DESIGN, SYNTHESIS AND EVALUATION OF SILVER-SPECIFIC LIGANDS

THESIS

Submitted to
Rhodes University
in fulfilment of the requirements for the degree of

DOCTOR OF PHILOSOPHY

by

ANDRÉ DAUBINET

January 2001

Department of Chemistry
Rhodes University
Grahamstown

Contents

ACKNOWLEDGEMENTS

I am extremely grateful to Professor Perry Kaye for allowing me to conduct this research under his supervision. Professor Kaye's willingness to explore new ideas combined with his extensive chemical knowledge, provided tremendous help. I also express my gratitude to Dr. Cheryl Sacht, the co-supervisor of the project, who provided valuable insights for the inorganic sections of the project.

I am indebited to MINTEK, the financial sponsors of the project, for their assistance and financial support.

A special thanks must go the Dr. Eric Hosten, of the Metal Separations Unit at Univeristy of Port Elizabeth, for his assistance in obtaining the ICP-MS data; to Paula Antunes, of the Heavy Metals Group in the Department of Biochemistry and Microbiology at Rhodes University, for her assistance in acquiring the AAS data; to Gerardo Medina, of the Chemistry Department at Rhodes University, for his assistance in interpreting the IR spectra of the complexes; to Dr. J. Basca from University of Cape Town, for the X-ray analysis; to Dr. P. Boshoff of the Cape Technikon for the mass spectroscopy; and to Mr. Aubrey Sonemann of the Chemistry Department of Rhodes University for his help in obtaining the GCQ mass spectroscopic data.

I would like to thank my fellow post-graduate students, my family and all my friends for the their tremendous support over the last five years.

ABSTRACT

Several series of ligands, designed to chelate silver(I) specifically in the presence of base metals, have been synthesised. The ligands include: - dithiodiamide compounds, prepared by the condensation of acetanilide derivatives with 1,2-dibromoethane; propanenitrile and propanoic ester derivatives prepared from pyridine-2-carbaldehyde *via* the Morita-Baylis-Hillman reaction; and novel malonamide ligands from the reaction of diethyl malonate with a range of primary amines. The malonamide derivatives were prepared under both conventional thermal and microwave-assisted conditions, the latter proving to be highly efficient. The ligands were all characterised using a combination of spectroscopic and, where appropriate, elemental analysis; in one case, the structural assignment was confirmed by single-crystal X-ray analysis. The fragmentation patterns in the electron-impact mass spectra of the malonamide derivatives have been explored using high-resolution and meta-stable peak scanning techniques.

Complexes of the malonamide ligands with copper(II) and silver(I) have been synthesised, and examination of these complexes has revealed distinct differences in their co-ordination preferences towards silver(I) and copper(II). Tentative, computer-modelled structures for the complexes have been proposed using the available spectroscopic and elemental analysis data. Computer modelling, at the Molecular Mechanics level, has also been used to assess the capacity of the ligand systems to adopt conformations suitable for the chelation of tetrahedral silver(I).

Solvent extraction studies have been undertaken using aqueous metal ion solutions and various organic solvents. The dithiodiamide derivatives typically presented solubility problems, but one of the ligands, *N*,*N*´-bis(3-chlorophenyl)-3,6-dithiaoctanediamide, exhibited significant but slow extraction of silver(I) into toluene. The malonamide derivatives, however, proved to be readily soluble in ethyl acetate and, in some cases, exhibited good to excellent selectivity for silver(I) in the presence of the base metals copper and lead. Atomic absorption analysis revealed rapid equilibration times (<15 min) and high extraction efficiencies over a wide pH range (2.78 - 9.0). Metal selectivity has been determined by ICP-MS analysis of the residual silver, copper and lead present in the aqueous phase after 15 min, and one of the ligands, *N*,*N*´-bis(2-benzylsulfanylethyl)malonamide, exhibits excellent (≥ 96 %) silver(I) specificity.

1 Introduction

1.1 Silver and its Compounds

Silver belongs to the same group as copper and gold in the periodic table, and they are collectively referred to as the "coinage metals" because of their usage since the late Stone Age for coins and jewelry. Silver occurs with an abundance of 0.08 parts per million (ppm) in the earth's crust, existing as the sulfide ore, Ag_2S (argentite), silver chloride salt, AgCl (horn silver) or as the native metal. The main producers of silver are Mexico (16 %), the United States of America (USA) (11 %), Russia (11 %), Canada (10 %), Peru (10 %), Australia (7.5 %) and Poland (7 %). Silver is obtained as a by-product during the extraction of copper, lead and zinc or is extracted as the cyanide complex during gold recovery. The main uses of silver are in photographic emulsions (AgCl or AgBr), jewelry, batteries and for silvering mirrors.[1,2]

Silver has the electronic configuration [Kr] $5s^1$ $4d^{10}$. It is easily oxidized to silver(I) (Ag^+), the standard reduction potential (SRP) being +0.80 V. The corresponding SRP's for silver(II) (Ag^{2+}) and silver(III) (Ag^{3+}) are +1.98 V and +2.1 V, respectively.[1] These values give an indication as to why the compounds formed with silver are dominated by silver(I) systems. The recent literature on silver is reviewed in the following chapter, but due to the volume of work reported only selected examples have been cited.

1.1.1 Silver (III) Complexes

Silver(III) is a rather unusual metal cation, and is therefore the focus of attention of specialist groups. Silver(III) compounds are used mainly as oxidizing agents, as the following examples from the recent literature illustrate.

Banerjee *et al.*[3] reported the kinetics of the silver(I) catalyzed oxidation of H_3PO_2 with the [(ethylenebis(biguanide)]silver(III) cation ($[Ag(H_2biguan)]^{3+}$) **1** in aqueous perchloric acid solution. The $[Ag(H_2biguan)]^{3+}$ cation is one of the few examples of water soluble silver(III) complexes.[4] The study revealed the mechanism of the

reaction and the structure of the intermediate generated, as illustrated in **Figure 1** below.

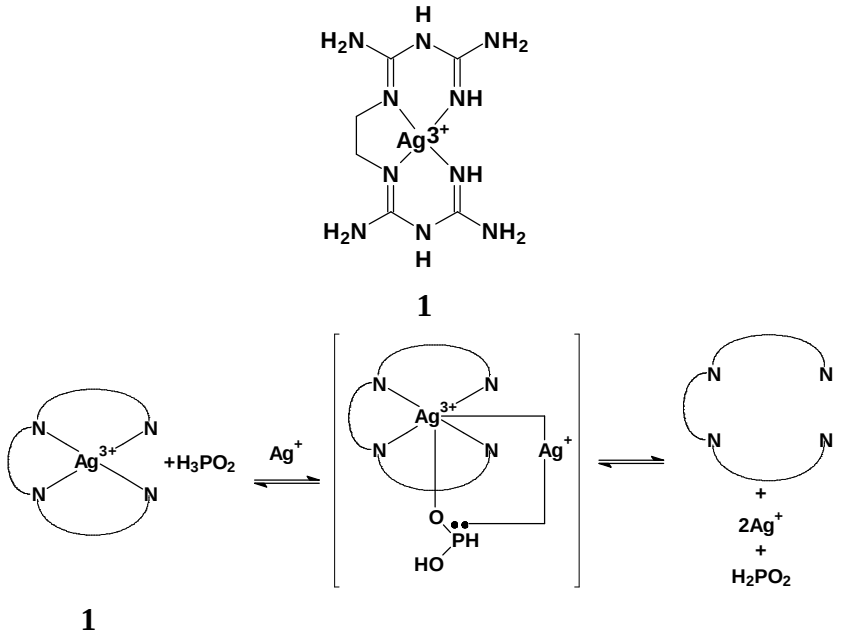

Figure 1. Mechanism for the silver(I) catalyzed oxidation of H_3PO_2 by complex **1**.

Dasgupta *et al.*[4] studied the electron transfer reaction between the $[Ag(H_2biguan)]^{3+}$ cation and ascorbic acid (H_2Asc) in acidic aqueous solution. The reaction was shown to involve the formation of a 1:1 intermediate between $[Ag(H_2bguan)]^{3+}$ and H_2Asc, which decomposes *via* a two electron transfer process, to yield dehydroascorbic acid, silver(I) and the free ligand. The authors identified three intermediate adducts in solution, *viz.*, $[Ag^{3+}(H_2biguan)(H_2Asc)]$, $[Ag^{3+}(H_2biguan)(HAsc)]$ and $[Ag^{3+}(H_3biguan)(H_2Asc)]$.

Gupta *et al.*[5] examined the kinetics of the oxidation of azide to N_2 by bis(dihydrogentellurato)silver(III) **2** (Equation 1). The reactant may be represented as $[M^{3+}\{(TeO_4)_2(OH)_4\}]^{5-}$ in which the metal, Ag^{3+}, adopts a square planar geometry and the hydroxyl ions (OH^-) are bound to the tellurium. The authors found that the reaction proceeded through a 1:1 intermediate complex with a one-step two-electron reduction of silver(III). The rate of the reaction increased with an increase in azide ion concentration but decreased with increasing alkalinity.

$$2N_3^- + [Ag^{3+}(H_2TeO_6)_2]^{5-} \rightarrow 3N_2 + [Ag^{+}(H_2TeO_6)_2]^{7-} \qquad \text{Equation 1}$$

2

1.1.2 Silver (II) Complexes

Silver(II) is also an unusual metal cation, but is more readily available to researchers than silver(III). The coordination chemistry of this cation has been explored, as is illustrated by the following examples from the current literature; the cation is commonly used as an oxidizing agent.

Lucier *et al.*[6] studied the preparation, structural and magnetic properties of silver(II) complexes of the type $AgF^{+}MF_6^{-}$ (M = Ir, Ru, Sb, Bi) and $Ag^{2+}(BiF_6^{-})_2$ systems. The authors found that for the $AgFMF_6$ systems they could identify three different structural types. For M = Ir the structure was found to contain two, linearly coordinating fluoride ligands in a one-dimensional chain. Where M = Ru the structure was found to be very different, consisting of a one-dimensional zig-zag ribbon, even though the RuF_6^{-} anion is only ~0.3 Å smaller in size than IrF_6^{-}. The structures of the complexes in which M = Sb and Bi are unknown but the complexes were shown by X-ray powder diffraction to be isostructural. For the $Ag(MF_6)_2$ systems the structures of $Ag(BiF_6)_2$, $AgBiF_6RuF_6$ and $Ag(SbF_6)_2$ were shown to be similar and correspond to structure **3**.

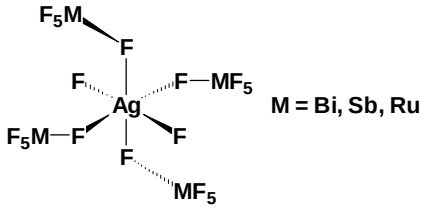

3

Giraudeau *et al.*[7] studied the complexation behavior of a phenanthroline-capped porphyrin **4** with silver. The authors found that when there is an excess of silver(I) in solution, the phenanthroline and porphyrin moieties each chelate a silver cation in the monovalent oxidation state, but, the silver(I) in the porphyrin complex is rapidly oxidized to silver(II), thus affording a homodinuclear multivalent complex.

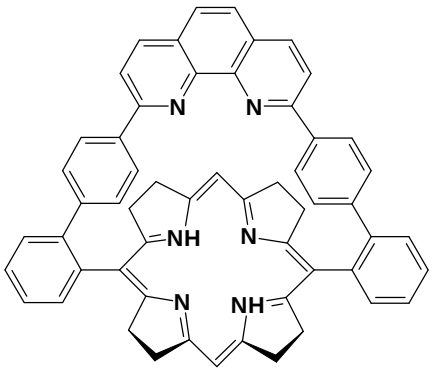

4

1.1.3 Silver (I) Complexes

Complexes containing silver(I) are clearly the most abundant of the silver complexes. What makes the silver(I) cation remarkable is its ability to coordinate in a range of geometries, from linear through to octahedral and, in some cases, even higher geometric orders. Silver(I) coordinates with a wide variety of donor atoms including the common donors, nitrogen, oxygen, phosphorous and sulfur, as well as unusual elements such as tellurium, arsenic and antimony. In the review of the recent literature, which follows, an attempt has been made to illustrate the range of geometries adopted by silver(I) and the nature of the complexes formed. In view of the number of such silver(I) complexes reported in the recent literature, only systems containing the donor atoms, nitrogen, oxygen and sulfur have been considered. The examples have been classified according to the donor atom involved, with each class further subdivided into (a) monomeric, (b) polymeric and (c) macrocyclic systems.[8,9,10]

1.1.3.1 *Silver(I) Complexes with Nitrogen*

(a) *Oligomeric Silver(I) Complexes*

Munakata *et al.*[11] have studied the coordination of 3,5-bis(2-pyridyl)pyrazole **5** with silver(I) and showed that this ligand has the ability to chelate in three different modes (**Figure 2**). The authors synthesised two silver(I) complexes and determined their structures by X-ray crystallography. The first complex was identified as a dinuclear silver(I) complex, $[Ag_2(\mathbf{5})_4][ClO_4]_2 \cdot 2Me_2CO$, in which each silver(I) is chelated to two ligand molecules, in mode **B**; each complex is then hydrogen bonded to another

complex. The silver(I) adopts a distorted trigonal-pyramidal geometry. The second silver(I) complex forms a polymeric substance, and is therefore discussed in the polymeric section.

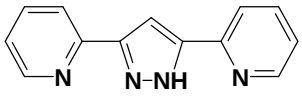

5

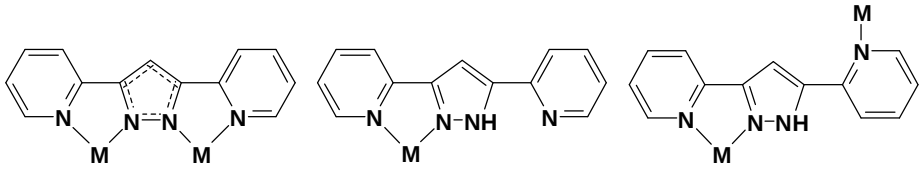

A **B** **C**

Figure 2. The possible coordination modes of ligand **5**.

Amoroso *et al.*[12] have determined the crystal structure of the complex formed between silver(I) and tris[3-(2-pyridyl)-pyrazol-1-yl]hydroborate **6**. The complex was characterized as a trinuclear silver(I) cluster, with formula $[Ag_3(\mathbf{6})_2][ClO_4]$. Each silver(I) atom adopts a distorted octahedral geometry and is coordinated to the other two silver atoms and in a bidentate fashion to one arm of each ligand.

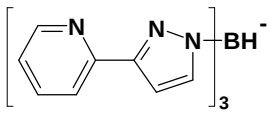

6

Hartshorn and Steel[13] reported on their study of the complexation between the bis(2-pyridyloxy)benzenes **7-9** and silver nitrate ($AgNO_3$). Their previous work involving the ligand **7** had produced a dinuclear complex of formula, $[Ag_2(\mathbf{7})_2]$, which has some interesting structural characteristics. In the complex, each silver(I) atom adopts a 'T-shaped' geometry, bridging the pyridyl nitrogen atoms from the two donor ligands and coordinating a solvent (H_2O) molecule. The benzene ring sub-units are also involved in π-π stacking. The authors were interested in determining whether similar effects would be observed for ligands **8** and **9.** They showed that in $[Ag_2(\mathbf{8})_2]$ the silver(I) centres are slightly distorted from the 'T-shape'. The complex formed with ligand **9** did not afford crystals suitable for X-ray crystallography, but from elemental analysis it was concluded that a complex of stoichiometry, $Ag_5(\mathbf{9})_4$, was formed.

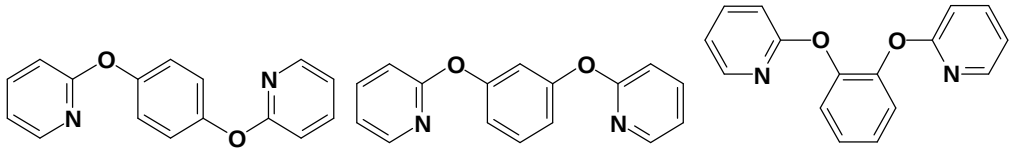

7 **8** **9**

Schneider *et al.*[14] studied the formation of the metallomacrocycle using silver hexafluorophosphate ($AgPF_6$) and the *p*-aminopyridine (1,5-dipyridin-4-yl-[1,5]diazonane) derivative **10**. The metallomacrocycle was shown to have the formula, $[Ag_2(\mathbf{10})_2](PF_6)_2$, and to exhibit C_{2v} symmetry. The silver(I) centres, which adopt a linear geometry, bridge the pyridyl nitrogen atoms from two ligand molecules, and there are Ag-aromatic interactions between adjacent units.

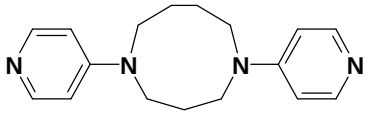

10

(b) *Polymeric Silver(I) Complexes*

The polymeric complex synthesised by Munakata *et al.*[11] using 3,5-bis(2-pyridyl)pyrazole **5** and silver(I), was shown to have the formula $\{[Ag(\mathbf{5})]ClO_4\}_\infty$. The polymer consists of silver(I) ions chelating adjacent ligands by coordinating the pyridyl nitrogen atom of one ligand and the pyridyl and pyrazolyl nitrogen atoms of a second ligand. The resulting structure, in which silver(I) ions adopt a distorted trigonal planar geometry, is similar to that observed for binding mode **C (Figure 2)**.

Masciocchi *et al.*[15] used X-ray powder diffraction to determine the structure of the polymeric complex formed between $AgNO_3$ and imidazole **11**. The silver(I) ions are linearly coordinated to two imidazole ligands, thus forming the polymeric chain $\{[Ag(\mathbf{11})]NO_3\}_\infty$, in which a close contact between silver(I) centres was observed (Ag-Ag = 3.161 Å).

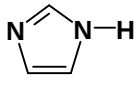

11

Carlucci *et al.*[16] studied the silver(I) complexes formed with pyrazine **12** and isolated four different polymeric products. With a ligand : metal ratio of 1:1, $\{[Ag(\mathbf{12})]BF_4\}_\infty$ was obtained, with silver(I) linearly coordinating two ligand molecules. With a ratio of 2:1, $\{[Ag_2(\mathbf{12})_3]BF_4\}_\infty$ was obtained, and was shown to comprise two different crystal morphologies, with the silver(I) centres adopting a planar geometry intermediate between 'T-shaped' and trigonal. At higher ligand - metal ratios, $\{[Ag(\mathbf{12})_3](BF_4)\}_\infty$ was obtained, with the silver(I) ions coordinating four ligand molecules in a distorted tetrahedral geometry.

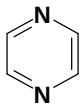

12

Venkataraman *et al.*[17] have reported zeolite-like behavior from a polymer formed between silver triflate (AgO_3SCF_3) and the symmetrical ligand **13**. In this system, the silver(I) ions adopt a trigonal pyramidal geometry, coordinating to the nitrile nitrogen atoms from three different ligands, with the triflate ($^-O_3SCF_3$) counterion in the axial position.

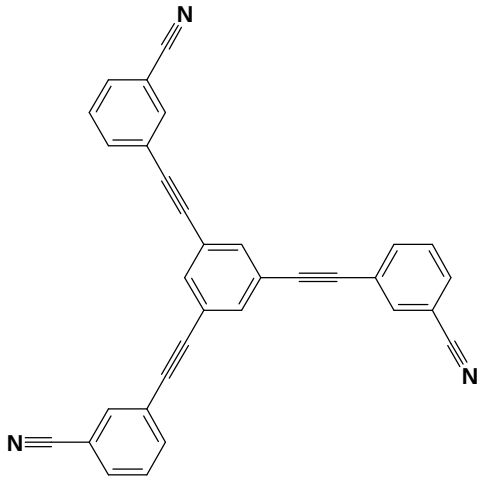

13

Carlucci *et al.*[18] observed rather different geometries in the X-ray crystal structures of the polymeric complexes $\{[Ag(\mathbf{14})_2]BF_4\}_\infty$ and $\{[Ag(\mathbf{12})_2]PF_6\}_\infty$, formed using piperazine **14** and pyrazine **12.** In the polymeric piperazine complex $\{[Ag(\mathbf{14})_2]BF_4\}_\infty$, the silver(I) cation adopts a distorted tetrahedral geometry, coordinating to the nitrogen atoms of four bridging ligands. In order to achieve this geometry, two of the ligands coordinate in a quasi equatorial-equatorial and the other

two in an axial-equatorial fashion. The polymer can be considered to consist of 2-dimensional sheets. Similar 2-dimensional sheets characterise the pyrazine complex $\{[Ag(\mathbf{12})_2]PF_6\}_\infty$, even though ligand **12** is far more rigid than ligand **14**. In the latter polymer, the silver(I) ions adopt a "see-saw" (disphenoidal) geometry.

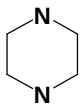

14

Hirsch *et al.*[19] investigated the influence of the counterion on the polymerization of silver(I) salts with the ligand 4,4´-biphenyldicarbonitrile **15**, and found that use of AgO_3SCF_3 afforded a linear polymeric chain of the formula $\{[Ag(\mathbf{15})(CF_3SO_3)]\}_\infty$. When $AgPF_6$ was used, a complex of formula $\{[Ag(\mathbf{15})_2]PF_6\}_\infty$ was isolated. The structure of this complex was described as comprising a nine-fold diamondoid network, in which the ligands bridge the tetrahedral silver(I) ions. The network structure is so large that eight similar networks fill the space within the framework, resulting in a nine-fold diamondoid arrangement.

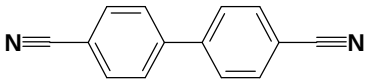

15

Robinson and Zaworotko[20] anticipated that the polymeric complex formed between $AgNO_3$ and 4,4´-bipyridine **16** would exhibit either linear or tetrahedral geometry. Unexpectedly, they found that the polymer consisted of silver(I) centres that adopted a 'T-shaped' geometry with one of the bonds to another silver(I) atom, and the others to two **16** ligands, forming, in total, three interpenetrated networks.

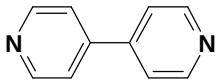

16

Plappert *et al.*[21] examined the silver complexes formed between $AgPF_6$ and the ligands bis(2-aminoethyl)amine **17**, tris(2-aminoethyl)amine **18**, *N*,*N*'-bis(2-amino-ethyl)propane-1,3-diamine **19**, and found that ligand **17** afforded a polymeric complex, $\{[Ag(\mathbf{17})PF_6]\}_\infty$, in which the silver(I) ions adopt a 'T-shaped' geometry, coordinating to two nitrogen atoms of one ligand unit, and one nitrogen atom of

another unit. In the case of the {[Ag(**18**)PF_6]}$_\infty$ polymer, the silver(I) ions adopt a distorted tetrahedral geometry, with one arm of the ligand coordinating to another silver(I) ion. Unfortunately the {[Ag(**19**)PF_6]}$_\infty$ polymer yielded no crystals suitable for analysis. The authors pursued the idea that the addition of monodentate ligands could hamper the formation of polymers, and, using this strategy, synthesised the following complexes $[Ag_2(\mathbf{17})_2(PMe_3)_2](PF_6)_2$, $[Ag(\mathbf{17})(PPh_3)]_n(PF_6)_n$ and $[Ag(\mathbf{17})(Bu^tNC)]_n(PF_6)_n$. From the analysis of these complexes they concluded that, while the addition of the monodentate ligands restricted polymerization, it resulted in dimeric structures.

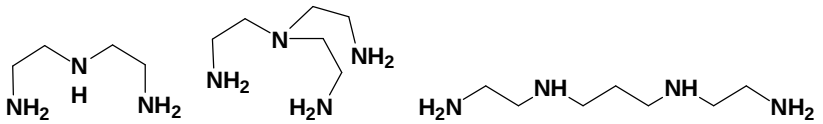

17 **18** **19**

The bis(2-pyridyl) ligands **20** and **21** were used by Hartshorn and Steel[13] to obtain polymeric complexes in which the silver(I) ions bridge the pyridyl nitrogen atoms from two ligands non-linearly, forming metallopolymers rather than metallocycles, with π-π stacking occurring between the aromatic rings.

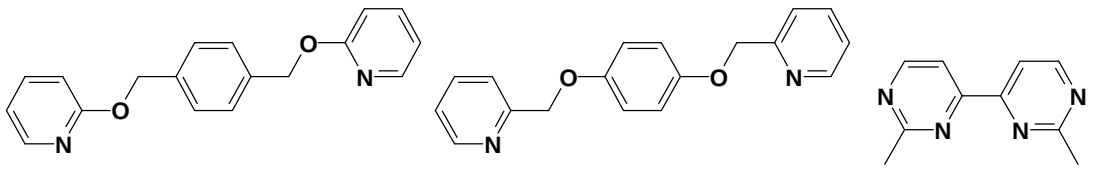

20 **21** **22**

Janiak *et al.*[22] considered the effect of metal - ligand ratio (1:1 or 2:1) and the nature of the counterions NO_3^-, BF_4^- or PF_6^- on the silver(I) complexes of 2,2´-dimethyl-4,4´-bipyrimidine **22**. Using a metal - ligand ratio of 1:1, and NO_3^- as the counterion, afforded a polymer comprising Ag-NO_3-Ag chains in which the silver(I) ions are bridged by the ligand molecules. With a metal - ligand ratio of 2:1, the polymeric framework illustrated in **Figure 3** was observed. Use of acetonitrile as the solvent and the salts, silver tetrafluoroborate ($AgBF_4$) and $AgPF_6$, afforded isostructural complexes, having the polymeric structure shown in **Figure 4**.

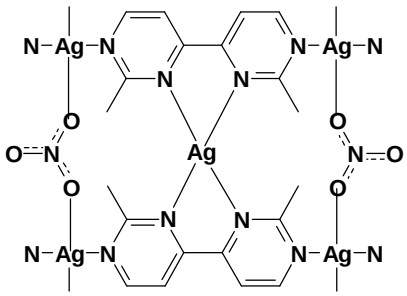

Figure 3. Polymeric framework.

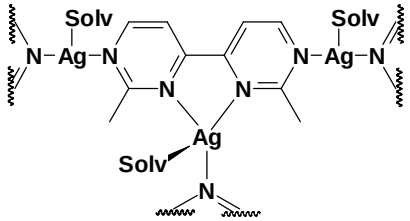

Figure 4. Polymeric framework.

(c) *Silver(I) Complexes of* N-*containing macrocycles*

The nitrogen-containing macrocyclic ligands **23-26** have been shown to chelate silver(I). Thus, Adams *et al.*[23] reported the synthesis and crystal structure of the decazine macrocycle disilver(I) complex **23**, which accommodates two, mutually non-bonded silver(I) ions. Each of the silver(I) ions is five-coordinate, and binds to four of the macrocycle nitrogens and to one of the nitrogen-containing pendant arms. Harding *et al.*[24] reported the encapsulation of two silver(I) ions using the octazine macrocycle **24**, but were unable to isolate crystals suitable for further analysis.

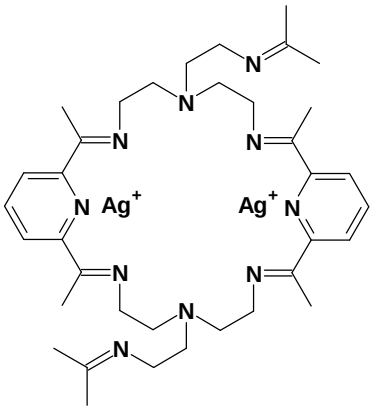

23

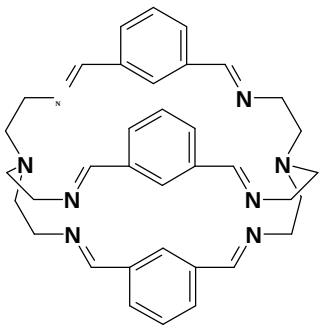

24

The decazine cage macrocycle **25** was shown by Takemura *et al.*[25] to accommodate either one or two silver(I) ions. From electrochemical studies, the authors showed that the single silver(I) species is very stable and does not demetallate easily. The ^{1}H NMR spectrum of this complex at low temperature (~ -90 °C) resembles that of the potassium salt, and therefore the conclusion was drawn that the silver(I) ion lies in the heart of the cavity; however, the coordination mode could not be established. In the

case of the disilver(I) complex the metal centres, which do not bond to each other, were shown to adopt a distorted tetrahedral geometry.

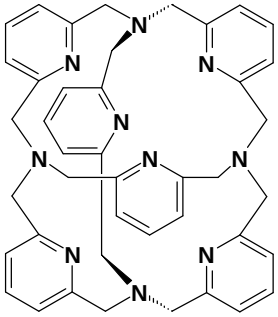

25

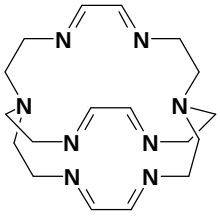

26

The disilver(I) complex formed with the octazine macrocycle **26** was shown by Coyle *et al.*[26] to have both silver(I) ions exposed on the surface of the macrocycle. Each silver(I) centre is trigonally coordinated to three nitrogen atoms and is bonded to the other silver(I) ion with an Ag-Ag axial bond.

1.1.3.2 *Silver(I) Complexes with Sulfur*

(a) *Monomeric and Oligomeric Silver(I) Complexes*

In the complex of silver(I) with the ferrocene ligand 1,1′-bis(diphenylthiophosphoryl)ferrocene **27**, reported by Gimeno *et al.*,[27] the silver(I) ion binds linearly to the two sulfur atoms (∠S-Ag-S = 176.83°), and no interaction with the ferrocene iron was observed.

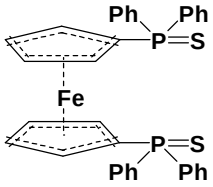

27

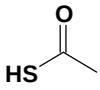

28

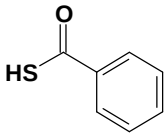

29

Sampanthar, Vittal and Dean[28] studied the complexation of silver(I) with the thiocarboxylate ligands thioacetic acid **28** and thiobenzoic acid **29**. The complex $[PPh_4][Ag(\mathbf{28})_2]$ also exhibits linear coordination between silver and the two sulfur donor atoms (∠S-Ag-S = 178.96°), whereas in the $[Et_3NH][Ag(\mathbf{29})_2]$ complex, some distortion from linearity was observed with the S-Ag-S angle reduced to 161.16°. This decrease has been ascribed to interactions with a second complex unit, involving

hydrogen bonding to the carbonyl oxygen and weak, additional silver-sulfur bonding; these interactions result in the silver(I) ion adopting a 'T-shaped' geometry.

Steiner *et al.*[29] have reported the synthesis of a multinuclear complex based on 2,4,6-triisopropylbenzenethiol, zinc and AgO_3SCF_3. As illustrated in **Figure 5**, each silver(I) centre adopts an essentially linear geometry [∠S-Ag-S = 174.7° (average)]. The complex is stable up to 70 °C, but is moisture sensitive, and on exposure to water, forms a polymeric product $[AgSR]_x$.

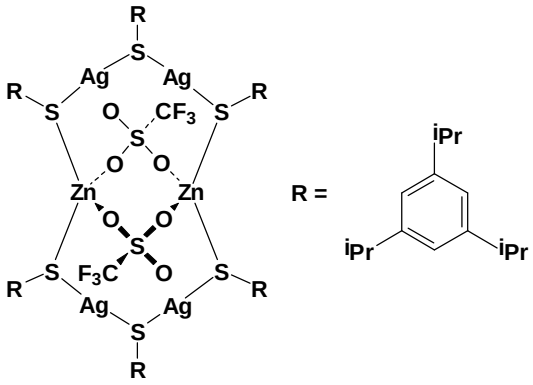

Figure 5. The structure of the multinuclear complex formed with silver(I) and Zinc.

(b) *Polymeric Silver(I) Complexes*

Texidor *et al.*[30] have reported the synthesis of a polymeric silver(I) complex with the cage compound exo-dithio-7,8-carba-*nido*-undecaborane **30**. The structure of the polymer consists of silver(I) ions trigonally coordinated to the sulfur atoms of three ligand units, with a very weak Ag-S interaction to additional sulfur atom of one of the three ligand units.

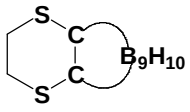

30

Black *et al.*[31] investigated the polymeric complexes arising from the coordination of the acyclic thioethers 1,3-bis(methylsulfanyl)propane **31** and 1,3-bis(phenylsulfanyl)-propane **32**. In the polymer $\{[Ag(\mathbf{31})]BF_4\}_\infty$ the silver(I) ions adopt a trigonal planar geometry coordinating to three ligand molecules. The authors noted that in the polymer of the three sulfur donor atoms coordinated to the silver(I) cation, two are

bidentate and one is monodentate. In the $\{[Ag(\mathbf{32})_2]BF_4\}_\infty$ polymer, however, the silver(I) ions coordinate tetrahedrally to four ligand molecules.

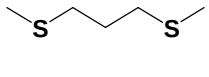

31

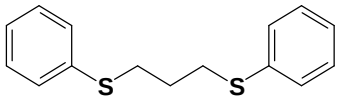

32

Nomiya *et al.*[32] investigated the use of electrospray ionization mass spectroscopy (ESI-MS) to identify and characterize silver(I) polymers. The authors identified the cyclic tetrameric subunit $\{Na_3[Ag(Htma)]_4\}_\infty$ in the MS spectrum of the polymer formed between thiomalic acid (H_3tma) **33** and $AgNO_3$. From ^{13}C and ^{109}Ag NMR spectroscopic evidence it was found that the silver(I) ion bridges the sulfur atoms, with no coordination to the carboxylic oxygen atoms.

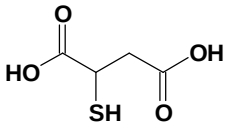

33

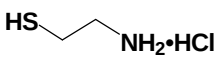

34

In the polymer generated by Su *et al.*[33] from silver chloride and 2-mercaptoethylamine hydrochloride **34** the base unit is an octanuclear cation $[Ag_8(\mathbf{34})_6Cl_6]^{2+}$. In this cation, six silver(I) ions adopt a distorted tetrahedral geometry, with three bonds to the sulfur atoms of the zwitterion ($^-SCH_2CH_2NH_3^+$) and one to a chlorine counterion. The other two silver(I) ions in the unit are trigonal planar, coordinating to three zwitterions, which exhibit μ_4 bridging *i.e.* linking four metal centres.

(c) *Silver(I) Complexes of S-containing macrocycles*

A number of macrocyclic silver(I) complexes have been reported in the recent literature - complexes that clearly illustrate the capacity of the silver(I) ion to adopt a variety of coordination geometries.

De Groot, Jenkins and Loeb[34] have explored the relationship between the counterion (X = ClO_4^-, BPh_4^-, $CF_3SO_3^-$ and BF_4^-) and the structure of the complexes formed between with the trithia macrocycle **35** and the corresponding silver(I) salts. While

all the complexes were observed to have the general formula $[Ag(\mathbf{35})_2]X$, their geometry proved to depend on the nature of the counterion. Thus, in the perchlorate ($X = ClO_4^-$) and tetrafluoroborate ($X = BF_4^-$) complexes the silver(I) coordinates with an approximately octahedral geometry. When $X = BPh_4^-$ the silver(I) ions adopt a distorted tetrahedral geometry, coordinating to the two sulfur atoms nearest the aromatic ring in each ligand, whereas for the triflate ($X = CF_3SO_3^-$) complex, the silver(I) ion adopts a tetrahedral geometry, coordinating to three sulfur atoms of one ligand and one sulfur atom of the other.

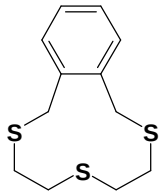

35

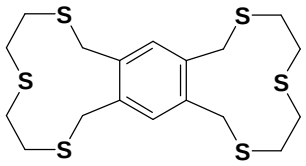

36

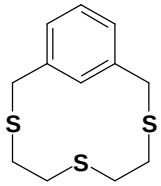

37

The analogous binuclear complex with the ligand 2,5,8,17,20,23-hexathia[9](1,2)[9](4,5)cyclophane **36** was shown by Loeb and Shimizu[35] to form a silver(I) complex, of formula $[Ag_2(\mathbf{36})(PPh_3)_2][BF_4]_2$, in which each of the silver(I) ions adopts a distorted tetrahedral geometry and coordinates in an *anti* arrangement (on opposite sides of the plane described by the aromatic ring) to three sulfurs and a PPh_3 ligand.

The meta-substituted trithia analogue 2,5,8-trithia[9]-m-cyclophane **37** was shown, by Casabó *et al.*[36], to form a polymeric complex with silver triflate. X-ray crystallography revealed that the silver(I) ions adopt a trigonal planar geometry and coordinate to the sulfur atoms of three ligands.

Complexes of 1,4,7,10,13-pentathiacyclopentadecane **38** with various silver(I) salts ($X = PF_6^-$, BPh_4^-, $B(C_6F_5)_4^-$) were studied by Blake *et al.*[37] In all the cases, the silver(I) ion is formally coordinated to all five sulfur atoms. With the counterion PF_6^- a polymeric complex is obtained, in which the silver(I) ions adopt a distorted octahedral geometry and the complex consists of two independent and antiparallel chains, formed by the coordination of the silver(I) ions to [4 + 2] S-donor sets. With the counterion BPh_4^-, a dimeric complex is obtained in which the two silver(I) ions

are tetrahedral and coordinate to a [3 + 1] S-donor set. With the counterion $B(C_6F_5)_4^-$, a simple mononuclear complex is formed.

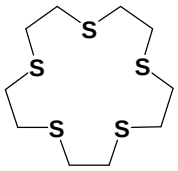

38

The macrocycle 1,5,9,13-tetrathiacyclohexadecane-3,11-diol **39**, synthesised and characterized by Munakata *et al.*[38], forms polymeric complexes with $AgNO_3$ and silver(I) acetate (CH_3CO_2Ag) in which the silver(I) ions adopt a tetrahedral geometry while coordinating to four ligand molecules. In the latter case, however, the tetrahedral geometry is very distorted.

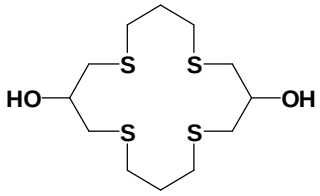

39

The silver(I) complexes of the trithia macrocyclic ligand **40** and hexathia macrocyclic ligand **41** have been investigated by Demirhan *et al.*[39], who found that with ligand **40**, in the presence of the neutral PPh_3 ligand, silver(I) coordinates tetrahedrally to all three sulfur atoms. Reacting $AgBF_4$ with ligand **41** gave a 1:1 adduct, in which the silver(I) ion coordinates to four of the six available sulfur atoms and exhibits a severely distorted tetrahedral geometry.

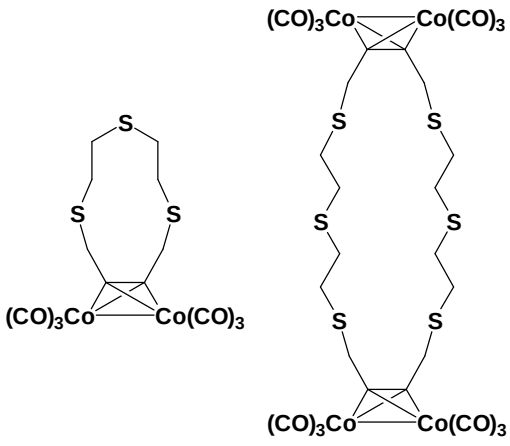

40 **41**

1.1.3.3 *Complexes with Oxygen*

(a) *Silver(I) Complexes with O-containing macrocycles*

Takeda *et al.*[40] studied the selectivity of the macrocycles 15,15-dimethyl-16-crown-5 **42** and 15-(2,5-dioxahexyl)-15-methyl-16-crown-5 **43** and found that while the presence of a side chain has no effect on the selectivity of the macrocycles for Na^+, Tl^+, K^+, Sr^{2+}, Ba^{2+} and Pb^{2+}, an enhancement in selectivity for Ag^+ was observed for ligand **43** over ligand **42**.

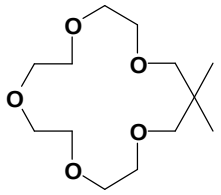

42

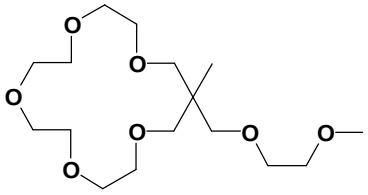

43

The properties associated with the silver(I) complexes of *C*-methylcalix[4]resorcinarene **44**, calix[6]arene **45** and calix[4]arene **46** have been investigated by Munakata *et al.*.[41] With $AgClO_4$, the ligand **44** was observed to form a dinuclear complex with the formula $[Ag_2(\mathbf{44})(C_6H_6)_2][ClO_4]\cdot 5C_4H_8O$. In this complex, the silver(I) ions each adopt a distorted tetrahedral geometry, coordinating to the solvent (benzene), the aromatic rings of resorcinarene and two phenolic groups. The macrocycles **45** and **46**, on the other hand, form complexes in which the silver(I) ions are tetrahedrally coordinated to the aromatic rings and the oxygen atoms of the counterions.

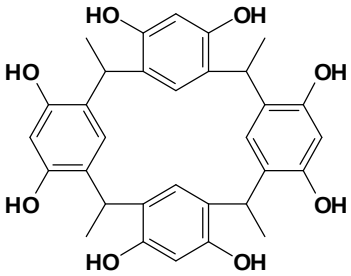

44

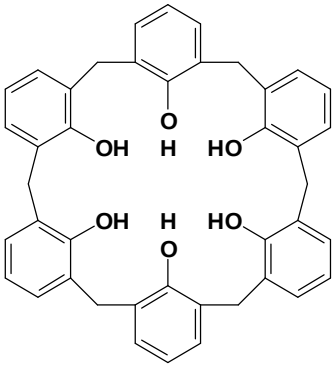

45

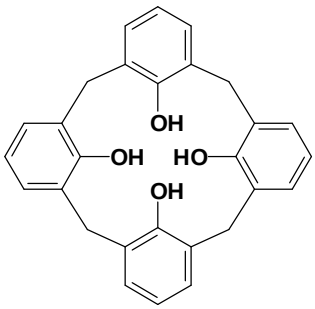

46

Nabeshima *et al.*[42] studied the extraction capabilities of a series of thiolariat ethers **47-53** and found that their affinity for alkali metal ions was almost the same as for the

corresponding lariat ethers, in which the sulfur atom in the pendant arm is replaced with oxygen. Selectivity for heavy metal ions, however, was only exhibited by thiolariat ethers which contained a 15-crown-5 ring, *i.e.* **48**, **50** and **51**, and these three ligands extracted Ag^+ with efficiencies of 95, 95 and 97 % respectively.

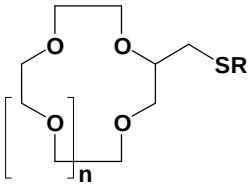

	n	R
47	1	Bu
48	2	Bu
49	1	Bn
50	2	Bn
51	2	$C_{12}H_{25}$

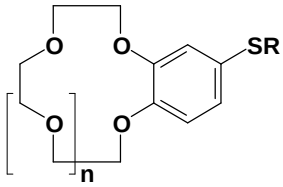

	n	R
52	2	Bu
53	2	Bn

(b) *Polymeric Silver(I) Complexes*

Two research groups have reported complexes of this class. Michaelides *et al.*[43] have prepared a polymeric complex from glutaric acid **54** and $AgNO_3$. The monomeric unit has the formula $[Ag_4(\mathbf{54})_2]$, and each silver(I) centre is coordinated to another silver(I) ion and the oxygen atoms of three ligand molecules, in a very distorted tetrahedral arrangement. Wu *et al.*[44] studied the coordination polymers formed using the ligands 2,5-*bis*(trimethylammonium)hexanedioic acid **55** and 2,5-dipyridin-1-ylhexanedioic acid **56** with $AgNO_3$ and $AgClO_4$. While the $AgClO_4$ complexes both exhibited 'T-shaped' coordination of the silver(I) atoms, the $AgNO_3$ complexes exhibited rather different coordination geometries. Thus in the $AgNO_3$ complex with ligand **55**, the silver(I) ion displays a distorted tetrahedral geometry, while in the corresponding system with ligand **56**, the silver(I) ion is square pyramidal.

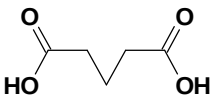

54

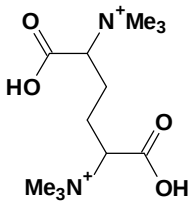

55

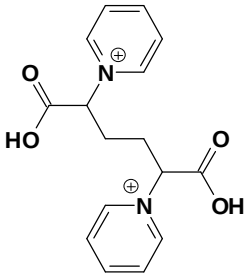

56

1.1.3.4 *Silver(I) Complexes with Nitrogen and Sulfur*

Silver(I) complexes containing the mixed donor atoms, nitrogen and sulfur, have been reported in the recent literature.

(a) *Monomeric Silver(I) Complexes*

The ketimine-based ligand *N,N'-bis*(1-thiophen-2-ylethylidene)ethane-1,2-diamine **57**, synthesised by Modder *et al.*[45], forms a silver(I) complex with the formula $[Ag(\mathbf{57})_2]O_3SCF_3$. The authors found that the flattened tetrahedral geometry of the silver(I) ion, in the solid state, was maintained in solution.

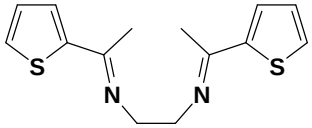

57

Ishikawa *et al.*[46] synthesised the cyclic and acyclic polythiazaalkane ligands **58-63** and used ^{1}H NMR spectroscopy, spectrophotometry and spectrofluorometry, to study the complexation of these ligands with silver(I). On addition of silver(I) the UV spectra of the ligands exhibited hypsochromic and hypochromic effects; there was also a decrease in the fluorescence intensity. However, no spectral changes were observed on the addition of other metal ions (Mn^{2+}, Co^{2+}, Ni^{2+}, Cu^{2+}, Zn^{2+}, Cd^{2+}, Pb^{2+} and Tl^{+}). From the NMR studies the authors concluded that the silver(I) ion binds *exo* to ligands **58** and **59**, but for the remaining ligands, the silver(I) ion appears to coordinate to all the donor atoms available within the cavity.

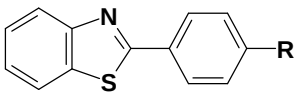

R				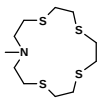	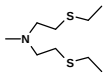	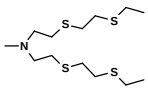
	58	**59**	**60**	**61**	**62**	**63**

(b) *Polymeric Silver(I) Complexes*

Haanstra *et al.*[47] synthesised a polymeric complex of $AgNO_3$ and 1,5-*bis*(3,5-dimethylpyrazol-1-yl)-3-thiapentane **64**, in which the silver(I) ion adopts a distorted tetrahedral geometry, coordinating to one sulfur atom, one nitrate counterion and two nitrogen atoms from different ligand molecules. In the polymeric complex of AgO_3SCF_3 and *N*-[*N*-((5-methyl-2-thienyl)methylidene)-L-methionyl]histamine **65**, however, Modder *et al.*[48] found that the silver(I) centres adopt a trigonal geometry and coordinate to three ligand molecules *via* the non-aromatic sulfur atom, the imine nitrogen and the aromatic nitrogen.

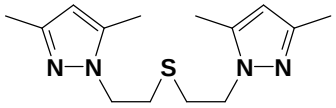

64

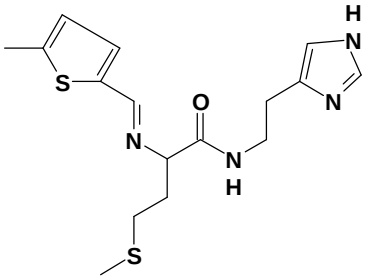

65

Hartshorn and Steel[49] investigated the complexation of the (2-pyridylsulfanylmethyl)benzene ligands **66**, **67** and **68** with $AgNO_3$, and observed that the silver(I) ions adopt different coordination geometries with each of the ligands. Thus, ligand **66** yielded a dimetalloparacyclophane, $[Ag_2(\mathbf{66})_2]$, in which the silver(I) ions are coordinated to nitrogen atoms from two ligand molecules and to the counterion in a distorted 'T-shaped' geometry. In the metallopolymer with ligand **67**, the silver(I) ions coordinate, in a distorted tetrahedral geometry, to the counterion, two pyridyl nitrogen atoms and one sulfur atom from different ligand molecules. In the metallopolymer with ligand **68**, the silver(I) ions coordinate to the counterion, to

another silver(I) ion, one sulfur atom and two pyridyl nitrogen atoms from different ligand molecules, in a distorted trigonal bipyramidal geometry.

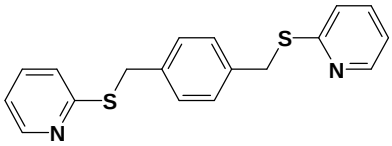

66

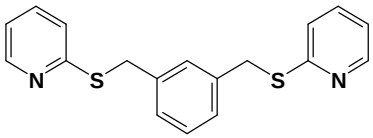

67

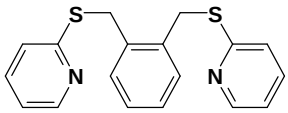

68

In the coordination polymer formed between $AgNO_3$ and 1,4-bis(2-pyridylmethylsulfanylmethyl)benzene **69**, Hanton and Lee[50] observed that the polymer consists of repeating units in which the silver(I) ions bridge two ligand molecules. The silver(I) ion coordinates in a distorted tetrahedral geometry to two oxygen atoms from the counterion, to the pyridyl nitrogen atom of one ligand and to the sulfur atom of another.

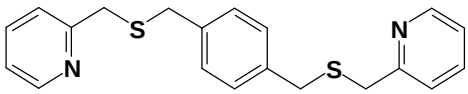

69

(c) *Silver(I) Complexes with N,S-containing macrocycles*

Mention has already been made of the macrocyclic ligands **58-63** developed by Ishikawa *et al.*[46] Chen *et al.*[51] have reported the formation of a complex between the diazatetrathia macrocycle **70** and $AgClO_4$, but have provided no details of the actual structure of the complex.

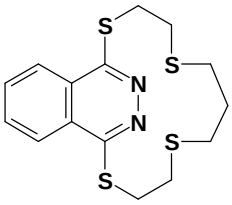

70

1.1.3.5 *Silver(I) Complexes with Nitrogen and Oxygen*

(a) *Dimeric Silver(I) Complexes*

The cytosine nucleobase, 1,5-dimethylcytosinate **71**, has been found, by Holthenric *et al.*[52], to form a tri-metal complex with one platinum(II) ion and two silver(I) ions.

The platinum ion is coordinated to the imine nitrogen atoms of two ligand molecules, while one of the silver(I) ions coordinates two carbonyl oxygen atoms, and the other to the two amine nitrogen atoms.

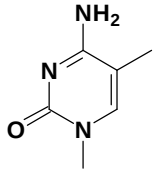

71

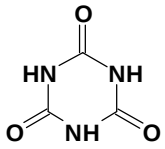

72

(b) *Polymeric Silver(I) Complexes*

Rao *et al.*[53] have reported the synthesis of the polymer formed between $AgNO_3$ and cyanuric acid **72**, in which the repeating unit [Ag_2(**72**)] contains two differently coordinated silver(I) ions. One of the silver(I) ions is linearly coordinated to the amine nitrogen atoms of two ligand molecules, while the other is coordinated to the carbonyl oxygen atoms of two ligand units and the amine nitrogen atom of another.

(c) *Silver(I) Complexes with N,O-containing macrocycles*

Medina *et al.*[54] investigated the silver(I) complexing potential of the ferrocenyl system, 1,1´-(1,4,10,13-tetraoxa-7,16-diazacyclooctadecane-7,16-dimethyl)ferrocene **73**. They found that the silver(I) ion is encapsulated within the cryptand, coordinating to all six donor atoms, and that there was an interaction between the iron and silver(I) ion, which serves to stabilize the complex.

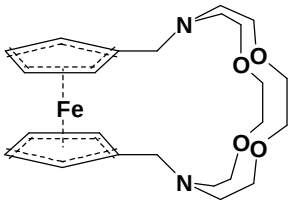

73

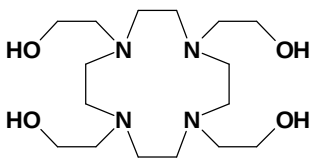

74

Potentiometric analysis and NMR spectroscopy was used by Turonek *et al.*[55] to study the complexation properties of 1,4,7,10-tetrakis(2-hydroxyethyl)-1,4,7,10-tetraazacyclododecane **74**. The stability constant of the silver(I) complex was found by potentiometric titration, to be 12.57 log(K/dm^{3}mol^{-1}) in methanol and 11.16

log(K/dm^{3}mol^{-1}) in dimethylformamide. The silver(I) complex had a higher stability constant than complexes of all the other metals tested (Na^+, K^+, Li^+, Rb^+, Cs^+).

The polyaza cryptand **75** was shown by Wang *et al.*[56] to encapsulate no less than five silver(I) ions. In the complex, each silver(I) ion exhibits distorted hexagonal-bipyramidal geometry, and is coordinated to a phenoxide oxygen atom, two imine nitrogen atoms and two, other silver(I) ions.

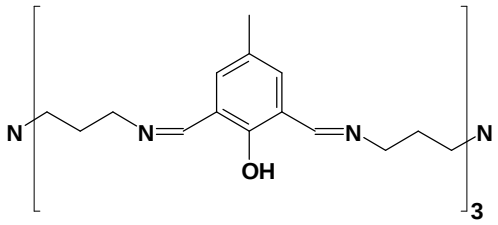

75

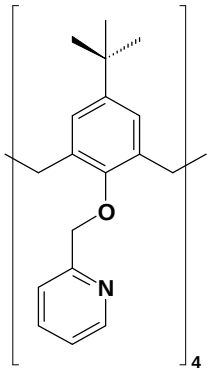

76

The crystal structure of the complex formed between $AgClO_4$ and 5,11,17,23-tetra-*tert*-butyl-[25,26,27,28-tetrakis(2-pyridylmethyl)oxy]calix[4]arene **76** was reported by de Namor *et al.*[57] In this unusual complex, the silver(I) ion is coordinated to four pyridyl nitrogen atoms and four ethereal oxygen atoms, in what is described as a "distorted Archimedean square antiprism".

Atkinson *et al.*[58] investigated the silver(I) complex of 14,22-di-*tert*-butyl-18-(2-pyridylmethyl)-2,10-dioxa-18,25-diazatetracyclopentaicosa-4,6,8(25),11,13,15,20,-22,24-nonaene **77**. The crystal structure revealed that the silver(I) ion is coordinated to the two ethereal oxygen atoms, the two pyridyl nitrogen atoms and the amine ring nitrogen atom in a distorted trigonal bipyramidal geometry.

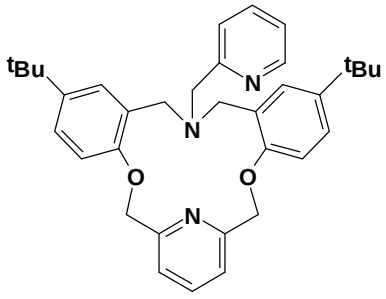

77

In an extensive investigation, Matsumoto *et al.*[59] explored the ability of the lariat ethers **78-104** to extract silver(I). They found that, for ion-selective *transport across a liquid membrane*, ligands **79-84**, **88-93** and **97-102** transport Ag^+ almost exclusively over Li^+, Na^+, K^+, Pb^{2+}, Cu^{2+} and Cd^{2+}. In contrast, the pyridylmethyl derivatives **85**, **94** and **103** effectively transport Li^+, Na^+, K^+, Pb^{2+} and Cu^{2+}, while the *N*-benzyl derivatives **86**, **95** and **104** showed high Na^+, K^+, Ag^{2+} and Pb^{2+} selectivity. From *extraction studies*, however, it was found that ligands **94**, **95**, **103** and **104** extracted Ag^+ competitively at 99, 96, 96 and 99 % respectively. The two lariat ether benzothiazolium styryl dyes **105** and **106**, were found[60] to coordinate with silver(I) but failed to show selectivity for silver over other metals. Surprisingly, the analogous lariat ether dye **107** does not complex Ag^+, whereas the unsubstituted aza-15-crown-5 ether does. [61]

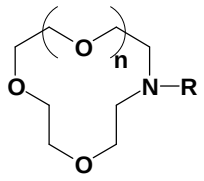

R	–H			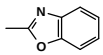	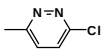		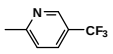		
n = 0	**78**	**79**	**80**	**81**	**82**	**83**	**84**	**85**	**86**
n = 1	**87**	**88**	**89**	**90**	**91**	**92**	**93**	**94**	**95**
n = 2	**96**	**97**	**98**	**99**	**100**	**101**	**102**	**103**	**104**

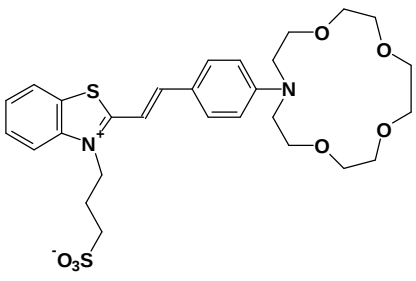

105

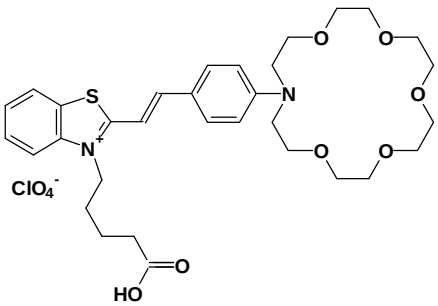

106

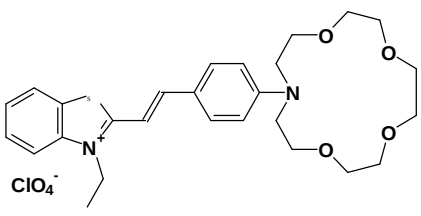

107

1.1.3.6 *Silver(I) Complexes with S,O-containing macrocycles*

In their study of the complexation of 1,4,7-trioxa-10,13-dithiacyclopentadecane **108** with silver(I), Blake *et al.*[62] isolated two products from the reaction of ligand **108** with $AgNO_3$ and NH_4PF_6, *viz.*, the polymeric complex $\{[Ag(\mathbf{108})]PF_6\}_\infty$ and the binuclear species $[Ag_2(\mathbf{108})_3](PF_6)_2$. In the polymeric complex, the silver(I) ions coordinate to all the donor atoms in the macrocycle as well as to the sulfur atom of another ligand molecule, thus forming a linear polymer in which the silver(I) ions adopt a distorted octahedral geometry. In the binuclear complex, each silver(I) ion is bound, in a distorted trigonal planar geometry, to two sulfur atoms of one ligand molecule, and one sulfur atom from a bridging ligand molecule.

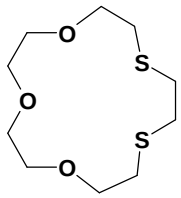

108

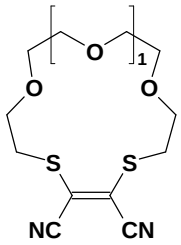

109

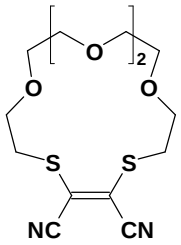

110

Sibert *et al.*[63] prepared silver(I) complexes with 1,4,7-trioxa-10,13-dithiacyclopentadec-11-en-11,12-dicarbonitrile **109** and 1,4,7,10-tetraoxa-13,16-dithiacyclooctadec-14-en-14,15-dicarbonitrile **110**. When the macrocycle **109** was used as the ligand, a monomeric and a polymeric product were obtained. In the monomeric product, the silver(I) ion exhibits distorted pentagonal pyramidal geometry and coordinates to all five macrocycle donor atoms and to the counterion. In the polymeric form the same geometry is observed around the silver centre, but the bond to the counterion is replaced by a bond to a nitrile group of an adjacent ligand unit. Complexation with the macrocycle **110** yielded a polymeric complex, in which the silver(I) centre adopts a distorted square pyramidal geometry and coordinates to one sulfur atom, three oxygen atoms and one of the nitrile groups of an adjacent macrocycle, thus forming a linear polymer.

1.1.3.7 *Silver(I) Complexes with N,S,O-containing macrocycles*

In the complex formed between the diazadithia ether macrocycle **111** and silver(I) the metal centre exhibits a distorted trigonal bipyramidal geometry through coordination to the two amine nitrogen atoms, the two sulfur atoms and the oxygen atom. [64]

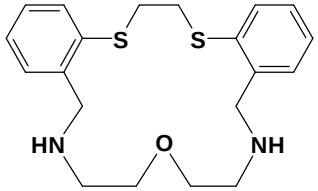

111

As can be readily seen from the examples cited in the above sections, the chemistry of silver, particularly that of silver(I), is very diverse and while the coordination chemistry of silver(I) is complicated, some general conclusions can be drawn.

i) Silver(I) prefers linear and tetrahedral coordination geometries, but other geometries can be expected.

ii) The nature of the donor atoms has a bearing on the coordination geometry, with silver(I) having a high affinity for soft donor atoms, *e.g.* sulfur.

iii) The number of donor atoms available in a system may influence the mode of coordination.

iv) The choice of counterion may determine whether the complex formed will be monomeric/oligomeric or polymeric and, in some cases, the counterion is involved in coordination to the silver(I) ion itself, complicating matters further.

These observations emphasise the need for caution in predicting what may be expected with a particular ligand and a silver(I) salt.

1.2 Solvent Extraction of Metal Ions

1.2.1 Theory

Solvent extraction is the process whereby a metal ion in an aqueous phase is selectively extracted into an organic phase by an appropriate organic reagent, thereby separating and purifying the particular metal ion. The process relies on the reversible formation of stable metal-ligand complexes of the specific metal ion. The rate of formation, and extraction, of these complexes determines the residence time required to achieve efficient extraction and, consequently, the choice and design of the extraction equipment. The rate of extraction is a function of the rate of diffusion of the various components.[65]

Of course, in order for extraction to occur, the metal ions and the extracting ligand must react. This can occur in three ways *viz.*, (a) diffusion of the ligand into the aqueous phase, (b) diffusion of the metal ion into the organic phase, or (c) reaction at the interface of the two phases. The products formed by the reaction must then diffuse away from the region of interest. These processes are shown schematically in **Figure 6**.[65]

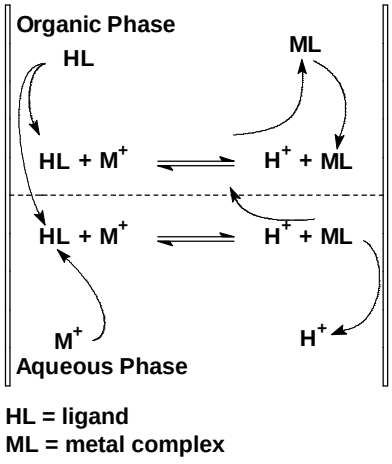

Figure 6. Reaction pathways in solvent extraction.

The diffusion processes are, typically, the slowest and, therefore, control the overall process. In most extraction processes, both the organic and aqueous phases are so efficiently stirred that the concentrations of all species in the system may be

considered to be the same in a given phase. At the interface, however, the role of diffusion can still be important.[65]

Whitman's two-film theory can be used to describe the diffusion process close to the interface. The first premise of the theory is that all turbulence due to the stirring of the phases dies out close to the interface, such that a laminar sub-layer exists in each of the phases near the interface. The theory assumes that, because there is no turbulence assisted transportation, there are no concentration gradients anywhere except in the laminar sublayer. This assumption implies that diffusion is the only mechanism for transportation across the laminar sub-layer and that the concentration gradient is linear as shown in **Figure 7**.[65]

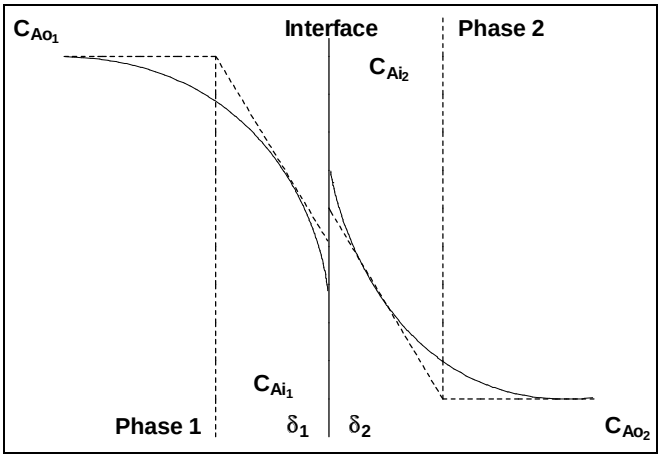

Figure 7. Concentration gradients at interface.

In the diagram, the dashed lines represent the theoretical concentration gradients, while the solid lines refer to the actual concentration gradient. It is assumed that an equilibrium exists at the interface and, therefore, C_{Ai1} and C_{Ai2} are in equilibrium. If the mass transfer is treated as a steady state process,

Ficks law $$N_A = D\frac{dc}{dz} \qquad (1)$$

becomes $$N_A = \frac{D_1}{\delta_1}\cdot\left(C_{Ao_1} - C_{Ai_1}\right) = k_1\cdot\left(C_{Ao_1} - C_{Ai_1}\right) \qquad (2)$$

or in the second phase terms, $$N_A = \frac{D_1}{\delta_2}\cdot\left(C_{Ai_2} - C_{Ao_2}\right) = k_2\cdot\left(C_{Ai_2} - C_{Ao_2}\right) \qquad (3)$$

Where, N_A = amount of substance diffusing;
D = diffusion coefficients;
$\frac{dc}{dz}$ = concentration gradient;
k_1 = rate of diffusion for phase 1;
k_2 = rate of diffusion for phase 2;
C_{Ao1} = original concentration of substance in phase 1;
C_{Ao2} = original concentration of substance in phase 2;
C_{Ai1} = concentration of substance at interface in phase 1;
C_{Ai2} = concentration of substance at interface in phase 2;
δ_1 = region of concentration change for phase 1 and
δ_2 = region of concentration change for phase 2.

Provided the complex does not accumulate at the interface, the two rates will be identical and can be related as follows[65] : -

$$\frac{k_1}{k_2} = \frac{\left(C_{Ai_2} - C_{Ao_2}\right)}{\left(C_{Ao_1} - C_{Ai_1}\right)} \qquad (4)$$

1.2.2 Silver-selective systems

In 1993, Paiva[66] published an exhaustive review on the recovery of silver from aqueous solution by solvent extraction. The following conclusions can be drawn from this compilation.

(a) Open-chain systems containing thiophosphorus exhibit remarkably good extraction properties. A commercially available extractant from Cyanamid, Cyanex® 471X **112**, selectively extracts silver from nitric, sulfuric and hydrochloric acid media, and can also be used to separate palladium from platinum.

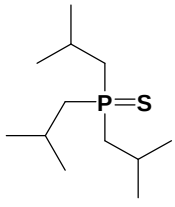

Cyanex® 471X

112

(b) Open-chain systems containing four sulfur donor atoms, *e.g.* as in ligand **113**, or a combination of sulfur and nitrogen, particularly aromatic nitrogen donor atoms, *e.g.* as in ligand **114**, also show excellent extraction behavior.

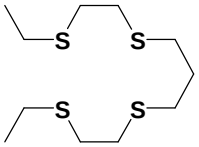

113

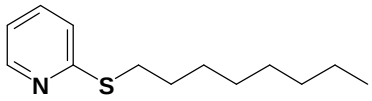

114

(c) Macrocyclic ligands containing nitrogen, oxygen and sulfur donor atoms in various combinations, whether in the ring or in pendant arms, show high selectivity for silver. Unfortunately, the contact times required tend to be longer than that for open-chain systems, and are more suited for other applications, such as ion-selective electrodes.

A concise overview of recent reports on the selective solvent extraction of silver follows. Examples of solvent extraction systems already cited in Section **1.1.3** are those of Takeda *et al.*[40] (page 16) and Matsumoto *et al.*[59] (page 22).

Ohmiya and Sekine[67] studied the extraction of silver by 2-thenoyltrifluoroacetone and 4-isopropyltropolone into chloroform, both in the presence and absence of tetrabutylammonium ions. Extraction in the presence of tetrabutylammonium ions was quantitative for both ligands, but proved poor in the absence of tetrabutylammonium ions. Mendoza and Kamata[68] examined the ability of ligand **115** to extract silver selectively. The authors found that this ligand forms a 1:1 complex with Ag^{+}, extracting it with an efficiency of 99.2 % in preference to Cd^{2+}, Co^{2+}, Cr^{3+}, Cu^{2+}, Fe^{3+}, Mn^{2+}, Ni^{2+}, Sn^{2+}, Pb^{2+}, Pt^{4+} and Zn^{2+}.

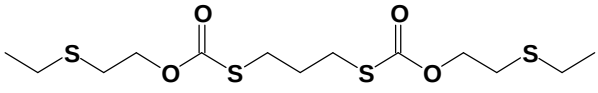

115

Tsukube *et al.*[69] synthesised a series of stereospecific acyclic podands **116-120**, each containing three pyridine moieties. Ligand **116a** forms an insoluble compound, ***SS*-117a** effecting 96 % extraction of silver in the presence of equimolar concentrations

of Cu^{2+}, Ni^{2+}, Pb^{2+}, Co^{2+} and Zn^{2+}, while the ***meso***-ligand **117a** effects 76 % extraction of Ag^{+} under the same conditions.

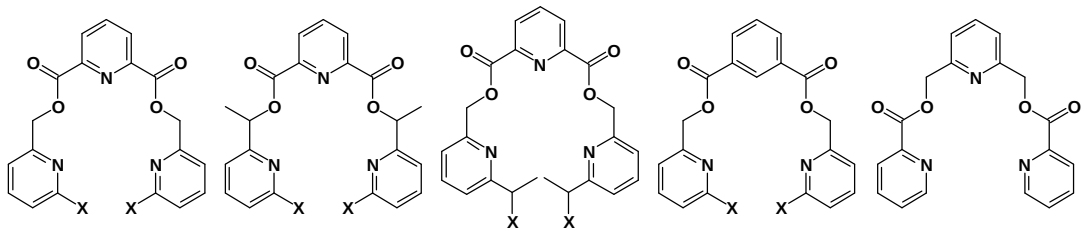

116 **117** **118** **119** **120**

116	**X**
a	H
b	$CH_2OTBDMS$
c	CH_2OPal
d	Br
e	CH_2OBn
f	CH_2OTr

117	**X**
a	H
b	$CH_2OTBDMS$
c	CH_2OPal

118	**X**
a	OAc
b	OTBDMS
c	OPal

119	**X**
a	H
b	$CH(CH_3)OPal$

Pal = $CO(CH_2)_{14}CH_3$

Kumar *et al.*[70] studied the factors which influence selectivity for silver in the acyclic and macrocyclic systems **121-135** and found that the acyclic systems **121-126** show good complexation of Ag^{+} and Pb^{2+}, but poor selectivity towards Ag^{+}. The conversion of the amino function to amide was found to lower complexation efficiency but increase selectivity for Ag^{+}. The macrocycles **127-135** on the other hand, showed higher extraction and selectivity properties.

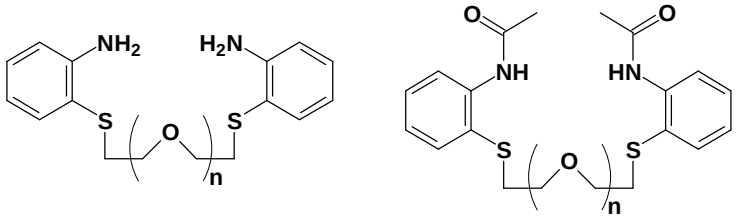

	n
121	**1**
122	**2**
123	**3**

	n
124	**1**
125	**2**
126	**3**

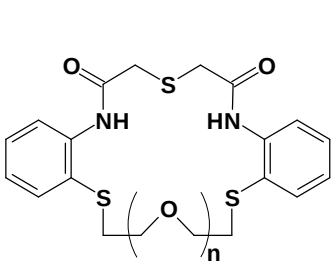

	n
127	**1**
128	**2**
129	**3**

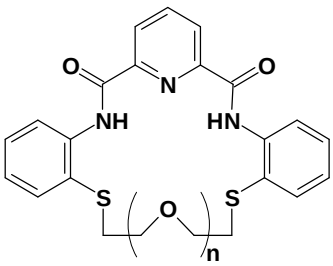

	n
130	**1**
131	**2**
132	**3**

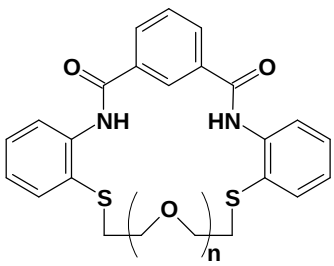

	n
133	**1**
134	**2**
135	**3**

The thiazacrown macrocycles **136-139**, investigated by Sakamoto *et al.*[71], showed good silver selectivity. The extraction efficiencies was found to decrease in the order: - **138** > **137** > **136** > **139**.

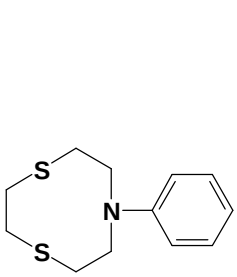

136

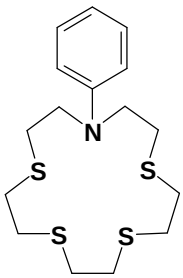

137

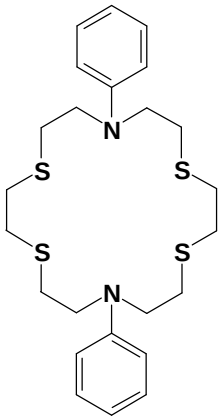

138

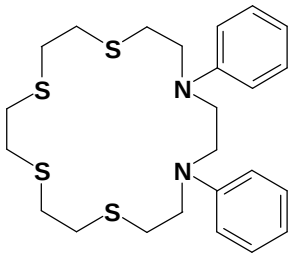

139

Other, crown ether ligands, developed by Kumar *et al.*[72] and Saito *et al.*[73] have shown silver chelation capacity. Thus, Kumar *et al.*[72] reported on the extraction capabilities of the trithiabenzenecyclophane **140** and dithiabenzenapyridinacyclophane **141**. The authors found that ligand **140** extracted Ag^+ 172 times more efficiently than Pb^{2+}. Ligand **141**, on the other hand, extracted Ag^+ 602 times more efficiently than Pb^{2+}. Saito *et al.*[73] determined the logarithmic distribution constant (log K_{DC}) and the logarithmic extraction constants [log $K_{ex(10)}$] for copper(II) and silver(I) into octan-1-ol for ligand **142** [for copper(II) log $K_{ex(10)}$ = -7.42, and for silver(I) log $K_{ex(10)}$ = -2.24 and log K_{DC} = 0.49].

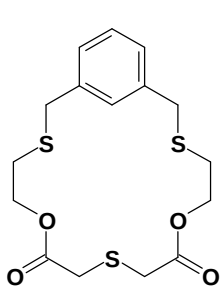

140

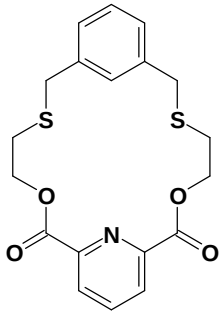

141

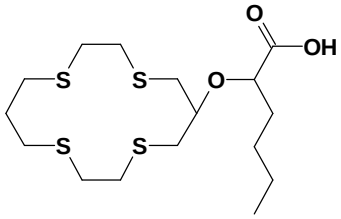

142

Calixarenes have also found application in silver extraction. Ohto *et al.*[74,75] found that a tetrameric ketonic calix[4]arene **143** was capable of separating silver selectively from palladium[74], and observed a similar result for the amide calix[4]arene **144**.[75] The amide analogues **145a-f**, developed by de Namor *et al.*[76], exhibited particularly good silver extraction abilities (log K_{ex} : 4.9-6.9).

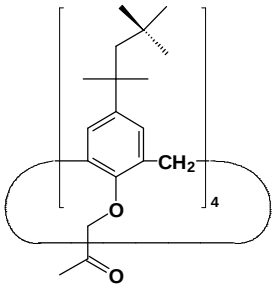

143

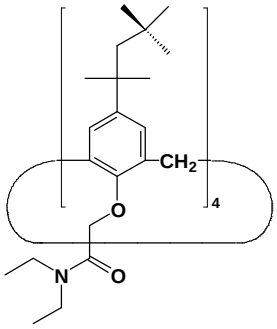

144

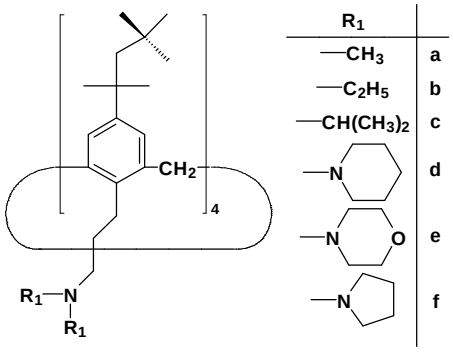

145a-f

Finally, Otsuka *et al.*[77] found that the capped calix[6]arene **146** showed remarkable selectivity towards Ag^+ and Cs^+.

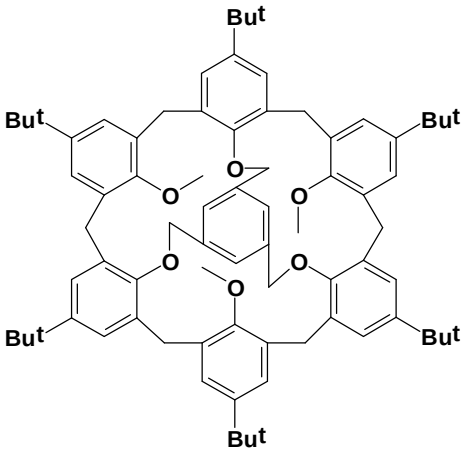

146

1.3 Previous work done in the group and aims of present investigation

It can be seen from the previous sections that there are many examples of systems designed and synthesised by research groups with a particular goal in mind. Previous research at Rhodes has focused on the design and synthesis of novel organic compounds with the potential to act as metal-specific or biomimetic ligands. Hagemann[78] developed a series of bidentate, tridentate[79] and tetradentate ligand systems[80] containing amide and sulfanyl groups, with the aim of selectively extracting platinum and palladium from mixtures containing base metals contaminants. Burton[81] and Wellington[82] have synthesised series of diamido, diamino and diimino ligands[83,84] with various spacer groups, with the intention of generating biomimetic copper complexes which would model the active site of the enzyme, tyrosinase.

Although there have been many recent attempts (Section **1.2.2**, p. 28) at developing a ligand-solvent extraction system which is specific for silver(I), there is still room for improvement, *i.e.* a) to increase selectivity for silver(I) by exploring more diverse ligand systems; b) to increase the efficiency of the system by decreasing the time taken to extract silver(I); and c) to develop simple systems which are readily synthesised and which do not require expensive reagents or complex synthetic methods. MINTEK had, in fact, identified a need to develop a ligand capable of extracting silver(I) selectively from a strongly acidic, ore-leach solution containing silver (*ca.* 100 g/l) and *ca.* 20 g/l of each of the metals, copper, gold, lead, mercury.

Specific objectives in the present study have included the following.

1. The design and synthesis of ligand systems containing combinations of nitrogen, oxygen and sulfur donor atoms to achieve selective extraction of silver(I).
2. The application of computer modelling in designing the ligands, and as an aid in predicting extraction ability.
3. An evaluation of the capabilities of the synthetic ligands in extracting silver(I) selectively from a nitric acid solution containing silver, copper, lead, mercury and gold ions.

2 Discussion

2.1 Ligand Design and Synthesis

The review published by Paiva[66] provides detailed examples of ligands that have been studied for the solvent extraction of silver (Section **1.2.2**, p. 28) and it is apparent, from this review, that many combinations of donor atoms, whether located in acyclic, macrocyclic or cryptand systems, have some extraction capability. On closer examination, however, it becomes evident that certain donor atom combinations achieve better extraction than others. These donor combinations may be identified as nitrogen and sulfur and, to a lesser degree, nitrogen and oxygen. Acyclic systems containing two, three or four donor atoms appear to be most efficient for silver extraction. Illustrated below (**Figure 8**) are some examples of previously investigated systems that showed good extraction potential.

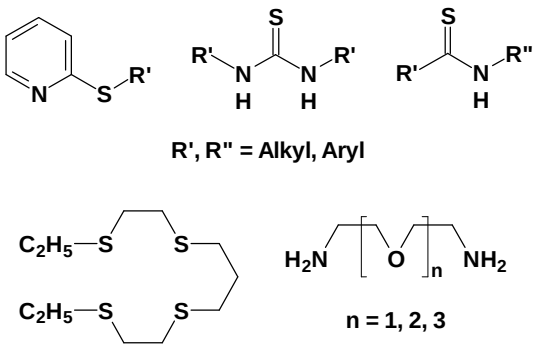

Figure 8. Examples of systems examined for the solvent extraction of silver.[66]

Designing ligands for solvent extraction application is a complex task, and the following ligand properties were identified as important design criteria.

(i) The ligand should contain a suitable combination of donor atoms, such as nitrogen, sulfur and oxygen, to effect selective and efficient solvent extraction of the metal.

(ii) The synthesis of the ligand should, ideally, be simple, efficient and cost-effective. This implies that the synthetic route should involve a minimal number of steps, each of which needs to be high-yielding, thus minimizing the overall cost and affording adequate quantities of the ligand.

(iii) The ligand system should be capable of extracting the metal efficiently at low pH, be impervious to oxidation and relatively inert towards acids.

(iv) The ligand, and the complex formed with the metal, should be sparingly soluble in the aqueous phase.

(v) Stripping of the metal from the organic phase and regeneration of the ligand should be easily achieved without significant degradation of the ligand.

An investigation of the coordination chemistry of silver revealed that two coordination geometries are favoured, *viz.*, linear and tetrahedral - as illustrated by the examples cited in the introduction (Section **1.1.3**). This suggests that ligands that are either bidentate or tetradentate should be suitable for chelation with silver(I). In light of the foregoing design criteria and the examples quoted in Sections **1.1.3** and **1.2**, the bidentate and tetradentate ligand templates illustrated in **Figure 9**, were targeted. The bidentate template **I** contains a pyridine moiety with a suitable side chain containing a second donor atom and a substituent '**R**', which could be varied to control metal selectivity. The tetradentate template **II** comprises versatile components with options for varying: - i) the donor atom combinations; ii) the type of spacer group(s) located between the donor atoms; and iii) the '**R**' substituents. Appropriate selection of these variables was expected to permit efficiency and selectivity in the solvent extraction of silver(I) to be optimized.

I : Bidentate template

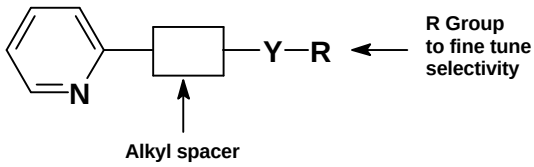

II : Tetradentate template

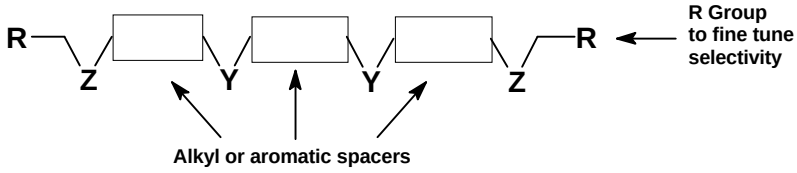

Y and Z = N, S, O donor atoms

Figure 9. Bidentate and tetradentate ligand templates.

2.1.1 3,6-Dithiaoctanediamide Derivatives

In previous work in our group, Hagemann[78] used acetanilide derivatives to produce tetradentate ligands of the type illustrated in **Figure 10** to extract platinum and palladium. These ligands, which contain appropriately spaced nitrogen and sulfur donors, correspond to the tetradentate template **II** (**Figure 9**) and were, therefore, also considered as candidates for silver extraction.

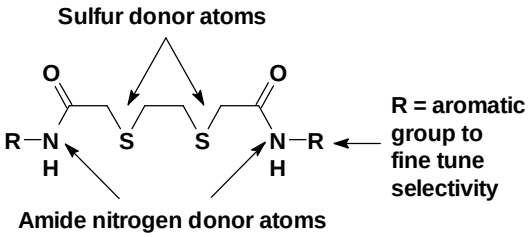

Figure 10. 3,6-Dithiaoctanediamide ligands with potential for chelating silver(I).

Applying Hagemann's synthetic methodolgy,[78] the aniline derivatives **147a-f** were reacted with sulfanylacetic acid **148** under nitrogen (**Scheme 1**), to produce the corresponding acetanilides **149a-f** in yields ranging from 29 to 99 % (**Table 1**). The ^{1}H NMR spectra of the products **149a-f**, illustrated for compound **149a** in **Figure 11**, are characterized by a sulfanyl proton triplet at δ_H *ca.* 2.0 ppm, a methylene doublet at *ca.* 3.4 ppm, a broad amide singlet at *ca.* 8.5 ppm and cluster of multiplets in the aromatic region.

Scheme 1. Synthesis of acetanilide derivatives.

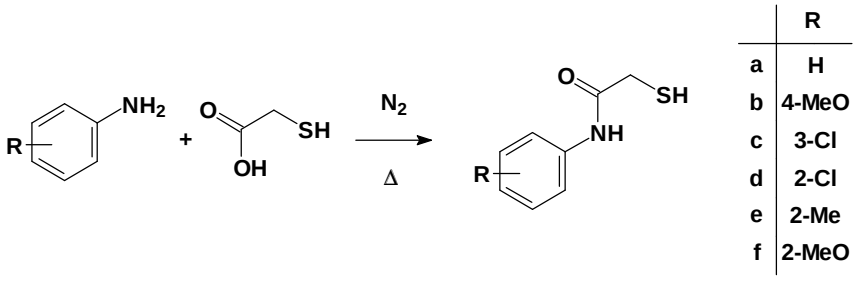

	R
a	H
b	4-MeO
c	3-Cl
d	2-Cl
e	2-Me
f	2-MeO

The acetanilides **149a-f**, which were all crystalline solids, were purified by recrystallisation before being reacted with dibromoethane and potassium hydroxide (**Scheme 2**) to yield the crystalline 3,6-dithiaoctanediamide derivatives **150a-f** in yields varying from 49 to 82 % (**Table 1**).

Scheme 2. Synthesis of 3,6-dithiaoctanediamide derivatives.

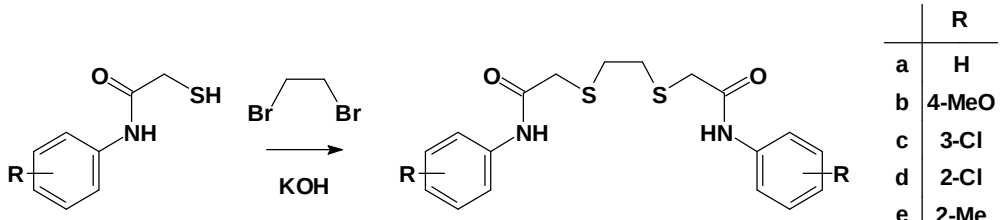

149a-f **150a-f**

The ^{1}H and ^{13}C NMR spectra illustrated for compound **150a** in **Figures 12** and **13**, respectively, are typical of the ligands **150**. The conversion of the acetanilide to the 3,6-dithiaoctanediamide is clearly evidenced in the ^{1}H NMR spectrum by:- the disappearance of the triplet at *ca.* 2.0 ppm; the appearance of the ethylene singlet at *ca.* 2.9 ppm; and the collapse of the methylene doublet at *ca.* 3.4 ppm into a singlet. The shift in the amide signal from *ca.* 8.5 ppm to *ca.* 10.1 ppm, while characteristic of the ligands **150**, may simply reflect the change in the NMR solvent from $CDCl_3$ to DMSO-d_6. The ^{13}C NMR spectrum (**Figure 13**) illustrates the symmetry of the 3,6-dithiaoctanediamide with only seven carbon signals being observed, each signal representing two carbons, with the exception of the signals at δ 119.1 and 128.6 which represent four carbons each.

Table 1. Data for the acetanilides **149a-f** and 3,6-dithiaoctanediamides **150a-f**.

		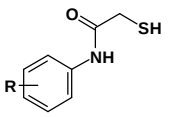		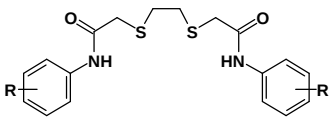	
		Acetanilides		3,6-Dithiaoctanediamides	
		149a-f		**150a-f**	
	R	Yield [a] / %	mp [b] / °C	Yield [a] / %	mp [b] / °C
a	H	57	111 (110-111)	56	159-161 (150-152)
b	4-MeO	99	118 (118-119)	82	180-182 (163-165)
c	3-Cl	93	72-73 (70-73)	49	137-139 (114-117)
d	2-Cl	29	60 (56-59)	61	169-172 (165-167)
e	2-Me	86	91 (88-91)	52	189-192 (176-178)
f	2-MeO	63	66 (64-66)	75	140-143 (137-140)

[a] Based on recrystallized product. [b] Followed in parentheses by the values reported by Hagemann.[78]

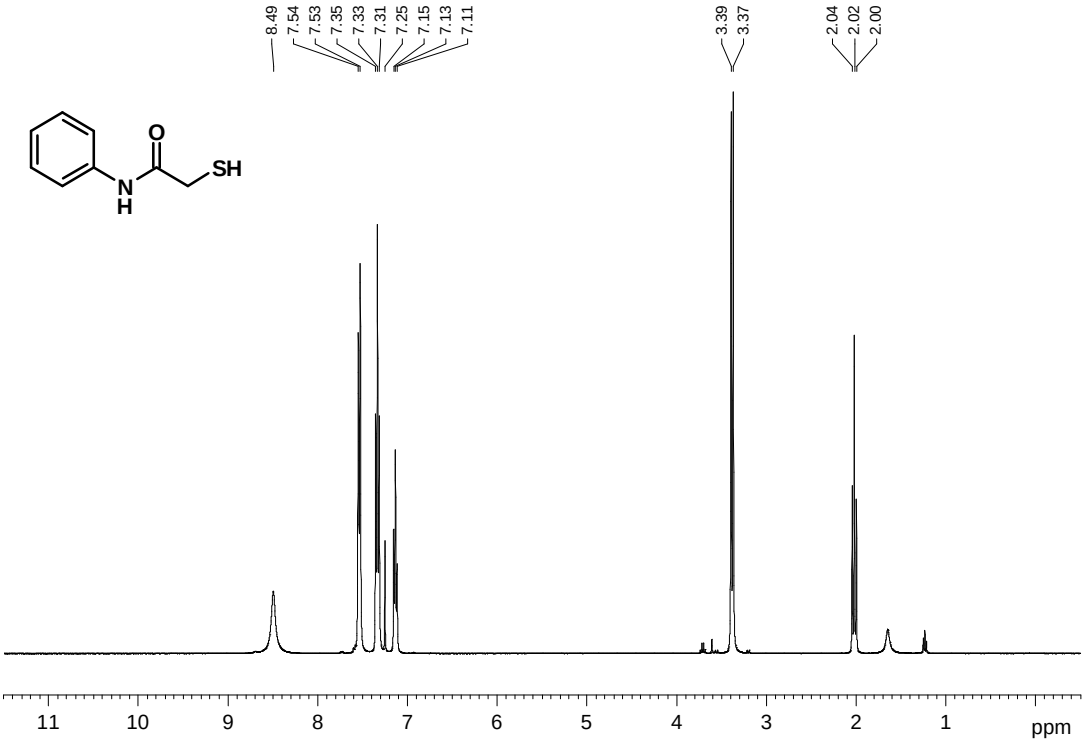

Figure 11. 400 MHz ^{1}H NMR spectrum of compound **149a** in $CDCl_3$.

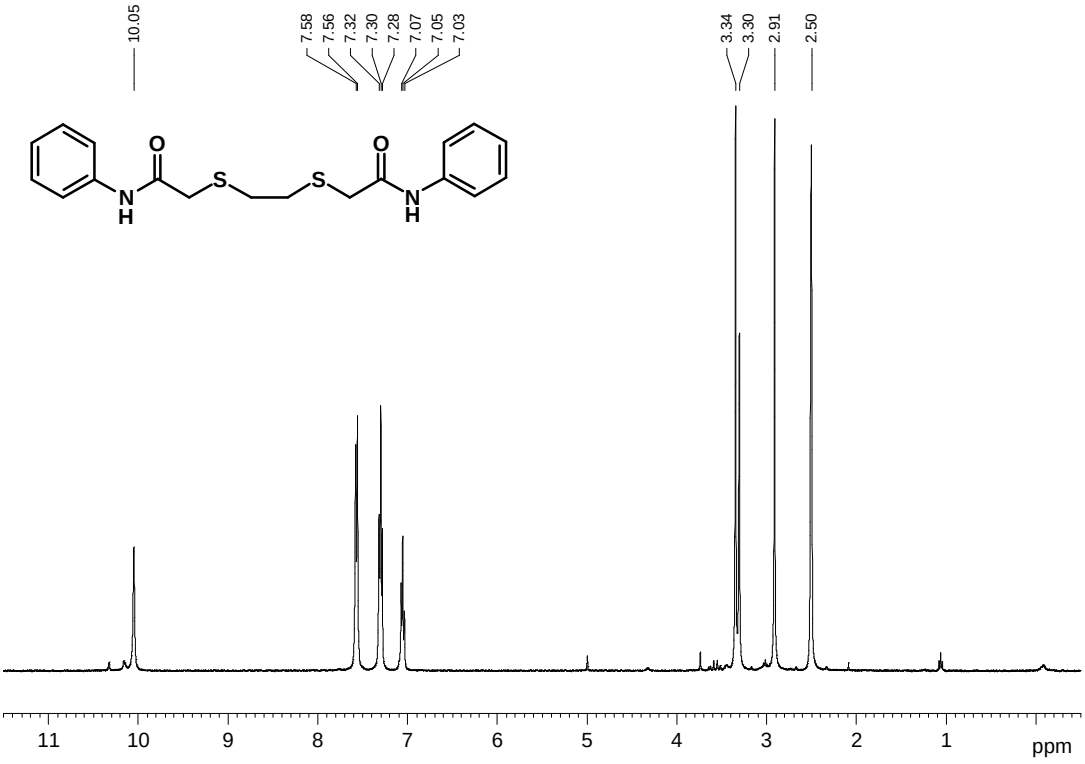

Figure 12. 400 MHz ^{1}H NMR spectrum of ligand **150a** in DMSO-d_6.

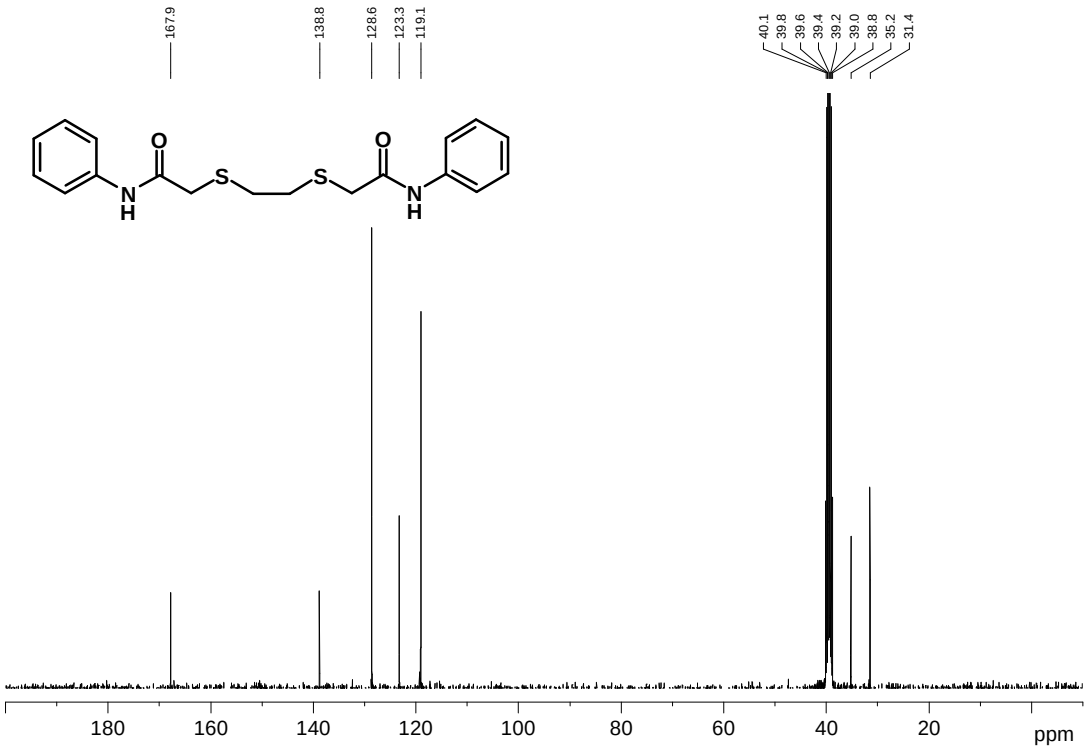

Figure 13. 100 MHz ^{13}C NMR spectrum of ligand **150a** in DMSO-d_6.

As can be seen from **Table 1**, the melting points obtained for the 3,6,-dithiaoctanediamides **150a-f** are consistently higher than those reported by Hagemann.[78] All other data (NMR, MS and IR) obtained in the process of characterizing the products confirmed that the compounds were, in fact, the 3,6-dithaioctanediamides **150a-f**. The higher melting points are, therefore, presumed to indicate that purer products were obtained in the present study.

The coordination potential of a ligand depends, in part, on its ability to accommodate a particular metal ion within its structure or to adjust its conformation to optimize chelation. Thus, for the tetradentate 3,6-dithiaoctanediamide ligands **150a-f**, the question is: "Can the ligands readily adopt an appropriate conformation to accommodate the silver(I) cation in a tetrahedral geometry ?". In order to estimate the steric energy* cost for effective chelation, the conformations of the ligands **150a-f** and their respective complexes **151a-f** (**Scheme 3**) were explored using computer-modelling techniques.

* The term steric energy can be defined as "the additional energy associated with the deviations of the structure with respect to an ideal situation where all geometrical elements would be in a reference state".[85]

Scheme 3. A schematic representation of the possible tetrahedral coordination of the ligands **150a-f** with silver(I) *via* formation of 5-membered chelates.

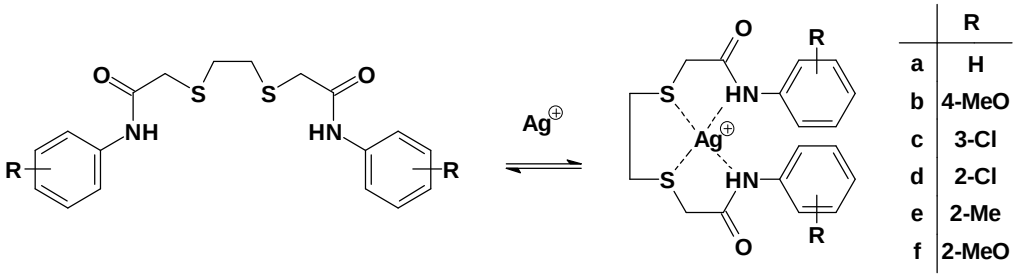

150a-f **151a-f**

Using a Molecular Mechanics (MM) approach, the ligand structures were constructed with the MSI Cerius$^{2®}$ modelling package.[86] Following minimization of each structure to a local minimum, the conformational space was explored to find the global minimum; for this purpose, a Molecular Dynamics - Simulated Annealing routine was applied. The lowest-energy conformer obtained for each ligand was then used to construct the corresponding silver(I) complex and, using the Universal Force Field (UFF), the same MM methodology was applied to identify the global minimum. Comparison of the steric energies of the free ligand and its "chelating conformation" (obtained by removing the silver ion) provided an estimate of the energy cost (ΔE_{MM}) associated with the conformational change necessary for chelation. The models obtained for the free ligand **150a** (Structure **I**), its silver(I) complex (Structure **II**) and the corresponding "chelating conformation" (Structure **III**) are illustrated in **Figure 14**. The ΔE_{MM} values obtained were relatively small (-12 to 78 kcal.mol^{-1}) and, while the application of Molecular Mechanics to metal centres may be problematic,[87] it appears that each of the ligands examined is, in fact, capable of adopting a conformation that should permit tetrahedral coordination of silver(I).

A detailed discussion of the application of Molecular Mechanics and other computational methods to the modelling of these and other complexes will be deferred to Section **2.3** (p. 92), while the complexation and solvent extraction abilities of the ligands will be discussed in Sections **2.4** (p. 103) and **2.5** (p. 112), respectively.

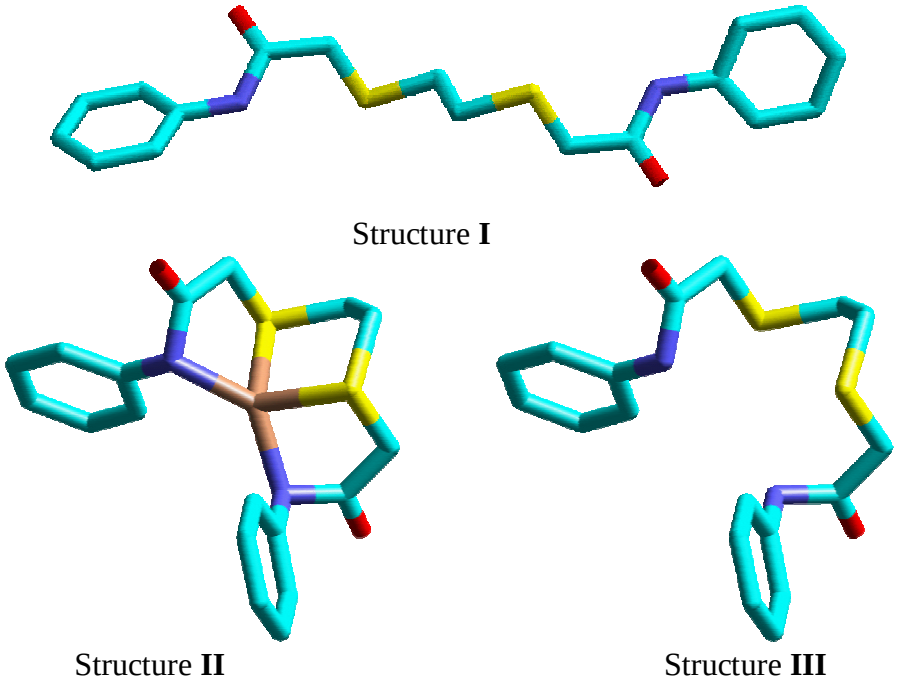

Structure **I**

Structure **II** Structure **III**

Figure 14. Computer models of: - **I**: the 3,6-dithiaoctanediamide **150a**; **II**: its silver(I) complex; and **III**: the "chelating conformation". The hydrogen atoms have been omitted for clarity and the elements colour-coded as follows:- carbon (cyan); oxygen (red); nitrogen (blue); sulfur (yellow); and silver (brown).

2.1.2 Applications of the Morita-Baylis-Hillman reaction in the construction of pyridine-containing ligands

Research conducted previously in our group by Bode[88] and George[89] involved the synthesis of indolizines **152** *via* the cyclisation of Morita-Baylis-Hillman (MBH) products **153,** obtained, in turn, by reacting pyridine-2-carbaldehyde with various vinyl derivatives in the presence of 1,4-diazabicyclo[2.2.2]octane (DABCO) (**Scheme 4**). Deane[90] and Whittaker[91] subsequently explored the conjugate addition of various nucleophiles to MBH products, obtaining compounds of type **154**.

Scheme 4. Cyclization and conjugate addition reaction of Morita-Baylis-Hillman products.

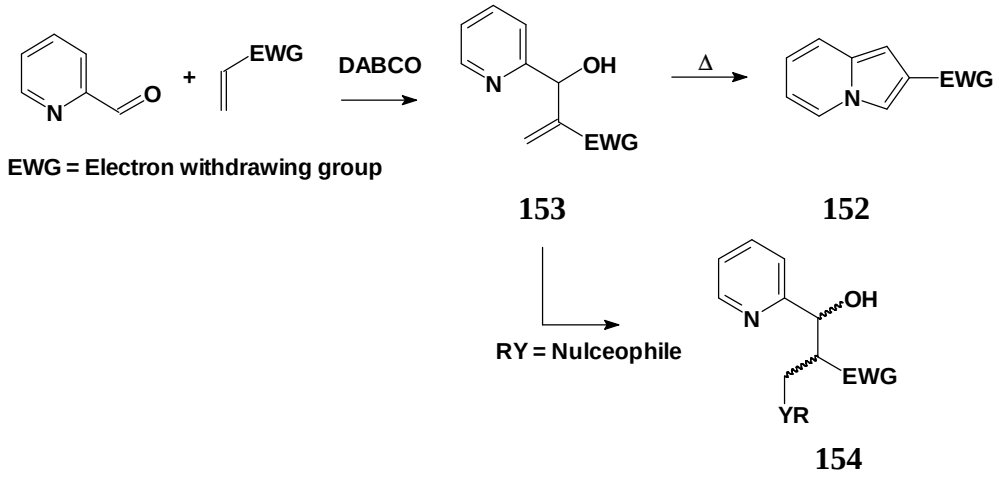

The latter compounds bear some resemblance to the pyridine system targeted as a template for silver-specific ligands (**Figure 9,** p. 35), and the structural correlations are evident in **Figure 15**; these include: - i) a pyridyl nitrogen as one of the donor atoms; ii) a second donor atom **Y**; iii) an alkyl spacer; and iv) a terminal group **R**, which can be varied to fine-tune selectivity.

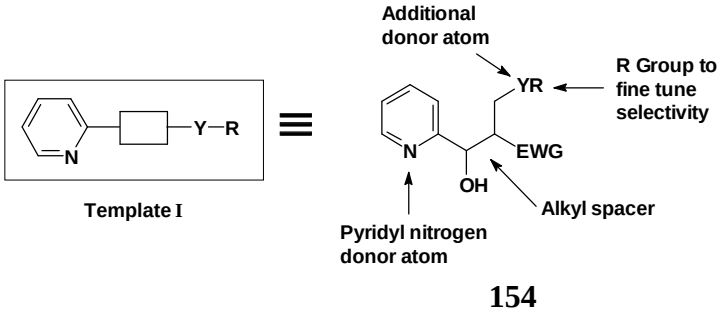

Figure 15. Structural correlations between template **I** and the conjugate addition products **154**.

The Morita-Baylis-Hillman reaction was thus identified as a potentially useful method for generating α-substituted pyridine derivatives as silver(I) ligands. Using pyridine-2-carbaldehyde **155** and pyridine-2,6-dicarbaldehyde **156** as substrates, various "single-" and "twin-chain" ligands (**Figure 16**) were envisaged as synthetic targets. Conjugate addition of selected nucleophiles to the MBH products was expected to permit the introduction of the additional donor atom(s) (Y = N, O, S) in each case.

(a) "Single-chain" ligands

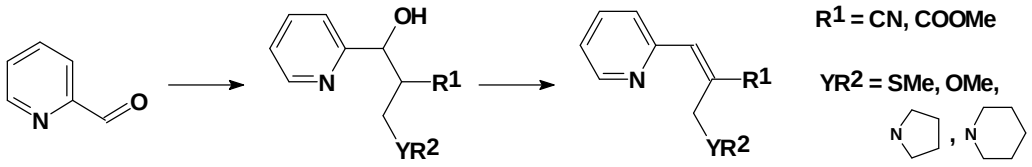

155

(b) "Twin-chain" ligands

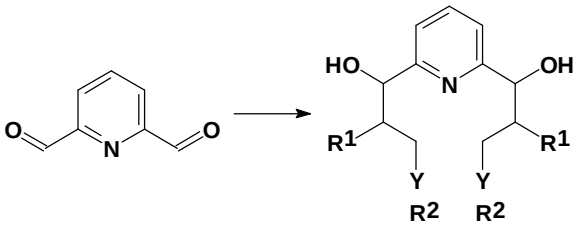

156

Figure 16. Proposed access to MBH-derived ligands: a) "single-chain" and b) "twin-chain" systems.

While metal chelation involving the pyridyl and '**Y**' donors would afford 7-membered rings, other combinations of donor atoms could afford 5- and 6-membered rings - as illustrated in **Figure 17**.

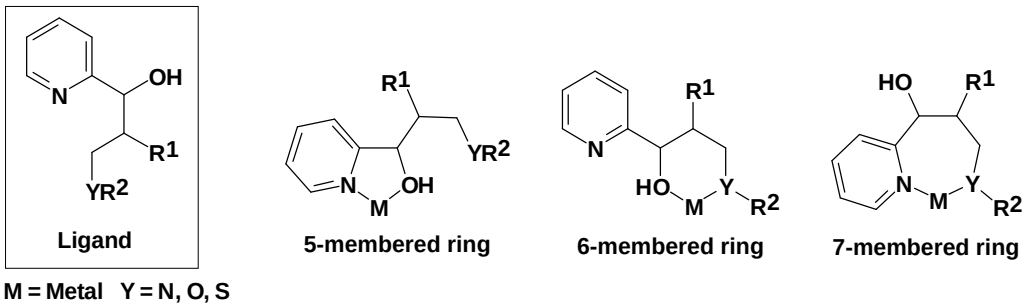

Figure 17. Chelation possibilities for ligands of type **154**.

In order to investigate the relative stability of such chelate rings, computer modelling was performed on the ligand **157**. The computer models generated for the free ligand, the 5-, 6- and 7-membered chelates and the corresponding chelating conformation adopted by each ligand are illustrated in **Figure 18**. Comparison of the steric energies of the free ligand (in its most favoured conformation) and the chelating conformations should permit qualitative prediction of the preferred ring size for the silver(I) complexes of ligands of the type **154**.

From the modelling data it seems that formation of a 6-membered chelate is least likely, the steric energy cost for the ligand to adopt the necessary chelating conformation being the greatest (ΔE_{MM} = 12.5 kcal.mol^{-1})‡. The steric energy costs for the formation of the 5- and 7-memebered rings, are significantly lower (ΔE_{MM} = 6.75 and 1.61 kcal.mol^{-1}, respectively). It is also, perhaps, significant, that, in the 7-membered chelate, the silver(I) atom adopts the favoured tetrahedral geometry. Some examples of silver(I) complexes involving various ring sizes have been reported and are illustrated in **Figure 19**.[52,92]

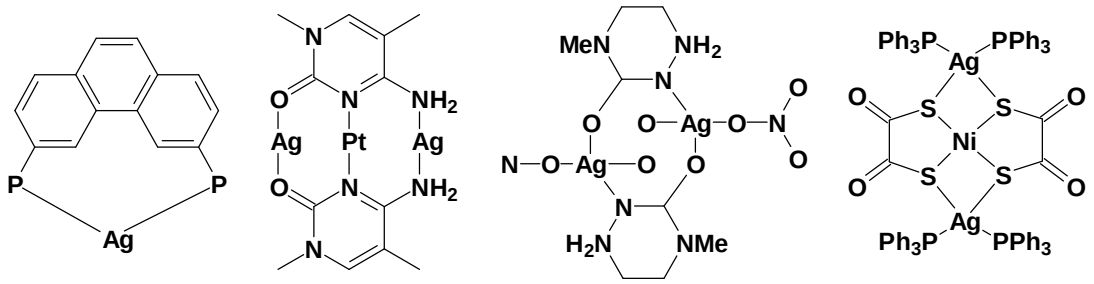

Figure 19. Examples of different Ag(I) chelate sizes.[52,92]

The generally accepted mechanism for the DABCO-catalyzed Morita-Baylis-Hillman reaction of an acrylic ester and an aldehyde is outlined in **Scheme 5**. The first, reversible step of the reaction is considered to involve nucleophilic attack of DABCO **158** on the acrylic ester **159** to form the zwitterionic intermediate **160**. This intermediate then attacks the aldehyde **161** to form a second zwitterion **162**, which has been proposed to undergo protonation and base-assisted *anti* E2 elimination of the catalyst to give the MBH product **163**.[93]

‡ ΔE_{MMf} represents the difference in steric energy between the lowest energy conformation of the ligand and the given chelating conformation.

(a)

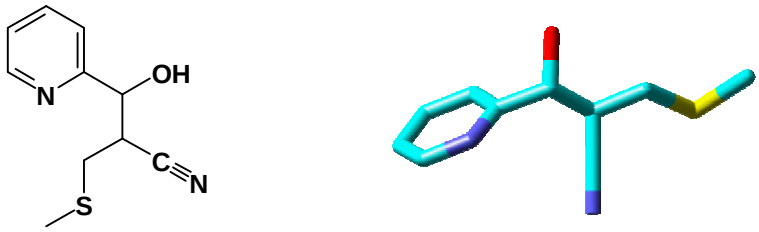

157

(b)

(c)

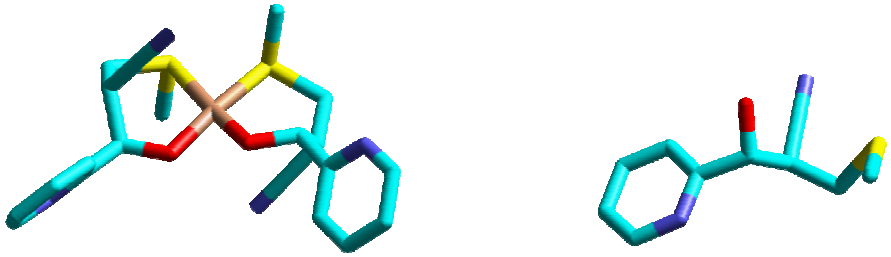

(d)

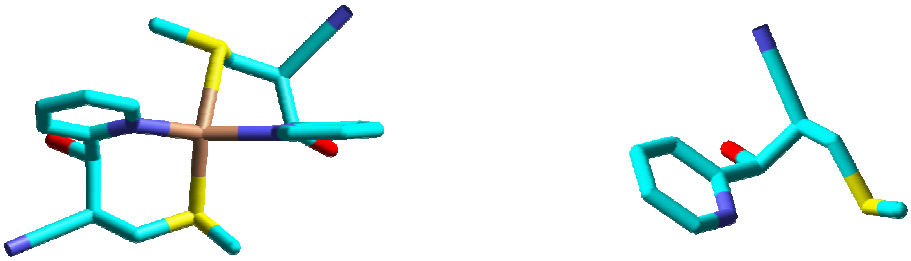

Figure 18. Computer-generated models for: - (a) the lowest energy conformation of ligand **157**; (b) the 5-membered ring complex and the corresponding chelating conformation of the ligand; (c) the 6-membered ring complex and the corresponding chelating conformation of the ligand; and (d) the 7-membered ring complex and the corresponding chelating conformation of the ligand. See **Figure 14** for the colour coding.

Recent computational studies, however, suggest that the elimination proceeds *via* the resonance-stabilized enolate intermediate **164**, *i.e. via* an E1cB mechanism.[94]

Scheme 5. Mechanism of Morita-Baylis-Hillman reaction.

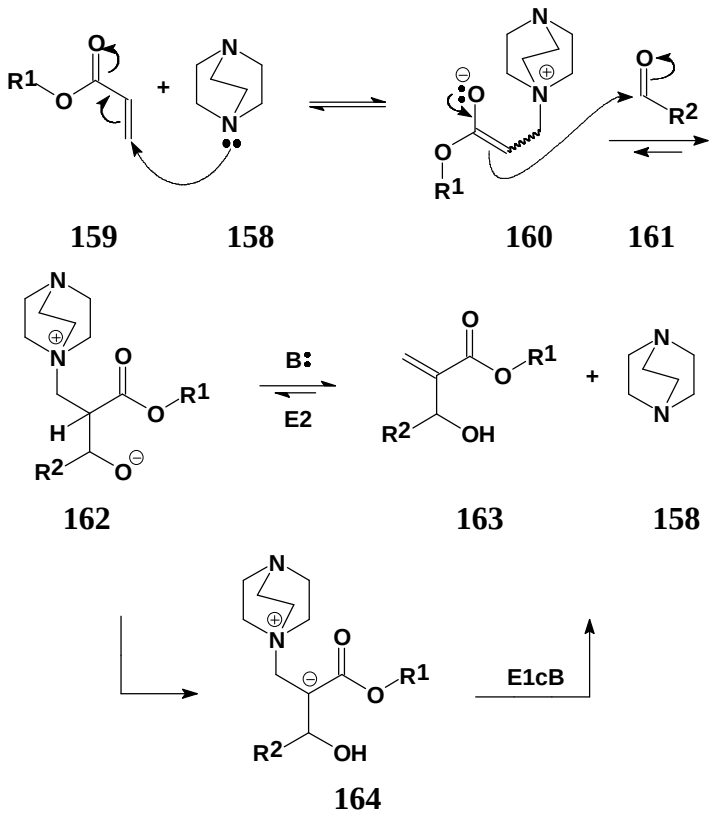

The Morita-Baylis-Hillman reaction was performed using pyridine-2-carbaldehyde **155** and, as the activated vinyl component, acrylonitrile **165a** or methyl acrylate **165b** (**Scheme 6**). The resulting MBH products, 2-[hydroxy(pyridin-2-yl)methyl]acrylonitrile **166a** and methyl 2-[hydroxy(pyridin-2-yl)methyl]acrylate **166b** were obtained in good yield (**Table 2**) and characterized by NMR spectroscopy. The ^{1}H and ^{13}C NMR spectra for methyl 2-[hydroxy(pyridin-2-yl)methyl]acrylate **166b** are shown in **Figures 20** and **21**. The ester methyl protons resonate at 3.61 ppm, while the corresponding methyl carbon signal appears at 51.5 ppm in the ^{13}C NMR spectrum. The changes in the vinylic region (δ_H 5-7 ppm) are particularly diagnostic of the transformation of the acrylate ester to the MBH product [see inset (b) in **Figure 20**], the apparent absence of coupling between the geminal vinyl protons being typical of MBH products.

Scheme 6. Application of the Morita-Baylis-Hillman reaction.

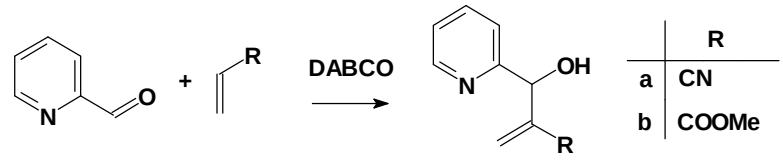

155 **165a,b** **166a,b**

Acetylation of the MBH products **166a** and **166b**, with acetic anhydride, as illustrated in **Scheme 7**, afforded 2-[acetoxy(pyridin-2-yl)methyl]acrylonitrile **167a** and methyl 2-[acetoxy(pyridin-2-yl)methyl]acrylate **167b**, respectively, in moderate yields (**Table 2**). The ^{1}H NMR spectrum of the ester **167b** (**Figure 22**) clearly reveals the disappearance of the hydroxyl signal at *ca.* 5.6 ppm, the presence of the acetyl methyl signal at 2.10 ppm and a down-field shift in the methine proton signal from 5.0 to 6.70 ppm.

Scheme 7. Acetylation of the Morita-Baylis-Hillman products.

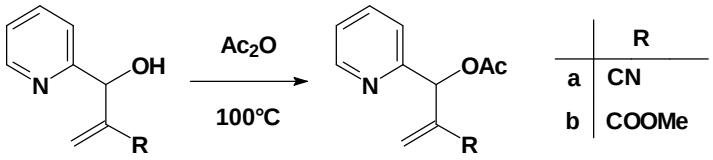

166a,b **167a,b**

Table 2. Yields of the MBH products **166** and their acetylated derivatives **167**.

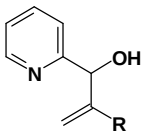

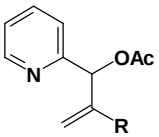

	MBH products		Acetylated derivatives	
R	Compound	Yield [a] / %	Compound	Yield [a] / %
CN	**166a**	88	**167a**	51
COOMe	**166b**	93	**167b**	46

[a] Based on pure product obtained following flash chromatography.

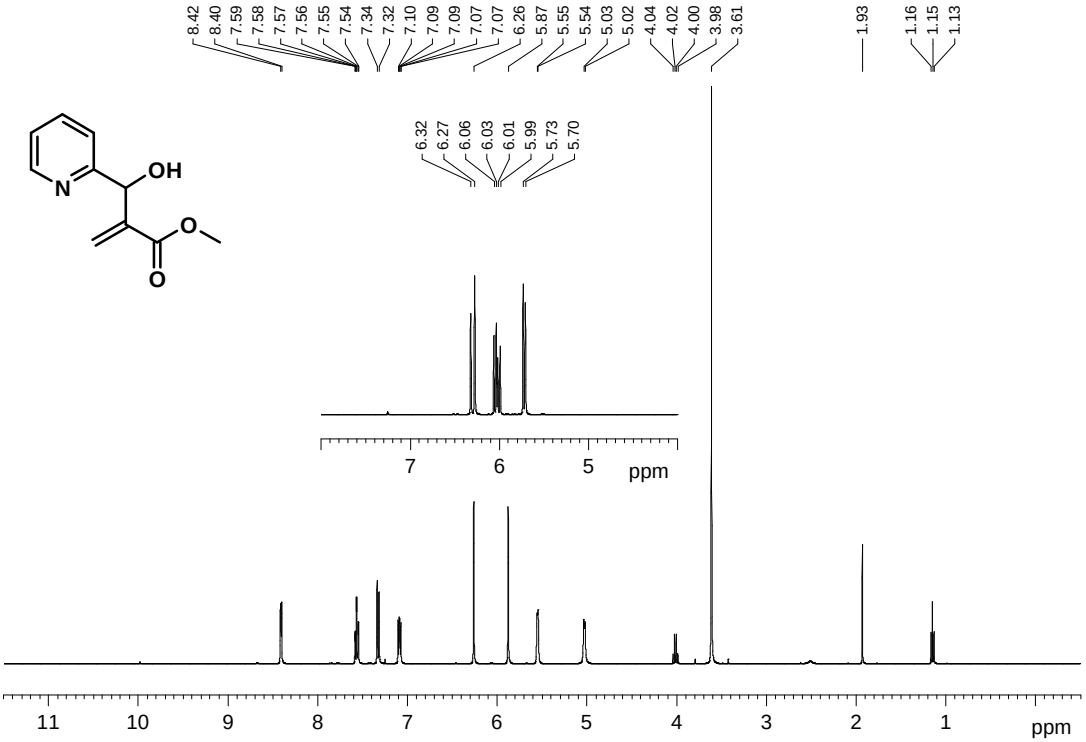

Figure 20. 400 MHz ^{1}H NMR spectrum in $CDCl_3$ of a) the ester **166b** and b) methyl acrylate (partial spectrum).

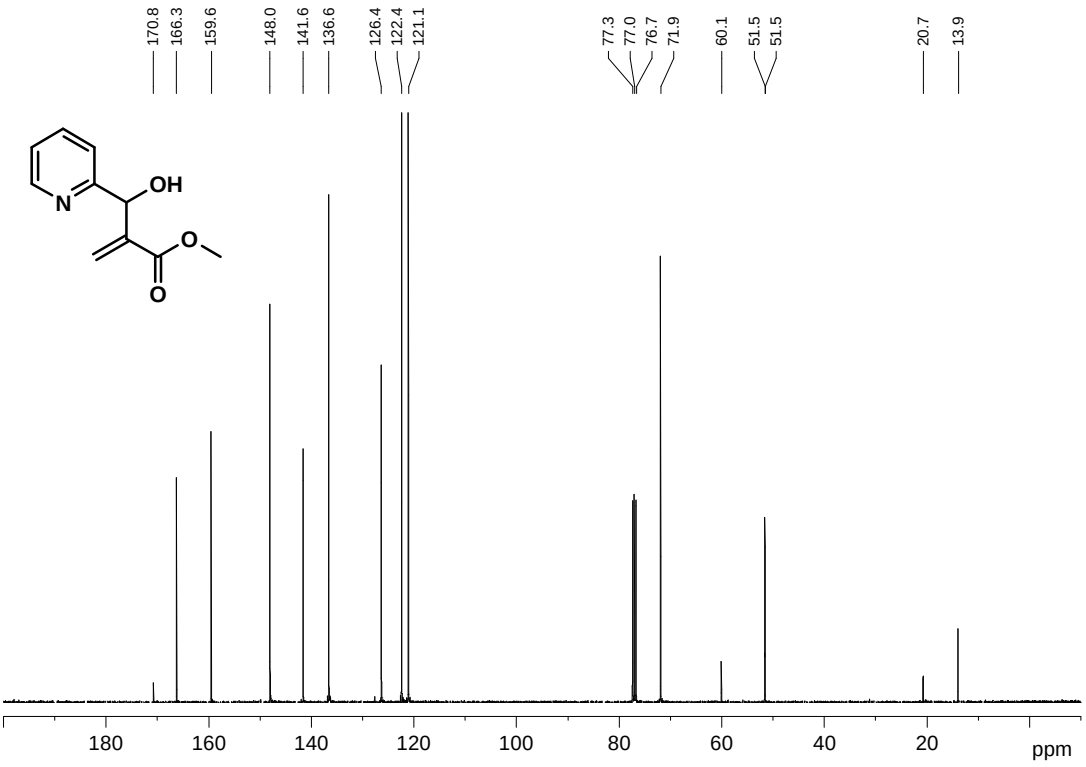

Figure 21. 100 MHz ^{13}C NMR spectrum of the ester **166b** in $CDCl_3$.

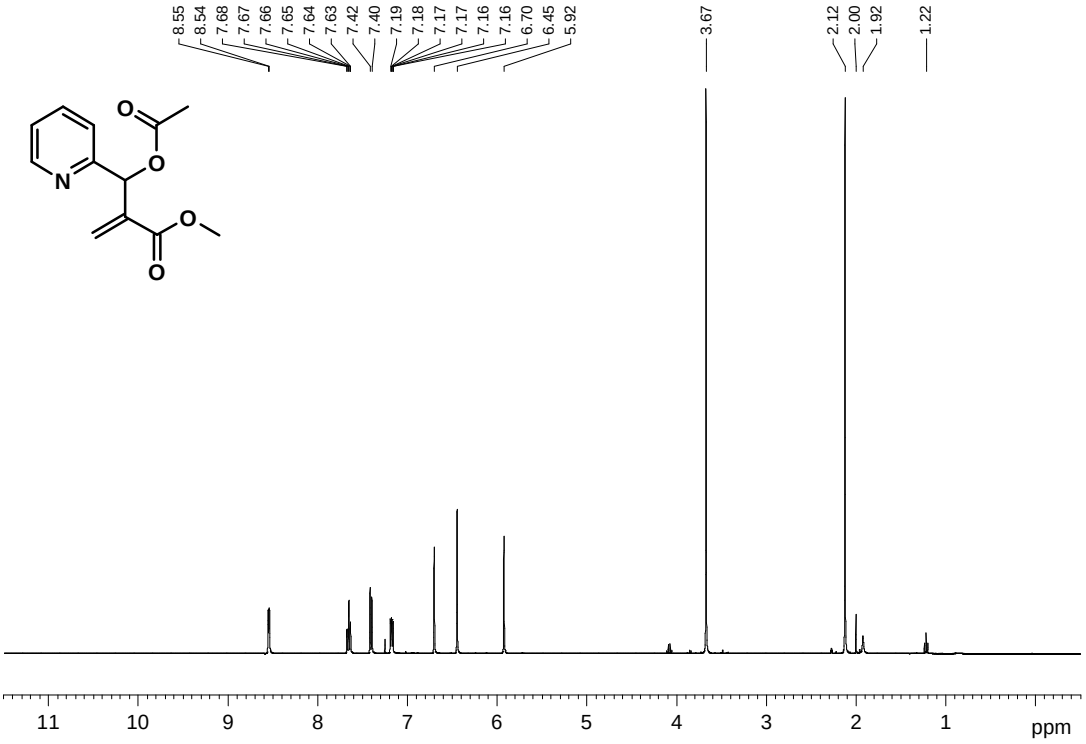

Figure 22. 400 MHz ^{1}H NMR spectrum of the acetylated ester **167b** in $CDCl_3$.

The first series of ligands, based on the MBH products, were obtained by conjugate addition of various nucleophiles (**Scheme 8**) to the MBH products **166a** and **166b**. The resulting propanenitriles **168a-d** and methyl propanonate derivatives **168e-h** were isolated in widely-ranging yields (5-90 %; **Table 3**). Under the conditions used, it is apparent that the nitrile **166a** underwent more efficient transformation; at this exploratory stage, yield optimization was not addressed.

Scheme 8. Formation of the conjugate addition products.

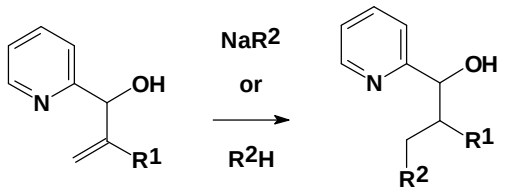

	R^1	R^2
a	CN	SMe
b	CN	OMe
c	CN	
d	CN	
e	COOMe	SMe
f	COOMe	OMe
g	COOMe	
h	COOMe	

166a,b **168a-h**

Table 3. Yields of the conjugate addition products **168**.

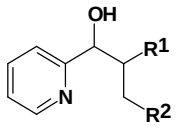

Compound	$\mathbf{R^1}$	$\mathbf{R^2}$	Yield [a] / %
168a	CN	SMe	80
168b	CN	OMe	90
168c	CN	1-Pyrrolidinyl	22
168d	CN	1-Piperidinyl	86
168e	COOMe	SMe	52
168f	COOMe	OMe	28
168g	COOMe	1-Pyrrolidinyl	6
168h	COOMe	1-Piperidinyl	8

[a] Based on pure product obtained following flash chromatography.

From the ^{1}H and ^{13}C NMR spectra of the nitrile **168c** (**Figures 23** and **24**, respectively), it can been seen that many of the signals are doubled due to the formation of diastereomers during the addition reaction. Based on the ^{1}H NMR spectrum of the nitrile **168c**, the calculated diastereomeric ratio is 2:1 [from a comparison of the integrals for each of the doubled signals in the aromatic region (7-9 ppm)]. To determine which diastereomer was favoured, the substrate **166a** was subjected to computer modelling. As indicated in **Figure 25(a)** the nucleophile can attack from either face of the alkene moiety, and the computer-generated model of the lowest energy conformer [**Figure 25(b**)] suggests that the "outer" face would be more open and thus favoured for nucleophilic attack.

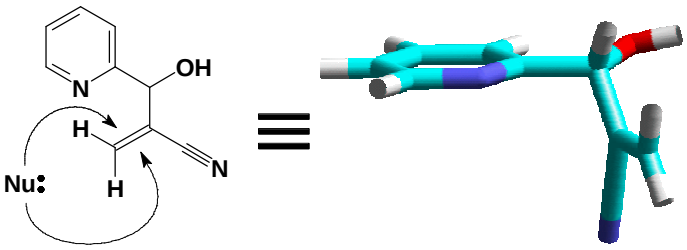

(a) **(b)**

Figure 25. Illustration of (a) nucleophilic attack on both faces of the nitrile **166a** and (b) the favoured conformation of the nitrile **166a**.

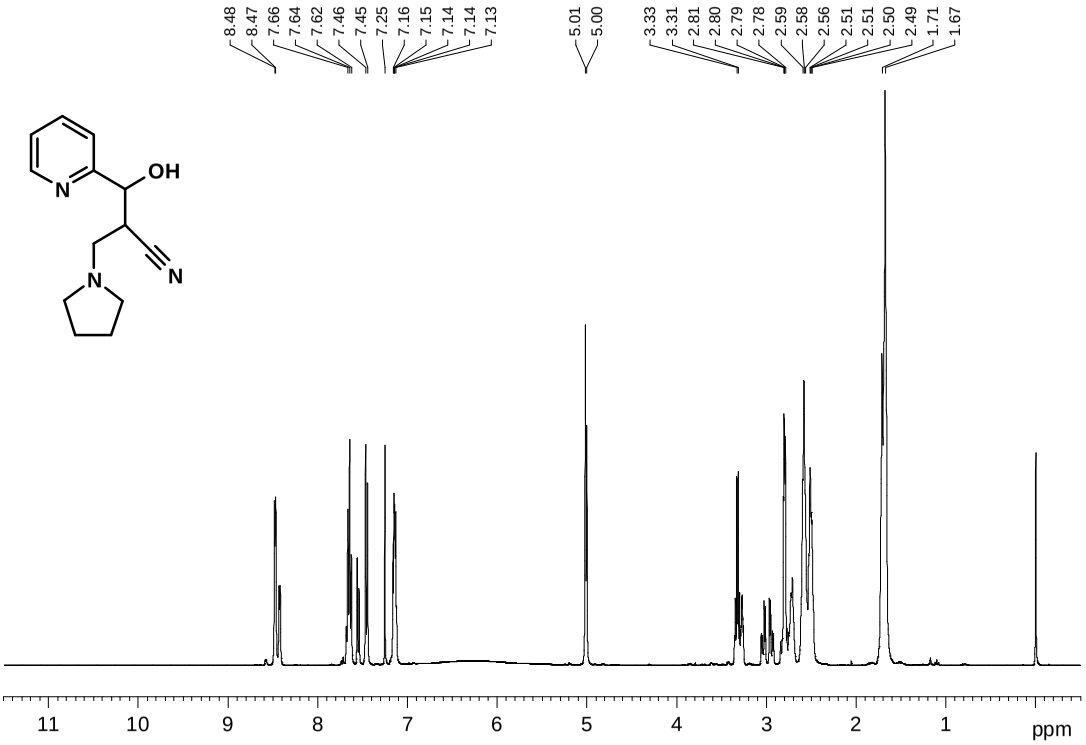

Figure 23. 400 MHz ^{1}H NMR spectrum of the nitrile **168c** in $CDCl_3$.

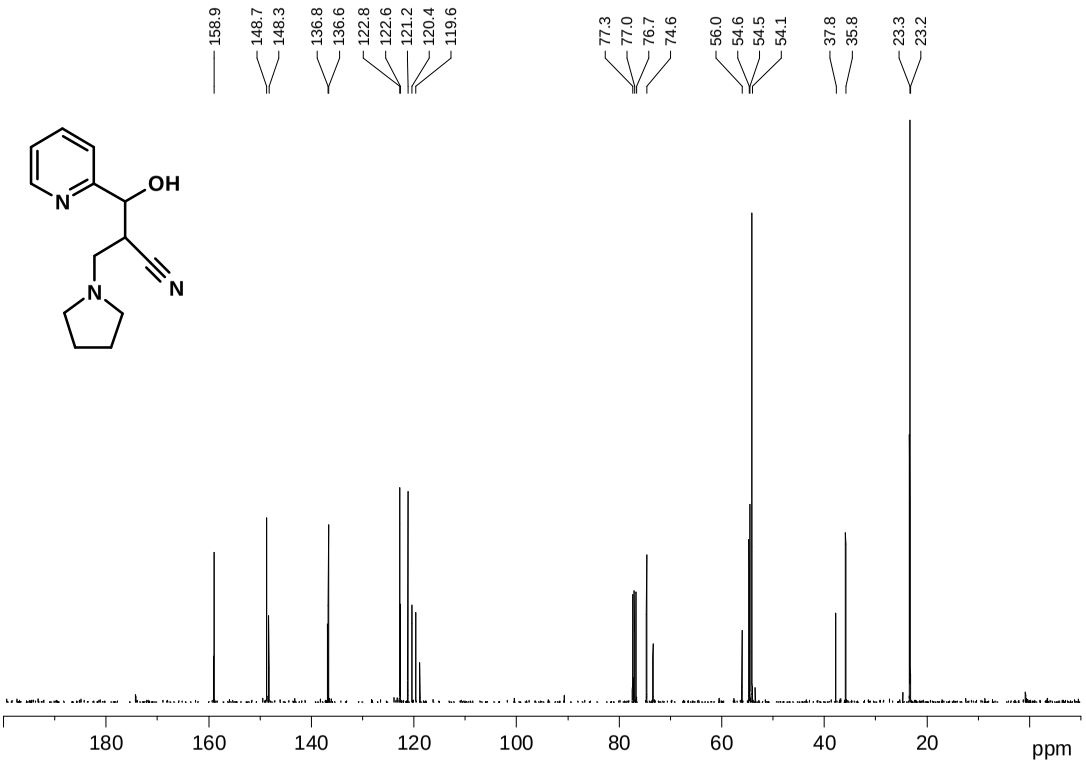

Figure 24. 100 MHz ^{13}C NMR spectrum of the nitrile **168c** in $CDCl_3$.

However, the new chiral centre is only generated on tautomerisation of the intermediate adduct **169** (**Scheme 9**), and the computer-modelled conformations of the intermediate **169** and the diastereomeric products **170** and **171** were inspected in an attempt to determine the relative configuration at the new chiral centre in the major diastereomer. While the relative access to the two faces of the intermediate **169** **[Figure 26(a)]** is not easy to assess by inspection, the steric energy of the *R*,*R*-product **170** **[Figure 26(b)]** is *ca.* 1 kcal/mol less than that of the diastereomeric *R*,*S*-product **171** **[Figure 26(c)]**. The operation of "product development control"[95] should then favour the *R*,*R*-product (and, of course, its *S*,*S*-enantiomer).

Scheme 9. Generation of the new chiral centre in the MBH-derived ligand **166a**.

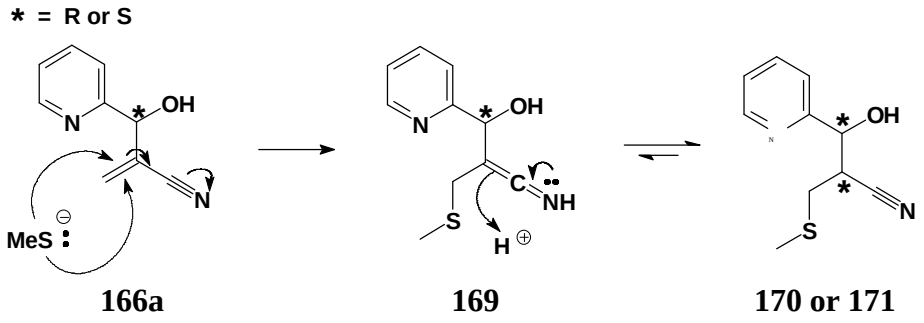

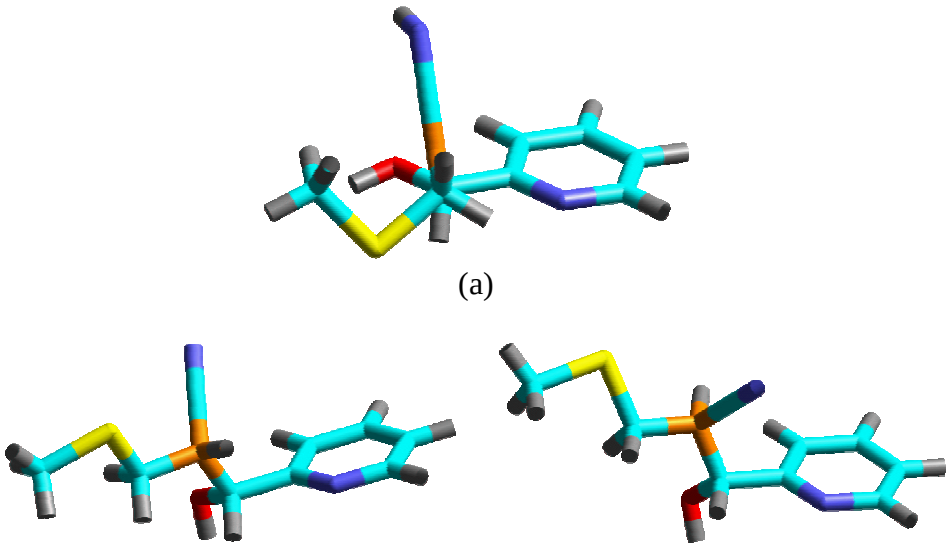

(a) (b) (c)

Figure 26. Computer-modelled structures of:- (a) the intermediate **169** formed during the nucleophilic attack on the *R*-substrate; (b) the *R*,*R* product **170**; and (c) the *R*,*S* product **171**. The carbon centre of interest is coloured orange. The hydrogen atoms are coloured gray, for the others see **Figure 14** for the colour coding.

The formation of the conjugate addition product is characterized, in each case, by an up-field shift of the hydroxyl signal from *ca.* 5.2 ppm to *ca*. 5.0 ppm and, more importantly, by the replacement of the methylene proton signals at *ca.* 6.0 ppm by a multiplet at *ca.* 2.8 ppm (*cf.* **Figure 20**).

In an attempt to obtain an additional set of potential ligands, reaction of the acetylated MBH products **167** with the same nucleophiles was examined (**Scheme 10**). These transformations, however, proved to be largely unsuccessful with side reactions leading to intractable mixtures in several cases. In fact, only the thiomethylated products **172a** and **172e** could be isolated (**Table 4**).

Scheme 10. Reaction of the acetylated MBH product.

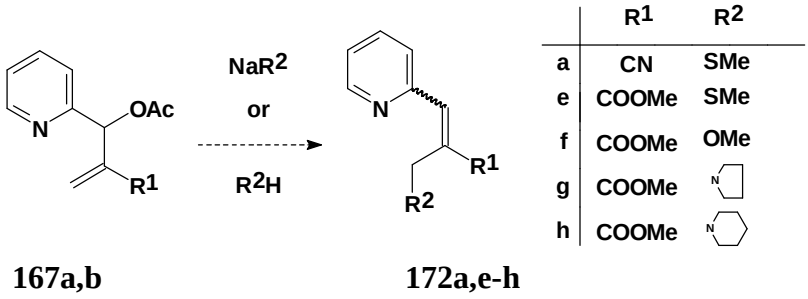

167a,b **172a,e-h**

Table 4. Yields for the reaction of the acetylated MBH products with various nucleophiles.

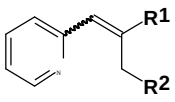

Compound	R^1	R^2	Yield [a] / %
172a	CN	SMe	49
172e	COOMe	SMe	93
172f	COOMe	OMe	-[b]
172g	COOMe	1-Pyrrolidinyl	-[b]
172h	COOMe	1-Piperidinyl	-[b]

[a] Based on pure product obtained following flash chromatography. [b] An intractable mixture was obtained.

Due to the formation of complex mixtures when the ester **167b** was treated with sodium methoxide, pyrrolidine or piperidine, no attempt was made to react these

nucleophiles with the nitrile **167b**. Although the mechanism of these transformations may well involve S_N' displacement of the acetate moiety, the possibility of a nucleophilic addition-elimination sequence cannot be excluded (as illustrated for the acrylonitrile substrate **167a**; **Scheme 11**).

Scheme 11. (a) S_N' displacement and (b) conjugate addition-elimination mechanisms for the reaction of acrylonitrile substrate **167a** with MeS^-.

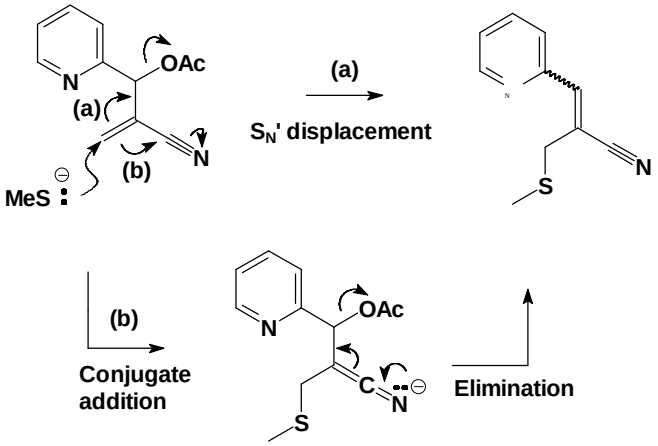

With the inefficiencies observed in some of the above reactions and, more significantly, the tendency of the products to degrade over time, it was decided not to investigate the formation of the envisaged "twin-chain" analogues derived from pyridine-2,6-dicarbaldehyde. The complexation properties of the ligands, which were prepared, will be discussed in Section **2.4** (p. 103).

2.1.3 Malonyl Derivatives as Silver(I) Ligands

A number of malonyl derivatives have found use as extraction agents for other metals. The *N,N′*-disubstituted malonamides **173** and **174**, for example, exhibit potential as lanthanide and actinide extractants.[96] Malonyl derivatives, with structures that clearly resemble template **II** (**Figure 27**) were considered as possible silver(I) ligands.

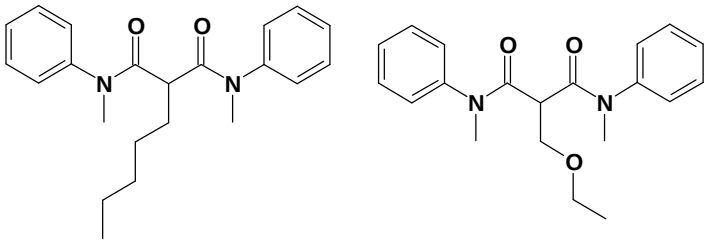

173 **174**

The presence of two acyl moieties and an active methylene group make simple malonyl derivatives ideal substrates for the introduction of the structural features considered necessary for silver(I) chelation, *viz.*, i) the appropriate donor atoms (Y and Z = NH, O or S); ii) a selection of spacer groups (alkyl or aromatic); and iii) the ability to fine tune selectivity and lipophilicity by varying the substituents **R'** and **R"**.

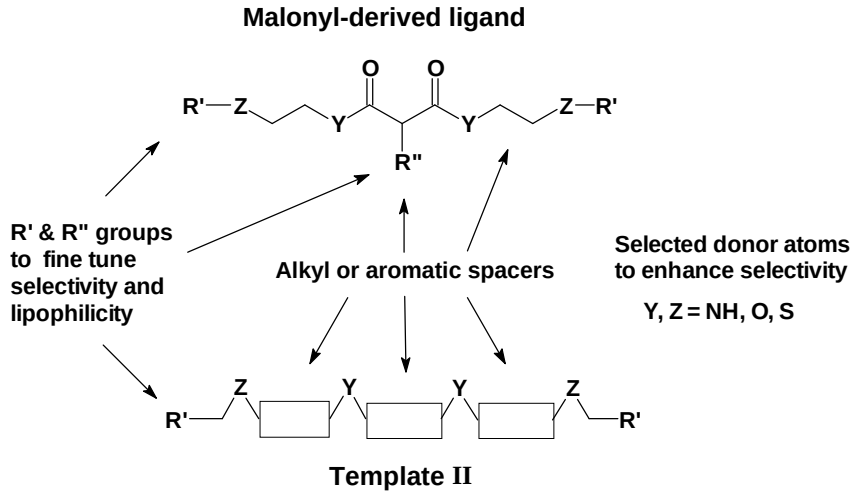

Figure 27. The malonyl system and its relationship to template **II**.

Diethyl malonate **175** and malonyl dichloride **176** were identified as substrates for the synthesis of several series of malonyl-derived ligands. The targeted tetradentate, acyclic and cyclic systems, illustrated in **Figure 28**, were expected to permit formation of 5-6-5- or 6-5-5-5-membered silver(I) chelates, respectively, and variation of the donor atoms (Y and Z = NH, O or S), the substituents (R^1, R^2) and the carbonyl moieties (C=O, C=S). The ester groups of diethyl malonate are susceptible to acyl substitution, while the introduction of alkyl groups at the methylene carbon can be effected by treating the enolate with an alkyl halide, thus providing ready access to a variety of substituted derivatives. Further variation may be achieved by functional elaboration of the carbonyl groups. Malonyl dichloride **176** is a very reactive acid halide, and could also be used as an activated substrate for the construction of the desired ligand systems.

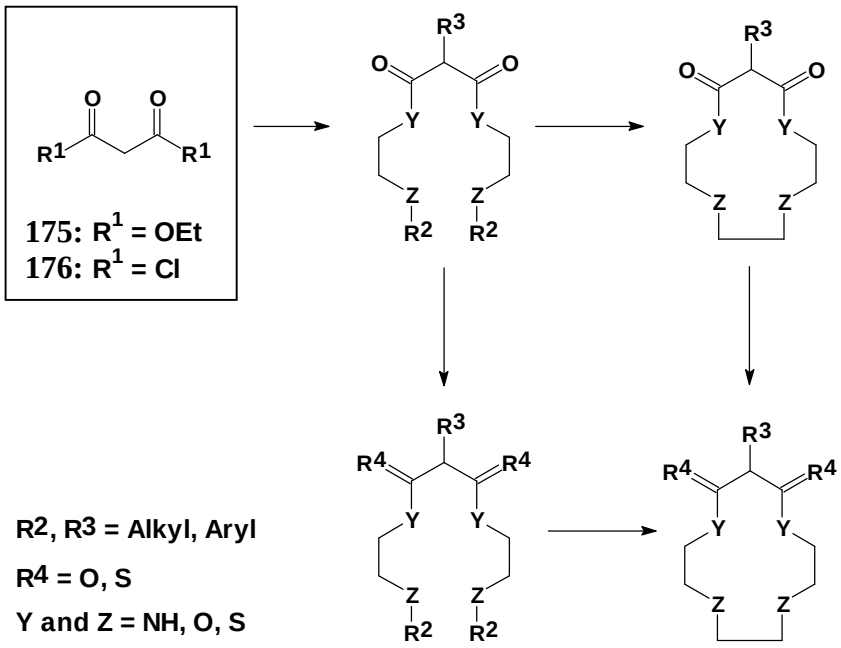

Figure 28. Malonyl-derived synthetic targets

2.1.3.1 *Substituted malonic esters*

In order to explore the relative solubility of the malonyl systems in aqueous and organic phases, a range of substituted malonic esters **177a-j** were prepared from diethyl malonate **175** (**Scheme 12**). The sodiomalonic ester enolate, prepared using sodium ethoxide, was reacted with various alkyl halides to afford the substituted products **177a-j**, typically, in good yield (**Table 5**). These compounds, which were to form the "backbone pool" for the synthesis of the ligand systems discussed in subsequent sections, were characterized by NMR, IR and MS analysis.

Scheme 12. Synthesis of substituted malonates **177a-j**.

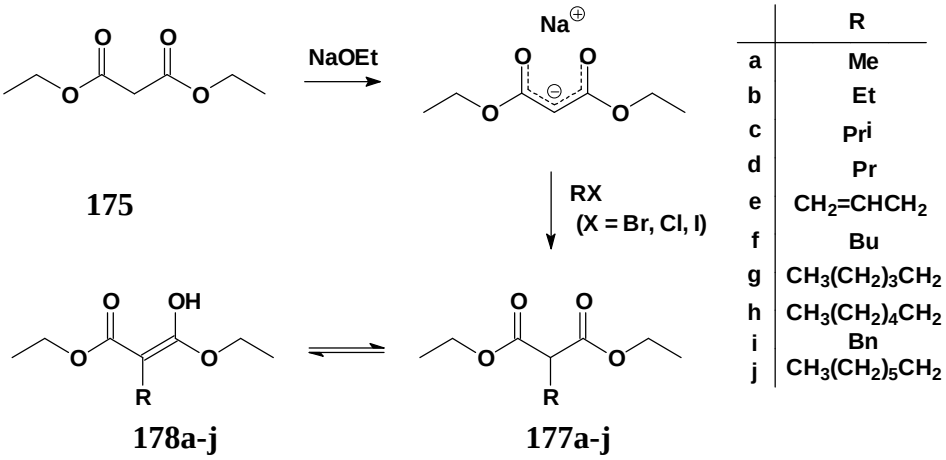

The keto-enol tautomerism, illustrated in **Scheme 12** (**177a-j** ⇌ **178a-j**), was evident in both the ^{1}H and ^{13}C NMR spectra of all the substituted malonic esters. In the ^{1}H NMR spectrum of diethyl ethylmalonate **177b** (**Figure 29**), for example, the methine proton of the keto form gives rise to a triplet at 3.36 ppm, while the corresponding hydroxy signal of the enol appears as a singlet at 3.45 ppm. The keto-enol tautomerism is also evidenced by the occurrence of two triplet signals, at 0.88 and 0.74 ppm, due to the methyl group of the ethyl chain being in different chemical environments in the keto and enol forms. In the ^{13}C NMR spectrum (**Figure 30**), the dominant signals are attributed to the keto tautomer, and the smaller signals to the enol tautomer.

Table 5. Yields for the substituted malonic esters **177a-f**.

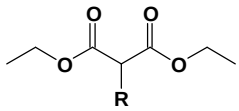

	Alkyl halide precusor	Substituted malonic ester		
		R	Yield [a] / %	bp [b] / °C
177a	methyl iodide	Me	65	104-107
177b	ethyl iodide	Et	70	105-107
177c	isopropyl iodide	Pr^i	83	110-113
177d	propyl iodide	Pr	72	112-115
177e	3-bromopropene	CH_2=$CHCH_2$	64	169-171
177f	butyl iodide	Bu	82	128-132
177g	pentyl iodide	$CH_3(CH_2)_3CH_2$	74	121-126
177h	hexyl iodide	$CH_3(CH_2)_4CH_2$	79	149-153
177i	benzyl chloride	Bn	47	178-181
177j	heptyl iodide	$CH_3(CH_2)_5CH_2$	77	161-165

[a] Based on pure product obtained following distillation. [b] At *ca.* 20 mm Hg; determined during distillation.

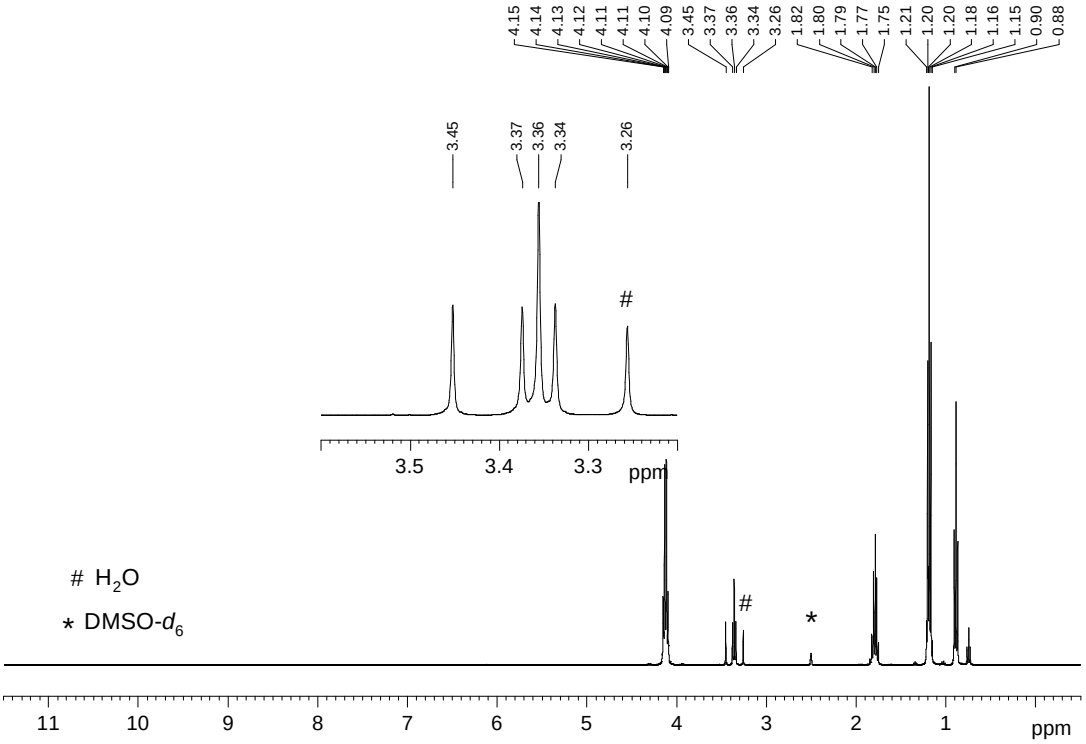

Figure 29. 400 MHz ^{1}H NMR spectrum of the substituted malonic ester **177b** in DMSO-d_6.

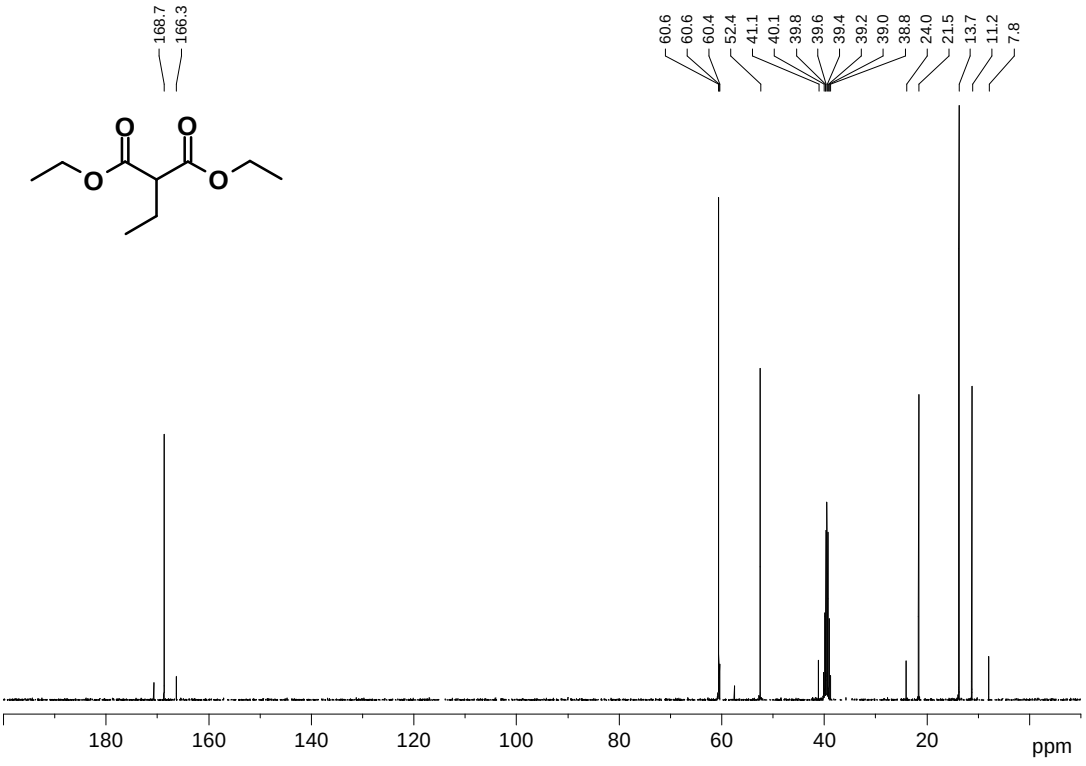

Figure 30. 100 MHz ^{13}C NMR spectrum of the substituted malonic ester **177b** in DMSO-d_6.

2.1.3.2 N,N′-*Bis(2-hydroxyethyl)malonamides*

As mentioned previously, malonamides have found use in solvent extraction systems,[96] mainly as *N*-alkylated derivatives. We proposed to lengthen the alkyl groups attached to the amide nitrogens and introduce additional donor atoms into these "side chains". To generate the malonamide precursors, the *C*-alkylated malonic esters (**175** and **177a-j**) obtained previously were reacted with excess ethanolamine **179** in the absence of added solvent (**Scheme 13)**, to afford the *N,N'*-bis(2-hydroxyethyl)malonamides **180a-d,f-k,** in varying yields (18-95 %) and reaction times (2-168 h) (**Table 6**).

Scheme 13. Reaction of substituted malonic esters with ethanolamine.

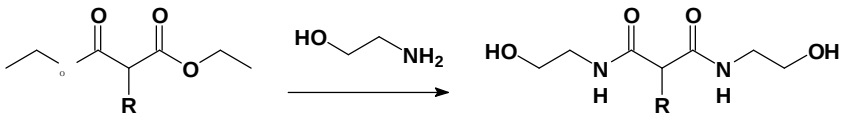

	R
a	Me
b	Et
c	Pr*i*
d	Pr
f	Bu
g	$CH_3(CH_2)_3CH_2$
h	$CH_3(CH_2)_4CH_2$
i	Bn
j	$CH_3(CH_2)_5CH_2$
k	H

175, 177a-d,f-j **179** **180a-d,f-k**

The products, which were all crystalline solids, were characterized by ^{1}H and ^{13}C NMR, MS and IR spectroscopy and elemental analysis (high-resolution MS). Surprisingly, the ligands **180b**, **180d**, **180f** and **180k** were the only known compounds of the series, as identified from a literature search of Chemical Abstracts and Beilstein (1908-2000). The formation of the *N,N'*-bis(2-hydroxyethyl)malonamides is evident from their ^{1}H NMR spectra in: - the disappearance of the triplet at δ_H *ca.* 1.2 ppm and the quartet at *ca.* 4.1 ppm, corresponding to the ethyl group of the ethyl ester substrate; the appearance of triplets at *ca.* 4.7 and 8.0 ppm, assigned to the hydroxyl and amide hydrogens respectively; and the presence of two quartets at *ca.* 3.1 and 3.4 ppm, ascribed to the ethylene protons in the product. The ^{1}H NMR spectrum for *N,N'*-bis(2-hydroxyethyl)malonamide **180k** is illustrated in **Figure 31**.

Table 6. Yields of the *N*,*N*'-bis(2-hydroxyethyl)malonamides **180a-d,f-k**.

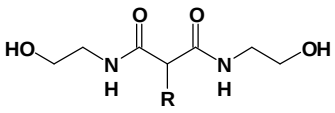

Compound	**R**	Yield [a] / %	Time / h	mp / °C
180a	Me	88	4	115-117
180b	Et	81	4	113-114
180c	Pr^i	35	24	120-122
180d	Pr	18	24	117-118
180f	Bu	89	48	123-125
180g	$CH_3(CH_2)_3CH_2$	45	168	124-126
180h	$CH_3(CH_2)_4CH_2$	43	168	108-109
180i	Bn	50	168	130-131
180j	$CH_3(CH_2)_5CH_2$	61	168	111-112
180k	H	95	2	125-126

[a] Based on pure product obtained following recrystalization.

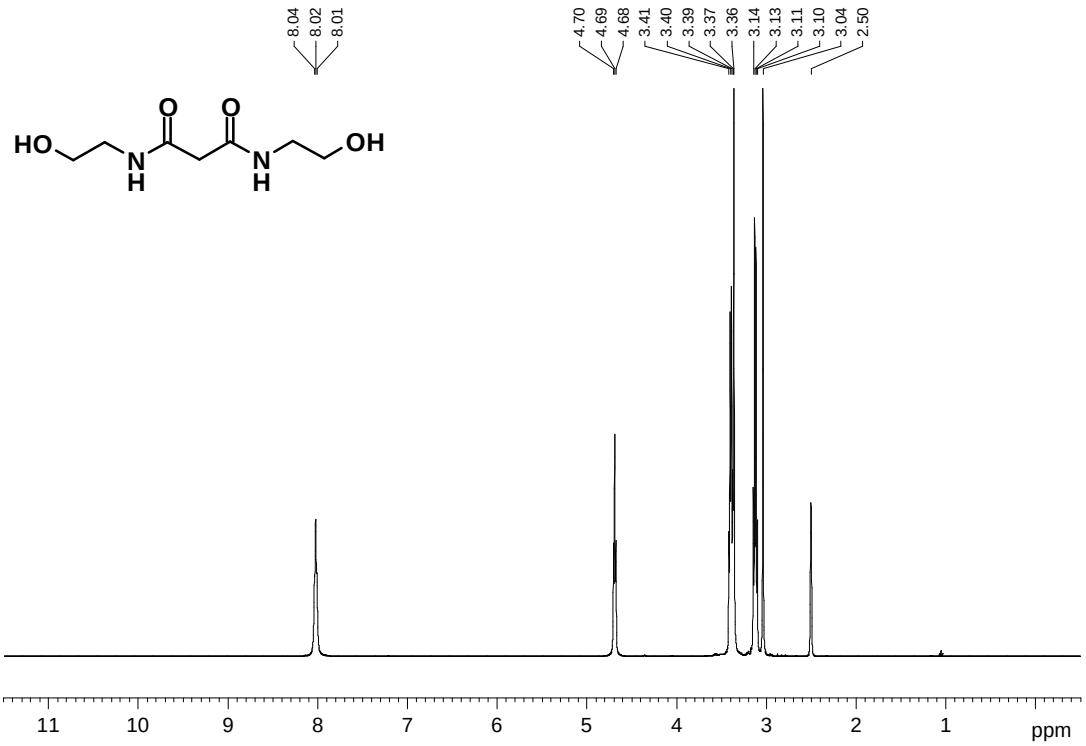

Figure 31. 400 MHz ^{1}H NMR spectrum of *N*,*N*'-bis(2-hydroxyethyl)malonamide **180k** in DMSO-d_6.

The keto-enol tautomerism observed in the NMR[†] spectra of the substituted malonic esters is not manifested in any of the spectra obtained for the *N*,*N*′-bis(2-hydroxyethyl)malonamides. To understand why this was the case the relative heats of formation (H_f) of representative examples of the substituted malonic esters and *N*,*N*′-bis(2-hydroxyethyl)malonamides were calculated using semi-empirical MO (AM1) methods. From these values, the Gibbs free energy ($\Delta G = \Delta H - T\Delta S$) were estimated, assuming the contribution of the entropy term to be negligible in the equilibrium between the enol and keto tautomers, *i.e.* $T\Delta S \approx 0$ and $\Delta G \approx \Delta H_f$.[‡] From the ΔG values, the equilibrium constants for the respective systems were estimated using the equation, $\Delta G = -RT \ln \boldsymbol{K}$. The ***K*** values thus obtained are listed in table **Table 7**.

Table 7. The equilibrium constants determined for keto-enol tautomerism in selected systems.

R	Compound	ΔH_f [a]	***K***	$\boldsymbol{K}_{obs}$ [b]
	Substituted Malonic Esters			
H	**175**	34.394	1.03×10^{-6}	-
Pr	**177d**	35.080	7.79×10^{-7}	0.428
$CH_3(CH_2)_5$	**177h**	35.186	7.47×10^{-7}	0.500
	N,*N*′-bis(2-hydroxyethyl)malonamides			
H	**180k**	76.136	5.53×10^{-14}	-
Pr	**180d**	70.898	4.52×10^{-13}	-
$CH_3(CH_2)_5$	**180h**	56.009	1.77×10^{-10}	-

[a] AM1 enthalpy differences for the equilibrium; keto form $\rightleftharpoons$ enol form in $kJ.mol^{-1}$. [b] Determined from the ratio of the integrals of the keto triplet and enol hydroxyl signals in the ^1H NMR spectra.[97]

As is evident from **Table 7**, the equilibrium constants for the substituted malonic esters examined are essentially of the same order of magnitude, while for the *N*,*N*′-bis(2-hydroxyethyl)malonamides the equilibrium constants vary significantly and are three to seven orders of magnitude lower than the values for the corresponding esters.

[†] keto-enol tautomerism is typically slow relative to the NMR time-scale.[98]
[‡] The assumption was based on the premise that, since the systems are chemically similar, the entropy would also be similar.

The significant difference between the calculated and observed equilibrium constants for the esters is attributed to the fact that the calculations assume isolated (gas phase) molecules, while the observed values are determined in solution. The effect of the solvent could explain the large differences, but the assumption that the entropy terms for the various systems are negligible could also play a role. However, the calculated data do indicate that: - i) the keto-enol tautomerism is more likely to be observed for the substituted malonic esters than for the *N,N'*-bis(2-hydroxyethyl)malonamides; and ii) since the equilibrium constants are very small, the keto tautomer should be dominant in the keto $\rightleftharpoons$ enol equilibrium.

The hydroxyl group is a poor-leaving group and, in order to facilitate nucleophilic displacement of oxygen by sulfur, an attempt was made to convert the "parent" bis(hydroxy)amide **180k** to the corresponding *p*-toluenesulfonate derivative **181** following the method reported by Kabalka *et al.*[99] (**Scheme 14)**. Treatment of the parent system **180k** with *p*-toluenesulfonyl chloride and pyridine afforded a complex mixture, shown by NMR spectroscopy to contain some of the desired product **181**. However, after purification by flash chromatography and recrystallisation, only 8 % of the *p*-toluenesulfonate derivative could be isolated. Repetition of the reaction failed to improve the yield and it was concluded that the tosyl group was being cleaved during purification, resulting in low yields. The tosylated malonamide **181** was reacted with 1,2-ethanedithiol in an attempt to obtain the cyclic ligand **182** (**Scheme 14)**, but without success. In an alternative approach to the replacement of oxygen by sulfur, *N,N'*-bis(2-hydroxyethyl)malonamide **180k** was treated with thiourea as the sulfur source, using the method of Kofod[100](**Scheme 14)**; unfortunately, only starting materials were isolated.

Scheme 14. Attempted replacement of hydroxyl groups by sulfanyl.

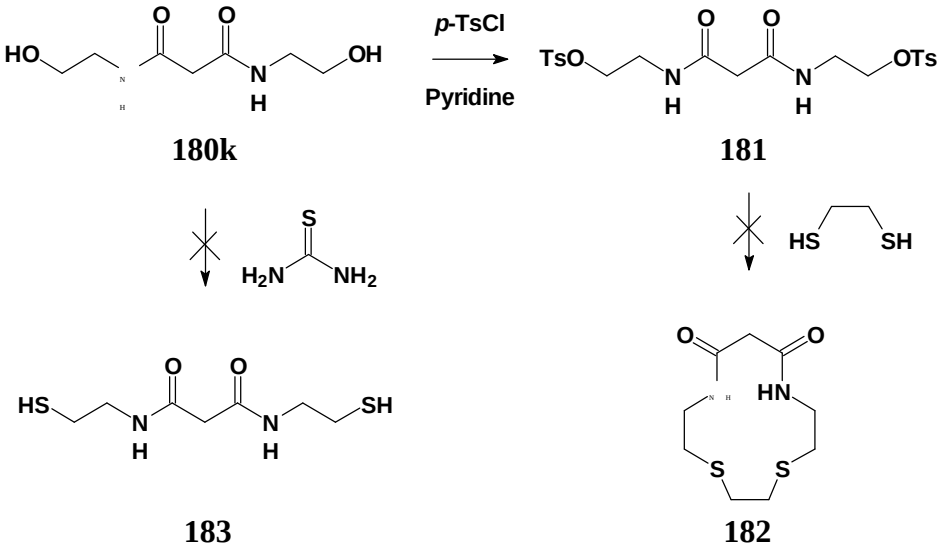

Attempts to access the cyclic ligands **184** and **185** by treating the *N*,*N*′-bis(2-hydroxyethyl)malonamide **180k** with 1,2-dibromoethane and 1,3-dibromopropane, respectively, were also unsuccessful (**Scheme 15**) and, consequently, alternative synthetic routes were explored; these are discussed in Section **2.1.3.4** (p. 65).

Scheme 15. Attempted ring-closure reactions.

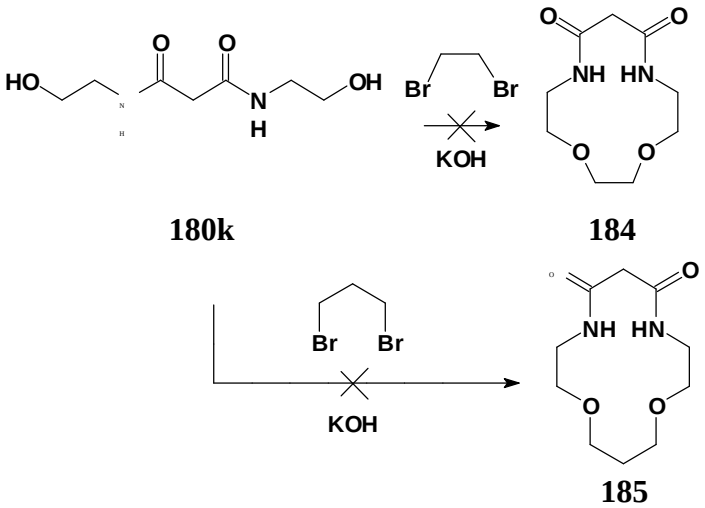

2.1.3.3 *Dithiomalonic esters*

Applying the same methodology used for the synthesis of the *N*,*N*′-bis(2-hydroxyethyl)malonamides **180a-k**, diethyl malonate was reacted with mercaptoethanol **186** in the presence of KOH, to yield the dithiomalonic ester **187**

(**Scheme 16**). The reaction proceeded with moderate yield (40 %), but the purification proved to be difficult and, in consideration of the criteria for synthesis outlined in **Section 2.1**, it was decided not to proceed further using this methodology. Attempts to generate the diamino dithiomalonic ester **188**, by reacting diethyl malonate **175** or malonyl dichloride **176** with 2-sulfanylethylamine hydrochloride under basic conditions, afforded complex mixtures and further investigation of this synthetic route was also discontinued.

Scheme 16. Synthesis of the dithiomalonic ester derivatives.

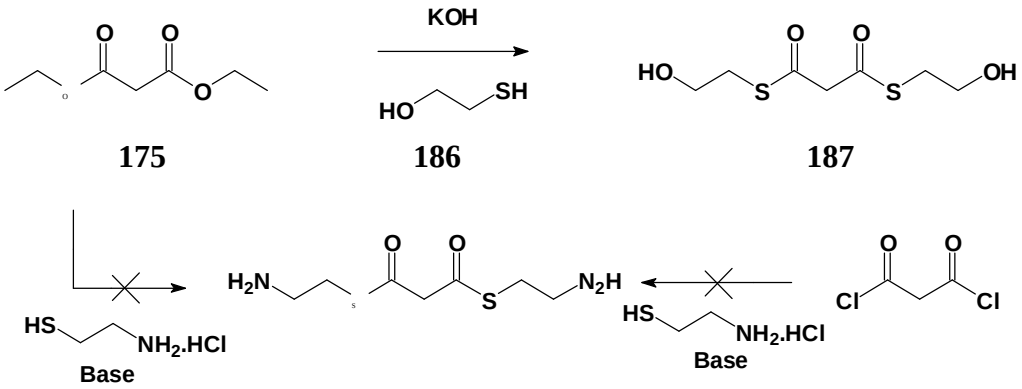

175 **186** **187** **188** **176**

2.1.3.4 *Synthesis of substituted malonamide derivatives*

Given the difficulties encountered in the syntheses discussed in the previous sections (**2.1.3.2** and **2.1.3.3)**, it was envisaged that greater success could be achieved by reacting malonic esters with amines which already contained additional donor atoms in the side-chains - an approach which was expected to provide access to a series of polydentate malonamide ligands. The functionalised amines **189-193** were identified as suitable candidates.

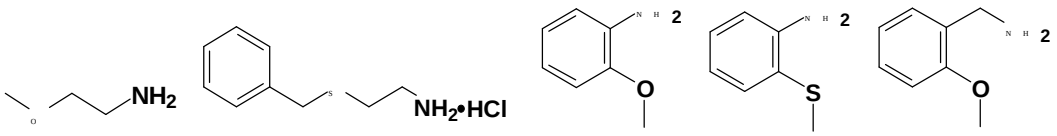

189 **190** **191** **192** **193**

Based on the knowledge gained in generating the *N*,*N'*-bis(2-hydroxyethyl)malonamides **180a-k**, it was envisaged that mild reaction conditions,

i.e. stirring at room temperature could be used to effect the formation of the desired products (**Scheme 17**).

Scheme 17. Reaction of malonic esters with amines (see **Table 8**).

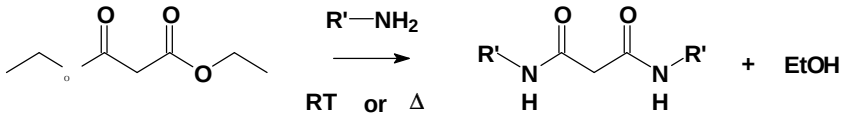

175 **194-197**

Consequently, the synthesis of the malonamides was first attempted by stirring the reagents together at room temperature. This proved to be a slow and inefficient (see **Table 8**). Closer examination of these reactions confirmed that ethanol was the only major side-product, and it was presumed that modification of the reaction conditions to promote the removal of ethanol would increase the yield of the malonamide. The simplest way to achieve this was to heat the reaction mixture under reflux. In fact, a search of the literature revealed that a number of malonamide derivatives (**Figure 32**) had been obtained in yields ranging between 3-50 %, by heating the reagents under reflux for 3-48 h.[101,102,103] The results of these reactions are also summarised in **Table 8**.

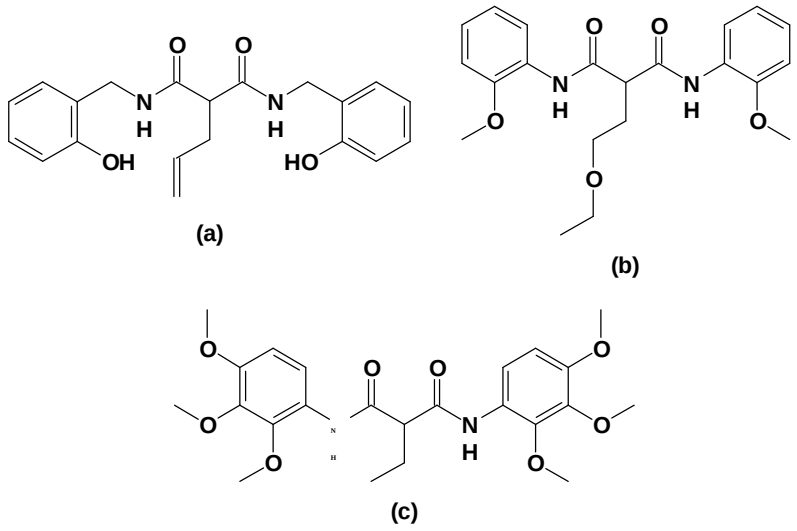

Figure 32. (a) 2-Allyl-*N*,*N*′-bis(2-hydroxybenzyl)malonamide; (b) 2-(2-ethoxyethyl)-*N*,*N*′-bis(2-methoxyphenyl)malonamide; and (c) 2-ethyl-*N*,*N*′-bis(2,3,4-trimethoxyphenyl)malonamide.

Table 8. Data for the synthesis of substituted malonamide derivatives.

Compound	Conditions	Time	Yield [a] / %
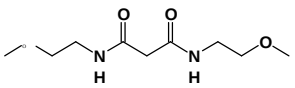 **194**	r.t. [b] reflux [b]	7 days 16 h	24 62
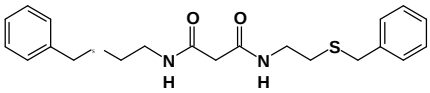 **195**	r.t. [b]	7 days	24
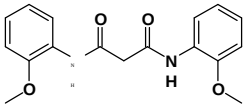 **196**	r.t. [b] r.t. [d] reflux	7 days 24 h 48 h	- [c] 23 66
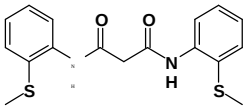 **197**	reflux [b]	48 h	30

[a] Calculated from recrystallized product. [b] Reaction performed using diethyl malonate. [c] No product was isolated from reaction mixture. [d] Reaction performed using malonyl dichloride.

As is clearly evident from **Table 8**, heating under reflux both decreased the reaction times and improved the overall yields. The yields observed under reflux conditions are, in fact, comparable with those reported for similar systems.[101,102,103] The malonamides obtained were characterized by elemental (high resolution MS) and spectroscopic (NMR, IR and MS) analysis. Selected NMR spectra of *N*,*N*´-bis(2-methoxyphenyl)malonamide **196** are illustrated in **Figures 33**, **34** and **35**. The ^{1}H NMR spectrum of the malonamide **196** (**Figure 33**) is characterized by the methylene singlet at 3.55 ppm, the methoxy singlet at 3.89 ppm, four signals in the region 6.87 - 8.35 ppm corresponding to the aromatic protons and the amide signal at 8.98 ppm. The most interesting features of the ^{13}C NMR spectrum (**Figure 34**) are: - the methylene carbon signal at 45.8 ppm, assigned on the basis of the DEPT spectrum (**Figure 35**); and the carbonyl signal at 164.8 ppm, as they are likely to be most sensitive to chelation, and hence useful as indicators of coordination. The structure of the malonamide **196** was confirmed by single-crystal X-ray analysis (see Section

2.3, p. 96). Crystal data, atomic coordinates and other relevant data are tabulated in the Appendix (p.185).

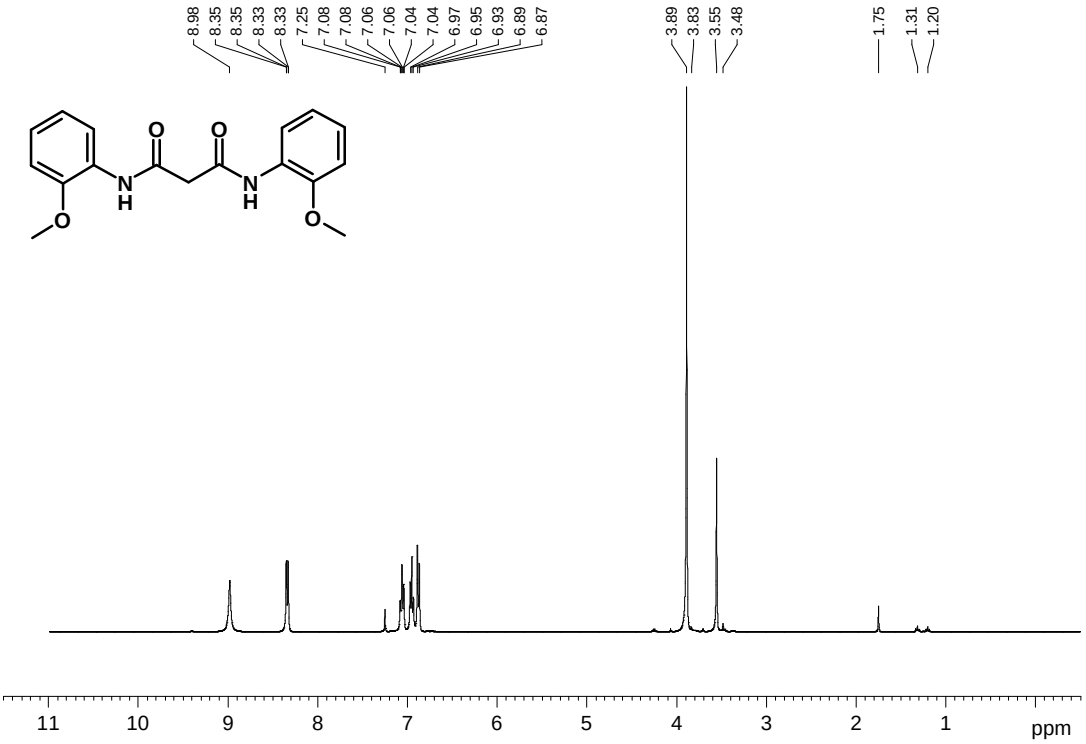

Figure 33. 400 MHz ^{1}H NMR spectrum of the malonamide **196** in $CDCl_3$.

Figure 34. 100 MHz ^{13}C NMR spectrum of the malonamide **196** in $CDCl_3$.

Figure 35. ^{13}C-DEPT-135 NMR spectrum of the malonamide **196** in $CDCl_3$.

In order to extend the range of malonamide-based ligands, the conversion of the carbonyl groups to thiocarbonyls was explored using Lawesson's reagent[104] (**Scheme 18**). After numerous unsuccessful attempts, the thiocarbonyl derivative of *N,N´*-bis(2-methoxyphenyl)malonamide **196,** *N,N´*-Bis(2-methoxyphenyl)dithiomalonamide **198,** was finally isolated in 1 % overall yield from the reaction mixture! The low yield was ascribed to the difficulty in obtaining adequate chromatographic separation of the components, due to streaking and, possibly, reaction of the components with the silica gel; no attempt was made to optimise this reaction. The novel dithiomalonamide **198** was fully characterised by elemental and spectroscopic analysis. In ^{13}C NMR spectrum (**Figure 36**), the methylene carbon is shifted downfield (relative to the dicarbonyl precursor **196**) from 45.8 to 69.6 ppm, and the carbonyl signal at 164.8 ppm is replaced by a thiocarbonyl signal at 192.3 ppm.

Scheme 18. Reaction of *N,N´*-bis(2-methoxyphenyl)malonamide with Lawesson's reagent.

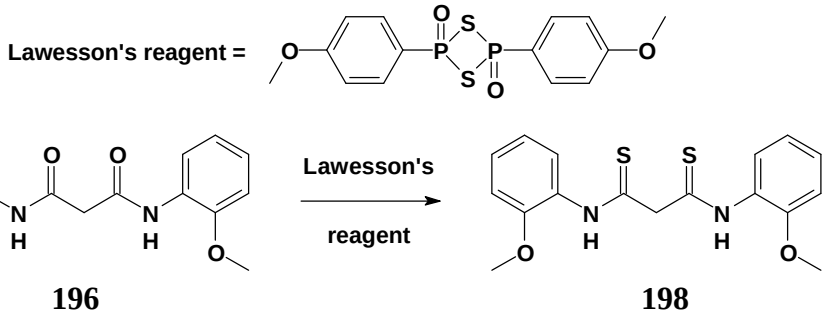

196 **198**

Figure 36. 100 MHz ^{13}C NMR spectrum of the dithiomalonamide **198** in $CDCl_3$.

2.1.3.5 *Synthesis of malonamide derivatives using microwave irradiation*

2.1.3.5.1 *Principles of microwave-assisted reactions*

The application of microwave irradiation in the field of organic synthesis is in its infancy, but it is a rapidly expanding field of research[105] - a field dogged by controversy over the question as to whether or not there is a "microwave effect". The controversy concerning the "microwave effect" arises from the enormous difference in results observed between various reactions carried out in a microwave environment, and those conducted using classical methods. In the cases studied, "microwave-assisted" reactions are completed in less time, are generally more efficient and, for some organic transformations, more product selective.[105] To explain these differences, many authors subscribe to a "microwave effect", although the evidence suggests that the kinetics of the reactions are not different to those measured for classical methods.[105,106]

The problem in studying these systems is in being able to control as many of the variables as possible.[105] In classical thermal reactions, variables such as reaction temperature and pressure are readily controlled, but the same cannot be said for microwave reactions. Controlling the pressure within the microwave system and the energy of the microwave radiation are relatively simple tasks, but controlling the temperature of the system is a non-trivial matter. The problem is due to the fact that, during irradiation, the temperature is not uniform throughout the reaction mixture. This non-uniform heat distribution is due to the mechanisms of heating involved in microwave radiation. It is generally accepted that such heating is due to either "dielectric heating" or "conduction loss", depending, largely, on the constituents of the system being irradiated. For the "dielectric heating" to operate in a system, the components of the reaction mixture must have dipoles with which the electric field can interact. The electric field enhances polarization of the dipoles, and the subsequent relaxation of this polarization leads to heat transfer to the reaction mixture. The "conduction loss" mechanism occurs in systems containing charge carriers and in which there is a high electrical resistance. The resistance of the system leads to a build-up of energy, which dissipates as heat. Both of these mechanisms lead to non-uniform heating, referred to as "hot-spots" within the reaction mixture.[105] A few

examples, discussed below, illustrate the attractiveness of microwave-assisted synthesis.

Scheme 19. Preparation of coumaran-2-one.[106]

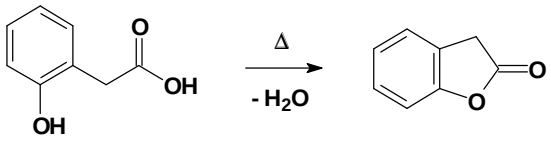

199 **200**

Goncalo *et al.* [106] studied the intramolecular cyclisation of 2-hydroxyphenylacetic acid **199** into 2,3-dihydro-2-oxo-1-benzofuran **200** (**Scheme 19**), using both microwave irradiation and classical heating methods. The product was isolated in 63 % yield after heating for 6 minutes, but in 85 % yield after exposure to microwave radiation for the equivalent time. Although there was only a moderate increase in yield, the major advantages for the authors were:- i) time saving, as the microwave reaction only took 6 minutes, whereas the classical heating method required preheating the oil bath for 0.5 h; and ii) energy saving, since the total energy cost for the microwave reaction was calculated at 108 kJ, compared to 540 kJ for the classical reaction (excluding the preheating energy of approximately 3000 kJ!).

Scheme 20. Sulfonation of napthalene.[105]

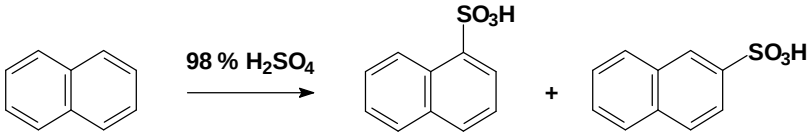

201 **202a** **202b**

The sulfonation reaction of naphthalene **201** (**Scheme 20**) is known to be a difficult reaction to perform, under both conventional and microwave conditions.[105] However, given adequate control of temperature and pressure, the microwave-assisted reaction affords, within 3 minutes, a 93 % yield of the sulfonic acids **202a** and **202b**, in a ratio of 18.6:1.[105]

Reactions performed in a microwave oven can also be applied to the synthesis of coordination compounds. Illustrated in **Scheme 21** is the preparation of a ruthenium(III) chloride complex with 2,2´-dipyridyl in DMF. The conventional

method requires 168 h, while the microwave-assisted synthesis involves three exposures, under pressure, of 20 seconds each, to yield the complex in an overall yield of 49 %.[105]

Scheme 21. Preparation of ruthenium coordination complex.[105]

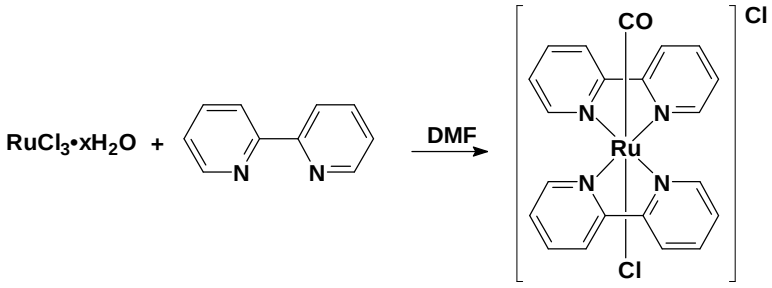

203 **204** **205**

2.1.3.5.2 *Application in malonamide synthesis*

We were interested to explore the possible benefit of using microwave-assisted methodology in the preparation of malonamide-based ligands, and the reaction between diethyl malonate **175** and *o*-anisidine **190** was studied under conventional and microwave conditions (**Scheme 22)**. The microwave-assisted reaction was performed in a conventional domestic microwave with the reagents placed in a 25 ml conical flask fitted with a condenser-vent.

Scheme 22. Preparation of the substituted malonamide **196**.

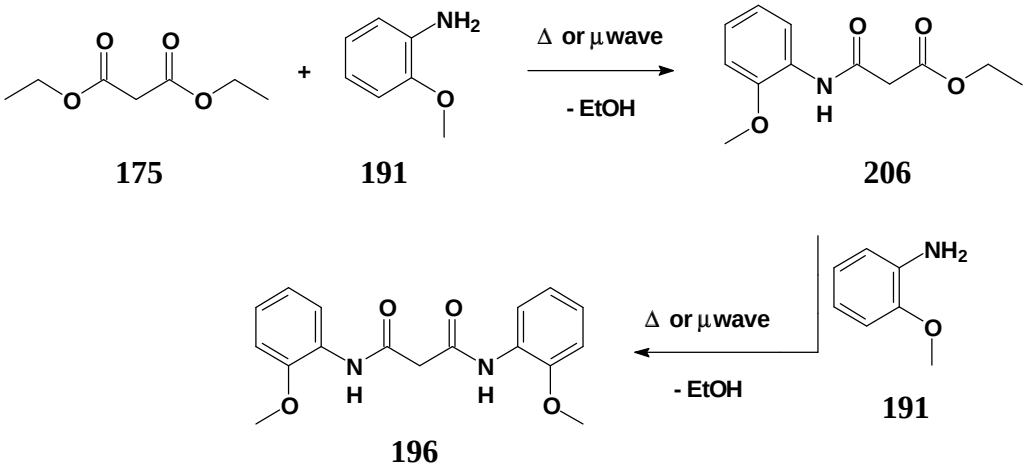

175 **191** **206**

196 **191**

In order to monitor the microwave-assisted synthesis of the malonamide derivative **196**, it was decided to use ^{1}H NMR spectroscopy as an analytical tool. Examination of the ^{1}H NMR spectra of the starting materials, the intermediate monoamide **206** and the final diamide product **196** revealed that the methylene proton signal could be used as an NMR probe. The chemical shift for the methylene nuclei in diethyl malonate is 3.35 ppm, for the diamide **196** 3.54 ppm, and for the intermediate monoamide **206** 3.47 ppm. A typical ^{1}H NMR spectrum of a crude reaction mixture, displaying the three tracer signals, is illustrated in **Figure 37**. Using these three tracer signals, the reaction mixture was analyzed at intervals and the resulting data is summarized in **Figures 38** and **39**. The distribution between the species after each interval was determined from the relative integrals of respective methylene signals, and is expressed as relative percentages. The classical reaction was performed over a 48-hour period, while the microwave reaction was limited to 5 minutes. For comparative purposes all the reactions were performed with neat reagents.

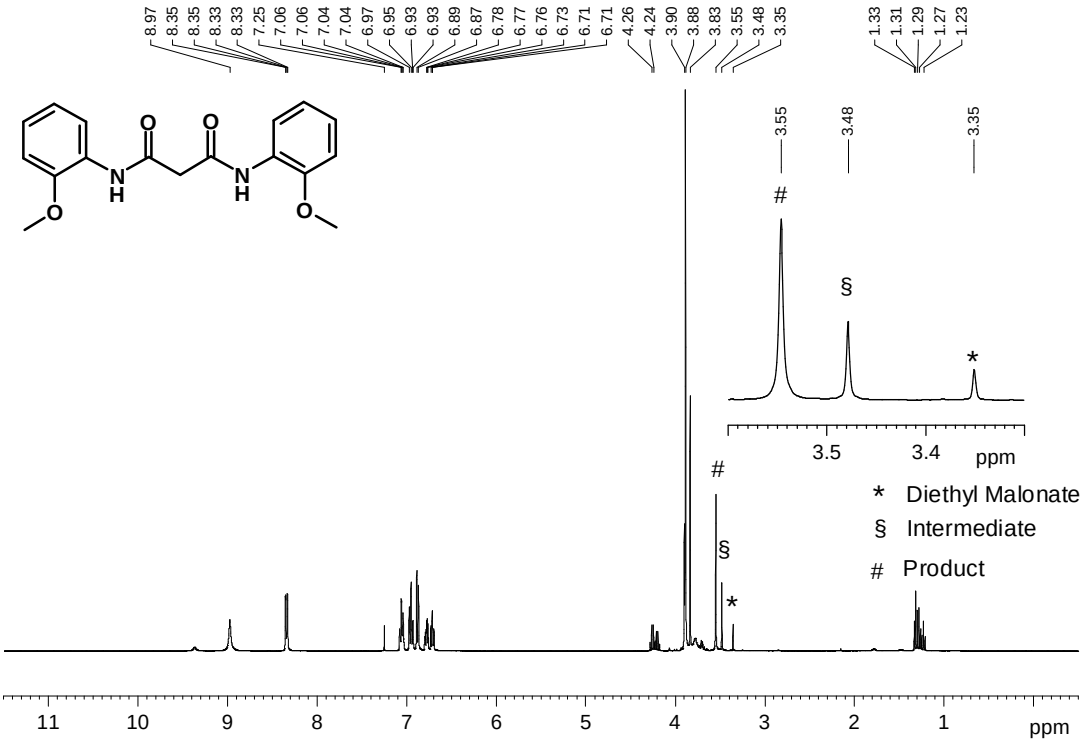

Figure 37. 400 MHz ^{1}H NMR spectrum in $CDCl_3$ of the crude mixture containing diethyl malonate **175**, the monoamide **206**, and the malonamide derivative **196**.

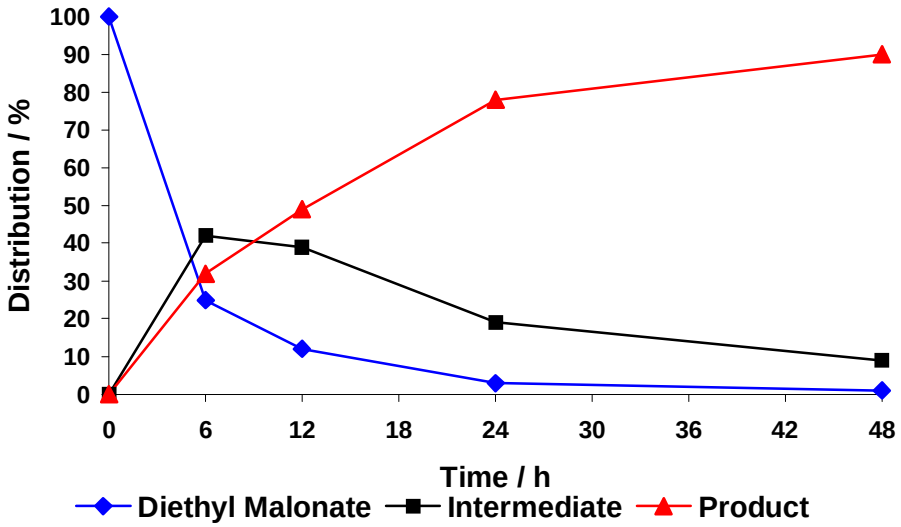

Figure 38. The percentage distribution of the starting material **175**, monoamide **206** and product **196** over time for the classical thermal reaction (**Scheme 22**).

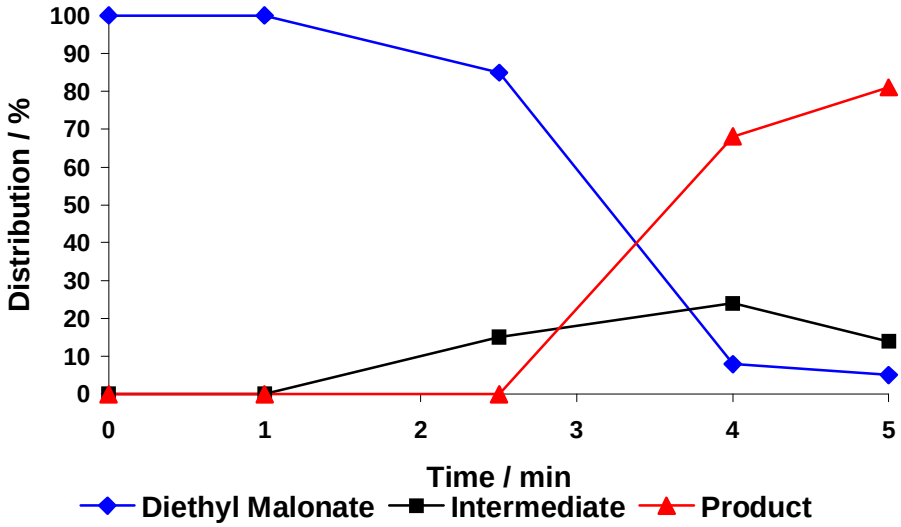

Figure 39. The percentage distribution of the starting material **175**, monoamide **206** and product **196** over time for the microwave-assisted reaction (**Scheme 22**).

Inspection of the figures reveals that, in both reactions, formation of the monoamide **206** precedes formation of the malonamide product **196**. It is also apparent that the consumption of the intermediate monoamide **206** is faster in the microwave-assisted reaction than in the conventional thermal reaction. This is evidenced by the relative abundance of the intermediate **206**, which peaks at 42 % for the thermal reaction but at 24 % for the microwave-assisted experiment. In the microwave-assisted process the intermediate **206** is the only product for the first 2.5 min, after which there is a rapid increase in the formation of the malonamide **196**. The "quiescent periods" of

ca. 1 minute and 2.5 minutes prior to the detection of the monoamide **206** and the malonamide **196**, respectively, presumably reflect the times needed to achieve reaction temperature under microwave-assisted conditions.

In order to determine whether the microwave-assisted reaction is influenced by bulk effects, the reaction was repeated for the same time period, but varying the amounts of the reagents. The distribution of the components was determined by inspection of the ^{1}H NMR spectra of the reaction mixtures after 5 minutes, and the results obtained are summarized in **Table 9**. Inspection of the data reveals that there is no apparent bulk effect on changing the total mass of the reactants in the microwave experiment, from 2.6 g to 13 g; in the cases examined the product was obtained in essentially the same yield (*ca.* 84 %).

Table 9. The effect of sample size on the microwave assisted synthesis of the malonamide derivative **196**.

	Ratio of Integrals of Signals after 5 minutes / %		
Compound	1 g / 1.6 g [a]	2.5 g / 4 g [a]	5 g/ 8 g [a]
Diethyl Malonate **175**	5	7	2
Monoamide **206**	11	7	16
Malonamide **196**	84	85	82

[a] Mass of diethyl malonate and *o*-anisidine.

Given the results obtained for the microwave-assisted generation of the malonamide derivative **196**, it was decided to apply the same methodology to the preparation of other malonamide ligands. The results are summarized in **Table 10**.

Table 10. Data for the malonamide derivatives obtained by microwave-assisted synthesis.

Compound	Time [a] / s	Yield [b] / %
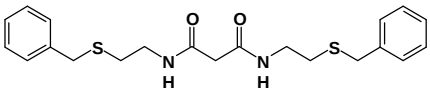 **195**	210 (7 days) [c]	55 (24) [c]
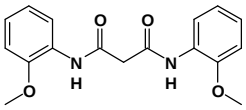 **196**	270 (48 h) [c]	65 (66) [c]
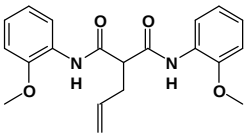 **207**	450	54
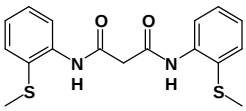 **197**	360 (48 h) [c]	56 (30) [c]
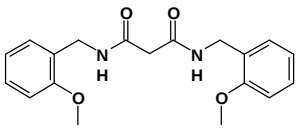 **208**	360	96

[a] Performed in a 2.45 GHz multimode 1000 W domestic oven using the defrost setting and neat reagents. [b] Calculated following recrystallisation. [c] Corresponding data for the conventional thermal reaction (see Table 8).

As can be seen from **Table 10**, the isolated yields, following recrystallisation, range from moderate to excellent (54 - 96 %) and, at the power levels used, the reaction times are six minutes or less. Interesting points to note are: - i) the increase in reaction time required for the allyl malonamide **207** compared to the unsubstituted analogue **196**; ii) the difference in reaction times for compounds **196** and **197**, where the ring substituent changes from methoxy to methylsulfanyl; and iii) the difference in reaction times and overall yields for the *N*-benzyl and *N*-phenyl analogues (**208** and **196**, respectively).

From these results it is apparent that the microwave-assisted reaction is of great use in generation of the malonamides. The reactions proceed in good yields and in short reaction times. The method used to isolate and purify of the products was the same as the one used in the thermal synthesis, *viz.*, filtration and washing of the precipitate formed on cooling. The main advantages of this synthetic method are clearly the ease of application and the short reaction times. The only disadvantage encountered was the degradation of the reaction mixture on prolonged exposure to the microwave radiation. A similar effect was observed when the heating period was extended in the classical thermal synthesis.

An attempt to generate a "mixed" malonamide ligand **209**, by isolating the monoamide intermediate **206** from the reaction mixture and reacting it further with a different reagent, proved difficult (**Scheme 23**). This was largely due to the rapid transformation of the monoamide intermediate **206** into the diamide product **196**.

Scheme 23. Proposed synthesis of "mixed" malonamide ligand **209**.

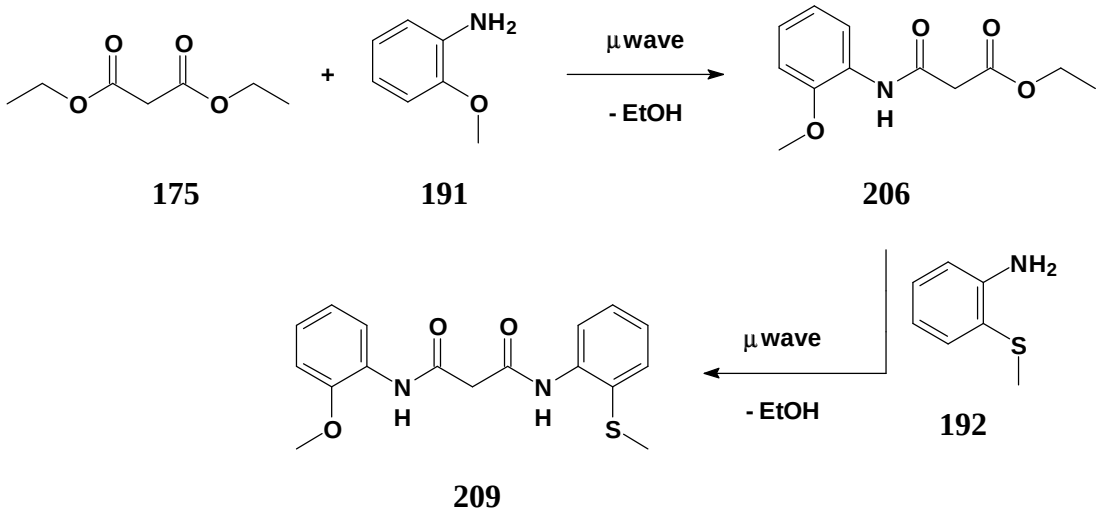

Discussion concerning the computer-modelling of the malonamide ligands and their respective complexes is deferred to Section **2.3** (p. 92).

2.2 Fragmentation Patterns in the Electron-impact Mass Spectra of Selected Malonamide Derivatives

Mass fragmentation studies were conducted on a series of selected malonamides to identify possible fragmentation patterns. High-resolution electron-impact (EI) mass spectra (illustrated for compound **180j** in **Figure 40**) and meta-stable peak data were obtained for the malonamides **180k**, **180j**, **194**, **195**, **196**, **197**, **198**, **207** and **208**. Examination of the spectra revealed that the fragmentation patterns which characterise the "alkyl-spacer"-containing malonamides (**180k**, **180j**, **194** and **195**) differ significantly from those which characterise the "aromatic-spacer"-containing malonamides (**196**, **197**, **198**, **207** and **208**). **Schemes 24-32**, which illustrate the proposed fragmentation patterns for each of the malonamides studied, are followed by analyses of the common features of each of the two sets of compounds (**Schemes 33** and **34**); the corresponding high-resolution data are summarised in the accompanying tables (**Tables 11-19**).

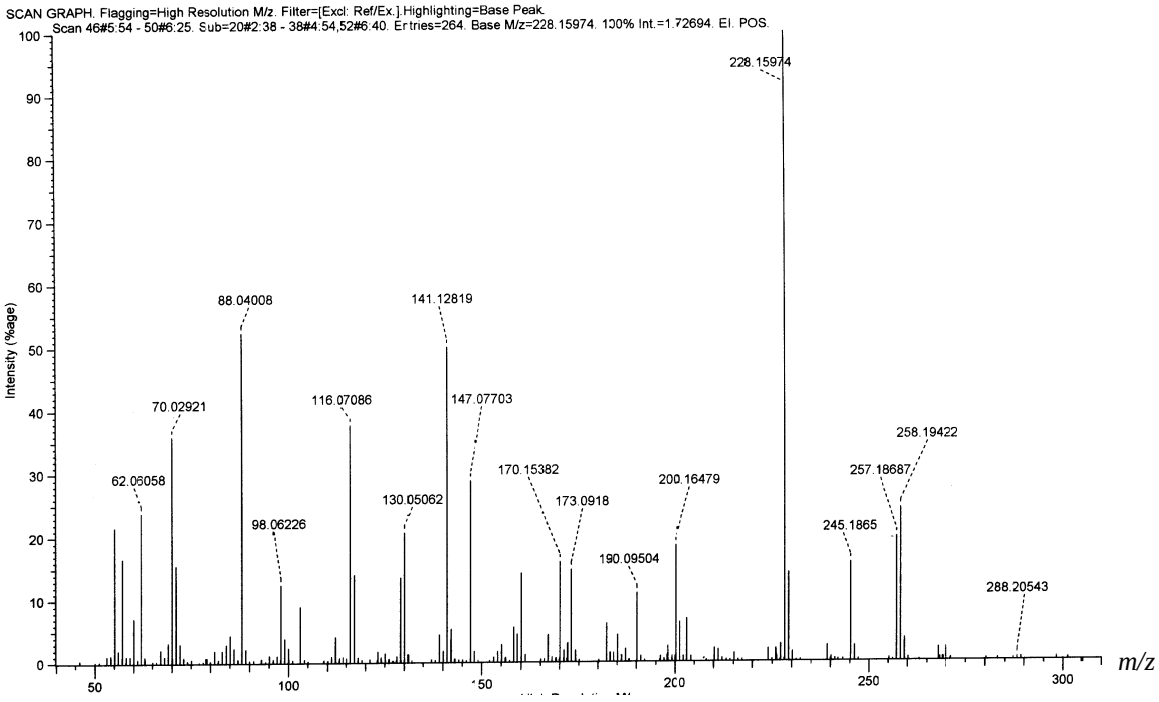

Figure 40. High-resolution electron-impact mass spectrum of compound **180j**.

Scheme 24. Proposed fragmentation of compound **180k**.

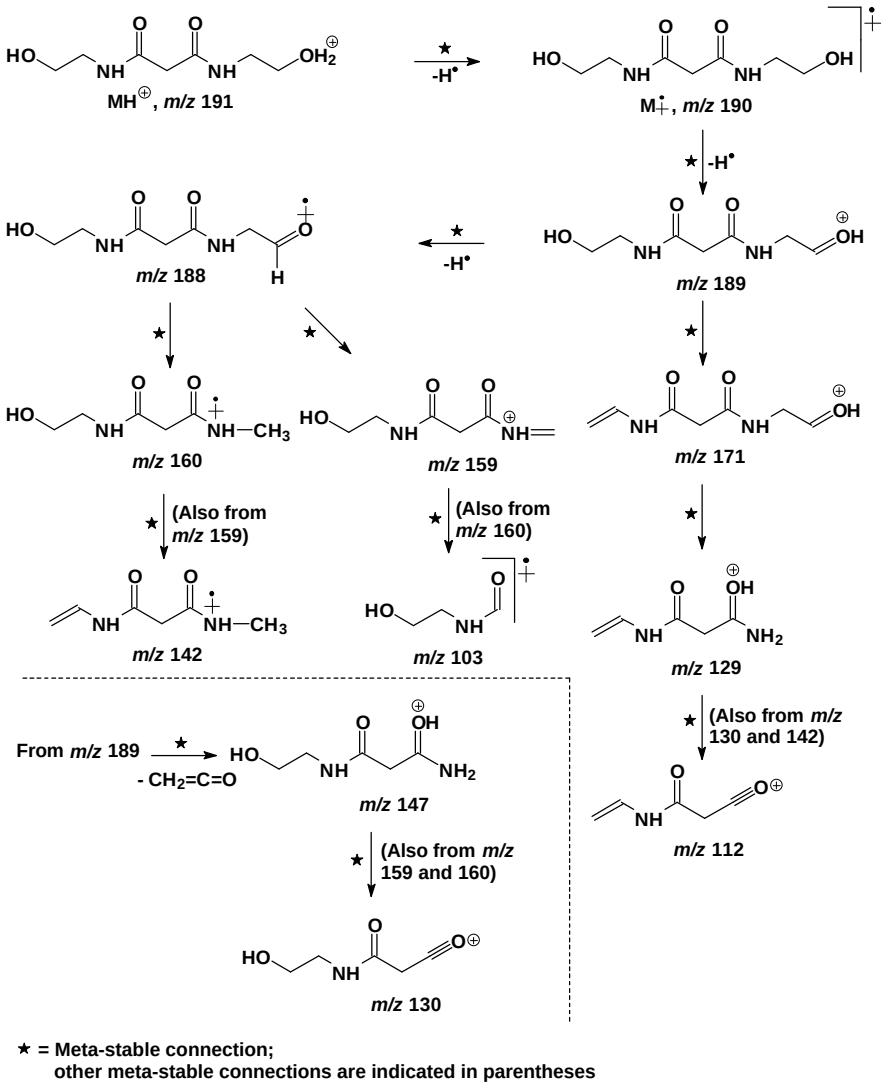

Table 11. Fragmentation (*m/z*) and relative abundance data for compound **180k**.

Observed	Formula	Calculated	Relative Abundance / %
191.1026	$C_7H_{15}N_2O_4$	191.1032	0.95
190.1 [a]	$C_7H_{14}N_2O_4$	190.0954	< 0.2
189.0881 [a]	$C_7H_{13}N_2O_4$	189.0876	< 0.2
188.1 [a]	$C_7H_{12}N_2O_4$	188.0797	< 0.2
171.1 [a]	$C_7H_{11}N_2O_3$	171.0770	0.48
160.0855	$C_6H_{12}N_2O_3$	160.0848	99.34
159.0778	$C_6H_{11}N_2O_3$	159.0770	75.57
147.0780	$C_5H_{11}N_2O_3$	147.0770	8.79
142.0744	$C_6H_{10}N_2O_2$	142.0742	10.53
130.0514	$C_5H_8NO_3$	130.0504	100
129.0666	$C_5H_9N_2O_2$	129.0664	16.29
112.0402	$C_5H_6NO_2$	112.0399	10.89
103.0634	$C_4H_9NO_2$	103.0633	25.39

[a] Present in the meta-stable peak spectrum.

Scheme 25. Proposed fragmentation of compound **180j**.

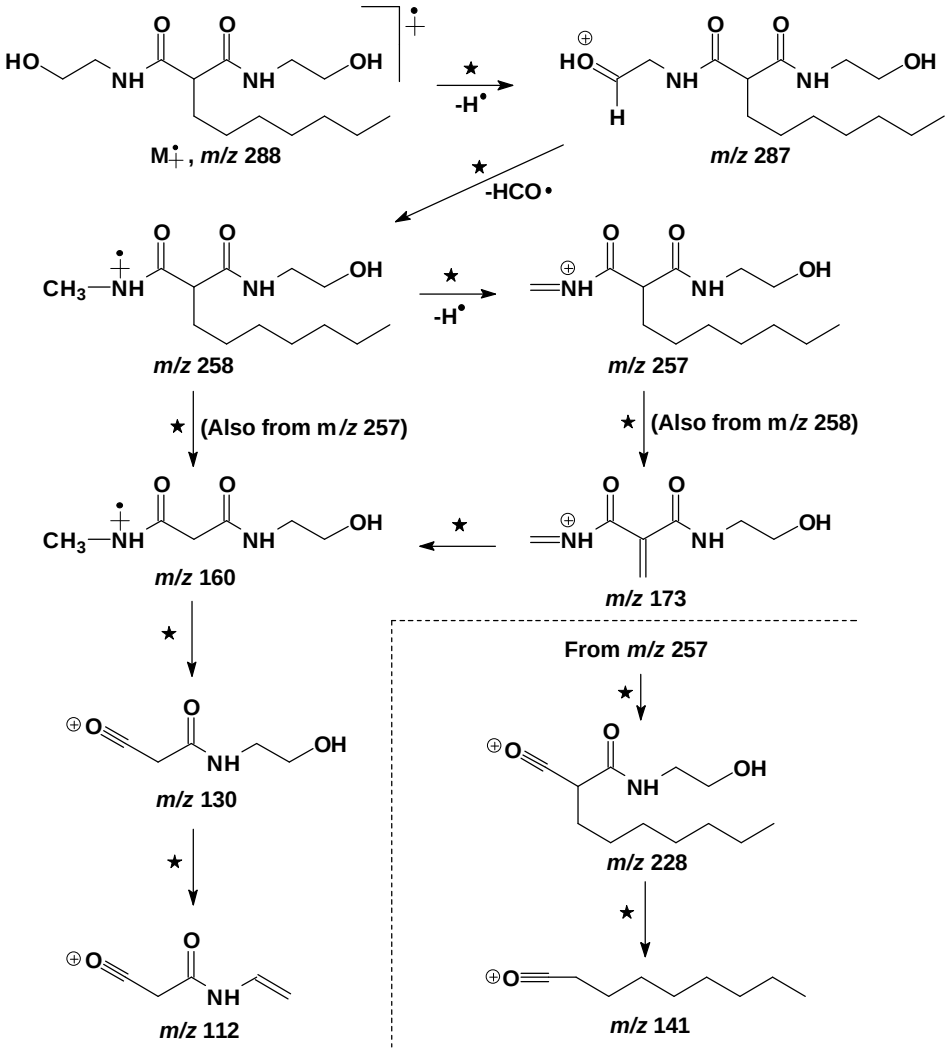

Table 12. Fragmentation (*m/z*) and relative abundance data for compound **180j**.

Observed	Formula	Calculated	Relative Abundance / %
288.20543	$C_{14}H_{28}N_2O_4$	288.2049	< 1.5
287.1 [a]	$C_{14}H_{27}N_2O_4$	287.1971	< 1.5
258.1942	$C_{13}H_{26}N_2O_3$	258.1943	24.32
257.1869	$C_{13}H_{25}N_2O_3$	257.1865	19.78
228.1597	$C_{12}H_{22}NO_3$	228.1600	100
173.0918	$C_7H_{11}N_2O_3$	173.0926	14.73
160.0854	$C_6H_{12}N_2O_3$	160.0848	14.15
141.1282	$C_9H_{17}O$	141.1279	50.06
130.0506	$C_6H_{10}N_2O_2$	130.0550	20.64
112.0398	$C_5H_8NO_3$	112.0399	4.11

[a] Present in the meta-stable peak spectrum.

Scheme 26. Proposed fragmentation of compound **194**.

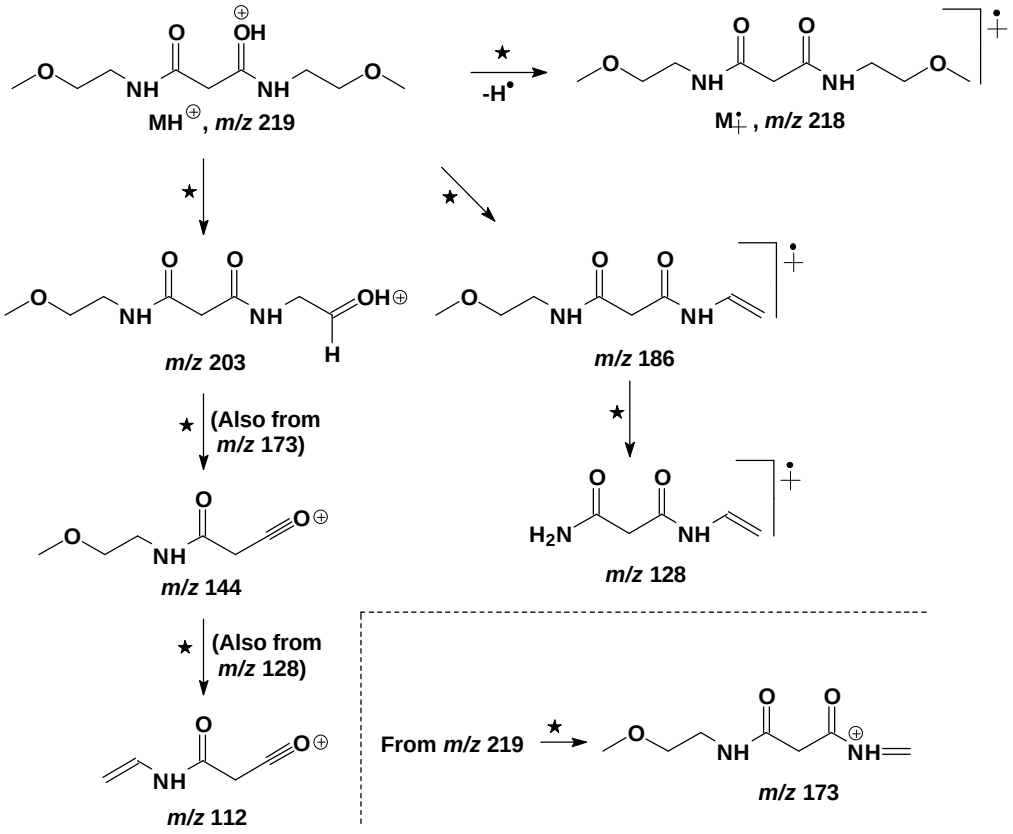

★ = Meta-stable connection;
other meta-stable connections are indicated in parentheses

Table 13. Fragmentation (*m/z*) and relative abundance data for compound **194**.

Observed	Formula	Calculated	Relative Abundance / %
219.1344	$C_9H_{19}N_2O_4$	219.1345	< 2
218.2 [a]	$C_9H_{18}N_2O_4$	218.1267	< 2
203.1034	$C_8H_{15}N_2O_4$	203.1032	2.12
186.1006	$C_8H_{14}N_2O_3$	186.1004	5.94
173.0929	$C_7H_{13}N_2O_3$	173.0926	57.00
144.0665	$C_6H_{10}NO_3$	144.0661	100
128.0585	$C_5H_8N_2O_2$	128.0586	39.87
112.0399	$C_5H_6NO_2$	112.0399	28.81

[a] Present in the meta-stable peak spectrum.

Scheme 27. Proposed fragmentation of compound **195**.

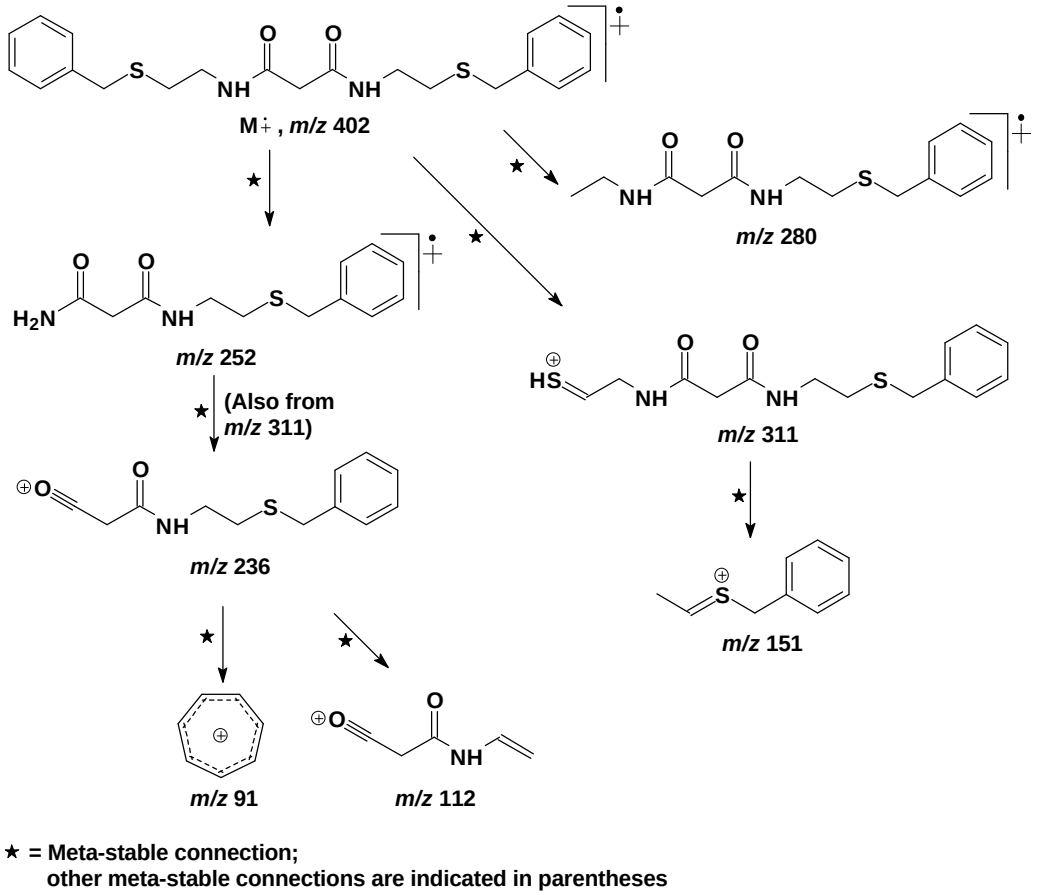

Table 14. Fragmentation (*m/z*) and relative abundance data for compound **195**.

Observed	Formula	Calculated	Relative Abundance / %
402.1444	$C_{21}H_{26}N_2O_2S_2$	402.1436	1.60
311.0895	$C_{14}H_{19}N_2O_2S_2$	311.0888	75.84
280.1247	$C_{14}H_{20}N_2O_2S$	280.1246	1.61
252.0934	$C_{12}H_{16}N_2O_2S$	252.0933	2.02
236.0745	$C_{12}H_{14}NO_2S$	236.0745	4.48
151.0578	$C_9H_{11}S$	151.0582	9.98
112.0399	$C_5H_6NO_2$	112.0399	3.22
91.0549	C_7H_7	91.0548	100

Scheme 28. Proposed fragmentation of compound **196**.

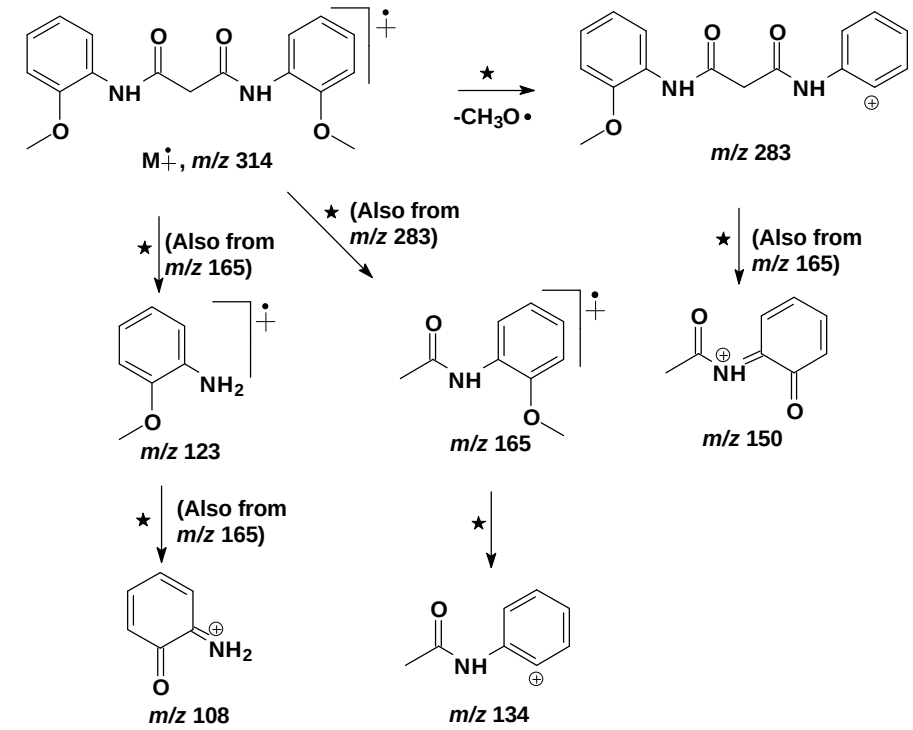

Table 15. Fragmentation (*m/z*) and relative abundance data for compound **196**.

Observed	Formula	Calculated	Relative Abundance / %
314.1273	$C_{17}H_{18}N_2O_4$	314.1267	93.20
283.1077	$C_{16}H_{15}N_2O_3$	283.1083	< 2
165.0795	$C_9H_{11}NO_2$	165.0790	60.72
150.0550	$C_8H_8NO_2$	150.0555	8.77
134.0604	C_8H_8NO	134.0606	17.27
123.0682	C_7H_9NO	123.0684	100
108.0451	C_6H_6NO	108.0449	56.89

Scheme 29. Proposed fragmentation of compound **197**.

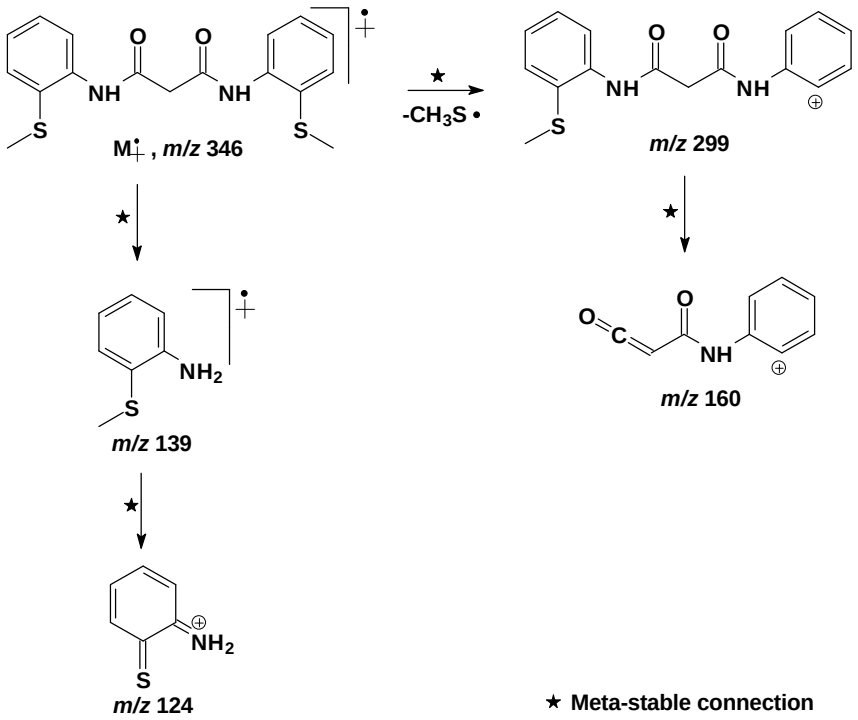

Table 16. Fragmentation (*m/z*) and relative abundance data for compound **197**.

Observed	Formula	Calculated	Relative Abundance / %
346.0820	$C_{17}H_{18}N_2O_2S_2$	346.0810	40.70
299.0857	$C_{16}H_{15}N_2O_2S$	299.0854	14.93
160.0410	$C_9H_6NO_2$	160.0399	10.54
139.0475	C_7H_9NS	139.0489	100
124.0221	C_6H_6NS	124.0221	30.85

Scheme 30. Proposed fragmentation of compound **207**.

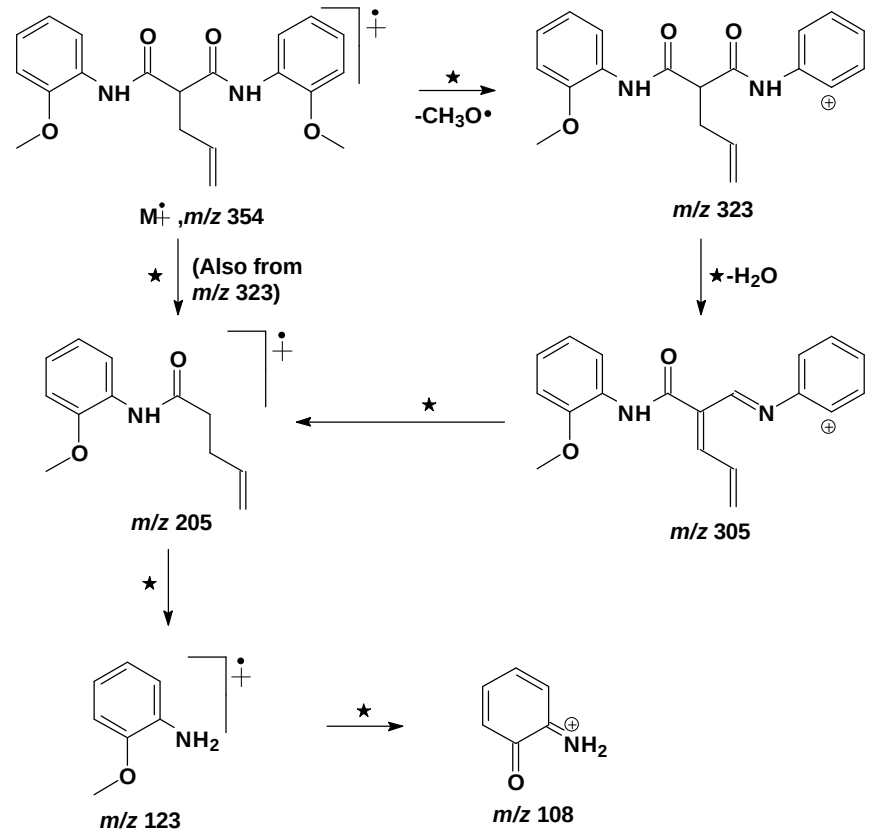

Table 17. Fragmentation (*m/z*) and relative abundance data for compound **207**.

Observed	Formula	Calculated	Relative Abundance / %
354.1585	$C_{20}H_{22}N_2O_4$	354.1580	46.55
323.1392	$C_{19}H_{19}N_2O_3$	323.1396	< 2
305.2 [a]	$C_{19}H_{17}N_2O_2$	305.1290	< 2
205.1101	$C_{12}H_{15}NO_2$	205.1103	25.08
123.0684	C_7H_9NO	123.0684	100
108.0451	C_6H_6O	108.0449	23.56

[a] Present in the meta-stable peak spectrum.

Scheme 31. Proposed fragmentation of compound **198**.

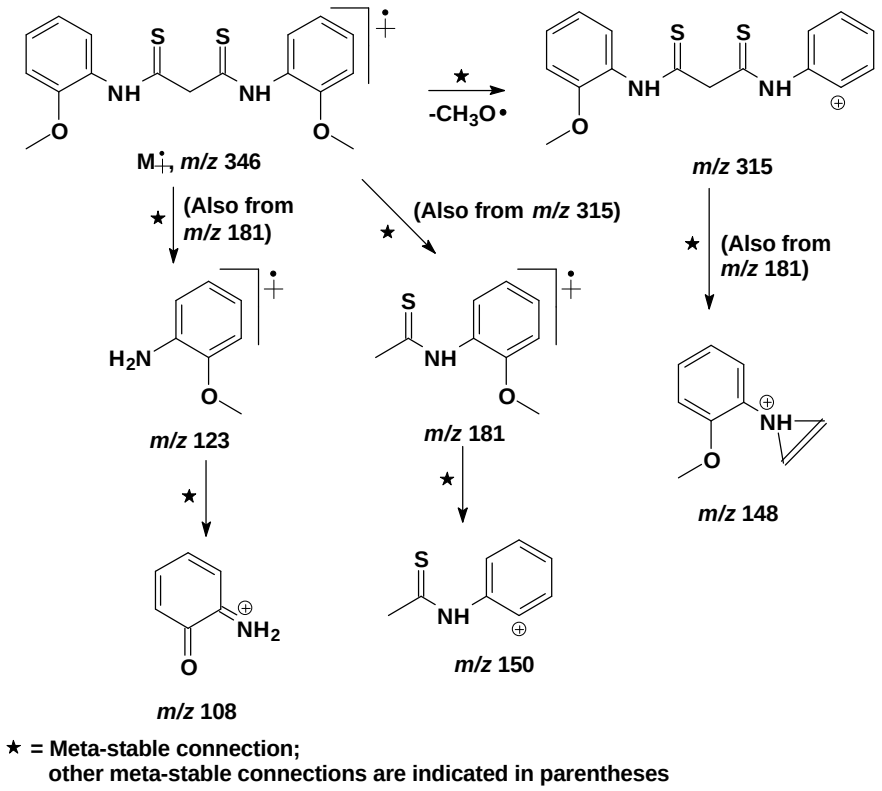

Table 18. Fragmentation (*m/z*) and relative abundance data for compound **198**.

Observed	Formula	Calculated	Relative Abundance / %
346.0818	$C_{17}H_{18}N_2O_2S_2$	346.0810	100
315.0644	$C_{16}H_{15}N_2OS_2$	315.0626	23.54
181.0555	$C_9H_{11}NOS$	181.0561	15.55
150.0380	C_8H_8NS	150.0378	37.07
148.0766	$C_9H_{10}NO$	148.0762	77.23
123.0683	C_7H_9NO	123.0684	25.38
108.0450	C_6H_6NO	108.449	18.98

Scheme 32. Proposed fragmentation of compound **208**.

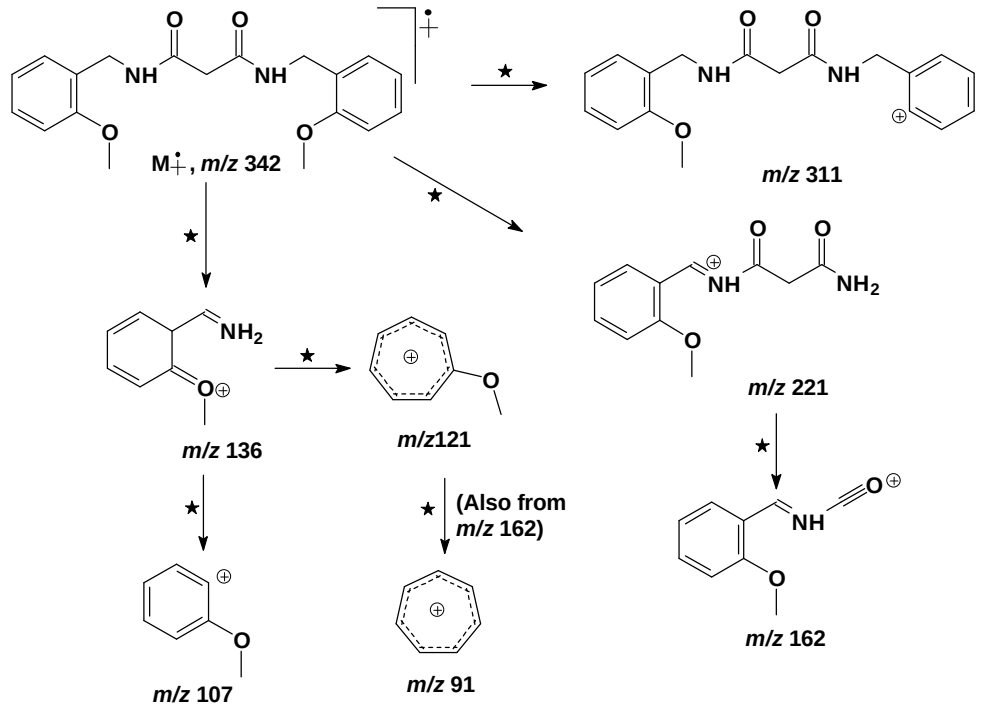

Table 19. Fragmentation (*m/z*) and relative abundance data for compound **208**.

Observed	Formula	Calculated	Relative Abundance / %
342.1588	$C_{19}H_{22}N_2O_4$	342.1580	17.85
311.1381	$C_{18}H_{19}N_2O_3$	311.1396	< 0.5
221.0928	$C_{11}H_{13}N_2O_3$	221.0926	15.57
162.0556	$C_9H_8NO_2$	162.0555	3.17
136.0763	$C_8H_{10}NO$	136.0726	100
121.0637	C_8H_9O	121.0653	17.48
107.0495	C_7H_7O	107.0497	2.17
91.0546	C_7H_7	91.0548	23.64

Inspection of the mass spectra of the "alkyl-spacer"-containing malonamides **180j**, **180k**, **194** and **195** revealed three fragmentation pathways common to all the spectra, and these are illustrated in **Scheme 33**. The corresponding fragments have been labelled as ion types **A**, **B**, **C** and **D**.

Scheme 33. Common fragmentation patterns for the malonamides **180j**, **180k**, **194** and **195**.

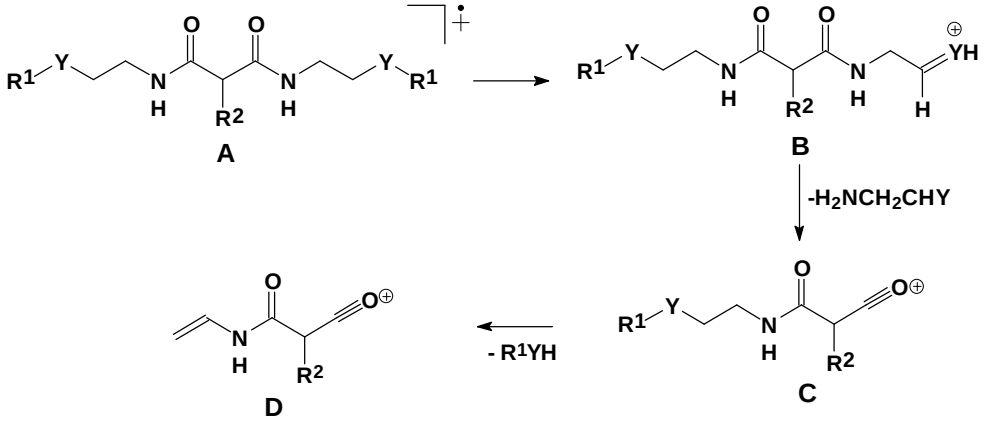

In the electron-impact mass spectra of these malonamides, the molecular ion **A** undergoes loss of the radical •R^1 to give the cation **B**, which fragments further to yield the acylium ion **C**. The acylium ion **C** fragments further to yield another acylium ion **D**. These fragmentation patterns were observed regardless of the substituents R^1 and R^2. The common fragment types and their respective nominal masses are listed in **Table 20**.

Table 20. Selected MS peaks (*m/z*) for the malonamides **180j**, **180k**, **194** and **195**.

				Ion Fragment Types			
Compound	Y	R^1	R^2	A	B	C	D
180k	O	H	H	190	189	130	112
180j	O	H	$CH_3(CH_2)_6$	288	287	228	112
194	O	Me	H	218	203	144	112
195	S	Bn	H	402	311	236	112

The "aromatic-spacer"-containing malonamides, however, exhibited significantly different fragmentation patterns to those of the "alkyl-spacer"-containing malonamides. Thus, acylium ions which characterise the mass spectra of the latter compounds were not observed in the spectra of the malonamides **196**, **197**, **198**, **207**

and **208**. Instead, the formation of a primary amine radical cation **B'**, *via* fragmentation of the molecular ion **A'**, and the subsequent fragmentation to yield ions of type **C'** were observed for all of the "aromatic spacer"-containing malonamides, except compound **208** (**Scheme 34**). Another common ion type, observed in the fragmentation of these malonamides, was cation **D'**, formed by loss of the substituent on one of the aromatic rings. In the case of malonamide **208**, the *N*-substituents are benzyl groups (rather than phenyl) precluding the formation of fragments of type **B'** and **C'**; instead of an ion of type **C'**, this compound affords the fragment **E'** (*m/z* 136). However, a fragment (*m/z* 311) corresponding to ion type **D'** is observed. The masses for the common fragment ions observed for the various malonamides are listed in **Table 21**.

Scheme 34. Common fragmentation ions for the malonamides **196**, **197**, **198**, **207** and **208**.

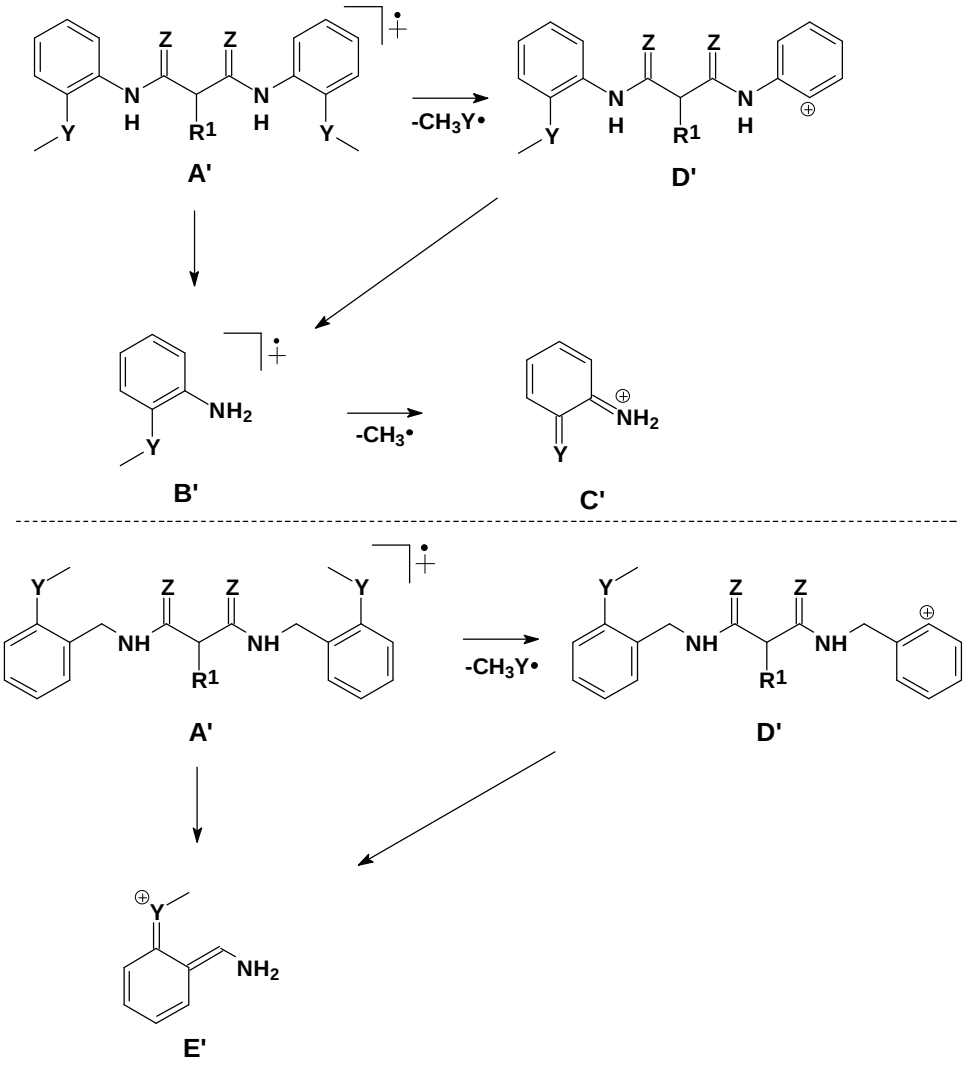

Table 21. Selected MS fragmentation peaks (*m/z*) for the malonamides **196**, **197**, **198** and **207**.

				Ion Fragment Types			
Compound	Y	Z	R^1	A'	B'	C'	D'
196	O	O	H	314	123	108	283
197	S	O	H	346	139	124	299
198	O	S	H	346	123	108	315
207	O	O	CH_2=$CHCH_2$-	354	123	108	323

Inspection of **Table 21** reveals that for compounds **196-198** and **207** the fragmentation patterns in **Scheme 34** are observed regardless of the substituent on the aromatic ring (Y = O or S), the presence of carbonyls or thiocarbonyls (Z = O or S), or the presence or absence of an alkyl chain (R^1 = CH_2=$CHCH_2$).

2.3 Computer Modelling Studies

2.3.1 Basic principles in computer modelling

The fundamental premise in molecular modelling is that all significant molecular properties, *i.e.* stability, reactivity, electronic properties, *etc.* are related to the structure of the compound concerned.[87] Consequently, if it is possible to model the structure of a compound, using an algorithm, it should be possible to compute the molecular properties, and *vice versa*. Various methods are available, including *ab initio* calculations, semi-empirical molecular orbital methods (MO), molecular mechanics (MM), ligand field calculations and density functional theory (DFT).

In contrast to the quantum mechanical-based calculations, the MM method calculates the forces between atoms using a classical mechanical approach. Thus, for example, bonded atoms are considered to be held together by mechanical springs, while non-bonding interactions are treated as a combination of attractive and repulsive forces which together produce a typical van der Waals curve. In order to optimize the geometry of a molecule, the total energy arising from these forces is minimized by a computational method. The resultant energy, referred to as the "steric energy", is related to the molecule's potential energy and stability. Early MM studies defined the steric energy U_{Total} as the sum of four principal energy terms (Equation 5).[87]

$$U_{Total} = \sum_{Molecule} \left(E_b + E_\theta + E_\phi + E_{nb} \right) \tag{5}$$

where: $\sum E_b$ is the total bond deformation energy,
$\sum E_\theta$ is the total valence angle deformation energy,
$\sum E_\phi$ is the total torsional (dihedral) angle deformation energy, and $\sum E_{nb}$ is the total nonbonded (van der Waals) interaction energy.

In more recent packages, additional terms have been added to this summation.[87] An out-of-plane deformation $\sum E_\delta$ is included for systems that contain aromatic or sp^2 hybridized atoms, while electrostatic $(\sum E_\varepsilon)$ and hydrogen bonding $(\sum E_{hb})$ terms are included in modelling the interaction of metal complexes with biological systems. These functions together with the values that describe their parameters constitute the

"force field". The goal of MM modelling, once a model and a force field have been chosen, is to find the geometry with the lowest steric energy.[87]

In the case of metal ion selectivity, MM has been used to study the chelate ring size, the macrocycle hole size and the effect of preorganization of the ligand on selectivity.[87] There are, however, major limitations to the prediction of metal ion selectivities using MM modelling alone. Application of the same force field for various metal ions leads to the assumption that the force field parameters do not change for different metal ions - an assumption that is hardly justified.[87] Moreover, different conformations and configurations of the ligands may lead to different cavity sizes, which also need to be considered. In the case of macrocycles, the method does not take into account the preference of a metal ion for a particular geometry or its electronic effects.[87] A further limitation is the fact that MM typically affords structures for isolated (gas phase) molecules; in solvent extraction systems, solvation effects are likely to be significant. On the positive side, MM calclulations are rapid and applicable to large molecular systems.

2.3.2 Application of computer modelling in the present study

In this project, an attempt has been made to use MM-based calculations to assist in the design of ligands for the solvent extraction of silver, and as a tool for predicting which systems might be most selective. For this purpose the MSI modelling programme Cerius$^{2®86}$ was used for all the MM-based calculations. In selected cases, some semi-empirical and *ab initio* calculations were performed using the PC-Spartan Pro[107] programme.

To ensure consistency throughout the MM modelling experiments, a general and rigorous method was required that could produce reliable and reproducible results. The following protocol was developed and applied to all the systems investigated (including the models presented in the previous sections).

(a) The models were constructed with the appropriate bonds, charges and conformational properties, *i.e.* for ligand systems the overall charge distribution was set to zero (neutral), while for the complexes containing

silver(I) the overall charge was set to +1; the Universal force-field (UFF) was used to type the atoms and bonds.

(b) Using a Newton-Raphson algorithm, the model was minimized to a local minimum.

(c) The model corresponding to the local minimum was then used as the initial structure in a Dynamics Simulation to search for the global minimum. The Dynamics Simulation was performed with the following "settings": -

i) volume and temperature were kept constant at 300 K;.

ii) 500 inter-dynamic annealing cycles, from 300 to 500 K, with 50 K increments per dynamic step, were used to overcome rotational energy barriers;

iii) after each annealing cycle the molecule was minimized ("quenched") using a truncated Newton algorithm;

iv) after each "quenching", the molecule's conformation was recorded; and

v) the Dynamic Simulation was run for 100000 steps, generating 500 different conformers of the molecule.

An example of the data obtained from such a simulation is illustrated in **Figure 41**.

(d) The 5 lowest-energy conformers were then inspected.

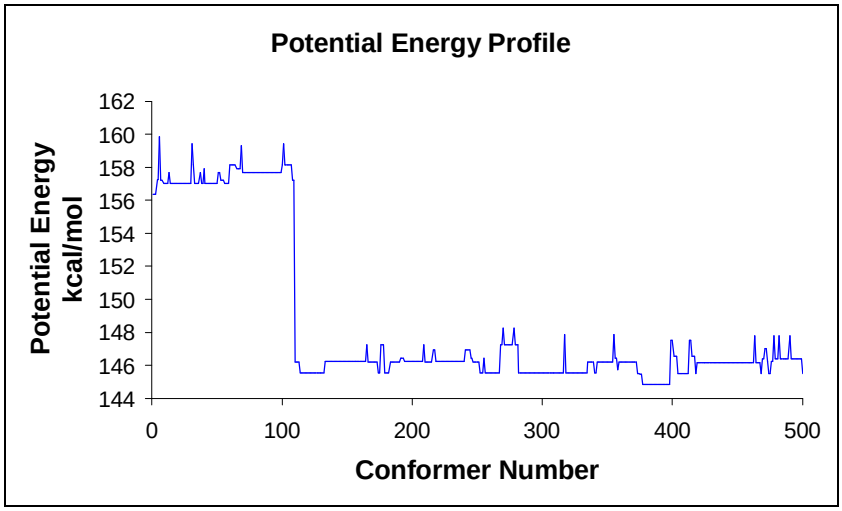

Figure 41. The potential energy profile obtained from a typical dynamic-annealing simulation.

This protocol lent itself to automation and the settings and script used are listed in the experimental section. It was hoped that the computer modelling would be of assistance in: -

i) determining the capacity of the various ligands synthesised to adopt conformations suitable for chelating silver(I) (see Sections **2.1.1**, p. 41; **2.1.2**, p. 45 and **2.3.2.1**, p. 97);

ii) predicting extraction efficiency trends within various series of ligands (see Sections **2.3.2.2**, p. 99 and **2.3.2.3**, p. 100); and

iii) visualising possible structures for the complexes (see Sections **2.4.1**, p. 104 and **2.4.3**, p. 107-109).

In an attempt to assess the ability of the Cerius[2®86] programme to model the ligands and the metal complexes satisfactorily, the crystal structure of the ligand **196**, prepared in this study, and the silver complex **210**, reported by Wong *et al.*,[108] were compared to their respective computer-generated models.

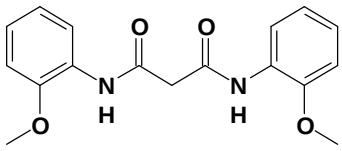

196

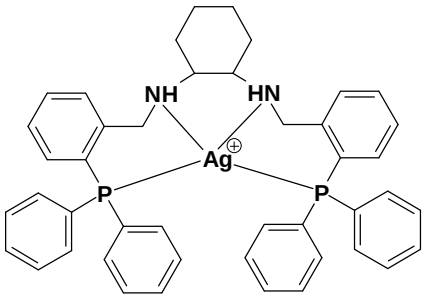

210

The X-ray crystal structure of ligand **196** is illustrated in **Figure 42**, while the crystal structure of the complex **210** was retrieved from the Cambridge Crystallographic Data Bank and is shown in **Figure 43**. The computer-generated models were constructed using the protocol mentioned previously, and are illustrated for the ligand **196** in **Figure 44** and the silver complex **210** in **Figure 45**. The representations of the crystal structures in **Figure 44** and **46** were obtained, for comparative purposes, by reading the crystallographic atomic coordinates into the Cerius[2] programme.

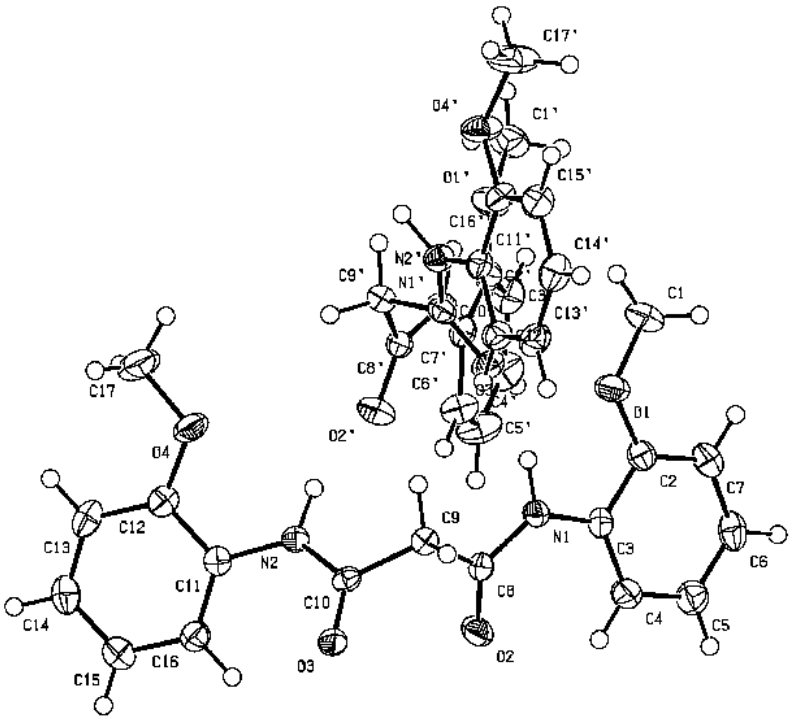

Figure 42. X-ray crystal structure of ligand **196**, showing the two ligands in the unit cell and the crystallographic numbering.

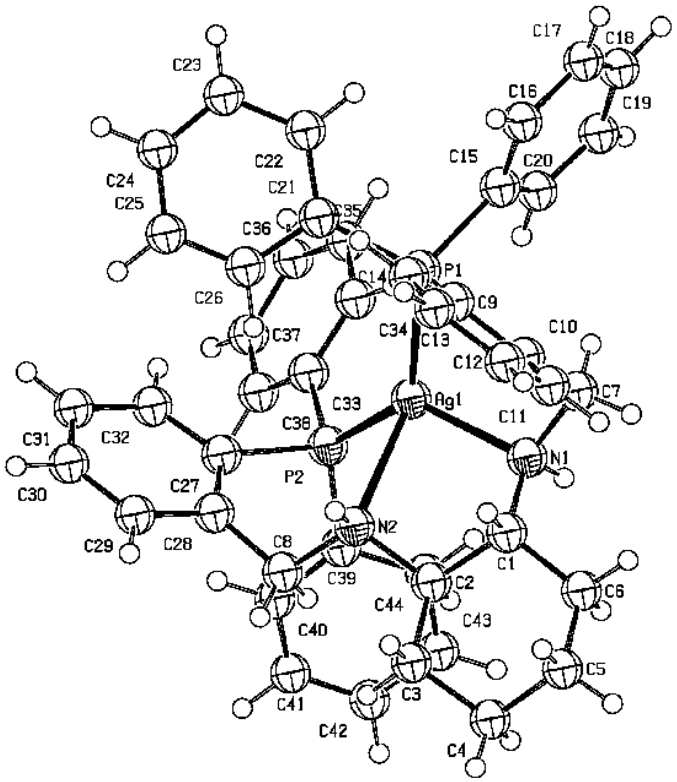

Figure 43. X-ray crystal structure of the complex **210**,[108] showing the crystallographic numbering.

(a) **(b)**

Figure 44. Comparison of the crystal structure (a) of ligand **196** with the computer-generated model (b).

Similarities between the crystal structure of the ligand **196** and the computer-generated, gas-phase model are clearly evident (**Figure 44**). The correspondence between the crystal structure of the complex **210** and its corresponding model (**Figure 45**), however, is less apparent, although closer inspection reveals a number of important correlations, *viz.*, the distortion of the silver(I) centre and the conformation of the ligand. The results serve to illustrate both the usefulness and limitations of the MM methodology.

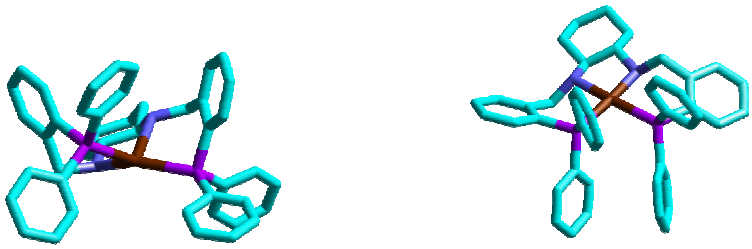

(a) **(b)**

Figure 45. Comparison of the crystal structure (a) of **210** with the computer-generated model (b).

2.3.2.1 *Modelling the silver(I) chelation capacity of the malonamide ligands*

To confirm that the malonamide ligands **180j**, **195**, **196**, **197** and **208** could chelate the silver(I) ion, MM models of the ligands and their proposed complexes were generated (**Figure 46**). The complexes exhibit silver(I) centres that are predominantly tetrahedral, and the "chelating" conformations (obtained by removing the metal ion from the complex) are not very different from the minimum-energy conformations of the respective "free" ligands. In fact, the steric energy differences between the "free" and "chelating" conformations in each case are $\leq$ 70 kcal.mol^{-1}, suggesting the capacity of these ligands to adopt conformations appropriate for coordination.

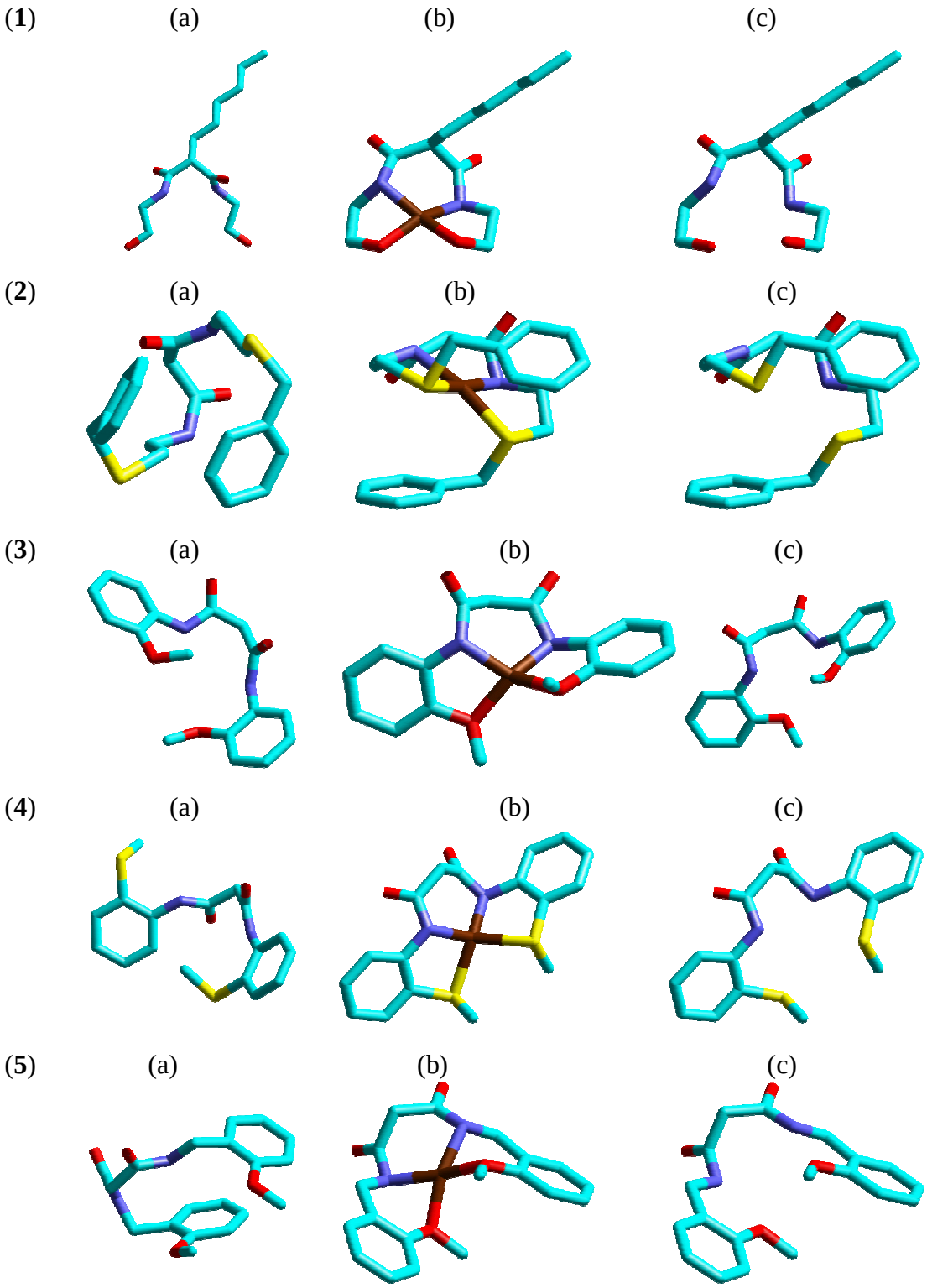

Figure 46. Computer-generated models for: - (a) the lowest energy conformation of the free ligand; (b) the corresponding silver(I) complex; and (c) the chelating conformation of the ligand; for the ligand systems: - (**1**) **180j**; (**2**) **195**; (**3**) **196;** (**4**) **197;** and (**5**) **208**. See **Figure 14** for the colour coding.

2.3.2.2 *Predicting the extraction efficiency of the 3,6-dithiaoctanediamide ligand series*

Scheme 35. Complexation of the 3,6-dithiaoctanediamides with Silver(I).

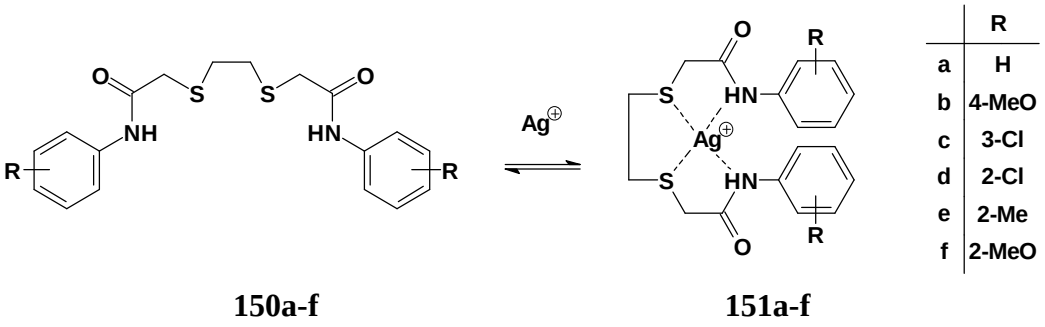

150a-f **151a-f**

In the case of the 3,6-dithiaoctanediamide series (**Scheme 35**), the ligands differ only in the nature and position of the substituent on the aromatic ring. If Equation 6 is assumed to represent silver(I) chelation in this series, Equation 7 can be used to predict the influence of the substituent since the metal centre will be the same for all the complexes. Of course, such analysis ignores speciation effects and the solubility distribution of the ligands and their respective complexes in the aqueous and organic media - factors which could contribute significantly to overall extraction efficiency.

$$ML_1 + L_2 \rightleftharpoons ML_2 + L_1 \qquad (6)$$

$$\Delta E_{MM} = \left(E_{ML_H} + E_{L_X}\right) - \left(E_{ML_X} + E_{L_H}\right) \qquad (7)$$

where : - E_{ML_H} and E_{ML_X} are the potential energies of the lowest-energy conformers for the metal complexes of the parent (R=H) and derivative ligands (R=X), respectively; and

E_{L_H} and E_{L_X} are the potential energies of the lowest-energy conformers of the parent (R=H) and derivative (R=X) ligands.

If the energy difference (ΔE_{MM}) is positive the ligand (R=X) should form a less stable metal complex than the parent system (R=H), if negative the opposite applies. From a plot of ΔE_{MM} for the 3,6-dithiaoctanediamide series **150a-f** (**Figure 47**) it seems that: -

(i) *ortho* substituents are likely to destabilize the silver(I) complexes (*cf.* **150b** and **150f**; **150c** and **150d**); and

(ii) the 3-chloro derivative **150c** should be the most efficient extractant for silver(I).

However the selectivity and efficiency of the system can only be proven by actual extraction studies.

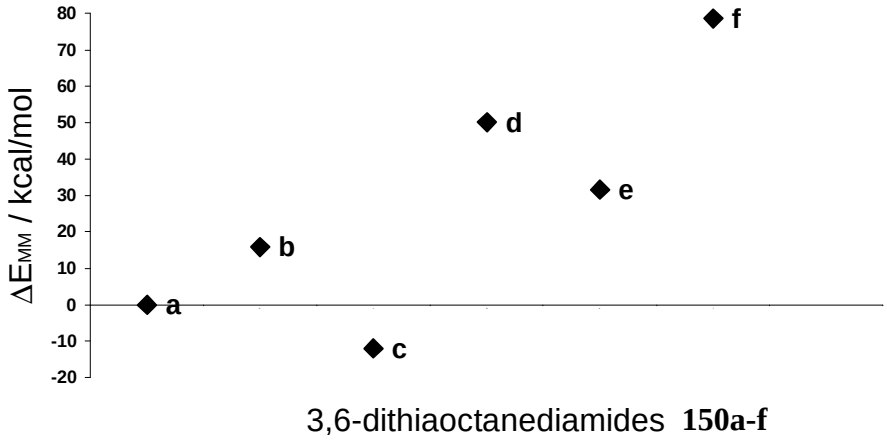

Figure 47. The effect of the substituent R, relative to R = H, on the potential energy for the silver(I) complexes with the 3,6-dithiaoctanediamide ligands **150a-f**.

2.3.2.3 *Predicting the extraction efficiency of the malonamide ligands*

The prediction of extraction efficiency in the malonamide series presented a different problem. In this series, the ligands are structurally diverse, and cannot be so readily related to one another. An additional problem in assessing metal selectivity is how to accommodate the influence of *different* metals on the potential energy of the complexes.

Steric energy differences (ΔE_{Diff}) obtained from MM analysis of *different* systems cannot be equated with heat of formation differences. It was hoped that higher-level calculations (AM1 or DFT) could be used to determine the latter but, unfortunately, parameters for silver were not included in the computational packages available to us (HyperChem/Momec and PC-Spartan Pro). Consequently, the MSI Cerius$^{2®86}$ package was simply used to assess the relative conformational (steric energy) costs associated with complexation of each of the ligands **180j**, **195**, **196**, **197** and **208** with the different metals, Ag(I), Cu(II), Hg(II) and Pb(II).

This was achieved by examining the conformations of the coordinated ligand in each complex, following removal of the metal ion. In all cases, it was assumed that the ligands remain neutral (*i.e.* chelate without deprotonation), and that the coordination sites were same, irrespective of the metal concerned (*i.e.* coordination through the amide nitrogens and the oxygen or sulfur donor atoms in the side chain).

Plots of the ΔE_{Diff} values (Equation 8) for complexation of: - a) the various ligands with silver(I); and b) selected ligands with the metals Ag(I), Cu(II), Hg(II) and Pb(II), are illustrated in the **Figures 48-50**.

$$\Delta E_{Diff} = \Delta E_{ML-M} - \Delta E_{L} \qquad (8)$$

where: - ΔE_{ML-M} is the potential energy of the coordinated ligand after the metal removed.
ΔE_{L} is the potential energy of the free ligand.

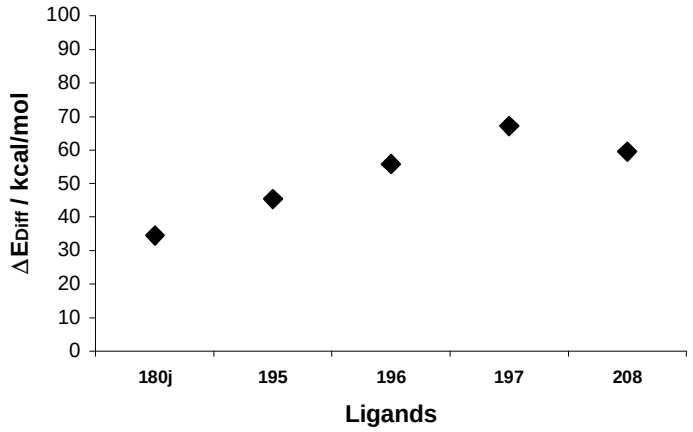

Figure 48. The steric energy costs (ΔE_{Diff}) for ligands **180j**, **195**, **196**, **197** and **208** to coordinate silver(I).

The trend exhibited by ligands (**Figure 48**), based on the ΔE_{Diff} values, suggest that the ligands **180j** and **195** could be possible candidates for silver extraction, while the derivatives **196**, **197** and **208** are less likely candidates. It must be stressed, however, that the steric energy data (ΔE_{Diff}) take no account of the crucial bond energy terms associated with chelation and solvation processes.

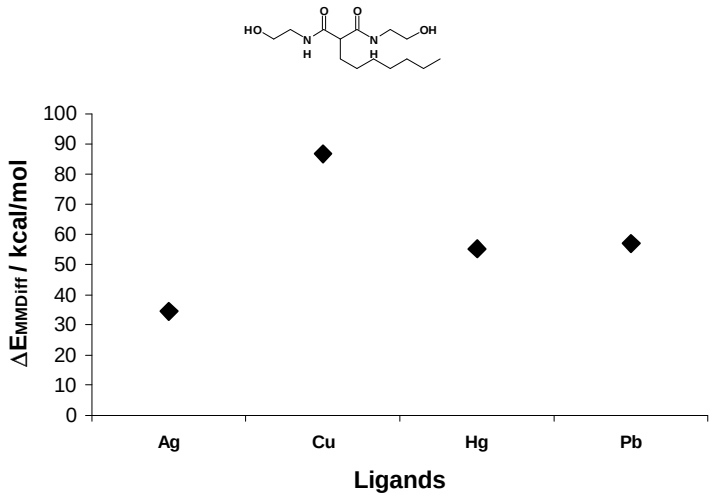

Figure 49. The steric energy cost (ΔE_{Diff}) for the ligand 2-heptyl-*N*,*N*´-bis(2-hydroxyethyl)malonamide **180j** to coordinate the metals ions Ag^{+}, Cu^{2+}, Hg^{2+} and Pb^{2+}.

The trends in selectivity in **Figures 49** and **50** suggest that both ligands **180j** and **195** should exhibit a higher selectivity for silver(I) than copper(II), but not discriminate readily between silver(I), mercury(II) and lead(II). From these predicted trends, its clear that ligands **180j** and **195** appear to be the most promising candidates. It was recognised, however, that the assumptions concerning the coordination sites may well have been unfounded, and that the trends indicated by the MM modelling data required confirmation by conducting extraction experiments.

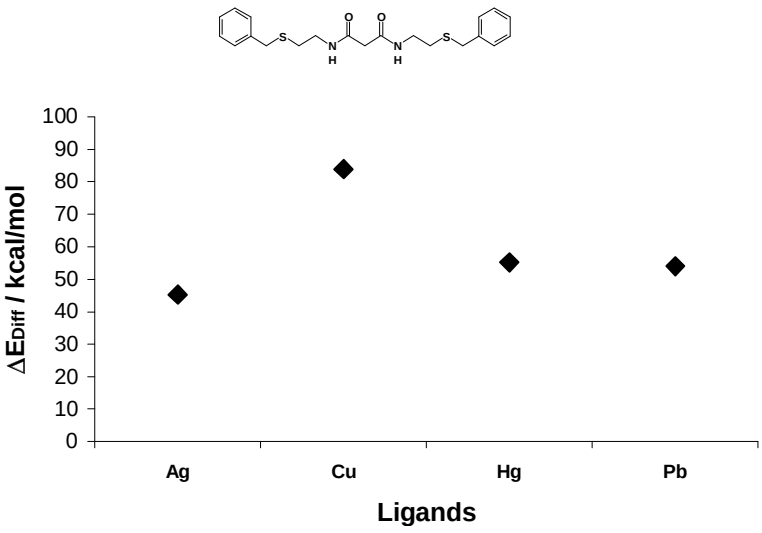

Figure 50. The steric energy cost (ΔE_{Diff}) for the ligand *N*,*N*´-bis(2-benzylsulfanylethyl)malonamide **195** to coordinate the metals ions Ag^{+}, Cu^{2+}, Hg^{2+} and Pb^{2+}.

2.4 Investigation of the silver(I) and other complexes

Since the extraction process involves the formation of metal-ligand complexes, it was decided, where possible, to explore their structures. None of the complexes afforded material suitable for single-crystal X-ray analysis and, consequently, our conclusions are based on a combination of spectroscopic, elemental (high resolution-MS and/or combustion) analysis and computer modelling. The computer-modelled structures are necessarily tentative and, of course, represent isolated systems.

2.4.1 Complexes of the 3,6-dithiaoctanediamide ligands

The formation of silver(I) complexes of the 3,6-dithiaoctanediamide ligands **150b-d**, using silver triflate (CF_3SO_3Ag) and silver nitrate ($AgNO_3$) was attempted.

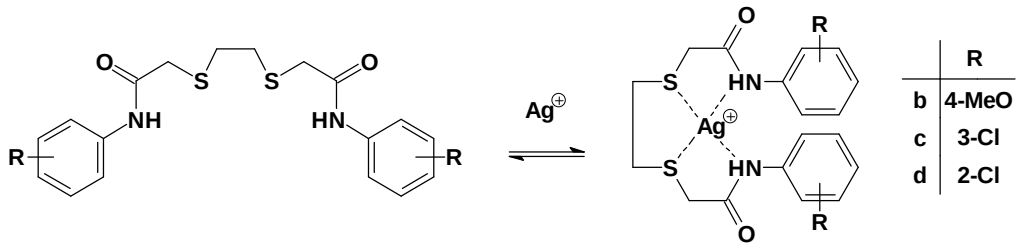

150b-d **151b-d**

The insolubility of these ligands in various organic solvents presented a major difficulty in preparing their silver complexes. The other major problem experienced was the tendency of the complexes to degrade rapidly, making analysis and complete characterization difficult. NMR analysis (^{1}H, ^{13}C, ^{19}F, and ^{109}Ag) of the complexes proved fruitless as, in the NMR solvents used (DMF, DMSO and MeCN), the complexes disproportionated into the free ligand and metal ion. Evidence of complex formation was provided, however, by IR spectroscopy. The changes observed between the IR spectra of the free ligand *N*,*N'*-bis(4-methoxyphenyl)-3,6-dithiaoctanediamide **150b** and its silver(I) complex **151b**, formed with CF_3SO_3Ag, include: - i) a decrease in intensity and a shift in the position of the NH band, from *ca.* 3304 to 3291 cm^{-1}; ii) the shift of a band, attributed to the C-S stretch, from 968 to 958 cm^{-1}; and iii) an increase in the frequency of the carbonyl (υC=O) band from 1655 to 1667 cm^{-1}. These changes suggest coordination between silver and the nitrogen and sulfur donor atoms, the increase in the υC=O band reflecting a decrease

in nitrogen lone-pair delocalization in the complex. The computer-modelled structure of the proposed complex **151b** (**Figure 51**) illustrates such coordination to give a tetrahedral silver(I) ion. The complexes **151c** and **151d** exhibited a similar trend in the shift of the υC=O band to higher frequency, *i.e.* 1664 to 1671 cm^{-1} for **151c** and 1656 to 1680 cm^{-1} for **151d**. No other, significant changes were observed in the IR spectra of these complexes, which we expected to adopt a structure similar to that of complex **151b**.

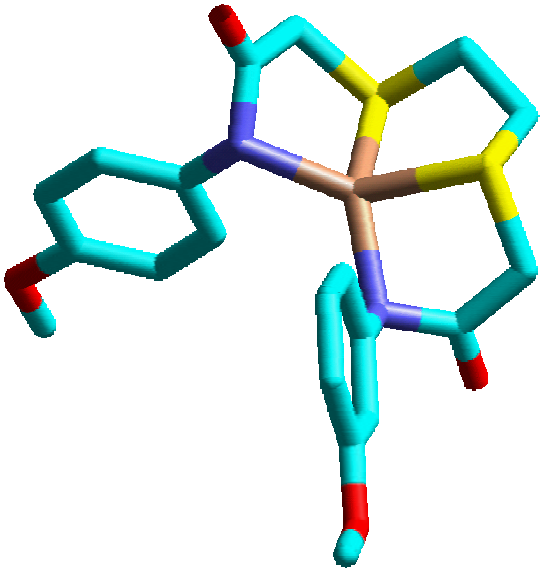

Figure 51. Proposed computer-modelled structure of silver(I) complex **151b**.

2.4.2 Complexes of the Morita-Baylis-Hillman-derived ligands

The formation of metal complexes of the ligands 3-hydroxy-2-(methylsulfanylmethyl)-3-(pyridin-2-yl)propanenitrile **168a** and 3-hydroxy-2-(methoxymethyl)-3-(pyridin-2-yl)propanenitrile **168b** was investigated using the following metal salts: - silver(I) nitrate, copper(II) nitrate, copper(I) acetonitrile hexafluorophosphate, mercury(II) nitrate and lead(II) nitrate.

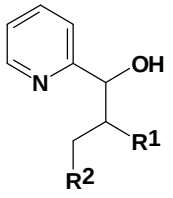

	R^1	R^2
a	CN	SMe
b	CN	OMe

168a,b

The ligands were dissolved in acetone to give 1.0 M solutions, while the metals were typically dissolved in H_2O-acetone (1:1) to 0.5 M solutions [$Pb(NO_3)_2$ was dissolved

in H_2O]. Equal volumes (2.5 ml) of the ligand and metal solutions were stirred together for 1 day and the mixture then left to stand and evaporate. Colour changes (blue to brown) were observed for the copper salts, while all the other solutions changed from colourless to brown. Soon after mixing, the silver solutions formed silver mirrors on the glass of the vessel; the other metal solutions afforded black, intractable masses - attributed to rapid degradation of the ligands in the presence of air and the metal salt. Attempts to prevent degradation of the ligands by performing the reactions under nitrogen were unsuccessful. It was therefore decided that the MBH-derived ligands would not be considered for solvent extraction experiments.

2.4.3 Complexes of the malonamide-derived ligands

The formation of silver(I) and copper(II) complexes of the ligands **180j**, **194-208** was explored using the metal salts, silver(I) triflate and copper(II) nitrate. The complexes were prepared by boiling solutions of the ligands and metal salts under reflux for several hours. IR spectroscopy provided an ideal tool for the identification of the complexes, and the results obtained for the various systems are reported in **Table 22**.

2.4.3.1 *Copper(II) complexes*

From an inspection of the data for the copper complexes (Entries 2, 4, 6, 9, 11 and 14), it is apparent that the NH stretching band (υNH) frequency varies little on complexation, while the υC=O band shows significant shifts to lower frequency. This suggests that coordination involves the carbonyl oxygen atoms, rather than the amide nitrogen donors. For the ligands containing oxygen in the side-chain (Entries 2, 4, 9 and 14), decreases in the C-O stretching band (υCOR) frequencies indicate coordination of copper to the side-chain oxygen atoms. Unfortunately, the C-S stretching band (υCSR) for the ligands containing sulfur atoms in the side-chains could not be identified, due to masking by stronger bands in the region 700 - 600 cm^{-1}.[109,110] Consequently, coordination involving the sulfur donors could not be deduced with any certainty.

Table 22. IR data (cm^{-1}) for the ligands **180j**, **194-208** and their silver(I) and copper(II) complexes.

Entry	Compound	υNH [a]	υC=O [a]	υCOR [a]
1	**180j** 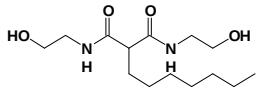	3103	1674	1089 1057 1043
2	**211** Cu(**180j**)$(NO_3)_2$	3092	1624	1077 1049 1040
3	**194** 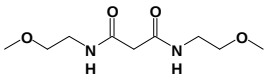	3292	1650 1633	1093
4	**212** Cu(**194**)$(NO_3)_2$	3280	1619	1070
5	**195** 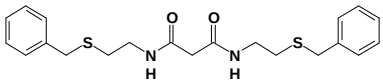	3300 3374 [b]	1630 1678 [b]	- -
6	**213** Cu(**195**)$(NO_3)_2$	3364 [b]	1656 [b]	-
7	**214** CF_3SO_3Ag(**195**)	3356 [b]	1678 [b]	-
8	**196** 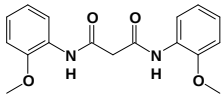	3369 3295	1676	-
9	**215** Cu(**196**)(NO_3)	3314	1676	-
10	**197** 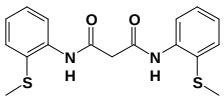	3225	1682 1673	-
11	**216** Cu(**197**)$(NO_3)_2$	3264	1634	-
12	**217** CF_3SO_3Ag(**197**)	3223	1644	-
13	**208** 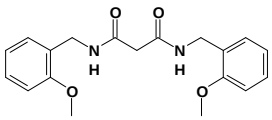	3297	1655	1049 1034 1028
14	**218** Cu(**208**)$(NO_3)_2$	3301	1622	1052 1030 1016

[a] Spectra recorded using KBr discs. [b] Spectra recorded in a CaF_2 solution cell, using MeCN as solvent.

Further information concerning the structures of the copper(II) complexes was provided by the nitrate stretching (υNO_3) band at *ca.* 743 cm^{-1}. All of the copper complexes changed colour on contact with KBr suggesting an ion exchange process. To overcome this, the spectra were recorded in nujol®, which revealed that the nitrate counterion was coordinated to the copper(II) ion in some of the complexes (**218**), but was free in others (**211- 216**). Combustion and FAB-MS analysis of the complexes provided further evidence for the elemental composition of the complexes. The copper complex formed with **195** yielded a paste, which was shown, by IR spectroscopy, to be solvated, but attempts to remove the solvent (EtOAc) proved fruitless. This solvation was also evident in the combustion analysis data of the complex.

The most intriguing copper(II) complex was that formed with ligand **196**. On addition of the ligand to the solution containing the copper(II) ion, a rapid colour change from blue through green to brown, was observed. The IR spectra of the complex formed (**215**) exhibited no changes in the any of the key bands. However, ^{1}H NMR analysis of the complex showed minimal broadening of the proton signals. These factors suggested that the paramagnetic copper(II) ion had been reduced to diamagnetic copper(I); this conclusion was confirmed by the combustion analysis data, which indicated the presence of only one nitrate unit. The composition of the other copper(II) complexes analyzed, proved to be as expected. The proposed, computer-generated structure of the copper(II) complex **211** is illustrated in **Figure 52**.

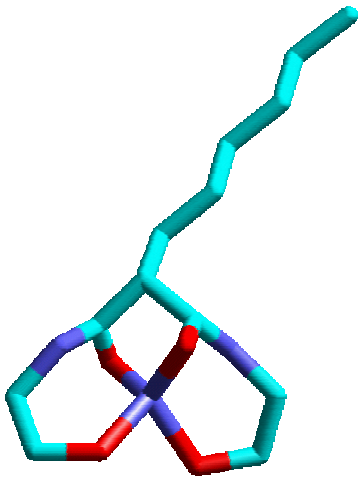

Figure 52. Computer-generated model of the proposed structure of the copper(II) complex **211**.

2.4.3.2 *Silver(I) complexes*

The data for the two-silver(I) complexes listed in **Table 22** (Entries 7 and 12) show some interesting patterns. Both of the ligands **195** and **197** contain sulfur atoms, and as mentioned previously, metal coordination involving these donor atoms could not be confirmed by IR spectroscopy. However, both complexes exhibit minor shifts in the υNH band frequency, while υC=O increases significantly. Unlike the paramagnetic copper(II) complexes, the silver(I) complexes can be studied by ^{1}H NMR spectroscopy and, by using appropriate organic solvents, dissociation of the complex in solution can be avoided. Unfortunately, the ^{1}H NMR spectrum of the complex **217** proved difficult to interpret as the NMR solvent chosen (MeOH-d_4) masks some of the signals. However, the singlet at δ 2.45 ppm, due to the methylsulfanyl group in the ligand, is not masked and its downfield shift to 2.64 ppm in the complex is clearly evident. From the IR and ^{1}H NMR spectroscopic data it is apparent that coordination of silver(I) to the ligand **197** is through the carbonyl oxygen atoms and the methylsulfanyl sulfur, with the triflate counterion coordinated to the metal. The combustion analysis confirmed the empirical formula of the complex, a computer-modelled structure of which is illustrated in **Figure 53**.

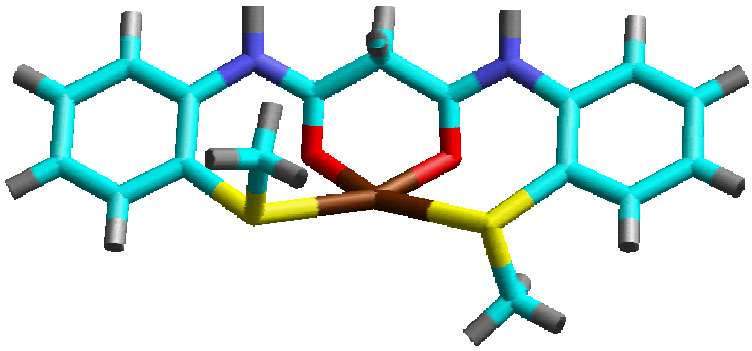

Figure 53. The computer-modelled structure for the silver(I) complex **217**.

The silver(I) complex of ligand **195** was obtained as a paste, and comparison of the IR spectra of the ligand and its complex **214** revealed no significant changes and no evidence of solvation. However, significant differences are apparent in the ^{1}H and ^{13}C NMR spectra (**Figures 54** and **55**, respectively). The broadening of signals in the ^{1}H NMR spectrum of the complex **214** is attributed to the coordination of the metal to the ligand, implying that the complex structure is maintained in solution. It is also

significant that the multiplicities of the signals do not change, suggesting that none of the protons, in particular the amide proton, are lost on complexation. Notable differences between the NMR spectra of the ligand and the complex include[‡] coalescence of the aromatic proton signals into a multiplet; downfield shifts of: - i) the benzyl methylene signal from 3.70 ppm to 3.87 ppm; ii) the signal corresponding to the methylene group nearest to the amide moiety from 3.38 ppm to 3.57 ppm; iii) the sulfanyl methylene signal from 2.55 ppm to 2.97 ppm; iv) the malonyl methylene singlet from 3.10 ppm to 3.32 ppm; and v) the amide proton signal from 7.12 ppm to 7.58 ppm. From the ^{1}H NMR data it is clear that coordination to silver occurs through the amide nitrogen and sulfanyl sulfur donors, while ^{19}F NMR spectroscopy confirmed that the triflate counterion is not coordinated to the metal centre. The FAB-MS spectrum of the product exhibited a fragmentation pattern corresponding to a homodinuclear [Ag_2(195)] complex. This is not totally unexpected, given the examples cited in the introduction. An X-ray crystal structure would be necessary to characterise the complex conclusively, but attempts to obtain a suitable crystal proved fruitless. A tentative, computer-modelled structure for the silver(I) complex **214**, which accommodates the above spectroscopic data, is illustrated in **Figure 56**.

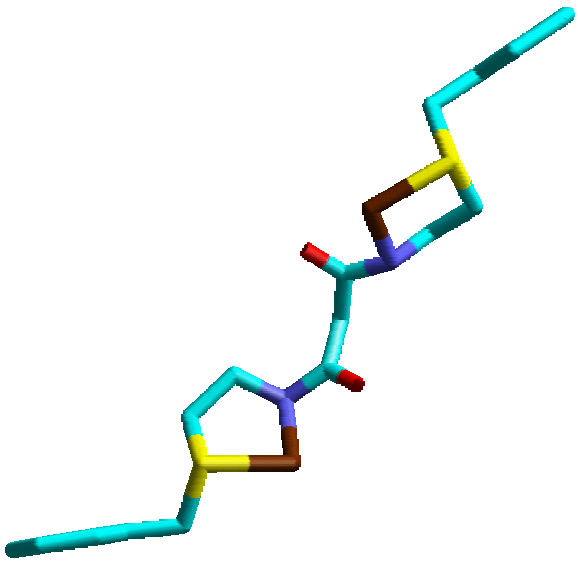

Figure 56. The computer-modelled structure for the silver(I) complex **214**.

[‡] The indicated changes are *from* the free ligand **195** to the complex **214**.

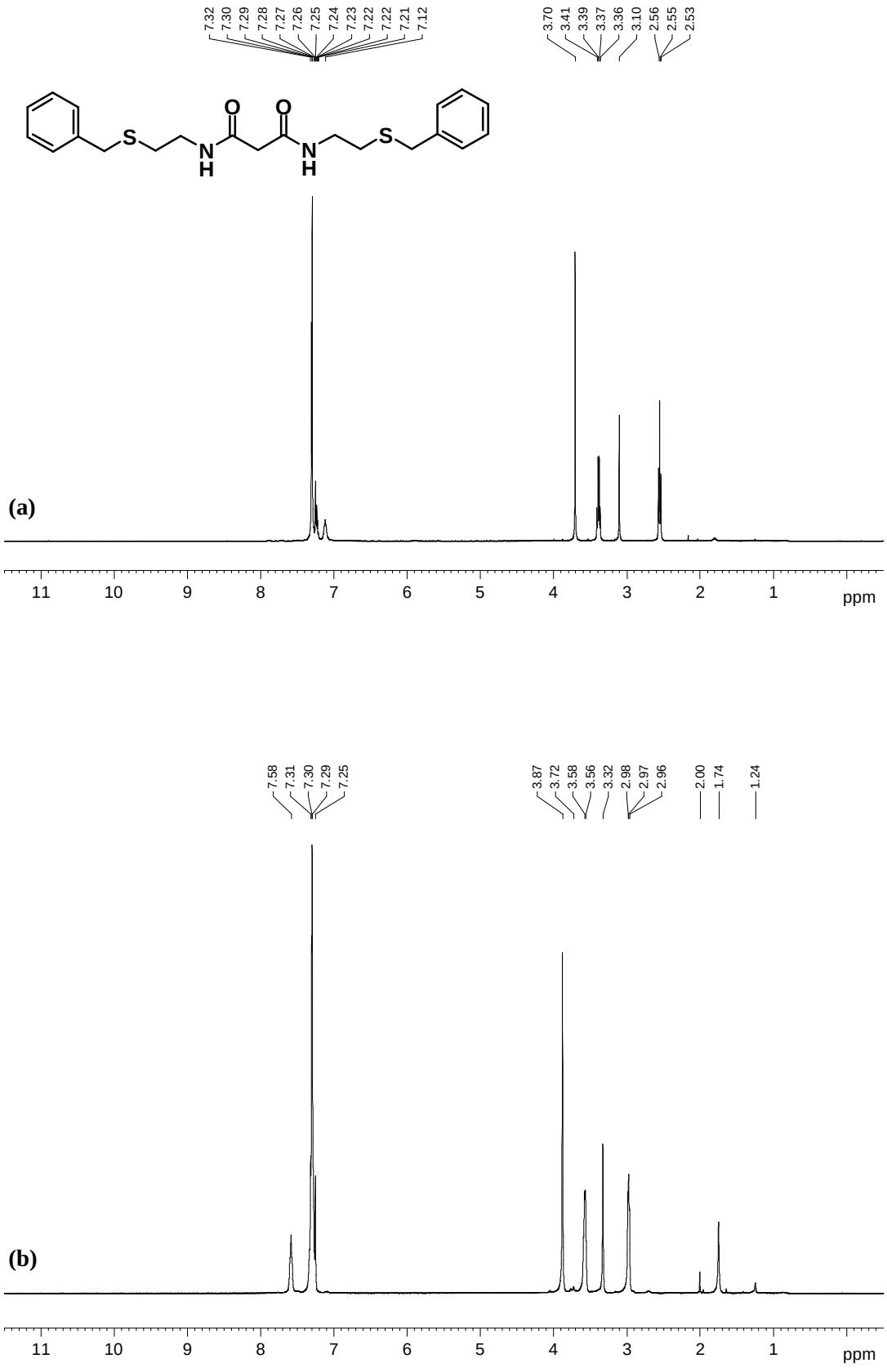

Figure 54. 400 MHz ^{1}H NMR spectrum (a) the free ligand **195**; and (b) the silver(I) complex **214** in $CDCl_3$.

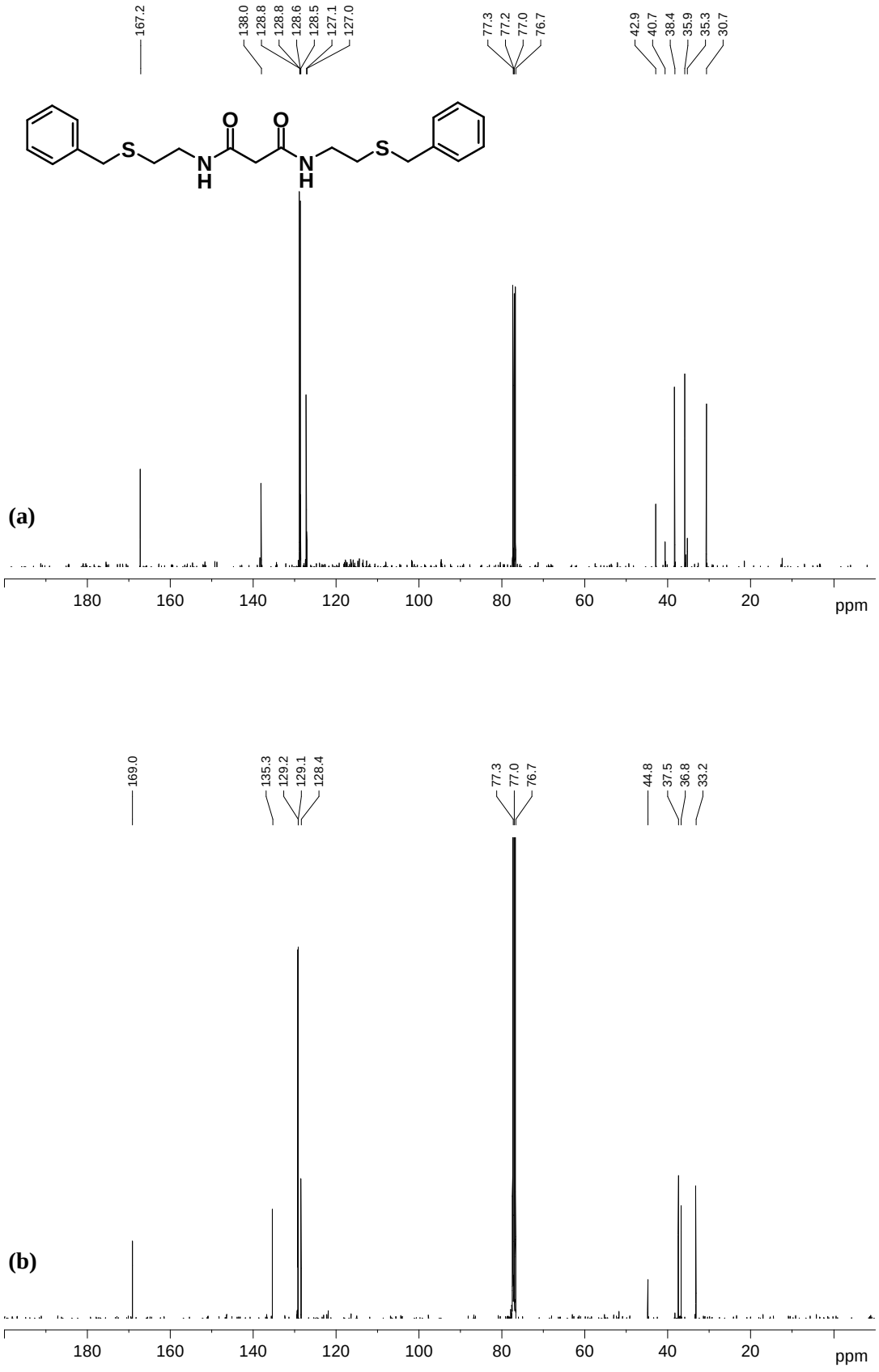

Figure 55. 100 MHz ^{13} C NMR spectrum (a) the free ligand **195**; and (b) the silver(I) complex **214** in $CDCl_3$.

2.5 Solvent Extraction Studies

The main focus of this project has been to extract silver from an ore stream containing 50-100 g/l Ag (4.6-9.3 x 10^{-1} M) in the presence of Cu (2.0-3.0 x 10^{-2} M), Hg (0.05-1.0 x 10^{-1} M), Pb (0.5-9.7 x 10^{-2} M) and possibly Au (0.05-1.0 x 10^{-1} M) in a 6M-nitric acid medium,[111] using a solvent extraction system. Certain conditions were placed on the solvent extraction abilities of the ligands, *viz.*, they should be stable under highly acidic conditions and should effect significant extraction of the metal within 5 minutes. In other words, the distribution equilibrium of the metal between the aqueous and organic phases should be reached within 5 minutes.[111]

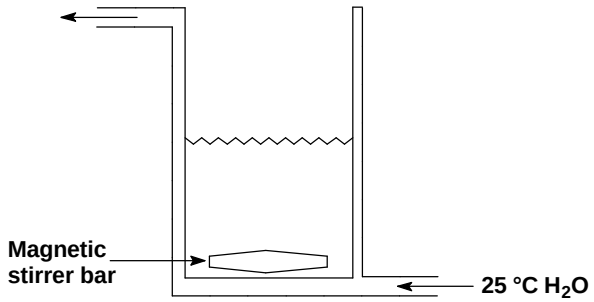

Figure 57. The jacketed beaker used in solvent extraction studies.

In order to study the efficiency of the ligands, which we had synthesised, the conditions used in industry were reproduced as closely as possible, but lower concentrations of metals ions (<25 ppm) and ligands were used. The methodology described by Sole[112] was followed for all extraction experiments, with the experiments being carried out in a jacketed 150 ml beaker (see **Figure 57**), kept at a constant temperature of 25 °C by circulating heated water through the jacket from a thermostatically-controlled water-bath. Equal volumes (50 ml) of aqueous and organic phases were mixed vigorously, for the duration of each experiment, in order to maximize the surface contact between the phases. At regular time intervals, suitable, equal aliquots (< 5 ml) of both the aqueous and organic phases were removed, and the aqueous phase was analyzed for the residual metal content. The influence of pH on the extraction ability of the ligands was studied using the same methodology, but small volumes of concentrated NaOH were added to increase the pH, which was measured using a pH meter. The results obtained for the various ligand systems studied are discussed below.

2.5.1 Metal extraction using the 3,6-dithiaoctanediamide ligands

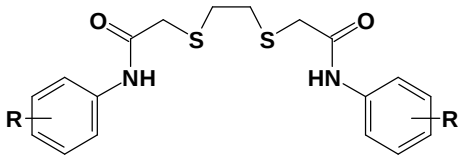

	R
a	H
b	4-MeO
c	3-Cl
d	2-Cl
e	2-Me
f	2-MeO

150a-f

The 3,6-dithiaoctanediamide ligands **150a-f** were investigated for their ability to extract silver(I) and palladium(II).[113] (Palladium extraction was examined in order to compare the results obtained in the present study with those reported previously by Hagemann.[78]) Due to the relative insolubility of these ligands in most organic solvents, the ligand concentration in the organic phase (toluene) was limited to the range 2.1-2.8 x 10^{-3} M (1000 ppm). In order to maintain the overall ionic strength of the aqueous phase during extraction, the aqueous phase comprised a 1.0 x 10^{-1} M $NaNO_3$ solution for the silver extraction and 1.0 x 10^{-1} M NaCl solution for the palladium extractions. For both metals, the starting concentrations were 2.3 x 10^{-4} M (25 ppm). The extraction studies were performed at 25 °C and pH 1.7. Unfortunately, under these conditions, vigorous stirring resulted in the formation of emulsions within 5 minutes. By increasing the temperature to 40 °C and the pH to 7, the formation of an emulsion was avoided only in the case of the ligand, *N*,*N´*-bis(3-chlorophenyl)-3,6-dithiaoctanediamide **150c**. The residual, aqueous metal concentrations were determined by atomic absorption spectroscopy (AAS), and the resulting extraction curves obtained for this ligand are illustrated in **Figure 58**. The ligand **150c** extracted palladium as expected, with similar efficiency (*ca.* 98 % for palladium within 10 minutes) to that reported by Hagemann.[78] However the ligand did not extract silver to the same extent; as can be seen from the curves, distribution equilibrium between the aqueous and organic phases was only reached after *ca.* 0.5 h, with an extraction efficiency of *ca.* 90 %. Given their tendency to form emulsions and the long equilibration period for the extraction of silver, the 3,6-dithiaoctanediamide ligands were not examined further.

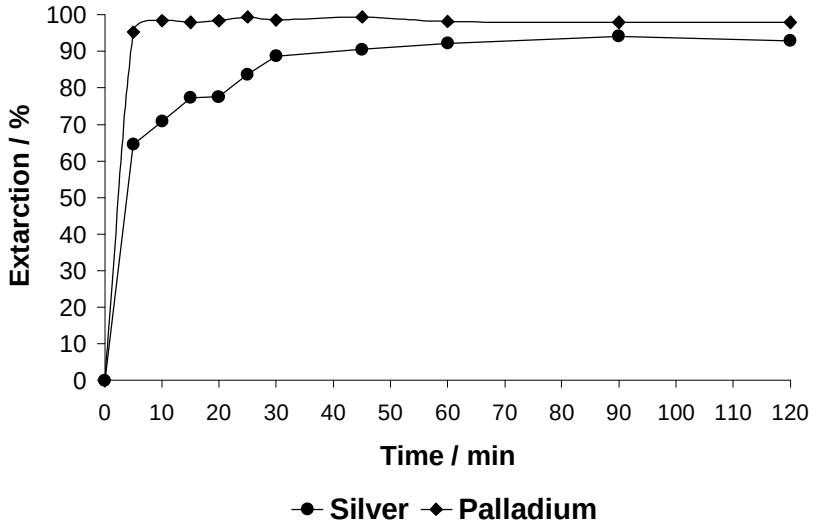

Figure 58. The extraction efficiency of *N,N´*-bis(3-chlorophenyl)-3,6-dithia-octanediamide **150c** in toluene at 40 °C and pH 7 for palladium(II) and silver(I).

2.5.2 Silver(I) extraction using the malonamide ligands

The ability of the malonamide ligands to extract silver(I) was investigated using the methodology described in the previous section. In preliminary extraction studies, the metal ion concentration was 9.3 x 10^{-5} M (10 ppm) and the ligand concentration approximately 1.8 x 10^{-2} M (*i.e.* a 200 fold excess with respect to silver). Ethyl acetate was used as the organic phase; and the ionic strength was maintained by a 2.5 x 10^{-2} M $NaNO_3$ solution. AAS was used to determine the residual aqueous silver(I) concentration, and a typical calibration curve, which exhibits the required linearity (R^2 = 0.996), is illustrated in **Figure 59**.

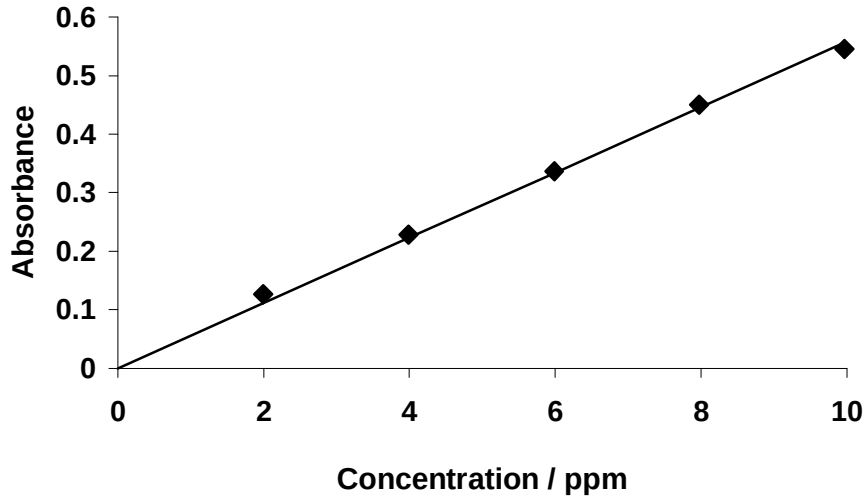

Figure 59. A typical calibration curve for the AAS analysis of silver(I).

To determine the appropriate time-scale for the extraction experiments, a study was undertaken using 2-hexyl-*N*,*N*´-bis(2-hydroxyethyl)malonamide **180h**, and the residual aqueous silver(I) concentration determined at 5-minute intervals during a 15-minute period. The resulting extraction curve is shown in **Figure 60**.

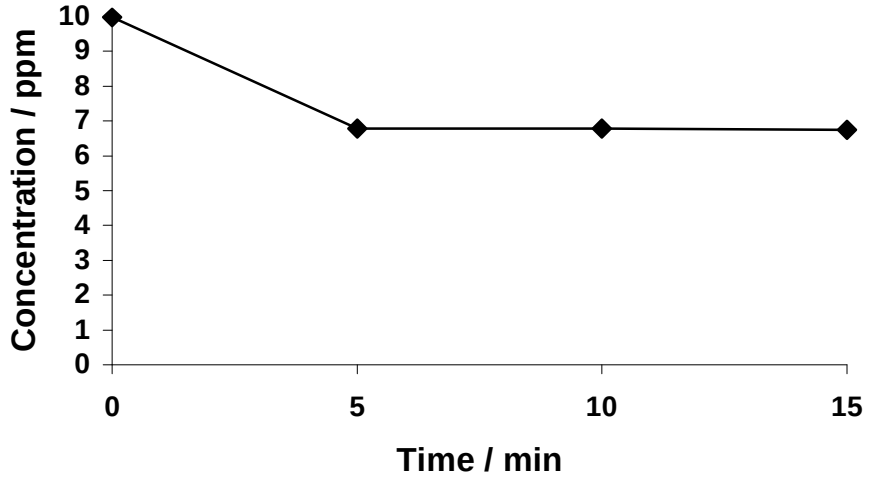

Figure 60. The change in silver(I) concentration during extraction using the ligand 2-hexyl-*N*,*N*´-bis(2-hydroxyethyl)malonamide **180h** in EtOAc.

From **Figure 60** it is apparent that 15 minutes was more than adequate for an extraction experiment, and this time limit was used for all subsequent extraction experiments. The results obtained for the extraction of silver(I) using the series of malonamide ligands are summarized in **Table 23**.

Table 23. Data for the extraction of silver(I) using the malonamide ligands.[a]

Ligand		Extraction efficiency [b] / %
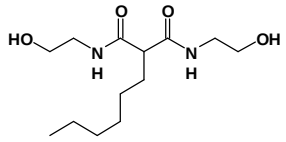	**180h**	32
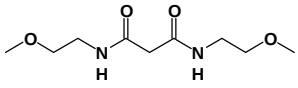	**194**	18
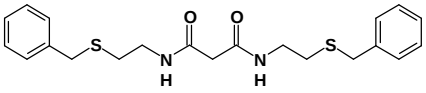	**195**	97
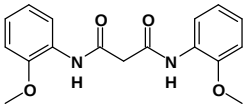	**196**	10 (42) [c]
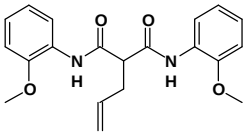	**207**	34
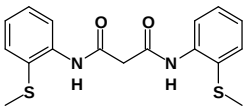	**197**	12 (35) [c]
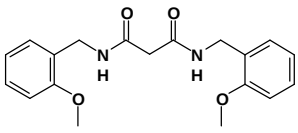	**208**	19

[a] All extractions performed at pH 2.78 and at 25 °C with EtOAc and an aqueous solution containing 10 ppm Ag in a 2.5 x10^{-2} M $NaNO_3$ solution. [b] Extraction efficiency determined by AAS analysis after 15 min. [c] Extraction performed using a 0.25 M $NaNO_3$ solution.

The first comment that can be made concerning the results listed in **Table 23**, is that very few of the ligands show any real potential to extract silver(I). Ligands **180h** and **207** show moderate extraction performance (*ca.* 33 %). Ligands **194** and **208** extract

silver(I) with even less efficiency (*ca.* 18 %), while ligands **196** and **197** perform very poorly (*ca.* 11 %).

Of all the malonamide ligands examined, *N*,*N*´-bis(2-benzylsulfanylethyl)malonamide **195** clearly performed the best with an extraction efficiency of no less than 97 % at pH 2.78. To determine whether the extraction ability of this ligand was affected by a change in pH, extraction studies were carried out at various pH values; the results are illustrated in **Figure 61**. It is evident from **Figure 61** that *N*,*N*´-bis(2-benzylsulfanylethyl)malonamide **195** extracts silver(I) most efficiently at lower pH, but maintains very good overall extraction efficiency (*i.e.* above 95 %) over the pH range 2.5-9.0. This ligand thus clearly meets the design criteria of efficient silver(I) extraction at low pH.

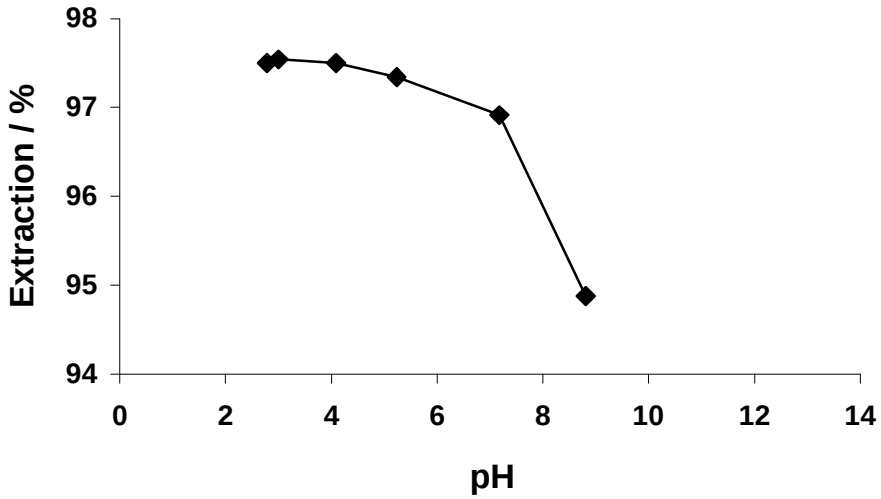

Figure 61. Effect of pH on the silver(I) extraction efficiency of the ligand *N*,*N*´-bis(2-benzylsulfanylethyl)malonamide **195**.

The various starting materials, used for the construction of the malonamide ligands, contain donor atoms and could, conceivably, act as ligands in their own right. Consequently, for comparative purposes, their ability to extract silver(I) was also examined; these results are reported in **Table 24**.

Table 24. Data for the extraction of silver(I) using malonamide ligand precursors.[a]

Compound		Extraction efficiency [b] / %
Diethyl malonate	**175**	15
2-Ethanolamine	**179**	16
Mercaptoethanol	**186**	38
2-Methoxyethylamine	**189**	14
S-Benzylcysteamine	**190**	13
o-Anisidine	**191**	15
2-Methylsulfanylphenylamine	**192**	15
2-Methoxybenzylamine	**193**	22

[a] All extractions performed at pH 2.78 and at 25 °C with EtOAc and a aqueous solution containing 10 ppm Ag in a 2.5 x10^{-2} M $NaNO_3$ solution. [b] Extraction efficiency determined by AAS analysis after 15 min.

Table 24 reveals that, in most cases, the precursors extract silver(I) with efficiencies that are similar to or less than the respective malonamide ligands of which they form part. It is interesting to note the efficiency with which mercaptoethanol extracts silver(I), as it is clearly the most efficient of all the precursors.

The project brief has been to design ligands which not only extract silver(I) efficiently at low pH, but do so in the presence of certain base metals, *viz.*, copper, lead, mercury and gold. To test how selective these ligands were for silver(I) in a competitive environment, extraction studies were performed using the malonamide ligands **180h**, **195**, **196**, **197** and **208** in EtOAc and a mixed metal ion aqueous phase, containing $NaNO_3$ (2.5 x 10^{-2} M) to maintain ionic strength and 10 ppm of each of the following metals: - a) silver (9.3 x 10^{-5} M); b) lead (4.8 x 10^{-5} M); c) mercury (5.0 x 10^{-5} M); and d) copper (1.6 x 10^{-4} M). The aqueous samples were analyzed by Inductively Coupled Plasma-Mass Spectroscopy (ICP-MS), with each metal ion being detected as two of its isotopes; the initial, overall results are illustrated in **Figure 62**.

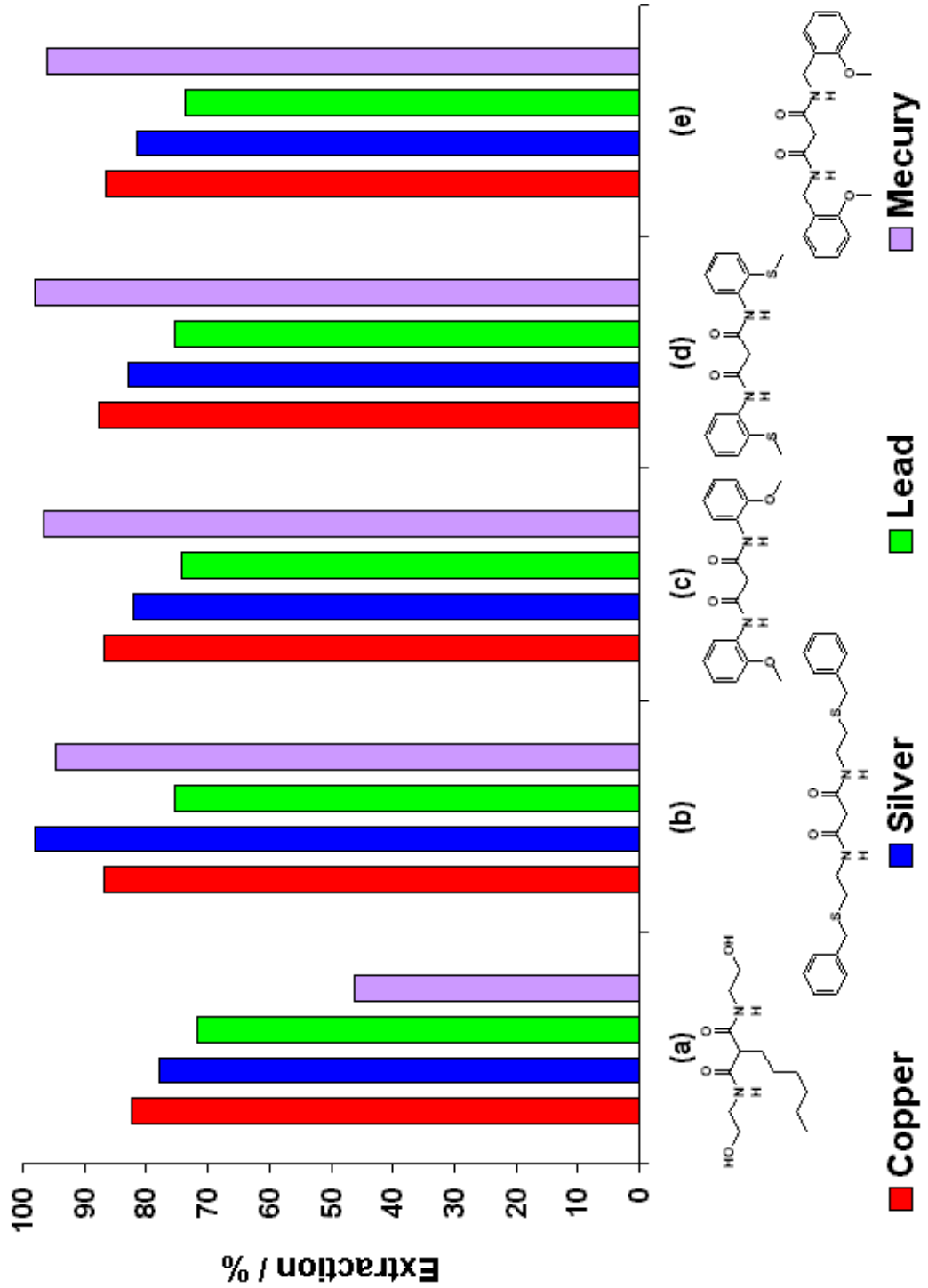

Figure 62. ICP-MS data for the extraction efficiency of the malonamide ligands for the metals, copper, silver, mercury and lead: -

a) 2-Hexyl-*N*,*N*´-bis(2-hydroxyethyl)malonamide **180h**,
b) *N*,*N*´-bis(2-benzylsulfanylethyl)malonamide **195**,
c) *N*,*N*´-bis(2-methoxyphenyl)malonamide **196**,
d) *N*,*N*´-bis(2-methylsulfanylphenyl)malonamide **197**,
e) *N*,*N*´-bis(2-methoxybenzyl)malonamide **208**.

A number of problems with the initial ICP-MS data set were immediately apparent.

1. It is clearly evident from a comparison of **Figure 62** and **Table 23** that the ICP-MS data for silver(I) do not correlate well with the AAS data.
2. With the exception of ligand **195**, the ligands all appear to exhibit the same trend in extraction efficiency, *i.e.* copper > silver > lead.
3. The mercury results show an increase in concentration with successive analyses and were discounted due to the apparent build up of mercury on the detector.
4. Careful investigation revealed that the ICP-MS results are severely influenced by the presence of any organic solvent in the aqueous phase - clearly a major problem since the aqueous phase was likely to be saturated with the organic solvent during the extraction process.

To correct for these problems, the extraction experiments and ICP-MS analyses were repeated, excluding mercury from the aqueous phase and concentrating each aqueous phase sample on a steam bath to remove all traces of the organic solvent; the samples were then diluted to the appropriate volume prior to analysis. The results obtained are illustrated in **Figure 63**, from which it is clearly evident that there is a radical improvement in the ICP-MS data obtained, using this method. In fact, these ICP-MS results for silver(I) are very similar to those obtained using AAS analysis.

In general, the malonamide ligands **180j**, **196**, **197** and **208** exhibit selectivity for silver over copper and lead, but with relatively low extraction efficiencies. In striking contrast are the results for the *N,N´*-bis(2-benzylsulfanylethyl)malonamide **195** - clearly the best in the series of ligands studied.

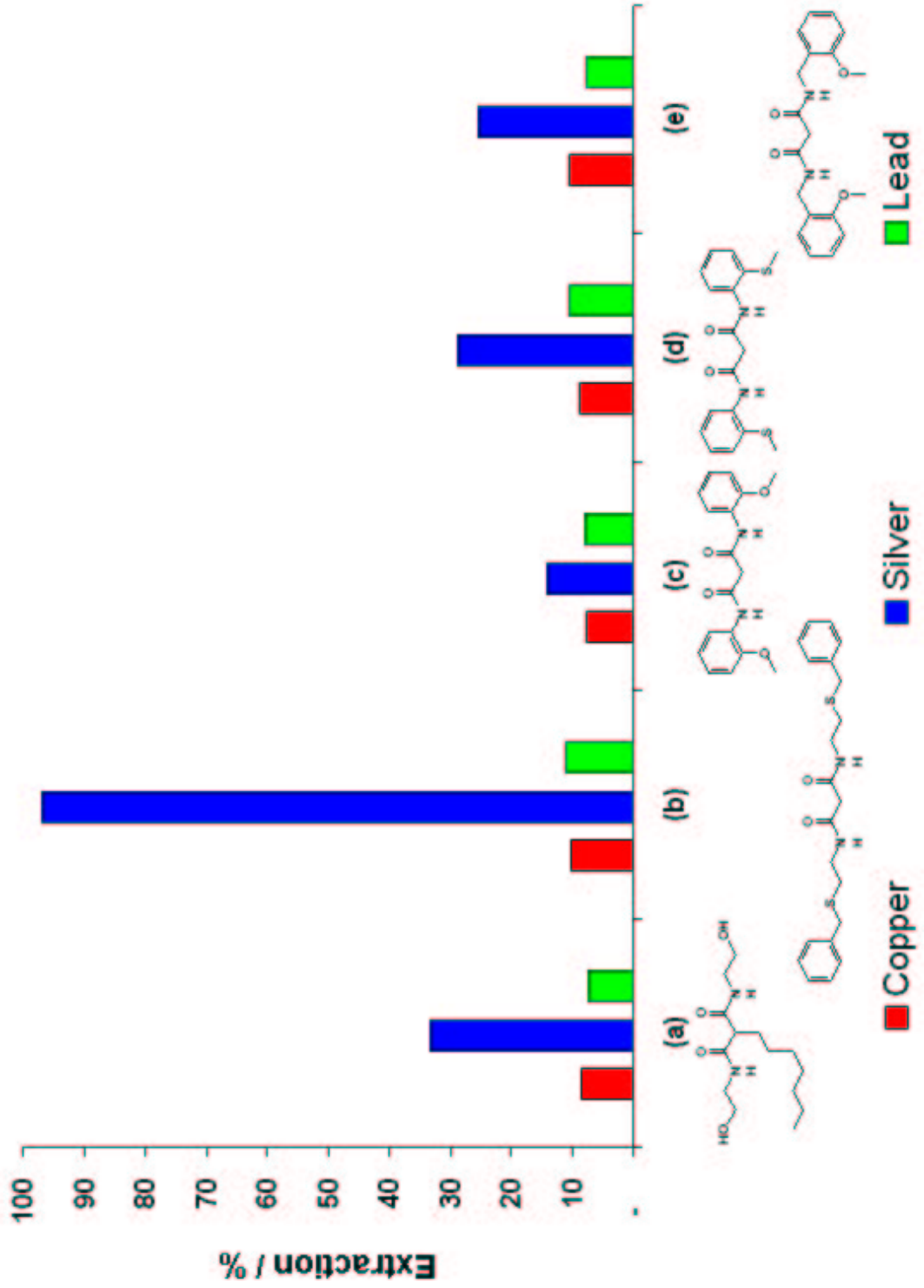

Figure 63. ICP-MS data for the extraction efficiency of the malonamide ligands for the metals, copper, silver and lead: -

a) 2-heptyl-*N*,*N*´-bis(2-hydroxyethyl)malonamide **180j**.
b) *N*,*N*´-bis(2-benzylsulfanylethyl)malonamide **195**.
c) *N*,*N*´-bis(2-methoxyphenyl)malonamide **196**.
d) *N*,*N*´-bis(2-methylsulfanylphenyl)malonamide **197**.
e) *N*,*N*´-bis(2-methoxybenzyl)malonamide **208**.

As can be seen from **Figures 63** and **64**, the ligand **195** exhibits remarkable selectivity, extracting silver(I) with an efficiency of no less than 97 % for both isotopes (a result which correlates well with the previously obtained data by AAS analysis), while copper(II) and lead(II) are extracted with efficiency levels of only *ca.* 10 %! The malonamide **195**, which contains two amide nitrogens and two alkyl sulfur donors, is clearly a highly efficient silver(I)-specific ligand.

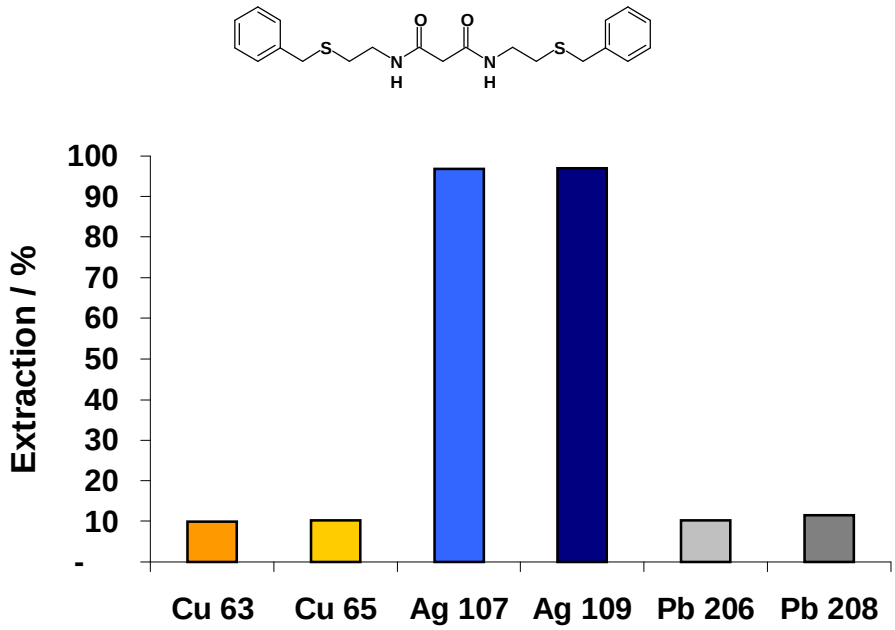

Figure 64. ICP-MS isotope extraction results for the ligand *N,N´*-bis(2-benzylsulfanylethyl)malonamide **195**.

2.6 Conclusions

The aim of this study was to develop a silver-specific ligand for the solvent extraction of silver(I) from nitric acid media containing base metals. A search of the literature revealed certain ligand characteristics necessary for silver(I) specificity, *viz.*, soft donor atoms (nitrogen and sulfur) and appropriate spacer groups. Certain ligands, previously synthesised by the Rhodes group, appeared to contain these desired features. Thus, a series of 3,6-dithiaoctanediamide derivatives were prepared by the condensing acetanilides with 1,2-dibromoethane, and a series of propanenitrile and propanoic ester derivatives were prepared from pyridine-2-carbaldehyde *via* the Morita-Baylis-Hillman (MBH) reaction. The 3,6-dithiaoctanediamides, however, proved too insoluble in organic solvents and formed emulsions during the extraction studies, rendering them useless as extraction reagents for silver(I). The MBH-derived ligands degraded rapidly in the presence of metals and, as a result, were not investigated further.

Attention was consequently turned to the use of malonic esters and malonamides which contained sulfur or oxygen donor atoms. A series of (2-hydroxyethyl)malonamides were prepared by reacting substituted malonic esters with ethanolamine, while a series of substituted malonamides were prepared from the reaction of diethyl malonate and various primary amines. A novel method of preparing the substituted malonamides was also developed, involving the use of microwave irradiation. The application of microwave-assisted synthesis afforded the target ligands rapidly and efficiently, with overall reaction times of 4.5 - 6 minutes, compared to the 24 h or more required for classical thermal reactions.

The electron-impact mass spectral fragmentation patterns exhibited by the malonamides **180j**, **194**, **195**, **196**, **197**, **198**, **207** and **208** were explored using high-resolution MS and meta-stable peak scanning techniques. Significant differences were apparent between the fragmentation patterns observed for the "alkyl-spacer"-containing ligands and the "aromatic-spacer"-containing ligands. The former fragmented to yield several common ion types, of which two were identified as acylium ions. The "aromatic-spacer"-containing ligands fragmented along simpler

pathways, to yield a number of common ion types, of which the most abundant was the primary amino radical cation.

The use of computer modelling at the molecular mechanics level provided useful insights into the coordination and solvent extraction potential of the ligands synthesised. Given the underlying assumptions, conclusions based on such modelling are necessarily tentative and, not surprisingly, there were discrepancies between the predicted and experimentally observed properties. Copper(II) and silver(I) complexes of the malonamide ligands were synthesised but, unfortunately, none of the complexes afforded material suitable for single crystal X-ray analysis. Consequently, IR, NMR, MS and elemental analysis data were used, together with molecular modelling, to propose structures for these complexes.

The metal extraction properties of the synthetic ligands were, of course, critical to the overall success of the project, and solvent extraction studies revealed that several of the malonamide ligands showed good selectivity towards silver(I) in the presence of copper(II) and lead(II) at low pH. All of the ligand-metal systems studied were shown to reach equilibrium within 5 minutes - an important property for a solvent extraction system intended for industrial application. Of the malonamide ligands examined, the *N*,*N*´-bis(2-benzylsulfanylethyl)malonamide **195** ligand emerged clearly as the most efficient and selective ligand [> 97 % for silver(I)] over a wide pH range (2.5 - 9.0); the base metals were extracted with much lower efficiencies [Cu(II): 10 %; Pb(II): 11 %]. This ligand system, which contains two amide nitrogen and two sulfur donor atoms, appears to have significant potential for commercial development.

Future research in this area is expected to include: -

(i) conclusive elucidation of the structures of the silver(I) complexes **214** and **217**, and the copper(II) complexes **211**, **212**, **213**, **215**, **216** and **218**;

(ii) the synthesis of malonamide derivatives, similar to ligand **195** but containing different spacer groups;

(iii) the synthesis and investigation of dithiomalonamide derivatives; and

(iv) refinement of the computer modelling methodology.

3 Experimental

All reagents were purchased from Aldrich, Merck or Fluka and used without further purification.

NMR spectra were recorded on a Bruker 400 MHz AVANCE spectrometer at 303 K. Chemical shifts are reported relative to the solvent peaks (δ_H : 7.25 ppm for $CDCl_3$ ($CHCl_3$), 2.50 ppm for DMSO-d_6 (DMSO-d_5); δ_C : 77.0 ppm for $CDCl_3$, 39.43 ppm for DMSO-d_6). IR spectra were recorded on a Perkin-Elmer FT-IR Spectrum 2000 spectrophotometer, using KBr discs, NaCl windows or a CaF_2 solution cell. The AAS data were acquired on a Varian AA-1275 spectrophotometer at MINTEK, and a GBC 909AA spectrophotometer using an air-acetylene flame. The ICP-MS data were obtained by the Metal Separations Group at the University of Port Elizabeth. Low-resolution mass spectra were recorded on a Finnigan GCQ instrument, the high-resolution mass spectra and FAB-MS spectra were recorded at the Cape Technikon Mass Spectroscopy Unit. All melting points were determined on a Kofler hot-stage and are uncorrected. Combustion analyses were obtained by Dr. Bencasa of the Department of Chemistry at the University of Cape Town.

The microwave oven used in synthesis was an unmodified 1000 W DEFY domestic multimode oven, operating at 2.45 GHz, with five power level settings.

The software programs Cerius$^{2®86}$ 4.0 and PC Spartan Pro[107] were used for the computer modelling on a SGI O^2 and pentium III machines, respectively.

3.1 Synthetic Procedures

3.1.1 Synthesis 3,6-dithiaoctanediamide-derived ligands

N-*Phenyl-2-sulfanylacetanilide* 149a[78]

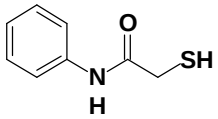

A mixture of aniline (4.10 g, 44.0 mmol) and 2-sulfanylacetic acid (3.93 g, 42.6 mmol) was stirred for 2 hours at 110-120 °C under a dry nitrogen atmosphere. The mixture solidified on cooling and was crushed into a fine powder under H_2O. The powder was then filtered off, washed with dilute HCl and then with H_2O, and dried *in vacuo*. The powder was recrystallised from EtOH and washed with Et_2O to afford, as colourless crystals, *N*-phenyl-2-sulfanylacetanilide **149a** (3.11 g, 57 %), mp 111 °C (from EtOH) (lit.,[78] 110-111 °C); δ_H(400 MHz; $CDCl_3$) 2.02 (1H, t, *J* 9.2 Hz, SH), 3.38 (2H, d, *J* 9.2 Hz, C***H***$_2$SH), 7.13 (1H, t, *J* 7.4 Hz, ArH), 7.33 (2H, t, *J* 7.9 Hz, ArH), 7.53 (2H, d, *J* 7.9 Hz, ArH) and 8.50 (1H, br s, NH); *m/z* (EI)167 (M^+, 60 %) and 93 (100).

N-*(4-Methoxyphenyl)-2-sulfanylacetanilide* 149b[78]

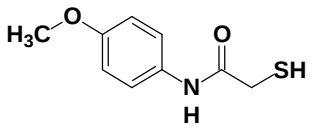

The experimental procedure described for the synthesis of *N*-phenyl-2-sulfanylacetanilide **149a** was followed, using 4-methoxyaniline (5.08g, 41.3 mmol) and 2-sulfanylacetic acid (3.74 g, 40.6 mmol). The crude product was recrystallised from aqueous EtOH to afford, as grey plates, *N*-(4-methoxyphenyl)-2-sulfanylacetanilide **149b** (7.89 g, 99 %), mp 118 °C (from EtOH) (lit.,[78] 118.5-119.5 °C); δ_H(400 MHz; $CDCl_3$) 1.86 (1H, t, *J* 8.3 Hz, SH), 2.81 (2H, d, *J* 8.3 Hz, C***H***$_2$SH), 3.29 (3H, s, CH_3O) 6.34 (2H, m, ArH), 7.03 (2H, m, ArH) and 9.26 (1H, br s, NH).

N-*(3-Chlorophenyl)-2-sulfanylacetanilide* 149c[78]

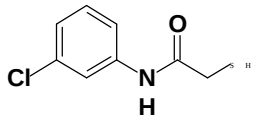

The experimental procedure described for the synthesis of *N*-phenyl-2-sulfanylacetanilide **149a** was followed using 3-chloroaniline (4.16 g, 32.6 mmol) and 2-sulfanylacetic acid (3.04 g, 33.0 mmol) to afford, as a white solid, *N*-(3-chlorophenyl)-2-sulfanylacetanilide **149c** (6.20 g, 93 %), mp 72-73 °C (from EtOH) (lit.,[78] 70-73 °C); δ_H(400 MHz; $CDCl_3$) 2.09 (1H, t, *J* 9.2 Hz, SH), 3.11 (2H, d, *J* 9.2 Hz, C***H***$_2$SH), 7.20-7.96 (4H, m, ArH) and 9.92 (1H, br s, NH).

N-*(2-Chlorophenyl)-2-sulfanylacetanilide* 149d[78]

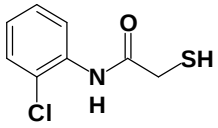

The experimental procedure described for the synthesis of *N*-phenyl-2-sulfanylacetanilide **149a** was followed using 2-chloroaniline (5.55 g, 43.5 mmol) and 2-sulfanylacetic acid (4.17 g, 45.3 mmol). No precipitate formed on pouring the mixture into cold water. The mixture was acidified by the addition of several drops of conc. HCl and then extracted with $CHCl_3$ (3x 30 ml). The combined $CHCl_3$ extracts were washed with 10 % aqueous NaOH. The NaOH washings were acidified with 32 % HCl before being extracted with $CHCl_3$. The combined $CHCl_3$ extracts were dried over anhyd. $MgSO_4$, and the solvent was removed *in vacuo* to yield, as a white solid, *N*-(2-chlorophenyl)-2-sulfanylacetanilide **149d** (2.61 g, 29 %), mp 60 °C (from $CHCl_3$) (lit.,[78] 56-59 °C); δ_H(400 MHz; $CDCl_3$) 2.08 (1H, t, *J* 9.3 Hz, SH), 3.48 (2H, d, *J* 9.3 Hz, C***H***$_2$SH), 7.09 (1H, t, *J* 7.6 Hz, ArH), 7.30 (1H, t, *J* 8.2 Hz, ArH), 7.41 (1H, d, *J* 8.0 Hz, ArH), 8.38 (1H, d, *J* 8.2 Hz, ArH) and 9.17 (1H, br s, NH).

N-*(2-Methylphenyl)-2-sulfanylacetanilide* 149e[78]

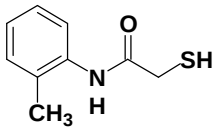

The experimental procedure described for the synthesis of *N*-phenyl-2-sulfanylacetanilide **149a** was followed using 2-methylaniline (3.68 g, 34.3 mmol) and 2-sulfanylacetic acid (3.13 g, 34.0 mmol) to afford, as a white powder, *N*-(2-methylphenyl)2-sulfanylacetanilide **149e** (5.29 g, 86 %), mp 91 °C (from EtOH) (lit.,[78] 88-91 °C); δ_H(400 MHz; $CDCl_3$) 2.03 (1H, t, *J* 9.3 Hz, SH), 2.30 (3H, s, CH_3Ar), 3.43 (2H, d, *J* 9.3 Hz, C***H***$_2$SH), 7.06-7.24 (3H, m, ArH), 7.89 (1H, d, *J* 8.0 Hz, ArH) and 8.51 (1H, br s, NH).

N-*(2-Methoxyphenyl)-2-sulfanylacetanilide* 149f[78]

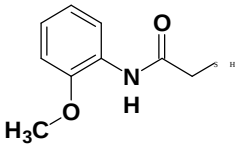

The experimental procedure described for the synthesis of *N*-phenyl-2-sulfanylacetanilide **149a** was followed using 2-methoxylaniline (4.09 g, 33.2 mmol) and 2-sulfanylacetic acid (3.05 g, 33.2 mmol) to afford, as light grey solid, *N*-(2-methoxylphenyl)-2-sulfanylacetanilide **149f** (4.14 g, 63 %), mp 66 °C (from EtOH) (lit.,[78] 64-66 °C); δ_H(400 MHz; $CDCl_3$) 2.00 (1H, t, *J* 8.7 Hz, SH), 3.12 (2H, d, *J* 8.7 Hz, C***H***$_2$SH), 3.61 (3H, s, CH_3O), 6.70 (3H, m, ArH), 7.93 (1H, d, *J* 7.3 Hz, ArH) and 8.77 (1H, br s, NH).

N,N´-*Diphenyl-3,6-dithiaoctanediamide* 150a[78]

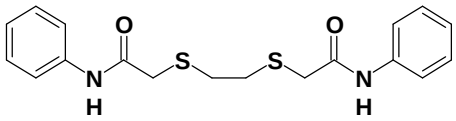

A solution of *N*-phenyl-2-sulfanylacetanilide **149a** (1.70 g, 10.2 mmol) and KOH (0.57 g, 10 mmol) in MeOH (60 ml) was added dropwise to a stirred solution of 1,2-dibromoethane (0.95 g, 5.1 mmol) in MeOH (20 ml). The mixture was stirred at room temperature for 24 h; H_2O (30 ml) was then added and the MeOH evaporated *in vacuo*. The residual aqueous solution was extracted with EtOAc (3x 30 ml). The

combined EtOAc extracts were dried over anhyd. $MgSO_4$ and the solvent was then removed *in vacuo*. The residue was recrystallised from EtOH to yield, as white crystals, *N,N´*-diphenyl-3,6-dithiaoctanediamide **150a** (1.02 g, 56%), mp 159-161 °C (from EtOH) (lit.,[78] 150-152 °C); ν_{max}(KBr)/cm^{-1} 3295 (NH) and 1660 (CO); δ_H(400 MHz; DMSO-d_6) 2.91 (4H, s, SC***H***$_2$CH$_2$), 3.34 (4H, s, COCH$_2$S), 7.05 (2H, t, *J* 7.3 Hz, ArH), 7.30 (4H, t, *J* 7.8 Hz, ArH), 7.57 (4H, d, *J* 7.8 Hz, ArH) and 10.05 (2H, br s, NH); δ_C(100 MHz; DMSO-d_6) 31.5 (C-4 and C-5), 35.2 (C-2 and C-7) 119.1, 123.3, 128.6 and 138.8 (ArC) and 167.9 (CO); *m/z* (EI) 360 (M^+, 12 %) and 120 (100).

N,N´-*Bis(4-methoxyphenyl)-3,6-dithiaoctanediamide* 150b[78]

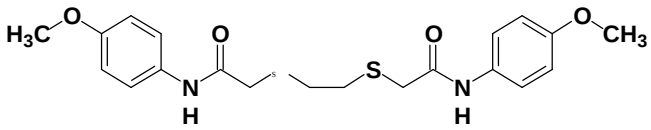

The experimental procedure described for the synthesis of *N,N´*-diphenyl-3,6-dithiaoctanediamide **150a** was followed, using *N*-(4-methoxyphenyl)-2-sulfanylacetanilide **149b** (5.36 g, 27.2 mmol), 1,2-dibromoethane (2.54 g, 13.5 mmol) and KOH (1.71 g, 30.6 mmol). The residue was recrystallised from EtOH-H_2O to afford, as light grey crystals, *N,N´*-bis(4-methoxyphenyl)-3,6-dithiaoctanediamide **150b** (4.66 g, 82 %), mp 180-182 °C (from EtOH-H_2O) (lit.,[78] 163-165 °C); ν_{max}(KBr)/cm^{-1} 3304 (NH) and 1659 (CO); δ_H(400 MHz; DMSO-d_6) 2.90 (4H, s, SC***H***$_2$CH$_2$), 3.31 (4H, s, COCH$_2$S), 3.71 (6H, s, OCH$_3$), 6.87 (4H, d, *J* 9.0 Hz, ArH), 7.47 (4H, d, *J* 9.0 Hz, ArH) and 9.99 (2H, br s, NH); δ_C(100 MHz; DMSO-d_6) 31.5 (C-4 and C-5), 35.1 (C-2 and C-7), 55.0 (OCH$_3$), 113.8, 120.6, 132.0 and 155.2 (ArC) and 167.4 (CO); *m/z* (EI) 420 (M^+, 27 %) and 223 (100).

N,N´-*Bis(3-chlorophenyl)-3,6-dithiaoctanediamide* 150c[78]

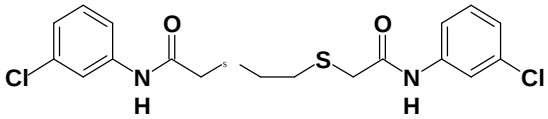

The experimental procedure described for the synthesis of *N,N´*-diphenyl-3,6-dithiaoctanediamide **150a** was followed, using *N*-(3-chlorophenyl)-2-sulfanylacetanilide **149c** (3.19 g, 15.8 mmol), 1,2-dibromoethane (1.45 g, 7.7 mmol)

and KOH (1.05 g, 18.6 mmol). The resulting aqueous phase was extracted using $CHCl_3$ (3x 30 ml), and the combined $CHCl_3$ extracts were washed with 10% aqueous NaOH before drying over anhyd. $MgSO_4$. The solvent was evaporated *in vacuo*, and the yellow residue was recrystallised from EtOH-H_2O to yield, as fine yellow needles, *N,N´*-bis(3-chlorophenyl)-3,6-dithiaoctanediamide **150c** (1.63 g, 49 %), mp 137-139 °C (from EtOH) (lit.,[78] 114-117 °C); ν_{max}(KBr)/cm^{-1} 3390 (NH) and 1665 (CO); δ_H(400 MHz; DMSO-d_6) 2.90 (4H, s, SC***H***$_2$CH$_2$), 3.44 (4H, s, COCH$_2$S), 7.11 (2H, d, *J* 7.9 Hz, ArH), 7.33 (2H, t, *J* 8.0 Hz, ArH), 7.42 (2H, d, *J* 8.2 Hz, ArH), 7.79 (2H, s, ArH) and 10.25 (2H, br s, NH); δ_C(100 MHz; DMSO-d_6) 31.4 (C-4 and C-5), 35.2 (C-2 and C-7), 117.4, 118.5, 123.0, 130.3, 133.0 and 140.3 (ArC) and 168.3 (CO); *m/z* (EI) 428 (M^+, 10 %) and 228 (100).

N,N´-*Bis(2-chlorophenyl)-3,6-dithiaoctanediamide* 150d[78]

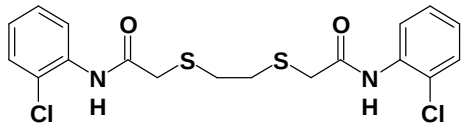

The experimental procedure described for the synthesis of *N,N´*-diphenyl-3,6-dithiaoctanediamide **150a** was followed, using *N*-(2-chlorophenyl)-2-sulfanylacetanilide **149d** (2.39 g, 11.9 mmol), 1,2-dibromoethane (1.20 g, 6.4 mmol) and KOH (0.73 g, 13 mmol). The crude product was recrystallised from EtOH to afford, as white crystals, *N,N´*-bis(2-chlorophenyl)-3,6-dithiaoctanediamide **150d** (1.68 g, 61 %), mp 169-172 °C (from EtOH) (lit.,[78] 165-167 °C); ν_{max}(KBr)/cm^{-1} 3401 (NH) and 1656 (CO); δ_H(400 MHz; DMSO-d_6) 2.93 (4H, s, SC***H***$_2$CH$_2$), 3.47 (4H, s, COCH$_2$S), 7.19 (2H, t, *J* 7.7 Hz, ArH), 7.32 (2H, t, *J* 7.7 Hz, ArH), 7.49 (2H, d, *J* 8.0 Hz, ArH), 7.76 (2H, d, *J* 7.9 Hz, ArH) and 9.65 (2H, br s, NH); δ_C(100 MHz; DMSO-d_6) 31.4 (C-4 and C-5), 34.6 (C-2 and C-7), 125.4, 125.9, 126.2, 127.3, 129.3 and 134.5 (ArC) and 168.2 (CO); *m/z* (EI) 428 (M^+, 6 %) and 228 (100).

N,N´-*Bis(2-methylphenyl)-3,6-dithiaoctanediamide* 150e[78]

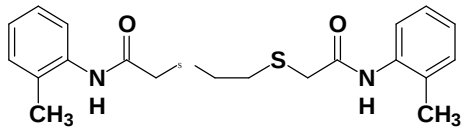

The experimental procedure described for the synthesis of *N,N´*-diphenyl-3,6-dithiaoctanediamide **150a** was followed, using *N*-(2-methylphenyl)-2-sulfanylacetanilide **149e** (2.69 g, 14.8 mmol), 1,2-dibromoethane (1.47g, 7.8 mmol) and KOH (0.97 g, 17 mmol). The crude product was recrystallised from EtOH to afford, as a white powder, *N,N´*-bis(2-methylphenyl)-3,6-dithiaoctanediamide **150e** (1.58 g, 52 %), mp 189-192 °C (from EtOH) (lit.,[78] 176-178 °C); ν_{max}(KBr)/cm^{-1} 3392 (NH) and 1659 (CO); δ_H(400 MHz; DMSO-d_6) 2.20 (6H, s, CH_3), 2.94 (4H, s, SC***H***$_2$CH$_2$), 3.39 (4H, s, COCH$_2$S), 7.06-7.22 (6H, m, ArH), 7.40 (2H, d, *J* 7.7 Hz, ArH) and 9.41 (2H, br s, NH); δ_C(100 MHz; DMSO-d_6) 17.6 (CH_3), 31.5 (C-4 and C-5), 34.6 (C-2 and C-7), 124.7, 125.1, 125.8, 130.2, 131.5 and 135.9 (ArC) and 167.9 (CO); *m/z* (EI) 388 (M^+, 14 %) and 207 (100).

N,N´-*Bis(2-methoxyphenyl)-3,6-dithiaoctanediamide* 150f[78]

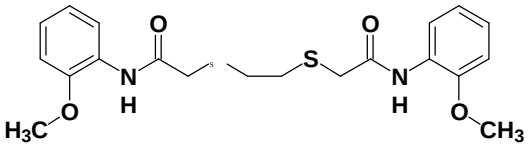

The experimental procedure described for the synthesis of *N,N´*-diphenyl-3,6-dithiaoctanediamide **150a** was followed, using *N*-(2-methoxyphenyl)-2-sulfanylacetanilide **149f** (2.98 g, 15.1 mmol), 1,2-dibromoethane (1.62 g, 8.6 mmol) and KOH (1.00 g, 17.9 mmol). The crude product was recrystallised from aqueous EtOH to afford, as a light grey powder, *N,N´*-bis(2-methoxyphenyl)-3,6-dithiaoctanediamide **150f** (2.73 g, 86 %), mp 140-143 °C (from EtOH) (lit.,[78] 137-140 °C); ν_{max}(KBr)/cm^{-1} 3394 (NH) and 1660 (CO); δ_H(400 MHz; DMSO-d_6) 2.90 (4H, s, 2 x SC***H***$_2$CH$_2$), 3.47 (4H, s, COCH$_2$S), 3.81 (6H, s, OCH_3), 6.90 (2H, t, *J* 6.8 Hz, ArH), 6.88-7.10 (4H, m, ArH), 7.97 (2H, d, *J* 7.9 Hz, ArH) and 9.33 (2H, br s, NH); δ_C(100 MHz; DMSO-d_6) 31.5 (C-4 and C-5), 35.0 (C-2 and C-7), 56.0 (OCH_3), 111.0, 120.2, 121.2, 124.3, 126.9 and 149.3 (ArC) and 167.8 (CO); *m/z* (EI) 420 (M^+ 8 %), 223 (100).

3.1.2 Synthesis of Morita-Baylis-Hillman products

2-[Hydroxy(pyridin-2-yl)methyl]acrylonitrile **166a**[88,114]

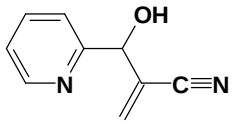

A solution of pyridine-2-carbaldehyde (4.06 g, 37.9 mmol), acrylonitrile (2.16 g, 40.8 mmol), and 1,4-diazabicyclo[2.2.2]octane (DABCO)(0.188 g, 1.7 mmol) in $CHCl_3$ (10 ml) was stirred for 3 days. The solvent was removed *in vacuo* and the crude product purified by flash chromatography [elution with EtOAc-hexane (40:60)] to yield, as an orange oil, 2-[hydroxy(pyridin-2-yl)methyl]acrylonitrile **166a** (5.34 g, 88 %); δ_H(400 MHz; $CDCl_3$) 5.25 (1H, s, C**H**OH), 5.55 (1H, s, OH), 5.95 and 6.11 (2H, 2 x s, C=CH_2), 7.23 (1H, t, *J* 5.0 Hz, ArH), 7.40 (1H, d, *J* 7.9 Hz, ArH), 7.71 (1H, t, *J* 7.7 Hz, ArH) and 8.48 (1H, d, *J* 5.7 Hz, ArH); δ_C(100 MHz; $CDCl_3$) 73.1 (CHOH), 116.5 (CN), 121.0 and 123.4 (ArC), 125.5 (***C***=CH_2), 130.9 (C=***C***H_2), 137.3, 148.2 and 156.6 (ArC).

Methyl 2-[hydroxy(pyridin-2-yl)methyl]acrylate **166b**[88,114]

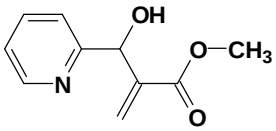

The method used to synthesise 2-[hydroxy(pyridin-2-yl)methyl]acrylonitrile **166a** was followed using pyridine-2-carbaldehyde (3.81 g, 35.6 mmol), methyl acrylate (3.23 g, 38.3 mmol) and DABCO (0.21 g, 1.9 mmol). The solvent was removed *in vacuo* and the crude product purified by flash chromatography [elution with EtOAc-hexane (40:60)] to yield, as a yellow oil, methyl 2-[hydroxy(pyridin-2-yl)methyl]acrylate **166b** (6.42 g, 93 %); δ_H(400 MHz; $CDCl_3$) 3.61 (3H, s, CH_3O), 5.03, (1H, d, *J* 5.2 Hz, C***H***OH), 5.55 (1H, d, *J* 3.9 Hz, OH), 5.88 and 6.26 (2H, 2 x s, C=CH_2), 7.09 (1H, t, *J* 6.9 Hz, ArH), 7.33 (1H, d, *J* 7.9 Hz, ArH), 7.57 (1H, t, *J* 7.7 Hz, ArH) and 8.44 (1H, d, *J* 4.8 Hz, ArH); δ_C(100 MHz; $CDCl_3$) 51.5 (CH_3O), 71.9 (CHOH), 121.1 and 122.4 (ArC), 126.4 (***C***=CH_2), 136.6 (ArC), 141.6 (C=***C***H_2), 148.1 and 159.6 (ArC) and 166.3 (CO).

***2-[Acetoxy(pyridin-2-yl)methyl]acrylonitrile* 167a**[88,114]

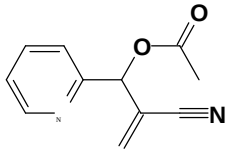

A mixture of 2-[hydroxy(pyridin-2-yl)methyl]acrylonitrile **166a** (4.09 g, 25.5 mmol) and acetic anhydride (13.25 g) was heated in a round-bottomed flask at 100 °C for 0.5 h. The mixture was cooled and poured into a $NaHCO_3$-ice slurry, and stirring continued for a further 0.5 h. The mixture was then basified with 1M-NaOH and extracted with Et_2O (3 x 30 ml). The Et_2O extracts were combined, washed with aqueous $NaHCO_3$ and then dried over anhyd. $MgSO_4$. The solvent was removed *in vacuo* and the crude product purified by flash chromatography [elution with EtOAc-hexane (70:30)] to yield, as an orange oil, 2-[acetoxy(pyridin-2-yl)methyl]acrylonitrile **167a** (2.65 g, 51 %); δ_H(400 MHz; $CDCl_3$) 2.14 (3H, s, CH_3CO), 6.13 and 6.16 (2H, 2 x s, C=CH_2), 6.37 (1H, s, CHOAc), 7.27 (1H, d, *J* 7.5 Hz, ArH), 7.40 (1H, d, *J* 7.7 Hz, ArH), 7.75 (1H, t, *J* 7.7 Hz, ArH) and 8.57 (1H, d, *J* 5.1 Hz, ArH); δ_C(100 MHz; $CDCl_3$) 20.9 (***C***H_3CO), 75.7 (CHOAc), 116.1 (CN), 121.0 (ArC), 121.6 (***C***=CH_2), 123.7 (ArC), 133.7 (C=***C***H_2), 137.3, 149.6 and 154.9 (ArC) and 169.2 (CO).

***Methyl 2-[acetoxy(pyridin-2-yl)methyl]acrylate* 167b**[88,114]

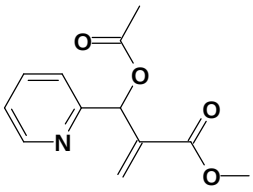

The method used to synthesise 2-[acetoxy(pyridin-2-yl)methyl]acrylonitrile **167a** was followed using methyl 2-[hydroxy(pyridin-2-yl)methyl]acrylate **166b** (4.34 g, 22.8 mmol) and acetic anhydride (22 ml) to yield, as an orange oil, methyl 2-[acetoxy(pyridin-2-yl)methyl]acrylate **167b** (2.45 g, 46 %); δ_H(400 MHz; $CDCl_3$) 2.12 (3H, s, CH_3CO), 3.67 (3H, s, CH_3O), 5.92 and 6.45 (2H, 2x s, C=CH_2), 6.70 (1H, s, CHOAc), 7.18 (1H, t, *J* 7.7 Hz, ArH), 7.41 (1H, d, *J* 7.8 Hz, ArH), 7.65 (1H, t, *J* 7.8 Hz, ArH) and 8.55 (1H, d, *J* 5.2 Hz, ArH); δ_C(100 MHz; $CDCl_3$) 20.6 (***C***H_3CO), 51.5 (CH_3O), 73.7 (CHOAc), 122.3 and 122.6 (ArC), 126.5 (***C***=CH_2), 136.2 (ArC), 138.7 (C=***C***H_2), 149.6 and 156.9 (ArC) and 164.3, 169.2 (CO).

***3-Hydroxy-2-(methylsulfanylmethyl)-3-(pyridin-2-yl)propanenitrile* 168a**[90]

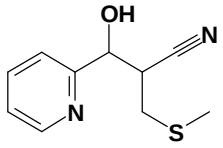

2-[Hydroxy(pyridin-2-yl)methyl]acrylonitrile **166a** (2.65 g, 16.5 mmol) and THF (5 ml) were placed in a three-necked, round-bottomed flask, fitted with scrubbers. Aqueous NaSMe (21%, 4.5 ml) was added dropwise over a five-minute period, and the resulting mixture was stirred for 0.5 h before being extracted with EtOAc (3 x 30 ml). The combined extracts were washed with satd. brine and dried over anhyd. $MgSO_4$, and the solvent was removed *in vacuo*. The crude product was purified by flash chromatography [elution with EtOAc-hexane (80:20)] to yield, as a yellow oil, 3-hydroxy-2-(methylsulfanylmethyl)-3-(pyridin-2-yl)propanenitrile **168a** (2.75 g, 80 %); δ_H(400 MHz; $CDCl_3$) 2.00/2.07[§] (3H, s, CH_3S), 2.60 (2H, m, CHC***H***$_2$S), 2.82 (1H, m, CHCN), 4.54 (1H, m, OH), 4.89 (1H, m, C**H**OH), 7.21 (1H, m, ArH), 7.44 (1H, m, ArH), 7.71 (1H, m, ArH), 8.44 (1H, m, ArH); δ_C(100 MHz; $CDCl_3$) 16.0 (CH_3S), 32.5 (***C***H_2SCH_3), 40.7 (***C***HCN), 71.2 (CHOH), 118.9 (CN), 121.2, 123.4, 137.0, 149.1 and 157.3 (ArC).

***3-Hydroxy-2-(methoxymethyl)-3-(pyridin-2-yl)propanenitrile* 168b**[90]

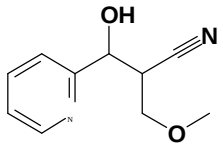

A methanolic solution of NaOMe (0.1 M, 130 ml) was added to a solution of 2-[hydroxy(pyridin-2-yl)methyl]acrylonitrile **166a** (2.04 g, 12.7 mmol) in THF (5 ml) and the resulting mixture was stirred for 1 h. The solvent was removed *in vacuo* and the product extracted into EtOAc (3x 30 ml). The combined extracts were washed with satd. brine and dried over anhyd. $MgSO_4$. The solvent was removed *in vacuo* and the crude product purified by flash chromatography [elution with EtOAc-hexane (80:20)] to yield, as an orange oil, 3-hydroxy-2-(methoxymethyl)-3-(pyridin-2-yl)propanenitrile **168b** (2.22 g, 90 %); δ_H(400 MHz; $CDCl_3$) 3.24 (1H, m, CHCN), 3.38/3.41 (3H, s, CH_3O), 3.67 (2H, m, CHC***H***$_2$O), 4.43 (1H, m, OH), 4.92 (1H, m,

[§] Chemical shifts reported in this format, here and elsewhere, reflect the signals for the diastereomeric components.

C**H**OH), 7.23 (1H, m, ArH), 7.43 (1H, m, ArH), 7.72 (1H, m, ArH) and 8.51 (1H, m, ArH); δ_C(100 MHz; $CDCl_3$) 40.0 (CHCN), 59.0 (CH_3O), 69.3 (CH***C***H_2O), 70.4 (CHOH), 118.1 (ArC), 120.8 (CN), 123.3, 137.1, 148.5 and 157.7 (ArC).

3-Hydroxy-2-[(pyrrolidin-1-yl)methyl]-3-(pyridin-2-yl)propanenitrile **168c**

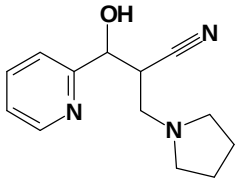

A solution of 2-[hydroxy(pyridin-2-yl)methyl]acrylonitrile **166a** (1.62 g, 10.0 mmol) and pyrrolidine (0.81 g, 11 mmol) in THF (5 ml) was stirred for 2 days. The crude product (2.28 g) was purified by flash chromatography [elution with EtOAc-hexane (80:20)] to yield, as a red oil, *3-hydroxy-2-[(pyrrolidin-1-yl)methyl]-3-(pyridin-2-yl)propanenitrile* **168c** (0.51 g, 22 %), (Found: **MH**$^+$, 232.144897. $C_{13}H_{18}N_3O$ requires *M*+1, 232.14487.); ν_{max}(NaCl)/cm^{-1} 3242 (OH) and 2243 (CN); δ_H(400 MHz; $CDCl_3$) 1.79 (4H, m, C***H***$_2$$CH_2$N), 2.65 (4H, m, CH_2C***H***$_2$N), 2.86 (2H, m, CHC***H***$_2$N), 3.21 (1H, m, CHCN), 3.39(1H, m, OH), 5.08 (1H, m, C**H**OH), 7.22 (1H, m, ArH), 7.56 (1H, m, ArH), 7.74 (1H, m, ArH) and 8.54 (1H, m, ArH); δ_C(100 MHz; $CDCl_3$) 23.5 (***C***H_2CH_2N), 36.0 (CHCN), 54.4 (CH_2***C***H_2N), 55.5 (CH***C***H_2N), 75.2 (**C**HOH), 119.3 (CN), 121.1, 122.7, 136.9, 148.9 and 159.0 (ArC); *m/z* (EI) 132 (M^+, 1.7 %) and 109 (100).

3-Hydroxy-2-[(piperidin-1-yl)methyl]-3-(pyridin-2-yl)propanenitrile **168d**

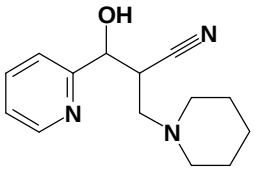

The method used to synthesise 3-hydroxy-2-[(pyrrolidin-1-yl)methyl]-3-(pyridin-2-yl)propanenitrile **168c** was followed using 2-[hydroxy(pyridin-2-yl)methyl]acrylonitrile **166a** (1.59 g, 9.9 mmol) and piperidine (1.00 g, 11.7 mmol) to yield, as a red oil, *3-hydroxy-2-[(piperidin-1-yl)methyl]-3-(pyridin-2-yl)propanenitrile* **168d** (2.09 g, 86 %), (Found: **MH+**, 246.160648. $C_{14}H_{20}N_3O$ requires *M*+1, 246.160637.); ν_{max}(NaCl)/cm^{-1} 3183 (OH) and 2243 (CN); δ_H(400 MHz; $CDCl_3$) 1.40 (2H, m, CH_2C***H***$_2$$CH_2$), 1.56 (4H, m, C***H***$_2$$CH_2$N), 2.45 (4H, m, CH_2C***H***$_2$N), 2.68

(2H, m, CHC***H***$_2$N), 2.81 (1H, m, CHCN), 3.34 (1H, m, OH), 5.03 (1H, m, C**H**OH), 7.19 (1H, m, ArH), 7.53 (1H, m, ArH), 7.69 (1H, m, ArH) and 8.52 (1H, m, ArH); δ_C(100 MHz; $CDCl_3$) 23.7 (CH_2***C***H_2CH_2), 25.9 (***C***H_2CH_2N), 35.5 (***C***HCN), 55.1 (CH_2***C***H_2N), 58.7 (CH***C***H_2N), 74.8 (***C***HOH), 119.2 (CN), 121.1, 123.0, 136.9, 148.8 and 159.0 (ArC); *m/z* (EI) 246 (M^+, 1.7 %) and 109 (100).

Methyl-3-hydroxy-2-(methylsulfanylmethyl)-3-(pyridin-2-ylmethyl)propanate **168e**[90]

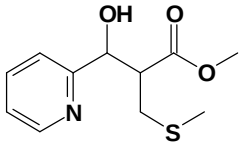

The method used to synthesise 3-hydroxy-2-(methylsulfanylmethyl)-3-(pyridin-2-yl)propanenitrile **168a** was followed using 2-[hydroxy(pyridin-2-yl)methyl]methylacrylate **166b** (1.19 g, 6.1 mmol) and NaSMe (21 % soln., 1.9 ml) to yield, as a yellow oil, methyl-3-hydroxy-2-(methylsulfanylmethyl)-3-(pyridin-2-yl)propanate **168e** (0.811 g, 52 %); δ_H(400 MHz; $CDCl_3$) 1.80/1.84 (3H, s, C**H**$_3$S), 2.42-2.75 (2H, m, CHC***H***$_2$S), 2.96-3.04 (1H, m, C**H**CO), 3.39/3.40 (3H, s, C**H**$_3$O), 4.52 (1H, s, OH), 4.81/4.86 (1H, s, C**H**OH), 7.00 (1H, m, ArH), 7.19 (1H, m, ArH), 7.49 (1H, m, ArH) and 8.30 (1H, m, ArH); δ_C(100 MHz; $CDCl_3$) 16.4/16.8 (***C***H_3S), 32.5/33.6 (***C***H_2SCH_3), 40.7/40.9 (***C***HCO), 51.2/52.3 (***C***H_3O), 70.4/71.6 (***C***HOH), 117.4/118.2, 120.9/121.6, 131.1/132.6, 136.9/137.5 and 148.7/149.8 (ArC) and 169.0/169.2 (CO).

Methyl-3-hydroxy-2-methoxymethyl-3-(pyridin-2-yl)propanate **168f**[90]

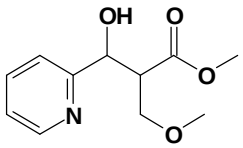

The method used to synthesise 3-hydroxy-2-methoxymethyl-3-pyridin-2-ylpropanenitrile **168a** was followed using methyl 2-[hydroxy(pyridin-2-yl)methyl] acrylate **166b** (1.94 g, 10.0 mmol) and methanolic NaOMe (0.1 M, 104 ml) to yield, as an orange oil, methyl 3-hydroxy-2-methoxymethyl-3-(pyridin-2-yl)propanoate **168f** (0.673 g, 28 %); δ_H(400 MHz; $CDCl_3$) 3.08/3.11 (3H, s, C***H***$_3$OCH_2), 3.17/3.43 (1H, m, C***H***CO), 3.52-3.63 (2H, m, CHC***H***$_2$O), 3.66/3.75 (3H, s, CH_3OCO), 4.43/4.52 (1H, s, OH), 5.04/5.06 (1H, s, C**H**OH), 7.11 (1H, m, ArH), 7.32 (1H, m, ArH), 7.62

(1H, m, ArH) and 8.44 (1H, m, ArH); δ_C(100 MHz; $CDCl_3$) 51.4/52.0 (***C***H_3O), 58.7/58.8 (***C***H_3OCH_2), 70.0/70.6 (CH***C***H_2O), 72.0/72.3 (***C***HOH), 82.2/82.8 (***C***$HCOCH_3$), 120.8/121.6, 122.4/122.9, 136.2/136.9, 148.4/149.1 and 158.7/160.0 (ArC) and 172.4/172.6 (CO).

Methyl-3-hydroxy-2-[(pyrrolidin-1-yl)methyl]-3-(pyridin-2-yl)propanate **168g**

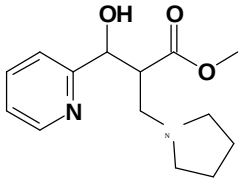

The method used to synthesise 3-hydroxy-2-[(pyrrolidin-1-yl)methyl]-3-(pyridin-2-yl)propanenitrile **168c** was followed using methyl 2-[hydroxy(pyridin-2-yl)methyl]acrylate **166b** (2.58 g, 13.3 mmol) and pyrrolidine (1.10 g, 15.5 mmol) to yield, as an red oil, *methyl-3-hydroxy-2-[(pyrrolidin-1-yl)methyl]-3-(pyridin-2-yl)propanate* **168g** (0.209 g, 5.6 %), (Found: **MH**$^+$, 265.155204. $C_{14}H_{21}N_2O_3$ requires *M*+1, 265.155218.); ν_{max}(NaCl)/cm^{-1} 3360 (OH) and 1737 (CO); δ_H(400 MHz; $CDCl_3$) 1.76 (4H, m, C***H***$_2$CH_2H), 2.55 (4H, m, CH_2C***H***$_2$H), 2.80/3.11 (2H, m, CHC***H***$_2$N), 3.30 (1H, m, C***H***CO), 3.55/3.61 (3H, s, C***H***$_3$O), 4.50 (1H, s, OH), 5.17/5.22 (1H, s, C**H**OH), 7.14 (1H, m, ArH), 7.46 (1H, m, ArH), 7.66 (1H, m, ArH) and 8.49 (1H, m, ArH); δ_C(100 MHz; $CDCl_3$) 23.5 (***C***H_2CH_2N), 48.6/49.5 (CH_2***C***H_2N), 51.6 (***C***$HCOCH_3$), 54.2/54.4 (***C***H_3CO), 56.8 (CH***C***H_2N), 74.9 (***C***HOH), 120.8/121.6, 122.1/122.4, 136.3/136.5, 148.5/148.7 and 161.3 (ArC) and 172.6/172.8 (CO); *m/z* (EI) 265 (M^+, 0.6 %), 156 (100).

Methyl-3-hydroxy-2-[(piperidin-1-yl)methyl]-3-(pyridin-2-yl)propanate **168h**

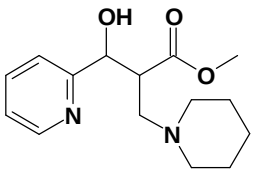

The method used to synthesise methyl-3-hydroxy-2-[(piperidin-1-yl)methyl]-3-(pyridin-2-yl)propanenitrile **168d** was followed using methyl 2-[hydroxy(pyridin-2-yl)methyl]acrylate **166b** (2.67 g, 13.8 mmol) and piperidine (1.38 g, 16.0 mmol) to yield, as an red oil, *methyl-3-hydroxy-2-[(piperidin-1-yl)methyl]-3-(pyridin-2-yl)propanate* **168h** (0.321 g, 8.0 %), (Found: **MH**+, 279.170822. $C_{15}H_{23}N_2O_3$ requires

M+1, 279.170868.); ν_{max}(NaCl)/cm^{-1} 3195 (OH) and 1737 (CO); δ_H(400 MHz; $CDCl_3$) 1.41 (2H, m, $CH_2C\boldsymbol{H}_2CH_2$), 1.57 (4H, m, $C\boldsymbol{H}_2CH_2N$), 2.27-2.55 (4H, m, $CH_2C\boldsymbol{H}_2N$), 2.70/3.02 (2H, m, $CHC\boldsymbol{H}_2N$), 3.12/3.50 (1H, m, C***H***CO), 3.52/3.64 (3H, 2x s, $C\boldsymbol{H}_3O$), 4.50 (1H, s, OH), 5.13/5.26 (1H, s, C**H**OH), 7.15 (1H, m, ArH), 7.40/7.46 (1H, 2x m, ArH), 7.66 (1H, m, ArH) and 8.50 (1H, m, ArH); δ_C(100 MHz; $CDCl_3$) 23.9/24.0 ($CH_2\boldsymbol{C}H_2CH_2$), 25.9/26.0 ($\boldsymbol{C}H_2CH_2N$), 46.4/47.7 (***C***HCO), 51.6 ($\boldsymbol{C}H_3CO$), 54.7 ($CH_2C\boldsymbol{H}_2N$), 56.9/60.3 ($CH\boldsymbol{C}H_2N$), 75.2 (***C***HOH), 120.7/121.2, 122.0/122.6, 136.2/136.5, 148.6/148.7 and 161.2/161.6 (ArC) and 172.5/172.6 (CO); *m/z* (EI) 279 (M^+, 2.1 %), 189 (100).

***2-Methylsulfanylmethyl-3-(pyridin-2-yl)acrylonitrile* 172a**[90]

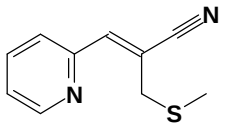

Method (a). 2-[Acetoxy(pyridin-2-yl)methyl]acrylonitrile **167a** (1.04 g, 5.56 mmol) and THF (5 ml) were placed in a three necked round bottomed flask, fitted with scrubbers. A solution of NaSMe (21 % soln., 2.3 ml) was added dropwise to the mixture over a five-minute period. The resultant mixture was stirred for 0.5 h and then extracted with EtOAc (3x 30 ml), washed with brine, and dried over anhyd. $MgSO_4$. The solvent was removed *in vacuo* and the crude product was then purified by flash chromatography (EtOAc-hexane 80:20) to yield, as an yellow oil, 2-methylsulfanylmethyl-3-(pyridin-2-yl)acrylonitrile **172a** (0.48 g, 49 %); δ_H(400 MHz; $CDCl_3$) 2.06 (3H, s, $C\boldsymbol{H}_3S$), 4.59 (2H, s, $C\boldsymbol{H}_2SCH_3$), 7.23 (1H, t, ArH), 7.44 (1H, d, ArH), 7.65 (1H, s, ***H***C=C), 7.72 (1H, t, ArH) and 8.65 (1H, d, ArH); δ_C(100 MHz; $CDCl_3$) 14.0 ($\boldsymbol{C}H_3S$), 20.6 ($\boldsymbol{C}H_2SCH_3$), 116.9 (CN), 122.3 (ArC), 124.6 (ArC), 136.7 (C=***C***H), 136.7, 136.9, 149.8 (ArC) and 156.3 (***C***=CH).

Method (b). A mixture of 3-hydroxy-2-(methylsulfanylmethyl)-3-(pyridin-2-yl)propanenitrile **168a** (0.4 g, 2.0 mmol) and *p*-toluenesulfonic acid (pTSA) (0.5 g, 3.0 mmol) were refluxed for 4 h in benzene (20 ml) in a three necked round bottomed flask, fitted to Dean-Stark apparatus. The mixture was allowed to cool, and the solvent removed *in vacuo*. ^{1}H NMR spectroscopic analysis of the crude product revealed only starting material present.

***Methyl 2-methylsulfanylmethyl-3-(pyridin-2-yl)acrylate* 172e**[90]

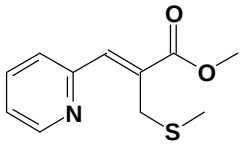

The method used to synthesise 2-methylsulfanylmethyl-3-(pyridin-2-yl)acrylonitrile **172a** was followed using methyl 2-[acetoxy(pyridin-2-yl)methyl]acrylate **167b** (1.18 g, 5.1 mmol) and NaSMe (21 % soln., 2.3 ml) to yield, as an yellow oil, methyl 2-methylsulfanylmethyl-3-(pyridin-2-yl)acrylate **172e** (1.05 g, 93 %); δ_H(400 MHz; $CDCl_3$) 1.99 (3H, s, C***H***$_3$S), 3.81 (3H, s C***H***$_3$O), 4.22 (2H, s, C***H***$_2$SCH$_3$), 7.16 (1H, t, ArH), 7.34 (1H, d, ArH), 7.56 (1H, s, ***H***C=C), 7.65 (1H, t, ArH) and 8.61 (1H, d, ArH); δ_C(100 MHz; $CDCl_3$) 14.1 (***C***H$_3$S), 15.1 (***C***H$_3$O), 28.8 (***C***H$_2$SCH$_3$), 122.5 (ArC), 126.5 (ArC), 133.2 (C=***C***H), 136.3, 136.5, 149.2 (ArC), 154.2 (***C***=CH) and 168.0 (CO).

***Attempted synthesis of Methyl 2-methoxymethyl-3-(pyridin-2-yl)acrylate* 172f**[90]

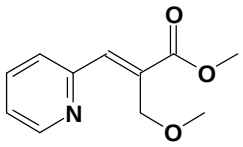

Methyl 2-[acetoxy(pyridin-2-yl)methyl]acrylate **167b** (1.979 g, 8.48 mmol) in THF (5 ml) was stirred with methanolic NaOMe (0.1 M, 104 ml) for 1 h. The solvent was removed *in vacuo*, and ^{1}H NMR spectroscopy of the crude product indicated the formation of a complex mixture, which could not be readily purified by flash chromatography.

***Attempted synthesis of Methyl-3-(pyridin-2-yl)-2-[(pyrrolidin-1-yl)methyl]acrylate* 172g**

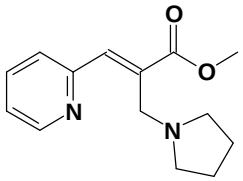

Methyl 2-[acetoxy(pyridin-2-yl)methyl]acrylate **167b** (2.10 g, 9.00 mmol) in THF (5 ml) was stirred with pyrrolidine (0.70 g, 9.86 mmol) for 2 days. The solvent was

removed *in vacuo*, and ^{1}H NMR spectroscopy of the crude product indicated the formation of a complex mixture, which could not be readily purified by flash chromatography.

***Attempted synthesis of Methyl 2-(piperidin-1-yl)methyl-3-(pyridin-2-yl)acrylate* 172g**

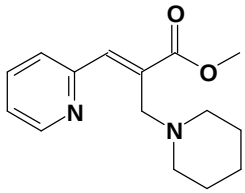

Methyl 2-[acetoxy(pyridin-2-yl)methyl]acrylate **167b** (1.99 g, 8.52 mmol) in THF (5 ml) was stirred with piperidine (0.84 g, 9.81 mmol) for 2 days. The solvent was removed *in vacuo*, and ^{1}H NMR spectroscopy of the crude product indicated the formation of a complex mixture, which could not be readily purified by flash chromatography.

3.1.3 Synthesis of malonamide ligands

3.1.3.1 *Substituted malonic esters*

***Diethyl methylmalonate* 177a**[78]

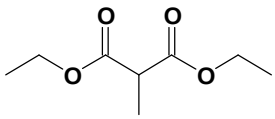

Diethyl malonate **175** (7.33 g, 45.3 mmol) was added to ethanolic NaOEt [generated *in situ* by reacting sodium (1.1 g, 48 mmol) with dry EtOH (60 ml)], and the resulting mixture was boiled under reflux for 2 h under dry nitrogen. Methyl iodide (6.39 g, 45.0 mmol) was then added dropwise and the mixture was boiled for a further hour. On cooling, water (50 ml) was added, and the resulting mixture was extracted with Et_2O (3 x 50 ml). The Et_2O extracts were combined, washed with brine and dried over anhyd. $MgSO_4$. The solvent was evaporated *in vacuo* to obtain the crude product (7.18 g, 92 %), which was then distilled *in vacuo* using a fractionating column to yield, as a colourless oil, diethyl methylmalonate **177a** (5.10 g, 65 %), bp 104-107 °C / *ca.* 20 mmHg (lit.,[115(a)] 198-199 °C), (Found: $\mathbf{M}^+$, 174.0887. $C_8H_{14}O_4$ requires *M*, 174.0892.); ν_{max}(NaCl)/cm^{-1} 1732 (CO); δ_H(400 MHz; DMSO-d_6)[†] 1.18 (6H, t, C***H***$_3$CH$_2$O), 1.27 (3H, d, *J* 7.2 Hz, C***H***$_3$CH), 3.53 (1H, q, *J* 7.2 Hz, CH$_3$C***H***) and 4.53 (4H, m, CH$_3$C***H***$_2$O); δ_C(100 MHz; DMSO-d_6)[†] 13.2 (***C***H$_3$CH), 13.7 (***C***H$_3$CH$_2$O), 45.2 (CH$_3$***C***H), 60.7 (CH$_3$***C***H$_2$O) and 169.5 (CO); *m/z* (EI) 174 (M^+, 60 %), 148 (100).

***Diethyl ethylmalonate* 177b**[78]

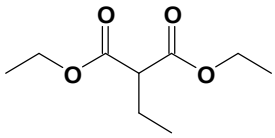

The experimental procedure described for the synthesis of diethyl methylmalonate **177a** was followed, using ethyl iodide (7.08 g, 45.4 mmol). The crude product (7.18 g, 92 %) was distilled *in vacuo* to yield, as a colourless oil, diethyl ethylmalonate **177b** (5.89 g, 70 %), bp 105-107 °C / *ca.* 20 mmHg (lit.,[115(b)] 75-77 °C / / 5 mmHg) (Found: $\mathbf{M}^+$, 188.1039. $C_9H_{16}O_4$ requires *M*, 188.1048); ν_{max}(NaCl)/cm^{-1} 1732 (CO);

[†] Shown by ^{1}H NMR spectroscopy to comprise a mixture of the keto and enol tautomers in DMSO-d_6. The cited NMR data refer to the major, keto tautomer.

δ_H(400 MHz; DMSO-d_6)† 0.88 (3H, t, *J* 7.4 Hz, C***H***$_3$CH$_2$CH), 1.18 (6H, t, *J* 7.2 Hz, C***H***$_3$CH$_2$O), 1.79 (2H, m, CH$_3$C***H***$_2$CH), 3.36 (1H, t, *J* 7.4 Hz, CH$_3$CH$_2$C***H***) and 4.12 (4H, q, *J* 7.2 Hz, CH$_3$C***H***$_2$O); δ_C(100 MHz; DMSO-d_6)† 11.2 (***C***H$_3$CH$_2$CH), 13.7 (***C***H$_3$CH$_2$O), 21.5 (CH$_3$***C***H$_2$CH), 52.4 (CH$_3$CH$_2$***C***H), 60.6 (CH$_3$***C***H$_2$O) and 168.7 (CO); *m/z* (EI) 188 (M^+, 31 %), 132 (100).

Diethyl isopropylmalonate **177d**[78]

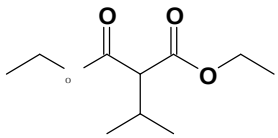

The experimental procedure described for the synthesis of diethyl methylmalonate **177a** was followed, using isopropyl iodide (7.63 g, 44.9 mmol). The crude product (7.57 g, 83 %) was distilled *in vacuo* to yield, as a colourless oil, diethyl isopropylmalonate **177d** (6.07 g, 67 %), bp 110-113 ° / *ca.* 20 mmHg (lit.,[116] 109-112 °C / 21 mmHg) (Found: $\mathbf{M}^+$, 202.1193. $C_{10}H_{18}O_4$ requires *M*, 202.1205.); ν_{max}(NaCl)/cm^{-1} 1735 (CO); δ_H(400 MHz; DMSO-d_6)† 0.94 (6H, d, *J* 6.7 Hz, (C***H***$_3$)$_2$CHCH), 1.18 (6H, t, *J* 7.1 Hz, C***H***$_3$CH$_2$O), 2.24 (1H, m, (CH$_3$)$_2$C***H***CH), 3.19 (1H, d, *J* 8.3 Hz, (CH$_3$)$_2$CHC***H***), and 4.14 (4H, q, *J* 7.2 Hz, CH$_3$C***H***$_2$O); δ_C(100 MHz; DMSO-d_6)† 13.7 (***C***H$_3$CH$_2$O), 19.7 [(***C***H$_3$)$_2$CHCH], 27.9 [(CH$_3$)$_2$***C***HCH], 57.9 [(CH$_3$)$_2$CHC***H***], 60.5 (CH$_3$***C***H$_2$O) and 168.0 (CO); *m/z* (EI) 202 (M^+, 37 %), 132 (100).

Diethyl propylmalonate **177d**[78]

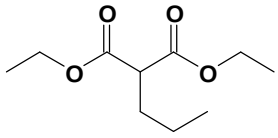

The experimental procedure described for the synthesis of diethyl methylmalonate **177a** was followed, using propyl iodide (7.66 g, 45.0 mmol). The crude product (7.92 g, 87 %) was distilled *in vacuo* to yield, as a colourless oil, diethyl propylmalonate **177d** (6.59 g, 72 %), bp 112-115 °C / *ca.* 20 mmHg (lit.,[117] 111 °C / 23 mmHg) (Found: $\mathbf{M}^+$, 202.1201. $C_{10}H_{18}O_4$ requires *M*, 202.1205.); ν_{max}(NaCl)/cm^{-1} 1732 (CO); δ_H(400 MHz; DMSO-d_6)† 0.88 (3H, t, *J* 7.3 Hz, C***H***$_3$CH$_2$CH$_2$), 1.18 (6H, t, *J* 7.0 Hz, C***H***$_3$CH$_2$O), 1.37 (2H, m, CH$_3$C***H***$_2$CH$_2$), 1.74 (2H, m, CH$_2$C***H***$_2$CH), 3.42 (1H,

t, *J* 7.5 Hz, $CH_2CH_2C\boldsymbol{H}$) and 4.12 (4H, q, *J* 7.0 Hz, $CH_3C\boldsymbol{H}_2O$); δ_C(100 MHz; DMSO-d_6)† 13.3 ($\boldsymbol{C}H_3CH_2CH_2$), 13.7 ($\boldsymbol{C}H_3CH_2O$), 19.7 ($CH_3\boldsymbol{C}H_2CH_2$), 30.2 ($CH_2\boldsymbol{C}H_2CH$), 50.8 ($CH_2CH_2\boldsymbol{C}H$), 60.6 ($CH_3\boldsymbol{C}H_2O$) and 168.8 (CO); *m/z* (EI) 202 (M^+, 33 %), 132 (100).

***Diethyl (3-propenyl)malonate* 177e**[78]

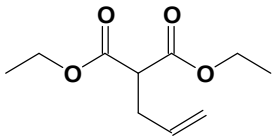

The experimental procedure described for the synthesis of diethyl methylmalonate **177a** was followed, using 3-bromopropene (5.44 g, 44.9 mmol). The crude product (8.21 g, 91 %) was distilled *in vacuo* to yield, as a colourless oil, diethyl (3-propenyl)malonate **177e** (5.77 g, 64 %), bp 169-171 °C / *ca.* 20 mmHg (lit.,[115] 104-105 °C / 5 mmHg) (Found: $\mathbf{M}^+$, 200.0968. $C_{10}H_{16}O_4$ requires *M*, 200.0970.); ν_{max}(NaCl)/cm^{-1} 1732 (CO); δ_H(400 MHz; DMSO-d_6)† 1.18 (6H, t, *J* 7.1 Hz, $C\boldsymbol{H}_3CH_2O$), 2.51 (2H, d, *J* 7.4 Hz, $CH_2{=}CHC\boldsymbol{H}_2$), 3.54 (1H, t, *J* 7.4 Hz, $CH_2C\boldsymbol{H}$), 4.13 (4H, q, *J* 7.1 Hz, $CH_3C\boldsymbol{H}_2O$), 5.06 (2H, m, $C\boldsymbol{H}_2{=}CH$) and 5.74 (1H, m, $CH_2{=}C\boldsymbol{H}$); δ_C(100 MHz; DMSO-d_6)† 13.7 ($\boldsymbol{C}H_3CH_2O$), 32.2 ($\boldsymbol{C}H_2CH$), 50.6 ($CH_2\boldsymbol{C}H$), 60.7 ($CH_3\boldsymbol{C}H_2O$), 117.2 ($\boldsymbol{C}H_2{=}CH$), 134.2 ($CH_2{=}C\boldsymbol{H}$) and 168.3 (CO); *m/z* (EI) 201 (M^+ 100 %) 127 (35).

***Diethyl butylmalonate* 177f**[78]

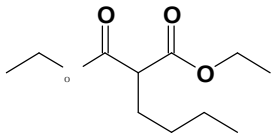

The experimental procedure described for the synthesis of diethyl methylmalonate **177a** was followed, using butyl iodide (8.28 g, 45.0 mmol). The crude product (9.07 g, 93 %) was distilled *in vacuo* to yield, as a red oil, diethyl butylmalonate **177f** (7.99 g, 82 %), bp 128-132 °C / *ca.* 20 mmHg (lit.,[115(c)] 235-240 °C), (Found: $\mathbf{M}^+$, 216.1360. $C_{11}H_{20}O_4$ requires *M*, 216.1361.); ν_{max}(NaCl)/cm^{-1} 1733 (CO); δ_H(400 MHz; DMSO-d_6)† 0.85 [3H, t, *J* 7.0 Hz, $C\boldsymbol{H}_3(CH_2)_3CH$], 1.19 (6H, t, *J* 7.1 Hz, $C\boldsymbol{H}_3CH_2O$), 1.26 [4H, m, $CH_3(C\boldsymbol{H}_2)_2CH_2CH$], 1.75 [2H, m, $CH_3(CH_2)_2C\boldsymbol{H}_2CH$], 3.39 [1H, t, *J* 4.1 Hz, $CH_3(CH_2)_3C\boldsymbol{H}$**]** and 4.12 (4H, q, $CH_3C\boldsymbol{H}_2O$); δ_C(100 MHz; DMSO-

d_6)† 13.5 [***C***$H_3(CH_2)_3CH$], 13.7 (***C***H_3CH_2O), 21.6, 27.8, 28.6 [CH_3(***C***$H_2)_3CH$], 51.0 [$CH_3(CH_2)_3$***C***H], 60.6 (CH_3***C***H_2O) and 168.8 (CO); *m/z* (EI) 216 (M^+ 100 %).

Diethyl pentylmalonate **177g**[78]

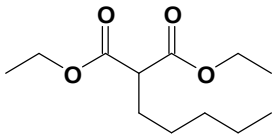

The experimental procedure described for the synthesis of diethyl methylmalonate **177a** was followed, using pentyl iodide (8.91 g, 45.0 mmol). The crude product (9.30 g, 90 %) was distilled *in vacuo* to yield, as a red oil, diethyl pentylmalonate **177g** (7.62 g, 74 %), bp 121-126 °C / *ca.* 20 mmHg (lit.,[118] 125 °C / 20 mmHg) (Found: **M**$^+$, 230.1520. $C_{12}H_{22}O_4$ requires *M*, 230.1518.); ν_{max}(NaCl)/cm^{-1} 1733 (CO); δ_H(400 MHz; DMSO-d_6)† 0.85 [3H, t, *J* 6.3 Hz, C***H***$_3(CH_2)_3CH_2CH$], 1.18 (6H, t, *J* 7.1 Hz, C***H***$_3CH_2O$), 1.25 [6H, br s, CH_3(C***H***$_2)_3CH_2CH$], 1.74 [2H, m, $CH_3(CH_2)_3$C***H***$_2$CH], 3.40 [1H, t, $CH_3(CH_2)_3CH_2$C***H***] and 4.13 (4H, q, CH_3CH_2O); δ_C(100 MHz; DMSO-d_6)† 13.6 [***C***$H_3(CH_2)_4CH$], 13.7 (***C***H_3CH_2O), 21.6, 26.0, 28.0, 30.7 [CH_3(***C***$H_2)_4CH$], 51.0 [$CH_3(CH_2)_4$***C***H], 60.6 (CH_3***C***H_2O) and 168.8 (CO); *m/z* (EI) 230 (M^+ 100 %).

Diethyl hexylmalonate **177h**[78]

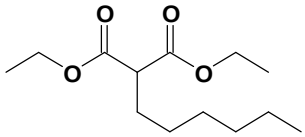

The experimental procedure described for the synthesis of diethyl methylmalonate **177a** was followed, using hexyl iodide (9.55 g, 45.0 mmol). The crude product (10.23 g, 93 %) was distilled *in vacuo* to yield, as a red oil, diethyl hexylmalonate **177h** (8.72 g, 79 %), bp 149-153 °C / *ca.* 20 mmHg (lit.,[119] 152-154 °C / 19 mmHg) (Found: **M**$^+$, 244.1669. $C_{13}H_{24}O_4$ requires *M*, 244.1674.); ν_{max}(NaCl)/cm^{-1} 1733 (CO); δ_H(400 MHz; DMSO-d_6)† 0.85 [3H, t, *J* 7.6 Hz, C***H***$_3(CH_2)_4CH_2CH$], 1.18 (6H, t, *J* 7.2 Hz, C***H***$_3CH_2O$), 1.25 [8H, br s, CH_3(C***H***$_2)_4CH_2CH$], 1.75 [2H, m, $CH_3(CH_2)_4$C***H***$_2$CH], 3.40 [1H, t, *J* 7.4 Hz, $CH_3(CH_2)_4CH_2$C***H***] and 4.11 (4H, q, CH_3C***H***$_2$O); δ_C(100 MHz; DMSO-d_6)† 13.6 [***C***$H_3(CH_2)_5CH$], 13.7 (***C***H_3CH_2O), 21.8,

26.3, 28.0, 28.1, 30.7 [$CH_3(\boldsymbol{C}H_2)_5CH$], 51.0 [$CH_3(CH_2)_5\boldsymbol{C}H$], 60.6 ($CH_3\boldsymbol{C}H_2O$) and 168.8 (CO); *m/z* (EI) 244 (M^+ 100 %).

***Diethyl benzylmalonate* 177i**[78]

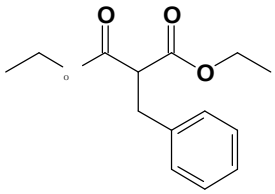

The experimental procedure described for the synthesis of diethyl methylmalonate **177a** was followed, using benzyl chloride (5.70 g, 45.0 mmol). The crude product (10.47 g, 93 %) was distilled *in vacuo* to yield, as a colourless oil, diethyl benzylmalonate **177i** (5.34 g, 47 %), bp 178-181 °C / *ca.* 20 mmHg (lit.,[115(d)] 162-163 °C / 10 mmHg) (Found: $\mathbf{M}^+$, 250.1203. $C_{14}H_{18}O_4$ requires *M*, 250.1205.); ν_{max}(NaCl)/cm^{-1} 1733 (CO); δ_H(400 MHz; DMSO-d_6)† 1.18 (6H, t, *J* 7.1 Hz, $C\boldsymbol{H}_3CH_2O$), 3.09 (2H, d, *J* 7.4 Hz, $PhC\boldsymbol{H}_2CH$), 3.80 (1H, t, *J* 7.4 Hz, $PhCH_2C\boldsymbol{H}$), 4.09 (4H, q, $CH_3C\boldsymbol{H}_2O$) and 7.26 (5H, m, ArH); δ_C(100 MHz; DMSO-d_6)† 13.8 ($\boldsymbol{C}H_3CH_2O$), 33.9 ($Ph\boldsymbol{C}H_2CH$), 52.8 ($PhCH_2\boldsymbol{C}H$), 60.7 ($CH_3\boldsymbol{C}H_2O$), 128.0, 128.6, 129.9 and 137.5 (ArC), and 168.8 (CO); *m/z* (EI) 250 (M^+ 48 %) 132 (100).

***Diethyl heptylmalonate* 177j**[78]

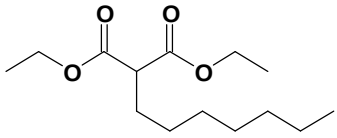

The experimental procedure described for the synthesis of diethyl methylmalonate **177a** was followed, using heptyl iodide (10.22 g, 45.0 mmol). The crude product (11.14 g, 96 %) was distilled *in vacuo* to yield, as a yellow oil, diethyl heptylmalonate **177j** (9.00 g, 89 %), bp 161-165 °C / *ca.* 20 mmHg (lit.,[120] 136-138 °C / 3 mmHg) (Found: $\mathbf{M}^+$, 258.1828. $C_{14}H_{26}O_4$ requires *M*, 258.1831.); ν_{max}(NaCl)/cm^{-1} 1736 (CO); δ_H(400 MHz; DMSO-d_6)† 0.85 [3H, t, *J* 7.5 Hz, $C\boldsymbol{H}_3(CH_2)_5CH_2CH$], 1.17 (6H, t, *J* 7.2 Hz, $C\boldsymbol{H}_3CH_2O$), 1.24 [10H, br s, $CH_3(C\boldsymbol{H}_2)_5CH_2CH$], 1.75 [2H, m, $CH_3(CH_2)_5C\boldsymbol{H}_2CH$], 3.42 [1H, t, *J* 7.6 Hz, $CH_3(CH_2)_5CH_2C\boldsymbol{H}$] and 4.14 (4H, q, *J* 7.2 Hz, $CH_3C\boldsymbol{H}_2O$); δ_C(100 MHz; DMSO-d_6)† 13.7 [$\boldsymbol{C}H_3CH_2O$ and $\boldsymbol{C}H_3(CH_2)_6CH$],

21.9, 26.3, 28.0, 28.2, 28.4, 30.9 [$CH_3(\boldsymbol{C}H_2)_6CH$], 51.0 [$CH_3(CH_2)_6\boldsymbol{C}H$], 60.6 ($CH_3\boldsymbol{C}H_2O$) and 168.8 (CO); *m/z* (EI) 258 (M^+ 33 %) 172 (100).

3.1.3.2 N,N´-*bis(2-hydroxyethyl)malonamide derivatives*

N,N´-*Bis(2-hydroxyethyl)malonamide* 180k[121]

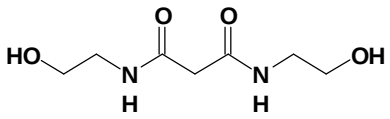

Diethyl malonate **175** (1.61 g, 10.0 mmol) was stirred with ethanolamine **179** (1.26 g, 20.6 mmol) for 2 hours. The resultant precipitate was filtered off and recrystallized from EtOH-Et_2O, yielding, as cream flakes, *N,N´*-bis(2-hydroxyethyl)malonamide **180k** (1.81 g, 95 %), mp 125-126 °C (from EtOH)(lit.,[121] 127-127.5 °C) (Found: $\mathbf{MH}^+$, 191.1031. $C_7H_{14}N_2O_4$ requires *MH*, 191.1032.); ν_{max}(NaCl)/cm^{-1} 3306 (OH), 3097 (NH) and 1639 (CO); δ_H(400 MHz; DMSO-d_6) 3.04 (2H, s, $C\boldsymbol{H}_2CO$), 3.12 (4H, q, *J* 5.8 Hz, $C\boldsymbol{H}_2NH$), 3.39 (4H, q, *J* 5.8 Hz, $C\boldsymbol{H}_2OH$), 4.69 (2H, t, *J* 5.3 Hz, OH) and 8.02 (2H, t, *J* 5.1 Hz, NH); δ_C(100 MHz; DMSO-d_6) 41.5 ($\boldsymbol{C}H_2NH$), 43.0 ($\boldsymbol{C}H_2CO$), 59.6 ($\boldsymbol{C}H_2OH$) and 167.0 (CO).

N,N´-*Bis(2-hydroxyethyl)-2-methyl-1,3-propanediamide* 180a

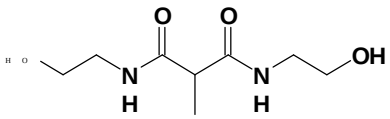

The experimental procedure described for the synthesis of N,N´-bis(2-hydroxyethyl)malonamide **180k** was followed, using diethyl methylmalonate **177a** (1.76 g, 10.1 mmol), ethanolamine **179** (1.23 g, 20.1 mmol) and stirring for 4 hours. The resultant precipitate was filtered off and recrystallized from EtOH-Et_2O, yielding, as cream flakes, *N,N´*-bis(2-hydroxyethyl)-2-methyl-1,3-propanediamide **180a** (1.82 g, 88 %), mp 115-117 °C (from EtOH) (Found: $\mathbf{MH}^+$, 205.1331. $C_8H_{16}N_2O_4$ requires *MH*, 205.1332.); ν_{max}(NaCl)/cm^{-1} 3311 (OH), 3099 (NH) and 1642 (CO); δ_H(400 MHz; DMSO-d_6) 0.91 (3H, d, *J* 7.1 Hz, $C\boldsymbol{H}_3CH$), 3.04 (1H, q, *J* 7.0 Hz, $C\mathbf{H}CH_3$), 3.12 (4H, q, *J* 5.8 Hz, $C\boldsymbol{H}_2NH$), 3.39 (4H, q, *J* 5.8 Hz, $C\boldsymbol{H}_2OH$), 4.69 (2H, t, *J* 5.4 Hz, OH) and 8.02 (2H, t, *J* 5.1 Hz, NH); δ_C(100 MHz; DMSO-d_6) 13.2 ($\boldsymbol{C}H_3CH$), 41.5 ($\boldsymbol{C}H_2NH$), 53.0 ($\boldsymbol{C}HCH_3$), 59.6 ($\boldsymbol{C}H_2OH$) and 169.2 (CO).

***2-Ethyl*-N,N´-*bis(2-hydroxyethyl)-1,3-propanediamide* 180b**[122]

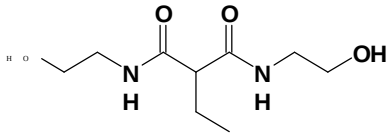

The experimental procedure described for the synthesis of N,N´-bis(2-hydroxyethyl)malonamide **180k** was followed, using diethyl ethylmalonate **177b** (1.88 g, 10.0 mmol), ethanolamine **179** (1.24 g, 20.2 mmol) and stirring for 4 hours. The resultant precipitate was filtered off and recrystallized from EtOH-Et_2O, yielding, as cream flakes, 2-ethyl-*N,N´*-bis(2-hydroxyethyl)-1,3-propanediamide **180b** (1.77 g, 81 %), mp 113-114 °C (from EtOH) (Found: $\mathbf{MH}^+$, 219.1631. $C_9H_{18}N_2O_4$ requires *MH*, 219.1632.); ν_{max}(NaCl)/cm^{-1} 3302 (OH), 3094 (NH) and 1636 (CO); δ_H(400 MHz; DMSO-d_6) 0.89 (3H, t, *J* 7.0 Hz, C***H***$_3$CH$_2$), 1.10 (2H, m, CH$_3$C***H***$_2$CH), 3.04 (1H, t, C***H***CH$_2$), 3.18 (4H, q, *J* 5.8 Hz, C***H***$_2$NH), 3.36 (4H, q, *J* 5.8 Hz, C***H***$_2$OH), 4.69 (2H, t, *J* 5.3 Hz, OH) and 8.01 (2H, t, *J* 5.1 Hz, NH); δ_C(100 MHz; DMSO-d_6) 13.7 (***C***H$_3$CH$_2$), 22.0 (CH***C***H$_2$), 41.6 (***C***H$_2$NH), 54.0 (***C***HCH$_2$), 59.4 (***C***H$_2$OH) and 168.0 (CO).

N,N´-*Bis(2-hydroxyethyl)-2-isopropyl-1,3-propanediamide* 180c[123]

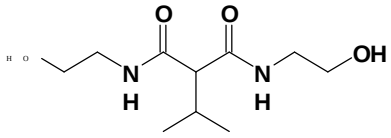

The experimental procedure described for the synthesis of N,N´-bis(2-hydroxyethyl)malonamide **180k** was followed, using diethyl isopropylmalonate **177c** (2.03g, 10.0 mmol), ethanolamine **179** (1.24 g, 20.2 mmol) and stirring for 24 hours. The resultant precipitate was filtered off and recrystallized from EtOH-Et_2O, yielding, as cream flakes, *N,N´*-bis(2-hydroxyethyl)-2-isopropyl-1,3-propanediamide **180c** (0.81 g, 35 %), mp 120-122 °C (from EtOH) (Found: $\mathbf{MH}^+$, 233.1220. $C_{10}H_{20}N_2O_4$ requires *MH*, 233.1219.); ν_{max}(NaCl)/cm^{-1} 3311 (OH), 3098 (NH) and 1631 (CO); δ_H(400 MHz; DMSO-d_6) 0.97 [6H, d , *J* 7.0 Hz, (C***H***$_3$)$_2$CH], 2.10 [1H, m, (CH$_3$)$_2$C***H***CH], 3.07 (1H, d, *J* 7.7 Hz, C***H***CH), 3.12 (4H, q, *J* 5.7 Hz, C***H***$_2$NH), 3.40 (4H, q, *J* 5.7 Hz, C***H***$_2$OH), 4.67 (2H, t, *J* 5.3 Hz, OH) and 8.01 (2H, t, *J* 5.2 Hz, NH); δ_C(100 MHz; DMSO-d_6) 20.0 [(***C***H$_3$)$_2$CH], 28.7 [(CH$_3$)$_2$***C***H], 41.5 (***C***H$_2$NH), 56.0 [(CH$_3$)$_2$CH***C***H], 59.6 (***C***H$_2$OH) and 168.4 (CO).

N,N´-*Bis(2-hydroxyethyl)-2-propyl-1,3-propanediamide* 180d

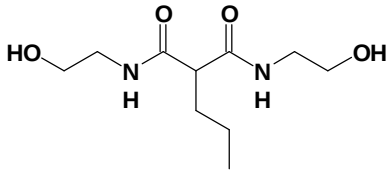

The experimental procedure described for the synthesis of N,N´-bis(2-hydroxyethyl)malonamide **180k** was followed, using diethyl propylmalonate **177d** (2.03g, 10.0 mmol), ethanolamine **179** (1.24 g, 20.2 mmol) and stirring for 24 hours. The resultant precipitate was filtered off and recrystallized from EtOH-Et_2O, yielding, as cream flakes, *N,N´*-bis(2-hydroxyethyl)-2-propyl-1,3-propanediamide **180d** (0.42 g, 18 %), mp 117-118 °C (from EtOH) (Found: $\mathbf{MH}^+$, 233.1220. $C_{10}H_{20}N_2O_4$ requires *MH*, 233.1219.); ν_{max}(NaCl)/cm^{-1} 3316 (OH), 3092 (NH) and 1620 (CO); δ_H(400 MHz; DMSO-d_6) 0.84 (3H, t, *J* 7.3 Hz, C***H***$_3$CH$_2$), 1.17 (2H, m, C***H***$_2$CH$_3$), 1.64 (2H, q, *J* 7.7 Hz, CHC***H***$_2$), 3.05 (1H, t, *J* 7.6 Hz, C***H***CH$_2$), 3.12 (4H, q, *J* 5.8 Hz, C***H***$_2$NH), 3.38 (4H, q, *J* 5.6 Hz, C***H***$_2$OH), 4.69 (2H, t, *J* 5.3 Hz, OH) and 8.02 (2H, t, *J* 5.4 Hz, NH); δ_C(100 MHz; DMSO-d_6) 13.6 (CH_3), 20.0 (***C***H$_2$CH$_3$), 32.5 (CH***C***H$_2$), 41.4 (CH_2NH), 52.8 (***C***HCH$_2$), 59.6 (***C***H$_2$OH) and 169.8 (CO).

***2-Butyl*-N,N´-*bis(2-hydroxyethyl)-1,3-propanediamide* 180f** [124]

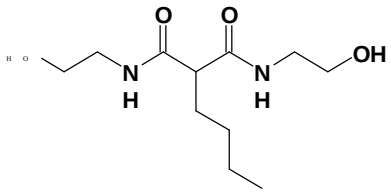

The experimental procedure described for the synthesis of N,N´-bis(2-hydroxyethyl)malonamide **180k** was followed, using diethyl butylmalonate **177f** (2.17g, 10.0 mmol), ethanolamine **179** (1.23 g, 20.1 mmol) and stirring for 48 hours. The resultant precipitate was filtered off and recrystallized from EtOH-Et_2O, yielding, as cream flakes, 2-butyl-*N,N´*-bis(2-hydroxyethyl)-1,3-propanediamide **180f** (2.21 g, 89 %), mp 123-125 °C (from EtOH) (Found: $\mathbf{MH}^+$, 247.1370. $C_{11}H_{22}N_2O_4$ requires *MH*, 247.1371.); ν_{max}(NaCl)/cm^{-1} 3310 (OH), 3089 (NH) and 1630 (CO); δ_H(400 MHz; DMSO-d_6) 0.83 (3H, t, *J* 7.3 Hz, C***H***$_3$CH$_2$), 1.14 (2H, m, CH$_2$C***H***$_2$CH$_2$), 1.24 (2H, m, CH$_3$C***H***$_2$), 1.65 (2H, q, *J* 7.6 Hz, CHC***H***$_2$), 3.02 (1H, t, *J* 7.6 Hz, C***H***CH$_2$), 3.12 (4H, q, *J* 5.8 Hz, C***H***$_2$NH), 3.44 (4H, q, *J* 5.8 Hz, C***H***$_2$OH), 4.70 (2H, s, *J* 5.4 Hz, OH) and 7.86 (2H, t, *J* 5.6 Hz, NH); δ_C(100 MHz; DMSO-d_6) 13.8 (***C***H$_3$CH$_2$), 21.9

($CH_3\boldsymbol{C}H_2$), 29.1 ($CH_2\boldsymbol{C}H_2CH_2$), 30.1 ($CH\boldsymbol{C}H_2$), 41.4 ($\boldsymbol{C}H_2NH$), 53.0 ($\boldsymbol{C}HCH_2$), 59.7 ($\boldsymbol{C}H_2OH$) and 169.9 (CO).

N,N´-*Bis(2-hydroxyethyl)-2-pentyl-1,3-propanediamide* 180g

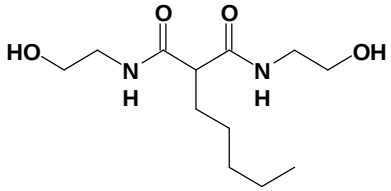

The experimental procedure described for the synthesis of N,N´-bis(2-hydroxyethyl)malonamide **180k** was followed, using diethyl pentylmalonate **177g** (2.31 g, 10.0 mmol), ethanolamine **179** (1.23 g, 20.2 mmol) and stirring for 1 week. The resultant precipitate was filtered off and recrystallized from EtOH-Et_2O to yield, as cream flakes, *N,N´*-bis(2-hydroxyethyl)-2-pentyl-1,3-propanediamide **180g** (1.18 g, 45 %), mp 124-125 °C (from EtOH) (Found: $\mathbf{MH}^+$, 261.1815. $C_{12}H_{24}N_2O_4$ requires *MH*, 261.1814.); ν_{max}(NaCl)/cm^{-1} 3283 (OH), 3074 (NH) and 1660 (CO); δ_H(400 MHz; DMSO-d_6) 0.84 [3H, t, *J* 7.1 Hz, $C\boldsymbol{H}_3(CH_2)_4CH$], 1.20 [6H, m, $CH_3(C\boldsymbol{H}_2)_3CH_2CH$], 1.64 [2H, q, *J* 7.3 Hz, $CH_3(CH_2)_3C\boldsymbol{H}_2CH$], 3.02 [1H, t, *J* 7.8 Hz, $CH_3(CH_2)_3CH_2C\boldsymbol{H}$], 3.12 (4H, q, *J* 5.6 Hz, $C\boldsymbol{H}_2NH$), 3.38 (4H, q, *J* 5.6 Hz, $C\boldsymbol{H}_2OH$), 4.69 (2H, t, *J* 5.3 Hz, OH) and 7.86 (2H, t, *J* 5.2 Hz, NH); δ_C(100 MHz; DMSO-d_6) 13.8 [$\boldsymbol{C}H_3(CH_2)_4CH$], 21.9, 26.4, 30.3, 30.9 [$CH_3(\boldsymbol{C}H_2)_4CH$], 41.4 ($\boldsymbol{C}H_2NH$), 53.0 [$CH_3(CH_2)_4\boldsymbol{C}H$], 59.7 ($\boldsymbol{C}H_2OH$) and 169.8 (CO).

***2-Hexyl*-N,N´-*bis(2-hydroxyethyl)-1,3-propanediamide* 180h**

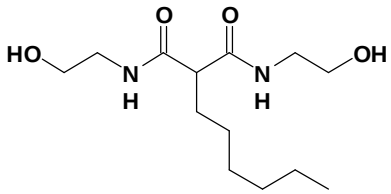

The experimental procedure described for the synthesis of *N,N´*-bis(2-hydroxyethyl)malonamide **180k** was followed, using diethyl hexylmalonate **177h** (2.47 g, 10.1 mmol), ethanolamine **179** (1.23 g, 20.1 mmol) and stirring for 1 week. The resultant precipitate was filtered off and recrystallized from EtOH-Et_2O to yield, as cream flakes, 2-hexyl-*N,N´*-bis(2-hydroxyethyl)-1,3-propanediamide **180h** (1.20 g, 43 %), mp 108-109 °C (from EtOH) (Found: $\mathbf{MH}^+$, 275.1970. $C_{13}H_{26}N_2O_4$ requires

MH, 275.1971.); ν_{max}(NaCl)/cm^{-1} 3337 (OH), 3120 (NH) and 1677 (CO); δ_H(400 MHz; DMSO-d_6) 0.85 [3H, t, *J* 7.1 Hz, C***H***$_3$(CH$_2$)$_5$CH], 1.22 [8H, m, CH$_3$(C***H***$_2$)$_4$CH$_2$CH], 1.64 [2H, q, *J* 7.6 Hz, CH$_3$(CH$_2$)$_4$C***H***$_2$CH], 3.02 [1H, t, *J* 8.3 Hz, CH$_3$(CH$_2$)$_4$CH$_2$C***H***], 3.12 (4H, q, *J* 5.6 Hz, C***H***$_2$NH), 3.38 (4H, q, *J* 5.6 Hz, C***H***$_2$OH), 4.69 (2H, t, *J* 5.4 Hz, OH) and 7.85 (2H, t, *J* 5.1 Hz, NH); δ_C(100 MHz; DMSO-d_6) 13.9 [***C***H$_3$(CH$_2$)$_5$CH], 21.9, 26.7, 28.3, 30.4, 31.0 [CH$_3$(***C***H$_2$)$_5$CH], 41.4 [***C***H$_2$NH], 53.0 [CH$_3$(CH$_2$)$_5$***C***H], 59.7 (***C***H$_2$OH) and 169.8 (CO).

***2-Benzyl*-N,N´-*bis(2-hydroxyethyl)-1,3-propanediamide* 180i**

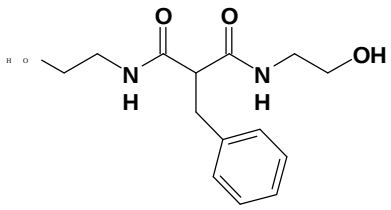

The experimental procedure described for the synthesis of N,N´-bis(2-hydroxyethyl)malonamide **180k** was followed, using diethyl benzylmalonate **177i** (2.51g, 10.0 mmol), ethanolamine **179** (1.23 g, 20.1 mmol) and stirring for 168 hours. The resultant precipitate was filtered off and recrystallized from EtOH-Et$_2$O, yielding, as cream flakes, 2-benzyl-*N*,*N*´-bis(2-hydroxyethyl)-1,3-propanediamide **180i** (1.41 g, 50 %), mp 130-131 °C (from EtOH) (Found: **MH**$^+$, 281.1523. $C_{14}H_{20}N_2O_4$ requires *MH*, 281.1527.); ν_{max}(NaCl)/cm^{-1} 3308 (OH), 3099 (NH) and 1642 (CO); δ_H(400 MHz; DMSO-d_6) 3.09 (2H, d, *J* 7.7 Hz, CHC***H***$_2$), 3.12 (4H, q, *J* 5.8 Hz, C***H***$_2$NH), 3.24 (1H, t, *J* 7.8 Hz, C***H***CH$_2$), 3.39 (4H, q, *J* 5.8 Hz, C***H***$_2$OH), 4.69 (2H, t, *J* 5.2 Hz, OH), 7.21 (5H, m, ArH) and 8.02 (2H, t, *J* 5.1 Hz, NH); δ_C(100 MHz; DMSO-d_6) 41.5 (***C***H$_2$NH), 47.0 (CHCH$_2$), 53.0 (***C***HCH$_2$), 59.6 (***C***H$_2$OH), 128.1, 128.6, 129.9 and 137.7 (ArC) and 168.9 (CO).

***2-Heptyl*-N,N´-*bis(2-hydroxyethyl)-1,3-propanediamide* 180j**

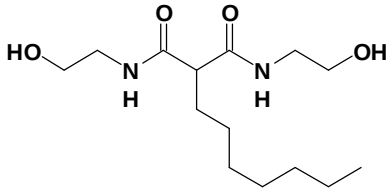

The experimental procedure described for the synthesis of *N,N´*-bis(2-hydroxyethyl)malonamide **180k** was followed, using diethyl heptylmalonate **177j** (2.59 g, 10.0 mmol), ethanolamine **179** (1.23 g, 20.1 mmol) and stirring for 1 week. The resultant precipitate was filtered off and recrystallized from EtOH-Et_2O to yield, as cream flakes, 2-heptyl-*N,N´*-bis(2-hydroxyethyl)-1,3-propanediamide **180j** (1.75 g, 61 %), mp 111-112 °C (from EtOH) (Found: $\mathbf{MH}^+$, 289.2123. $C_{14}H_{28}N_2O_4$ requires *MH*, 289.2127.); ν_{max}(NaCl)/cm^{-1} 3337 (OH), 3108 (NH) and 1675 (CO); δ_H(400 MHz; DMSO-d_6) 0.85 [3H, t, *J* 7.1 Hz, C***H***$_3$(CH$_2$)$_6$CH], 1.22 [10H, m, CH$_3$(C***H***$_2$)$_5$CH$_2$CH], 1.64 [2H, q, *J* 7.6 Hz, CH$_3$(CH$_2$)$_5$C***H***$_2$CH], 3.02 [1H, t, *J* 8.6 Hz, CH$_3$(CH$_2$)$_5$CH$_2$C***H***], 3.12 (4H, q, *J* 5.8 Hz, C***H***$_2$NH), 3.38 (4H, q, *J* 5.6 Hz, C***H***$_2$OH), 4.70 (2H, s, OH) and 7.86 (2H, t, *J* 5.1 Hz, NH); δ_C(100 MHz; DMSO-d_6) 13.9 [***C***H$_3$(CH$_2$)$_6$CH], 22.0, 26.8, 28.4, 28.6, 30.4, 31.1 [CH$_3$(***C***H$_2$)$_6$CH], 41.4 (***C***H$_2$NH), 53.0 [CH$_3$(CH$_2$)$_6$***C***H], 59.7 (***C***H$_2$OH) and 169.8 (CO).

3.1.3.3 *Substituted malonamides*

N,N´-*Bis(2-tosylethyl)malonamide* 181[99]

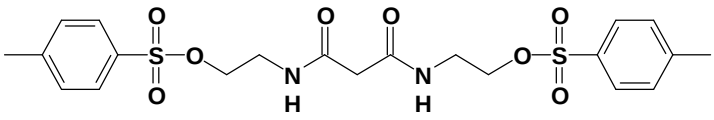

The synthetic method for tosylation of alcohols described by Kabalka *et al.*[99] was followed using *N,N´*-bis(2-hydroxyethyl)malonamide **180k** (1.00 g, 5.2 mmol) dissolved in $CHCl_3$ (10 ml) and cooled in an ice bath (0 °C). Pyridine (1.6 ml, 20 mmol) was added, followed, in small portions, by the addition of *p*-toluenesulfonyl chloride (2.85 g, 15 mmol) while stirring. The resulting mixture was allowed to stir for a further 4 h. Ether (30 ml) and water (10 ml) were then added, after which the organic layer was separated off, washed with HNO_3 (2 M), $NaHCO_3$ (5 %), and water, and dried over anhyd. $MgSO_4$. The solvent was removed *in vacuo* and the crude

product purified by flash chromatography [CH_2Cl_2-hexane (80:20)] to yield, as an orange oil, *N,N´*-bis(2-*p*-tosylethyl)malonamide (0.21 g, 8 %); δ_H(400 MHz; DMSO-d_6) 2.29 (6H, s, CH_3), 3.04 (2H, s, CH_2CO), 3.13 (4H, q, C***H***$_2$NH), 3.41 (4H, q, C***H***$_2$O), 7.14 (4H, d, ArH), 7.51 (4H, d, ArH) and 8.59 (2H, t, NH).

***Attempted synthesis of 1,4-Dithia-7,11-diazacyclotridecane-8,10-dione* 182**

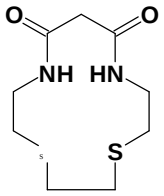

N,N´-Bis(2-tosylethyl)malonamide **181** (0.05 g, 0.1 mmol) was stirred with 1,2-dithioethane (0.01 g, 0.1 mmol) and KOH (0.006 g, 0.1 mmol) in MeOH (3 ml) for 1 week. NMR spectroscopy of the crude mixture revealed that reaction had not occurred.

***Attempted synthesis of* N,N´*-Bis(sulfanylethyl)malonamide* 183**

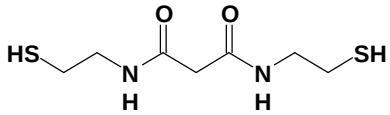

N,N´-bis(2-hydroxyethyl)malonamide **180k** (0.5 g, 2.5 mmol) was refluxed with thiourea (0.4 g, 5.0 mmol) and conc. HCl (2 ml) for 4 h. NMR spectroscopy of the crude mixture revealed that reaction had not occurred.

***Attempted synthesis of 1,4-Dioxa-7,11-diazacyclotridecane-8,10-dione* 184**

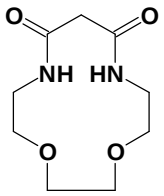

N,N´-bis(2-hydroxyethyl)malonamide **180k** (0.5 g, 2.5 mmol) was stirred with 1,2-dibromoethane (0.47 g, 2.5 mmol) and KOH (0.14 g, 2.5 mmol) in MeOH (5 ml) for 1 week. NMR spectroscopy of the crude mixture revealed that reaction had not occurred.

***Attempted synthesis of 1,11-Dioxa-4,8-diazacyclotetradecane-5,7-dione* 185**

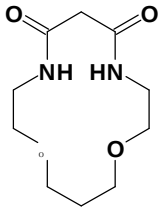

N,N´-bis(2-hydroxyethyl)malonamide **180k** (0.5 g, 2.5 mmol) was stirred with 1,3-dibromopropane (0.5 g, 2.5 mmol) and KOH (0.14 g, 2.5 mmol) in MeOH (5 ml) for 1 week. NMR spectroscopy of the crude mixture revealed that reaction had not occurred.

***Attempted synthesis of Dithiomalonic acid bis-S-(2-hydroxyethyl) ester* 187**

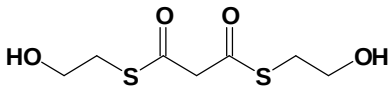

Diethyl malonate **175** (0.5 g, 3.0 mmol) was stirred with mercaptoethanol **186** (0.25 g, 3.0 mmol) and KOH (0.17 g, 3.0 mmol) in MeOH (5 ml) for 1 week. The solvent was removed *in vacuo* to give a pale yellow paste (0.26 g, 40 %). NMR spectroscopy of the crude mixture revealed a complex mixture and the presence of inorganic material. Isolation of the product from the crude mixture by flash chromatography [EtOAc:hexane (80:20)] proved fruitless.

***Attempted synthesis of Dithiomalonic acid bis-S-(2-aminoethyl) ester* 188**

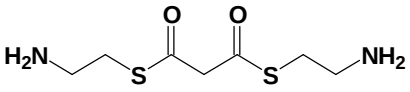

Method (a). Diethyl malonate **175** (0.5 g, 3.0 mmol) was stirred with 2-sulfanylethylamine hydrochloride (0.34 g, 3.0 mmol) and triethylamine (0.17 g, 3.0 mmol) in MeOH (5 ml) for 1 week. NMR spectroscopy of the crude mixture revealed a complex mixture and isolation of the product from the crude mixture was not attempted.

Method (b). Malonyl dichloride **176** (0.42 g, 3.0 mmol) was stirred with 2-sulfanylethylamine hydrochloride (0.34 g, 3.0 mmol) and triethylamine (0.17 g, 3.0 mmol) in dry MeOH (5 ml), under nitrogen overnight. NMR spectroscopy of the

crude mixture revealed a complex mixture and isolation of the product from the crude mixture was not attempted.

N,N´-*Bis(2-methoxyethyl)malonamide* 194

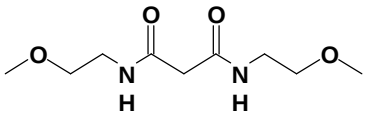

Method (a). A solution of diethyl malonate **175** (1.0 g, 6.2 mmol) and 2-methoxyethylamine **189** (0.978 g, 13.0 mmol) in MeOH was heated under reflux for 16 hours. The solvent was then removed *in vacuo*, and the crude product was recrystallised from EtOAc-hexane to yield, as a colourless needles, N,N´-*bis(2-methoxyethyl)malonamide* **194** (0.837 g, 62 %), mp 93-94 °C (EtOAc:hexane), (Found:, $\mathbf{M}^+$, 218.1258. $C_9H_{18}N_2O_4$ requires *M*, 218.1266); ν_{max}(KBr)/cm^{-1} 3280 (NH) and 1667 (CO); δ_H(400 MHz; $CDCl_3$) 3.16 (2H, s, CH_2CO), 3.33 (6H, s, CH_3O), 3.42 (8H, m, $OC\boldsymbol{H}_2C\boldsymbol{H}_2NH$) and 7.17 (2H, s, NH); δ_C(100 MHz; $CDCl_3$) 39.3 ($CH_2\boldsymbol{C}H_2NH$), 43.0 (CH_2CO), 58.7 (CH_3O), 70.8 ($CH_2\boldsymbol{C}H_2O$) and 167.3 (CO); *m/z* (EI) 219 (M^+, 10 %), and 112 (100).

Method (b). A solution of diethyl malonate **175** (2.1 g, 12.8 mmol) and 2-methoxyethylamine **189** (2.0 g, 26.5 mmol) in hexane (10 ml) was stirred for 7 days. The solvent was then removed *in vacuo*, and the crude product was recrystallised from EtOAc-hexane to yield, as a colourless needles, *N,N´*-bis(2-methoxyethyl)malonamide **194** (0.674 g, 24 %).

N,N´-*Bis(2-benzylsulfanylethyl)malonamide* 195

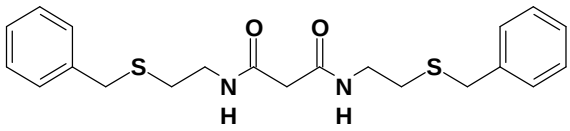

Method (a). Diethyl malonate **175** (1.60 g, 10.0 mmol) and *S*-benzylcysteamine [3.34 g, 20.0 mmol; obtained by the reaction of *S*-benzylcysteamine hydrochloride **190** with 0.1 M methanolic NaOMe] were placed in a conical flask (25 ml) fitted with a bleed and exposed to microwave irradiation (defrost setting) for 210 seconds. The mixture was allowed to cool, the resulting precipitate filtered off, washed with Et_2O

and then recrystallised from EtOH to yield, as yellow crystals, N,N´-*bis(2-benzylsulfanylethyl)malonamide* **195** (2.21 g, 55 %), mp 105-106 °C (from EtOH), (Found: $\mathbf{M}^+$, 402.1441. $C_{21}H_{26}N_2O_2S_2$ requires 402.1435); ν_{max}(KBr)/cm^{-1} 3300 (NH) and 1630 (CO); ν_{max}(CaF_2)/cm^{-1} 3374 (NH) and 1678 (CO); δ_H(400 MHz; $CDCl_3$) 2.53 (4H, m, C***H***$_2$S), 3.10 (2H, s, $COCH_2CO$), 3.38 (4H, m, CONHC***H***$_2$), 3.70 (4H, s, PhC***H***$_2$S), 7.18 (2H, t, NH) and 7.30 (10H, d, ArH); δ_C(100 MHz; $CDCl_3$) 35.9 (CH_2***C***H_2S), 39.3 ($PhCH_2S$), 42.9 (CH_2CO), 70.8 (CH_2***C***H_2NH), 127.1, 128.5, 128.7 and 138.0 (ArC) and 167.2 (CO); *m/z* (EI) 403 (M^+, 4 %), 311 (100).

Method (b). A solution of diethyl malonate **175** (0.401 g, 2.5 mmol) and *S*-benzylcysteamine hydrochloride **190** (0.991 g, 4.9 mmol) in methanolic NaOMe (0.1 M, 50 ml) was stirred for 7 days. The solvent was then removed *in vacuo*, and the crude product recrystallised from EtOAc-hexane to yield, as a fine yellow powder, *N,N´*-bis(2-benzylsulfanylethyl)malonamide **195** (0.237 g, 24 %).

N,N´-*Bis(2-methoxyphenyl)malonamide* 196[125]

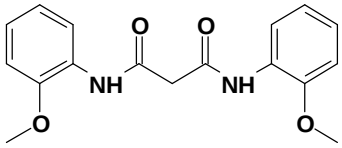

Method (a). Diethyl malonate **175** (1.02 g, 6.4 mmol) and *o*-anisidine **191** (1.63 g, 13.2 mmol) were placed in a conical flask (25 ml) fitted with a bleed, and subjected to microwave irradiation (defrost setting) for 300 seconds. NMR analysis of the crude product (1.76 g) revealed that 81% of the diethyl malonate **175** had been converted to the desired product. The crude mixture was recrystallised from EtOAc-hexane to yield, as colourless needles, *N,N´*-bis(2-methoxyphenyl)malonamide **196** (1.13 g, 65 %), mp 163-5 °C (from EtOH-hexane)(lit.,[125] 160-163 °C; from EtOH) (Found: $\mathbf{M}^+$, 314.1256. $C_{17}H_{18}N_2O_4$ requires *M*, 314.1266); ν_{max}(KBr)/cm^{-1} 3369 (NH) and 1676 (CO); δ_H(400 MHz; $CDCl_3$) 3.54 (2H, s, CH_2CO), 3.89 (6H, s, CH_3O), 6.88 (2H, d, ArH), 6.95 (2H, t, ArH), 7.04 (2H, t, ArH), 8.33 (2H, d, ArH) and 8.96 (2H, br s, NH); δ_C(100 MHz; $CDCl_3$) 45.8 (CH_2CO), 55.8 (CH_3O), 110.1, 120.3, 120.9, 124.3, 127.2 and 148.4 (ArC) and 164.8 (CO); *m/z* (EI) 314 (M^+, 100 %), 165 (52).

Method (b). Diethyl malonate **175** (1.0 g, 6.2 mmol) was stirred with *o*-anisidine **191** (1.6 g, 13.0 mmol) for 7 days. The desired product, *N,N´*-bis(2-methoxyphenyl)malonamide **196** could not be isolated from the resulting mixture.

Method (c). A solution of malonyl dichloride **176** (0.5 ml, 4.0 mmol) in anhyd. THF (100 ml) was added dropwise, over 3.5 hours, to a solution of *o*-anisidine **191** (1.02 g, 8.3 mmol) and pyridine (0.7 ml) in dry THF (200 ml), under dry nitrogen. The reaction mixture was stirred overnight, water (20 ml) was then added and the resulting mixture extracted with EtOAc (3 x 50 ml). The EtOAc extracts were dried over anhyd. $MgSO_4$, and the solvent was removed *in vacuo* to yield the crude product (1.51 g). The crude product was filtered through a silica plug and recrystallised from EtOH-Et_2O to yield, as colourless needles, *N,N´*-bis(2-methoxyphenyl)malonamide **196** (0.293 g, 23 %).

Method (d). A mixture of diethyl malonate **175** (1.0 g, 6.2 mmol) and *o*-anisidine **191** (1.6 g, 13.0 mmol) was heated under reflux for 48 hours. Volatile material was removed *in vacuo*, and the residue was dissolved in a mixture of EtOAc (1 ml) and hexane (5 ml). The resulting precipitate was filtered off and washed with hexane until the organic phase remained colourless. The residue was then dried to yield, as a fine, light-brown powder, *N,N´*-bis(2-methoxyphenyl)malonamide **196** (1.283 g, 66 %), which was shown by TLC and NMR analysis to be pure.

N,N´-*Bis(2-methylsulfanylphenyl)malonamide* 197

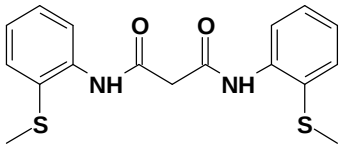

Method (a). The experimental procedure described for the synthesis of N,N´-*bis(2-methoxybenzyl)malonamide* **196 [**method (**a**)] was followed, using diethyl malonate **175** (1.0 g, 6.2 mmol) and 2-methylsulfanylphenylamine **192** (1.74 g, 12.5 mmol). The reagents were subjected to microwave radiation (defrost setting) for 360 seconds. NMR analysis of the crude product (2.22 g) revealed that 62% of the diethyl malonate **175** had been converted to the desired product. The crude mixture was recrystallised from EtOAc-hexane to yield, as a fine, light-yellow crystals, N,N´-*bis(2-*

methylsulfanylphenyl)malonamide **197** (1.076 g, 49 %), mp 114-116 °C (from EtOAc-hexane) (Found: $\mathbf{M}^+$, 346.0822 $C_{17}H_{18}N_2O_2S_2$ requires *M*, 346.0809); ν_{max}(KBr)/cm^{-1} 3225 (NH), 1682 and 1673 (CO); δ_H(400 MHz; $CDCl_3$) 2.39 (6H, s, CH_3S), 3.63 (2H, s, CH_2CO), 7.09 (2H, t, ArH), 7.27 (2H, t, ArH), 7.46 (2H, d, ArH), 8.26 (2H, d, ArH) and 9.33 (2H, br s, NH); δ_C(100 MHz; $CDCl_3$) 18.6 (CH_3S), 45.6 (CH_2CO), 121.3, 125.0, 126.7, 128.4, 132.2 and 137.4 (ArC) and 165.0 (CO); *m/z* (EI) 346 (M^+, 85 %), 299 (100).

Method (b). The experimental procedure described for the synthesis of N,N´-*bis(2-methoxybenzyl)malonamide* **196** [method (**d**)] was followed, using diethyl malonate **175** (1.0 g, 6.2 mmol) and 2-methylsulfanylphenylamine **192** (1.74 g, 12.5 mmol). Volatile material was removed *in vacuo*, and the crude product was then dissolved in a mixture of $CHCl_3$ (1 ml) and hexane (5 ml). The resulting mixture was filtered and the residual solid washed with hexane until the organic phase was colourless. The product was dried to yield, as a fine, light-yellow powder, N,N´-*bis(2-methylsulfanylphenyl)malonamide* **197** (0.643 g, 30 %), which was shown by TLC and NMR analysis to be pure.

N,N´-*Bis(2-methoxyphenyl)thiomalonamide* 198

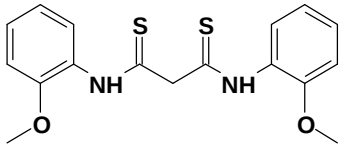

A mixture of *N,N´*-bis(2-methoxyphenyl)malonamide **196** (0.5 g, 1.6 mmol) and Lawesson's reagent (0.6 g, 1.6 mmol) in anhyd. THF (10 ml) was stirred overnight at room temperature. The solvent was removed *in vacuo* and the crude product purified by rotating plate chromatography [elution with CH_2Cl_2-Et_2O (90:10)] to yield, as a fine, light-yellow powder, N,N´-*bis(2-methoxyphenyl)thiomalonamide* **198** (0.035 g, 1 %), mp 116-118 °C (from CH_2Cl_2:Et_2O), (Found: $\mathbf{M}^+$, 346.0814. $C_{17}H_{18}N_2O_2S_2$ requires *M*, 346.0809); ν_{max}(KBr)/cm^{-1} 3232 (NH) and 1399, 1254 and 1113 (N-C=S); δ_H(400 MHz; $CDCl_3$) 3.89 (6H, s, CH_3O), 4.43 (2H, s, CH_2CS), 6.92 (2H, d, ArH), 6.99 (2H, t, ArH), 7.19 (2H, t, ArH), 8.91 (2H, d, ArH) and 10.24 (2H, br s, NH); δ_C(100 MHz; $CDCl_3$) 56.0 (CH_3O), 69.6(***C***H_2CS), 110.6, 120.2, 121.6, 126.9, 128.1 and 150.2 (ArC) and 192.3 (CS).

***2-Allyl*-N,N'-*bis(2-methoxyphenyl)-1,3-propanediamide* 207**

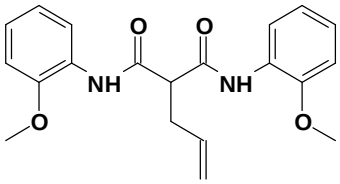

Diethyl (3-propenyl)malonate **177e** (2.0 g, 10 mmol) and *o*-anisidine **191** (2.47 g, 20.0 mmol) were placed in a conical flask (25 ml) fitted with a bleed, and subjected to microwave irradiation (defrost setting) for 450 seconds. The mixture was allowed to cool, and the resulting precipitate filtered off, washed with Et_2O and then recrystallised from EtOH to yield, as colourless crystals, *2-allyl*-N,N'-*bis(2-methoxybenzyl)-1,3-propanediamide* **207** (1.91 g, 54 %), mp 144-146 °C (from EtOH) (Found: $\mathbf{M}^+$, 354.1585. $C_{20}H_{22}N_2O_4$ requires *M*, 354.1579); ν_{max}(KBr)/cm^{-1} 3371 (NH) and 1677 (CO); δ_H(400 MHz; $CDCl_3$) 2.84 (2H, t, C***H***$_2$CH), 3.37 (1H, t, CHCO), 3.89 (6H, s, CH_3O), 5.18 (2H, dd, C***H***$_2$=CH), 5.88 (2H, m, CH_2=C***H***), 6.87 (2H, d, ArH), 6.95 (2H, t, ArH), 7.05 (2H, t, ArH), 8.34 (2H, d, ArH) and 8.79 (2H, br s, NH); δ_C(100 MHz; $CDCl_3$) 36.6 (***C***H_2CH), 55.8 (CH_3O), 57.5 (CO***C***HCO), 110.1 (ArC), 118.3 (***C***H_2=CH), 120.1, 120.9, 124.3 and 127.2 (ArC), 133.7 (CH_2=***C***H), 148.4 (ArC) and 167.7 (CO); *m/z* (EI) 354 (M^+, 79 %), 205 (100).

N,N´-*Bis(2-methoxybenzyl)malonamide* 208

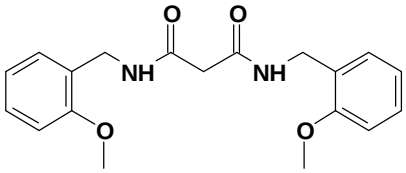

The experimental procedure described for the synthesis of N,N´-*bis(2-methoxybenzyl)malonamide* **196** [method (**a**)] was followed, using diethyl malonate **175** (1.0 g, 6.2 mmol) and 2-methoxybenzylamine **193** (1.74 g, 12.5 mmol). The reagents were subjected to microwave radiation (defrost setting) for 210 seconds. NMR analysis of the crude product (2.15 g) revealed that the sample contained only the desired product. The crude mixture was recrystallised from EtOAc-hexane to yield, as a fine, white crystals, N,N´-*bis(2-methoxyphenyl)malonamide* **208** (2.04 g, 96 %), mp 120-122 °C (from EtOAc-hexane) (Found: $\mathbf{M}^+$, 342.1586. $C_{19}H_{22}N_2O_4$ requires *M*, 342.1579); ν_{max}(KBr)/cm^{-1} 3297 (NH) and 1655 (CO); δ_H(400 MHz; $CDCl_3$) 3.14 (2H, s, CH_2CO), 3.82 (6H, s, CH_3O), 4.41 (4H, d, ArC***H***$_2$NH$_2$), 6.86

(4H, m, ArH), 7.22 (4H, m, ArH) and 7.41 (2H, br s, NH); δ_C(100 MHz; $CDCl_3$) 39.2 ($ArCH_2$), 43.2 (***C***H_2CO), 55.2 (CH_3O), 110.3, 120.5, 125.9, 128.7, 129.3 and 157.4 (ArC) and 167.0 (CO); *m/z* (EI) 342 (M^+, 40 %), 136 (100).

N-(*2-methoxyphenyl*)-N´-*(2-methylsulfanylphenyl)malonamide* 209

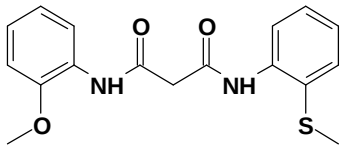

The experimental procedure described for the synthesis of N,N´-*bis(2-methoxybenzyl)malonamide* **196 [**method (**a**)] was followed, using diethyl malonate **175** (1.0 g, 6.2 mmol) and 2-methylsulfanylphenylamine (0.87 g, 6.2 mmol). The reagents were subjected to microwave radiation (defrost setting) for 360 seconds. On cooling, *o*-anisidine (0.82 g, 6.6 mmol) was added to the mixture, which was then exposed to further microwave irradiation (defrost setting) for 300 seconds. ^{1}H NMR analysis of the crude product (2.40 g) revealed a complex mixture, and isolation of the desired product was not attempted.

3.1.4 Synthesis of selected silver(I) and copper(II) complexes

Silver(I) [*N,N´*-bis(4-methoxyphenyl)-3,6,-dithiaoctanediamide]triflate 151b

To a solution of *N,N´*-bis(4-methoxyphenyl)-3,6,-dithiaoctanediamide **150b** (0.202 g, 0.5 mmol) in DMF (4.5 ml), CF_3SO_3Ag (0.123 g, 0.5 mmol) was added. The mixture was allowed to stir overnight in a dark room. Diethyl ether (20 ml) was added to the mixture and the resultant precipitate was filtered off, to yield, as a fine, brown powder, silver(I)[*N,N´*-bis(4-methoxyphenyl)-3,6,-dithiaoctanediamide]triflate **151b** (0.139 g, 41 %); ν_{max}(NaCl)/cm^{-1} 3291(NH) and 1667 (CO).

Copper(II) [2-heptyl-*N,N´*-bis(2-hydroxyethyl)-1,3-propanediamide]nitrate 211

A solution of $Cu(NO_3)_2$ (0.1 g, 0.5 mmol) and 2-heptyl-*N,N´*-bis(2-hydroxyethyl) -1,3-propanediamide **180j** (0.163 g, 0.5 mmol) in MeOH was boiled under reflux for 2 h. The solvent was removed *in vacuo*, to yield a fine, blue powder, which was recrystallised from MeOH to afford, as blue crystals, *copper(II) [2-heptyl*-N,N´*-bis(2-hydroxyethyl)-1,3-propanediamide]nitrate* **211** (0.202 g, 80 %), mp 126-128 °C (from MeOH) (Found: C, 37.5; H, 6.7; N, 10.9. $C_{14}H_{28}N_4O_{10}Cu{\bullet}2(CH_3OH)$ requires C, 35.6; H, 6.7; N, 10.4 %); ν_{max}(KBr)/cm^{-1} 3265 (OH), 3092 (NH) and 1624 (CO)..

Copper(II) [*N,N´*-bis(2-methoxyethyl)malonamide]nitrate 212

A solution of $Cu(NO_3)_2$ (0.199 g, 1.0 mmol) and *N,N´*-bis(2-methoxyethyl)malonamide **194** (0.231 g, 1.0 mmol) in MeOH was boiled under reflux for 2 h. The solvent was removed *in vacuo*, to yield a fine, blue powder, which was recrystallised from MeOH to afford, as blue crystals, *copper(II) [*N,N´*-bis(2-methoxyethyl)malonamide]nitrate* **212** (0.345 g, 85 %), mp 144-146 °C (from MeOH) (Found: C, 25.6; H, 5.2; N, 12.1. $C_9H_{18}N_4O_{10}Cu{\bullet}2CH_3OH$ requires C, 27.4; H, 5.1; N, 12.8 %); ν_{max}(KBr)/cm^{-1} 3280 (NH) and 1619 (CO).

Copper(II) [*N,N´*-bis(2-benzylsulfanylethyl)malonamide]nitrate 213

A solution of $Cu(NO_3)_2$ (0.10 g, 0.5 mmol) and *N,N´*-bis(2-benzylsulfanylethyl)malonamide **195** (0.212 g, 0.5 mmol) in EtOAc was boiled under reflux for 2 h. The solvent was removed *in vacuo*, to yield, as a green paste, *copper(II) [*N,N´*-bis(2-benzylsulfanylethyl)malonamide]nitrate* **213** (0.246 g, 78 %) (Found: C, 48.6; H, 4.7; N, 7.7. $C_{21}H_{26}N_4O_8S_2Cu$•1.5(EtOAc) requires C, 43.9; H, 5.2; N, 7.6 %); $\nu_{max}(CaF_2)/cm^{-1}$ 3364 (NH) and 1656 (CO).

Silver(I) [*N,N´*-bis(2-benzylsulfanylethyl)malonamide]triflate 214

A solution of CF_3SO_3Ag (0.13 g, 0.5 mmol) and *N,N´*-bis(2-benzylsulfanylethyl)malonamide **195** (0.212 g, 0.5 mmol) in EtOAc was boiled under reflux for 15 minutes. The solvent was removed *in vacuo*, to yield, as a yellow paste, *silver(I) [*N,N´*-bis(2-benzylsulfanylethyl)malonamide]triflate* **214** (0.316 g, 90 %) (Found: C, 40.6; H, 4.1; N, 4.7. $C_{21}H_{26}N_2O_2S_2F_3Ag$•2($CH_3OH$) requires C, 42.9; H, 4.7; N, 4.4 %); $\nu_{max}(CaF_2)/cm^{-1}$ 3356 (NH) and 1678 (CO). *m/z* (FAB) 618.8 (M_2L^{2+}, 2.4 %) and 106.9 (100).

Copper(I) [*N,N´*-bis(2-methoxyphenyl)malonamide]nitrate 215

A solution of $Cu(NO_3)_2$ (0.186 g, 1.0 mmol) and *N,N´*-bis(2-methoxyphenyl)malonamide **196** (0.310 g, 1.0 mmol) in MeOH was boiled under reflux for 4 h. The solution, which was initially green, turned brown after 4 h. The solvent was removed *in vacuo*, to yield a fine, brown powder, which was recrystallised from MeOH to afford, as brown crystals, *copper(I) [*N,N´*-bis(2-methoxyphenyl)malonamide]nitrate* **215** (0.410 g, 93 %), mp 93-94 °C (from MeOH) (Found: C, 47.9; H, 4.4; N, 9.95. $C_{17}H_{18}N_3O_7Cu$ requires C, 46.5; H, 4.1; N, 9.6 %); $\nu_{max}(KBr)/cm^{-1}$ 3314 (NH) and 1676 (CO).

Copper(II) [*N,N´*-bis(2-methylsulfanylphenyl)malonamide]nitrate 216

A solution of $Cu(NO_3)_2$ (0.108 g, 0.5 mmol) and *N,N´*-bis(2-methylsulfanylphenyl)malonamide **197** (0.194 g, 0.5 mmol) in MeOH was boiled under reflux for 4 h. The solvent was removed *in vacuo*, to yield a fine, olive-coloured powder, which was recrystallised from MeOH to afforded, as olive-coloured crystals, *copper(II) [*N,N´*-bis(2-methylsulfanylphenyl)malonamide]nitrate* **216** (0.206 g, 72 %), mp 78-80 °C (from MeOH) (Found: C, 39.9; H, 4.0; N, 9.3. $C_{17}H_{18}N_4O_8S_2Cu$ requires C, 38.2; H, 3.4; N, 10.5 %); ν_{max}(KBr)/cm^{-1} 3264 (NH) and 1634 (CO).

Silver(I) (*N,N´*-bis(2-methylsulfanylphenyl)malonamide)triflate 217

A solution of CF_3SO_3Ag (0.258 g, 1.0 mmol) in acetonitrile (1 ml) was added to a solution of *N,N´*-bis(2-methylsulfanylphenyl)malonamide **197** (0.347 g, 1.0 mmol) in $CHCl_3$ (10 ml) and the resulting solution was stirred overnight. The resultant precipitate was filtered off, washed with Et_2O, to afford, as a fine, white powder, *silver(I) [*N,N´*-bis(2-methylsulfanylphenyl)malonamide]triflate* **217** (0.419 g, 77 %), mp 228-230 °C (from MeCN-$CHCl_3$) (Found: C, 38.7; H, 2.9; N, 5.0. $C_{18}H_{18}N_2O_5S_3F_3Ag$ requires C, 35.8; H, 3.0; N, 4.6 %); ν_{max}(KBr)/cm^{-1} 3223 (NH) and 1644 (CO).

Copper(II) (*N,N´*-bis(2-methoxybenzyl)malonamide)nitrate 218

A solution of $Cu(NO_3)_2$ (0.188 g, 1.0 mmol) and *N,N´*-bis(2-methoxybenzyl)malonamide **208** (0.344 g, mmol) in MeOH was boiled under reflux for 4 h under a dry nitrogen atmosphere. The solvent was removed *in vacuo*, to yield, as fine, blue powder, *copper(II) [*N,N´*-bis(2-methoxybenzyl)malonamide]nitrate* **218** (0.40 g, 68 %), mp 176-178 °C (from MeOH) (Found: C, 46.0; H, 4.4; N, 10.0. $C_{19}H_{22}N_4O_{10}Cu$ requires C, 43.1; H, 4.2; N, 10.6 %); (Found:, **ML(NO$_3$)**$^+$, 467.94. $C_{19}H_{22}N_3O_7Cu$ requires *M*, 467.0753); ν_{max}(KBr)/cm^{-1} 3301 (NH) and 1622 (CO). *m/z* (FAB) 467.9 (*ML*$^+$, 3.7 %) and 121.1 (100).

3.2 Computer Modelling Data

A typical script used to perform Molecular Mechanics Dynamic Simulation on a structure in the Cerius$^{2®86}$ modeling package is listed below. For the free ligands the mid-cycle anneal temperature was set at 500 K, while for the metal complexes it was increased to 1000 K.

```
FILES/LOAD "./Model.msi"
FORCE-FIELD/LOAD_FORCE_FIELD "./Cerius2-Resources/FORCEFIELD/UNIVERSAL1.02"
FORCE-FIELD/CALCULATE_TYPING
FORCE-FIELD/CALCULATE_BOND_ORDER
CHARGE/CALCULATE
MECHANICS/METHOD "NEWTON RAPHSON"
MECHANICS/MINIMIZE
FILES/SAVE "./Model.min.msi"
DYNAMICS/METHOD "CONSTANT NVT"
DYNAMICS/QUENCH YES
DYNAMICS/ANNEAL YES
DYNAMICS/RUN_TIME 100000
DYNAMICS/ANNEAL_CYCLES 500
DYNAMICS/MID-CYCLE_TEMPERATURE 500
DYNAMICS/TRAJECTORY_PERIOD 1
DYNAMICS/ANNEAL_TRAJECTORY YES
DYNAMICS/TRAJECTORY_FILENAME "Model_anneal"
DYNAMICS/RUN_SIMULATION
SYSTEM/REINIT_ALL
```

The resultant data consisted of a collection of 500 conformers, which were analyzed to determine the conformer with the lowest potential (steric) energy. The steric energy (kcal.mol^{-1}) of this conformer was then used in the subsequent calculations. Unless indicated to the contrary, the modelling data cited in the following tables were obtained using the MM package Cerius^2.

3.2.1 Modelling data for the 3,6-Dithiaoctanediamide ligands and complexes

Table 25. Steric energies of the free ligand and complex with silver(I) for the ligand series **150a-f**.

150	Ligand / kcal.mol^{-1}	Complex / kcal.mol^{-1}	ΔE_{MM} [a] / kcal.mol^{-1}
a	-40.98	145.45	-
b	-25.74	144.83	15.9
c	-67.06	131.40	-12.0
d	42.03	178.36	50.1
e	-8.94	145.94	31.6
f	111.29	219.06	78.6

[a] $\Delta E_{MM} = (E_{ML_H} + E_{L_X}) - (E_{ML_X} + E_{L_H})$ where ΔE_{ML_H} and ΔE_{L_H} are the energies of the complex and free ligand of **150a**, respectively, and ΔE_{ML_X} and ΔE_{L_X} are the energies of the complex and free ligand of **150b-f**.

3.2.2 Modelling data for the Morita-Baylis-Hillman ligands

The steric energy values were determined by the method described previously, using the Cerius$^{2®86}$ 4.0 package.

Table 26. Data for the steric energy cost for coordination of silver(I) by ligand **157**.

Coordination Conformer	Steric Energy / kcal.mol^{-1}	ΔE_{MM} [a] / kcal.mol^{-1}
Free	27.2810	-
5-membered	34.0257	6.7447
6-membered	39.7873	12.506
7-membered	28.8894	1.6084

[a] Relative to the free ligand.

Table 27. Data for the generation of the new chiral centre in the MBH-derived ligand **166a**.

Compound	Stereochemistry	Steric Energy / kcal.mol^{-1}
170	RR	27.2810
171	RS	28.2712

3.2.3 Modelling data for the Malonamide ligands and Complexes

3.2.3.1 *Keto-enol tautomerism data*

The H_f values were determined using the semi-empirical MO (AM1) calculation option in the PC Spartan Pro[107] computer modelling package.

Table 28. Calculated ΔH_f values for the substituted malonic esters.

R	Compound	$H_{f_{keto}}$ / kJ.mol^{-1}	$H_{f_{enol}}$ / kJ.mol^{-1}	ΔH_f / kJ.mol^{-1}
H	**175**	-778.630	-744.237	34.394
Pr	**177d**	-852.056	-816.976	35.080
$CH_3(CH_2)_5$	**177h**	-935.004	-899.819	35.186

Table 29. Calculation of the equilibrium constant ***K*** for tautomerism in the substituted malonic esters.

R	Compound	ΔH_f / kJ.mol^{-1}	ln ***K*** [a]	***K***
H	**175**	34.394	-13.790	1.03 x10^{-06}
Pr	**177d**	35.080	-14.065	7.79 x10^{-07}
$CH_3(CH_2)_5$	**177h**	35.186	-14.107	7.47 x10^{-07}

[a] Assuming $\Delta H_f \approx \Delta G = -RT \ln K$.

Table 30. Calculated ΔH_f values for the tautomeric forms of the *N*,*N'*-bis(2-hydroxyethyl)malonamides..

R	Compound	$H_{f_{keto}}$ / kJ.mol^{-1}	$H_{f_{enol}}$ / kJ.mol^{-1}	ΔH_f / kJ.mol^{-1}
H	**180k**	-807.059	-730.923	76.136
Pr	**180d**	-879.375	-808.477	70.898
$CH_3(CH_2)_5$	**180h**	-943.323	-887.314	56.009

Table 31. Calculation of the equilibrium constant ***K*** for tautomerism in the *N,N'*-bis(2-hydroxyethyl)malonamides..

R	Compound	ΔH_f / kJ.mol^{-1}	ln ***K*** [a]	***K***
H	**180k**	76.136	-30.525	5.53 x10^{-14}
Pr	**180d**	70.898	-28.425	4.52 x10^{-13}
$CH_3(CH_2)_5$	**180h**	56.009	-22.456	1.77 x10^{-10}

[a] Assuming $\Delta H_f \approx \Delta G = -RT \ln K$.

3.2.3.2 *Coordination trend data*

The steric energy values were determined by the method described previously, using the package Cerius$^{2®86}$ 4.0.

Table 32. Coordination trend for the malonamide ligands **180j**, **195**, **196**, **197**, **208**.

Ligand Number	**180j**	**195**	**196**	**197**	**208**
Free Ligand / kcal.mol^{-1}	92.297	-52.375	16.566	-30.021	38.754
Ag(I) Complex / kcal.mol^{-1}	216.348	149.639	93.821	119.511	186.839
Chelating Conformer / kcal.mol^{-1}	126.822	-7.043	72.363	37.095	98.346
ΔE_{Diff} / kcal.mol^{-1}	34.525	45.332	55.797	67.117	59.592
Cu(II) Complex / kcal.mol^{-1}	-53.690	152.443	-102.851	-165.385	-136.698
Chelating Conformer / kcal.mol^{-1}	179.007	31.544	70.867	56.281	138.684
ΔE_{Diff} / kcal.mol^{-1}	86.710	83.918	54.301	86.303	99.930
Hg(II) Complex / kcal.mol^{-1}	338.426	202.091	116.134	214.804	239.993
Chelating Conformer / kcal.mol^{-1}	147.535	2.838	74.258	39.857	84.770
ΔE_{Diff} / kcal.mol^{-1}	55.238	55.212	57.692	69.879	46.016
Pb(II) Complex / kcal.mol^{-1}	127.831	76.192	-110.420	28.868	89.739
Chelating Conformer / kcal.mol^{-1}	149.355	1.662	70.643	37.016	76.927
ΔE_{Diff} / kcal.mol^{-1}	57.058	54.037	54.077	67.037	38.173

[a] ΔE_{Diff} = difference in steric energy between the chelating conformer and the free ligand.

3.3 Solvent Extraction Studies

3.3.1 General Method

All studies were performed in a 150 ml jacketed beaker at 25 °C. Equal volumes of the organic and aqueous phase (50 ml) were stirred together vigorously. The organic phase (toluene or EtOAc) contained the ligand in excess with respect to the metal concentration, and was pre-saturated with 0.5 M acid (HNO_3 or HCl) by shaking a 4:1 mixture of solvent and acid for 15 minutes. The aqueous phase consisted of a known concentration of metal and the appropriate sodium salt ($NaNO_3$ or NaCl), to maintain the overall ionic strength of the aqueous phase. At regular time intervals, aliquots (<5 ml) of each phase were removed, and the aqueous phase was analyzed for the residual metal concentration, by AAS or ICP-Ms methods

For the pH dependence experiment, small volumes of aqueous NaOH (10 M) were added to the original mixture, and the resultant pH determined with a pH meter. The extraction study was conducted following the general method, with the aqueous phase being analyzed for the residual metal concentration.

3.3.2 Extraction data for the 3,6-dithiaoctanediamide ligand 150c

The 3,6-dithiaoctanediamide ligand **150c** was dissolved in toluene to yield a concentration of 1000 ppm. For the silver studies, the aqueous phase contained 25 ppm Ag in a 0.1 M $NaNO_3$ solution, while, for the palladium studies, the metal concentration was 25 ppm in 0.1 M NaCl solution. The experiments were conducted at 40 °C and pH 7. The aqueous samples were diluted by 2/5 prior to analysis, and the results are summarised in **Tables 33-36**.

3.3.2.1 *Silver extraction using the 3,6-dithiaoctanediamide ligand 150c*

Table 33. AAS calibration data.

Concentration / ppm	Absorbance		
	Reading 1	Reading 2	Average
0	0.000	0.004	0.002
2	0.079	0.078	0.079
4	0.132	0.137	0.135
6	0.177	0.177	0.177
8	0.216	0.214	0.215
10	0.239	0.236	0.238

Regression Statistics [a]

Multiple R	0.9670
R Square	0.9351
Adjusted R Square	0.7351
Standard Error	0.02259
Observations	6

[a] Determined using the regression analysis tool in Microsoft Excel 97 and the average absorbance values.

Table 34. AAS extraction analysis data.

Time	Absorbance		Concentration [a]	Extraction efficiency [b] / %
	Reading 1	Reading 2		
0	0.240	0.237	22.42	0
5	0.082	0.087	7.94	65
10	0.068	0.071	6.53	71
15	0.053	0.055	5.08	77
20	0.053	0.054	5.03	78
25	0.038	0.040	3.67	84
30	0.025	0.029	2.54	89
45	0.021	0.024	2.11	91
60	0.018	0.019	1.74	92
90	0.013	0.015	1.32	94
120	0.018	0.016	1.60	93

[a] In the aqueous phase (ppm); calculated from the calibration curve and multiplied by the dilution factor 2.5. [b] Expressed as a percentage change in concentration relative to the original concentration.

3.3.2.2 *Palladium extraction using the 3,6-dithiaoctanediamide ligand 150c*

Table 35. AAS calibration data.

	Absorbance		
Concentration / ppm	Reading 1	Reading 2	Average
0	0.000	0.004	0.001
2	0.113	0.114	0.110
4	0.223	0.227	0.222
6	0.315	0.310	0.313
8	0.397	0.403	0.396
10	0.468	0.458	0.460

Regression Statistics [a]

Multiple R	0.9930
R Square	0.9861
Adjusted R Square	0.7861
Standard Error	0.02052
Observations	6

[a] Determined using the regression analysis tool in Microsoft Excel 97 and the average absorbance values.

Table 36. AAS extraction analysis data.

Time	Absorbance	Concentration [a]	Extraction efficiency [b] / %
0	0.459	24.95	0
5	0.023	1.177	95
10	0.008	0.409	98
15	0.010	0.512	98
20	0.008	0.409	98
25	0.003	0.154	99
30	0.007	0.358	99
45	0.003	0.154	99
60	0.009	0.461	98
90	0.010	0.512	98
120	0.010	0.512	98

[a] In the aqueous phase (ppm); calculated from the calibration curve and multiplied by the dilution factor 2.5. [b] Expressed as a percentage change in concentration relative to the original concentration.

3.3.3 Extraction data for the malonamide ligands

3.3.3.1 *Silver extraction analysis by AAS*

The malonamide ligands **180h**, **194**, **195**, **196**, **207**, **197** and **208** (and the synthetic precursors **175**, **179**, **186**, **189**, **190**, **191**, **192** and **193**) were dissolved in EtOAc to yield concentrations of approximately 1.8 x 10^{-2} M. For the silver studies, the aqueous phase contained 10 ppm Ag in a 2.5 x 10^{-2} M $NaNO_3$ solution. The experiments were conducted at 25 °C and pH 2.78. The aqueous samples were analysed undiluted. Calibration curves were determined for each data set, before analysis.

Table 37. AAS extraction analysis data for the malonamide ligands.

Time	Absorbance	Concentration [a]	Extraction efficiency [b] / %
		Ligand **180h**	
0	0.5456	9.72	0
5	0.3704	6.60	32
10	0.3711	6.61	32
15	0.3691	6.58	32
		Ligand **194**	
0	0.5416	9.65	0
5	0.4523	8.06	16
10	0.4457	7.94	18
15	0.4516	8.05	17
		Ligand **195**	
0	0.4530	10.50	0
5	0.0167	0.39	97
10	0.0155	0.36	97
15	0.0151	0.35	97

[a] In the aqueous phase (ppm); calculated from the calibration curve. [b] Expressed as a percentage change in concentration relative to the original concentration.

Table 37 (continued). AAS extraction analysis data for the malonamide ligands.

Ligand **196** at 2.5 x 10^{-2} M $NaNO_3$			
0	0.4967	8.85	0
5	0.4458	7.94	10
10	0.4608	8.21	7
15	0.4630	8.25	7
at 0.25 M $NaNO_3$			
0	0.4697	10.11	0
5	0.2719	5.85	42
10	0.2701	5.81	42
15	0.2719	5.85	42
Ligand **207**			
0	0.5910	10.00	0
5	0.4093	6.93	31
10	0.3927	6.65	34
15	0.3902	6.60	34
Ligand **197** at 2.5 x 10^{-2} M $NaNO_3$			
0	0.5411	9.64	0
5	0.4888	8.71	10
10	0.4834	8.61	11
15	0.4776	8.51	12
at 0.25 M $NaNO_3$			
0	0.4607	9.91	0
5	0.3640	7.83	21
10	0.3018	6.49	34
15	0.3013	6.48	35
Ligand **208**			
0	0.5717	9.68	0
5	0.4817	8.15	16
10	0.4755	8.05	17
15	0.4603	7.79	19

Table 38. AAS analysis data for the pH dependence of extraction by ligand **195**.

pH	Absorbance	Concentration [a]	Extraction efficiency [b] / %
	Ligand **195**		
-	0.4839	10.26	-
2.78	0.0024	0.29	97
3.00	0.0022	0.25	97
4.09	0.0024	0.27	97
5.24	0.0032	0.30	97
7.17	0.0053	0.39	96
8.81	0.0154	0.58	94

[a] In the aqueous phase (ppm); calculated from the calibration curve. [b] Expressed as a percentage change in concentration relative to the original concentration.

Table 39. AAS extraction analysis data for the precursors.

Time	Absorbance	Concentration [a]	Extraction efficiency [b] / %
		Compound **175**	
0	0.5632	9.55	0
5	0.5043	8.55	10
10	0.5085	8.62	10
15	0.4798	8.14	15
		Compound **179**	
0	0.5275	9.40	0
5	0.4624	8.24	12
10	0.4574	8.15	13
15	0.4429	7.89	16
		Compound **186**	
0	0.5276	9.40	0
5	0.3267	5.82	38
10	0.3374	6.01	36
15	0.3305	5.89	37
		Compound **189**	
0	0.5450	9.71	0
5	0.4900	8.73	10
10	0.4816	8.58	12
15	0.4662	8.31	14

[a] In the aqueous phase (ppm); calculated from the calibration curve. [b] Expressed as a percentage change in concentration relative to the original concentration.

Table 39 (continued). AAS extraction analysis data for the precursors.

		Compound **190**	
0	0.5314	9.47	0
5	0.4699	8.37	12
10	0.4629	8.25	13
15	0.4676	8.33	12
		Compound **191**	
0	0.5421	8.98	0
5	0.4885	8.09	10
10	0.4756	7.88	12
15	0.4594	7.61	15
		Compound **192**	
0	0.5429	8.99	0
5	0.4616	7.65	15
10	0.4667	7.73	14
15	0.4664	7.73	14
		Compound **193**	
0	0.5886	9.75	0
5	0.4881	8.09	17
10	0.4883	8.09	17
15	0.4577	7.58	22

3.3.3.2 *Competitive metal extraction analysis by ICP-MS*

The same experimental conditions used for the AAS analyses were applied for the competitive extraction studies. The aqueous phase contained 10 ppm of each of the metals, silver, lead and copper in a 2.5 x 10^{-2} M $NaNO_3$ solution. Aliquots (25 ml) of the aqueous phases, obtained following extraction, were concentrated on a steam bath for 0.5 h, after which the samples were re-diluted up to 25 ml. All standards and samples were diluted 20-fold for the ICP-MS analysis, and two isotopes of each metal were used in the analysis, *i.e.* ^{63}Cu and ^{65}Cu; ^{107}Ag and ^{109}Ag; and ^{206}Pb and ^{208}Pb. Each ICP-MS result represents the average of 6 successive readings.

Table 40. Calibration data for the ICP-MS analytes.

	Metal Isotope [a]					
Concentration / ppm	^{63}Cu	^{65}Cu	^{107}Ag	^{109}Ag	^{206}Pb	^{208}Pb
0	2116	1786	8579	8081	1850	2527
2	37330	19500	52051	49630	42271	79317
4	71532	36891	111618	106774	75487	140139
6	108672	55295	160278	151359	120058	225867
8	146465	74045	214565	204563	160672	300580
10	182597	92131	274182	260547	197979	373886
R^{2} [b]	0.9996	0.9992	0.9978	0.9977	0.9989	0.9988
coefficient of x	18230	9236	27139	25802	19873	37354

[a] Expressed as its MS intensity. [b] Determined using the regression analysis tool in Microsoft Excel 97.

Table 41. ICP-MS extraction analysis data for the malonamide **180j**.

	Metal Isotope [a]					
Time	^{63}Cu	^{65}Cu	^{107}Ag	^{109}Ag	^{206}Pb	^{208}Pb
0	145939	73702	213912	204346	160590	303731
15	170562	85358	182303	174379	192601	363763
	Metal Concentration / ppm					
0 [b]	10.01	9.97	9.85	9.90	10.10	10.16
15 [c]	9.16	9.08	6.58	6.59	9.34	9.37
	Extraction Efficiency [d]					
	8	9	33	33	8	8

[a] Expressed as its MS intensity. [b] Corrected for dilution of 4/50. [c] Corrected for dilution of 5/50. [d] Expressed as a percentage change in concentration relative to the original concentration.

Table 42. ICP-MS extraction analysis data for the malonamide **195**.

	Metal Isotope [a]					
Time	^{63}Cu	^{65}Cu	^{107}Ag	^{109}Ag	^{206}Pb	^{208}Pb
0	180467	91017	265840	253537	198930	375732
15	165638	83265	7979	7659	184935	344252
	Metal Concentration / ppm					
0	9.90	9.85	9.80	9.83	10.01	10.06
15	9.09	9.01	0.29	0.30	9.31	9.22
	Extraction Efficiency [b]					
	8	9	97	97	7	8

[a] Expressed as its MS intensity. [b] Expressed as a percentage change in concentration relative to the original concentration.

Table 43. ICP-MS extraction analysis data for the malonamide **196**.

	Metal Isotope [a]					
Time	^{63}Cu	^{65}Cu	^{107}Ag	^{109}Ag	^{206}Pb	^{208}Pb
0	143763	72410	210291	200839	160086	301709
15	168471	85549	231247	220574	190581	359981
	Metal Concentration / ppm					
0 [b]	9.86	9.80	9.69	9.73	10.07	10.10
15 [c]	9.24	9.26	8.52	8.55	9.59	9.64
	Extraction Efficiency [d]					
	6	5	12	12	5	5

[a] Expressed as its MS intensity. [b] Corrected for dilution of 4/50. [c] Corrected for dilution of 5/50. [d] Expressed as a percentage change in concentration relative to the original concentration.

Table 44. ICP-MS extraction analysis data for the malonamide **197**.

	Metal Isotope [a]					
Time	^{63}Cu	^{65}Cu	^{107}Ag	^{109}Ag	^{206}Pb	^{208}Pb
0	183030	91500	270248	257370	203449	383569
15	169584	85331	196183	187334	188708	355869
	Metal Concentration / ppm					
0	10.04	9.91	9.96	9.97	10.24	10.27
15	9.30	9.24	7.23	7.26	9.50	9.53
	Extraction Efficiency [b]					
	7	7	27	27	7	7

[a] Expressed as its MS intensity. [b] Expressed as a percentage change in concentration relative to the original concentration.

Table 45. ICP-MS extraction analysis data for the malonamide **208**.

	Metal Isotope [a]					
Time	^{63}Cu	^{65}Cu	^{107}Ag	^{109}Ag	^{206}Pb	^{208}Pb
0	181682	91208	268971	256641	203360	383724
15	165852	83190	203145	194251	192403	362553
	Metal Concentration / ppm					
0	9.95	9.90	9.81	9.85	10.11	10.14
15	8.92	8.87	7.33	7.34	9.35	9.36
	Extraction Efficiency [b]					
	10	10	25	25	7	8

[a] Expressed as its MS intensity. [b] Expressed as a percentage change in concentration relative to the original concentration.

4 References

(**1**) Lee, J. D., *Concise Inorganic Chemistry*, 4th ed, Chapman and Hall, London, 1991, pp. 816-834.

(**2**) Greenwood, N.N. and Earnshaw, A., *Chemistry of the Elements*, 1st ed, Pergamon Press, Oxford, 1984, pp. 1364-1394.

(**3**) Banerjee, R., Das, R. and Mukhopadhyay, S., *J. Chem. Soc., Dalton Trans.*, 1992, 1317-1321.

(**4**) Dasgupta, S., Herlinger, E. and Linert, W., *J. Chem. Soc., Dalton Trans.*, 1993, 567-570.

(**5**) Gupta, K. K. S., Sanyal, A. and Ghosh, S. P., *J. Chem. Soc., Dalton Trans.*, 1995, 1227-1232.

(**6**) Lucier, G., Münzenberg, J., Casteel, W. J. Jr. and Bertlett, N., *Inorg. Chem.*, 1995, **34**, 2692-2698.

(**7**) Giraudeau, A., Gisselbrecht, J. P., Gross, M. and Weiss, J., *J. Chem. Soc., Chem. Commun.*, 1993, 1103-1105.

(**8**) Housecroft, C. E., *Coord. Chem. Rev.*, 1995, **146**, 211-233.

(**9**) Housecroft, C. E., *Coord. Chem. Rev.*, 1996, **152**, 87-105.

(**10**) Cortez, S. M., Raptis, R. G., *Coord. Chem. Rev.*, 1998, **169**, 363-426.

(**11**) Munakate, M., Wu, L. P., Yamamoto, M., Kuroda-Sowa, T., Maekawa, M., Kawata, S. and Kitagawa, S., *J. Chem. Soc., Dalton Trans.*, 1995, 4099-4106.

(**12**) Amoroso, A. J., Jeffery, J. C., Jones, P. L., McCleverty, J. A., Psilakis, E. and Ward, M. D., *J. Chem. Soc., Chem. Commun.*, 1995, 1175-1176.

(**13**) Hartshorn, C. M. and Steel, P. J., *J. Chem. Soc., Dalton Trans.*, 1998, 3927-3933.

(**14**) Schneider, R., Hosseini, M. W., Planeix, J. M., De Cian, A. and Fischer, J., *J. Chem. Soc., Chem. Commun.*, 1998, 1625-1626.

(**15**) Masciocchi, N., Moret, M., Cairati, P., Sironi, A., Ardizzoia, G. A. and La Monica, G., *J. Chem. Soc., Dalton Trans.*, 1995, 1671-1675.

(**16**) Carlucci, L., Ciani, G., Proserpio, D. M. and Sironi, A., *J. Am. Chem. Soc.*, 1995, **117**, 4562-4569.

(**17**) Venkataraman, D., Gardner, G. B., Lee, S. and Moore, J. S., *J. Am. Chem. Soc.*, 1995, **117**, 11600-11601.

(**18**) Carlucci, L., Ciani, G., Proserpio, D. M. and Sironi, A., *Inorg. Chem.*, 1995, **34**, 5698-5700.

(**19**) Hirsch, K. A., Venkataraman, D., Wilson, S. R., Moore, J. S. and Lee, S., *J. Chem. Soc., Chem. Commun.*, 1995, 2199-2200.

(**20**) Robinson, F. and Zaworotko, M. J., *J. Chem. Soc., Chem. Commun.*, 1995, 2413-2414.

(**21**) Plappert, E. C., Minagos, D. M. P., Lawrence, S. E. and Williams, D. J., *J. Chem. Soc., Dalton Trans.*, 1997, 2119-2123.

(**22**) Jarnick, C., Uehlin, L., Wu, H., Klüfers, P., Piotrowski, H. and Scharmann, T. G., *J. Chem. Soc., Dalton Trans.*, 1999, 3121-3131.

(**23**) Admas, H., Bailey, N. A, Fenton, D. E., Fukuhara, C., Hellier, P. C. and Hempstead, P. D., *J. Chem. Soc., Dalton Trans.*, 1992, 729-730.

(**24**) Harding, C. J., Lin, Q., Malone, J. F., Marrs, D. J., Martin, N, McKee, V. and Nelson, J., *J. Chem. Soc., Dalton Trans.*, 1995, 1739-1747.

(**25**) Takemura, H., Kon, N., Tani, K., Takehara, K., Kimoto, J., Shinmyozu, T. and Inazu, T., *J. Chem. Soc., Perkin Trans. 1*, 1997, 239-246.

(**26**) Coyle, J. L., McKee, V. and Nelson, J., *J. Chem. Soc., Chem. Commun.*, 1998, 709-710.

(**27**) Gimeno, M. C., Jones, P. G., Laguna, A. and Sarroca, C., *J. Chem. Soc., Dalton Trans.*, 1995, 3563-3564.

(**28**) Sampanthar, J. T., Vittal, J. J. and Dean, P. A. W., *J. Chem. Soc., Dalton Trans.*, 1999, 3153-3156.

(**29**) Steiner, M., Grützmacher, H., Zolnai, L. and Huttner, G., *J. Chem. Soc., Chem. Commun.*, 1992, 689-690.

(**30**) Texidor, F., Ayllón, J. A., Viñas, C., Rius, J., Miravitlles, C. and Casabó, J., *J. Chem. Soc., Chem. Commun.*, 1992, 1279-1280.

(**31**) Black, J. R., Champness, N. R., Levason, W. and Reid, G., *J. Chem. Soc., Chem. Commun.*, 1995, 1277-1278.

(**32**) Nomiya, K., Kondoh, Y., Nagano, H. and Oda, M., *J. Chem. Soc., Chem. Commun.*, 1995, 1679-1680.

(**33**) Su, W., Cao, R., Hong, M., Chen, J. and Lu, J., *J. Chem. Soc., Chem. Commun.,* 1998, 1389-1390.

(**34**) de Groot, B., Jenkins, H. A. and Loeb, S. J., *Inorg. Chem.,* 1992, **31**, 203-208.

(**35**) Loeb, S. J. and Shimizu, G. K. H., *Inorg. Chem.,* 1993, **32**, 1001-1006.

(**36**) Casabó, J., Flor, T., Hill, M. N. S., Jenkins, A., Lockhart, J. C., Loeb, S. J., Romero, I. and Teixidor, F., *Inorg. Chem.,* 1995, **34**, 5410-5415.

(**37**) Blake, A. J., Collison, D., Gould, R. O., Reid, G. and Scröder, M., *J. Chem. Soc., Dalton Trans.,* 1993, 521-531.

(**38**) Munakata, M., Wu, L. P., Yamamoto, M., Kuroda-Sowa, T. and Maekawa, M., *J. Chem Soc., Dalton Trans.,* 1995, 3215-3220.

(**39**) Demirhan, F., Gelling, A., Irisli, S., Jeffery, J. C., Salek, S. N., Sentürk, O. S. and Went, M. J., *J. Chem Soc., Dalton Trans.,* 1993, 2765-2773.

(**40**) Takeda, Y., Kimura, T., Ochiai, S., Yajima, S., Kudo, Y., Ouchi, M. and Hakushi, T., *J. Chem. Soc., Faraday Trans.,* 1995, 4079-4082.

(**41**) Munakata, M., Wu, L. P., Kuroda-Sowa, T., Maekawa, M., Suenaga, Y., Sugimoto, K. and Ino, I., *J. Chem. Soc., Dalton Trans.,* 1999, 373-378.

(**42**) Nabeshima, T., Nishijima, K., Tsukada, N., Furusawa, H., Hosoya, T. and Yano, Y., *J. Chem. Soc., Chem. Commun.,* 1992, 1092-1094.

(**43**) Michaelides, A., Skoulika, S., Kiritsis, V. and Aubry, A., *J. Chem. Soc., Chem. Commun.,* 1995, 1415-1416.

(**44**) Wu, D. and Mak, T. C. W., *J. Chem. Soc., Dalton Trans.,* 1995, 2671-2678.

(**45**) Modder, J. F., Leijen, R. J., Vrieze, K., Smeets, W. J. J., Spek, A. L. and van Koten, G., *J. Chem. Soc., Dalton Trans.,* 1995, 4021-4028.

(**46**) Ishikawa, J., Sakamoto, H. and Wada, H., *J. Chem. Soc., Perkin Trans. 2,* 1999, 1273-1279.

(**47**) Haanstra, W. G., Driessen, W. L., van Roon, M., Stoffels, A. L. E. and Reedijk, J., *J. Chem. Soc., Dalton Trans.,* 1992, 481-486.

(**48**) Modder, J. F., Vrieze, K., Spek, A. L., Challa, G. and van Koten, G., *Inorg. Chem.,* 1992, **31**, 1238-1247.

(**49**) Hartshorn, C. M. and Steel, P. J., *J. Chem. Soc., Dalton Trans.,* 1998, 3935-3940.

(**50**) Hanton, L. R. and Lee, K., *J. Chem. Soc., Dalton Trans.,* 2000, 1161-1166.

(**51**) Chen, L., Thompson, L. K., Tandon, S. S. and Bridson, J. N., *Inorg. Chem.,* 1993, **32**, 4063-4068.

(**52**) Holthenrich, D., Krumm, M., Zangrando, E., Pichierri, F., Randaccio, L. and Lippert, B., *J. Chem. Soc., Dalton Trans.,* 1995, 3275-3279.

(**53**) Rao, C. N. R., Ranganathan, A., Pedireddi, V. R. and Raju, A. R., *J. Chem. Soc., Chem. Commun.,* 2000, 39-40.

(**54**) Medina, J. C., Goodnow, T. T., Rojas, M. T., Atwood, J. L., Lynn, B. C., Kaifer, A. E. and Gokel, G. W., *J. Am. Chem. Soc.,* 1992, **114**, 10583-10595.

(**55**) Turonek, M. L., Clarke, P., Laurence, G. S., Lincoln, S. F., Pittet, P. A., Politis, S. and Wainwright, K. P., *Inorg. Chem.,* 1993, **32**, 2195-2198.

(**56**) Wang, J., Luo, Q. H.., Shen, M. C., Huang, X. Y. and Wu, Q. J., *J. Chem. Soc., Chem. Commun.,* 1995, 2373-2374.

(**57**) de Namor, A. F. D., Piro, O. E., Salazr, L. E. P., Aguilar-Cornejo, A. F., Al-Rawi, N., Castellano, E. E. and Velarde, F. J. S., *J. Chem. Soc., Faraday Trans.,* 1998, **94**, 3097-3104.

(**58**) Atkinson, I. M., Chartres, J. D., Everett, G. W., Ji, X. K., Lindoy, L. F., Matthes, O. A., Meehan, G. V., Skelton, B. W., Wei, G. and White, A. H., *J. Chem. Soc., Dalton Trans.,* 2000, 1191-1198.

(**59**) Matsumoto, K., Hashimoto, M., Toda, M. and Tsukube, H. *J. Chem. Soc., Perkin Trans. 1,* 1995, 2497-2502.

(**60**) Lednev, I. K., Hester, R. E. and Moore, J. N., *J. Chem. Soc., Faraday Trans.,* 1997, **93**(8), 1551-1558.

(**61**) Alfimov, M. V., Churakov, A. V., Fedorov, Y. V., Fedorova, O. A., Gromov, S. P., Hester, R. E., Howard, J. A. K., Kuz'mina, L. G., Lednev, I. K. and Moore, J. N., *J. Chem. Soc., Perkin Trans. 2,* 1997, 2249-2256.

(**62**) Blake, A. J., Reid, G. and Schröder, M., *J. Chem. Soc., Chem. Commun.,* 1992, 1074-1076.

(**63**) Sibert, J. W., Lange, S. J., Williams, D. J., Barrett, A. G. M. and Hoffman, B. M., *Inorg. Chem.*, 1995, **34**, 2300-2305.

(**64**) Adam, K. R., Baldwin, D. S., Duckworth, P. A., Lindoy, L. F., McPartlin, M., Bashall, A., Powell, H. R. and Tasker, P. A., *J. Chem. Soc., Dalton Trans.*, 1995, 1127-1131.

(**65**) Stevens, G. W. and Perera, J. M., *Min. Pro. Ext. Met. Rev.*,1997, **17**, 205-226.

(**66**) Paiva, A. P., *Sep. Sci. Tech.*, 1993, **28**(4), 947-1008.

(**67**) Ohmiya, Y. and Sekine, T., *Anal. Sci.*, 1996, **12**, 249-254.

(**68**) Mendoza, C. S. and Kamata, S., *Anal. Sci.*, 1996, **12**, 495-497.

(**69**) Tsukube, H., Shinoda, S., Uenishi, J., Hiraoka, T., Imakoga, T. and Yonemitsu, O., *J. Org Chem.*, 1998, **63**, 3884-3894.

(**70**) Kumar, S., Bhalla, V. and Singh, H., *Tetrahedron*, 1998, **54**, 5575-5586.

(**71**) Sakamoto, H., Ishikawa, J. and Otomo, M., *Bull. Chem. Soc. Jpn*, 1995, **68**, 2831-2836.

(**72**) Kumar, S., Hundal, M. S., Hundal, G., Singh, P., Bhalla, V. and Singh, H., *J. Chem. Soc., Perkin Trans. 2*, 1998, 925-932.

(**73**) Saito, K., Taninaka, I., Murakami, S. and Muromatsu, A., *Talanta*, 1998, **46**, 1187-1194.

(**74**) Ohto, K., Murakami, E., Shinohara, T., Shiratsuchi, K., Inoue, K. and Iwasaki, M., *Anal. Chim. Acta*, 1997, **341**, 275-283.

(**75**) Ohto, K., Yamaga, H., Murakami, E. and Inoue, K., *Talanta*, 1997, **44**, 1123-1130.

(**76**) de Namor, A. F., Goitía, M. T., Casal, A. R., Verlarde, F. J. S., González, M. I. B., Villanueva-Salas, J. A. and Zapata-Ormachea, M. L., *Phys. Chem. Chem. Phys.*, 1999, **1**, 3633-3638.

(**77**) Otsuka, H., Suzuki, Y., Ikeda, A., Araki, K. and Shinkai, S., *Talanta*, 1998, **54**, 423-446.

(**78**) Hagemann, J.P., Ph.D. Thesis, Rhodes University, 1997.

(**79**) Hagemann, J.P., and Kaye, P.T., *Tetrahedron*, 1998, **55**, 869-874.

(**80**) Hagemann, J.P., and Kaye, P.T., *J. Chem. Soc., Perkin Trans. 1*, 1999, 341-347.

(**81**) Burton, S.G., Ph.D. Thesis, Rhodes University, 1994.

(**82**) Wellington, K.W., Ph.D. Thesis, Rhodes University, 1999.

(**83**) Burton, S.G., Kaye, P.T. and K. Wellington, *Synth. Commun.*, in press.

(84) Kaye, P.T. and K. Wellington, *Synth. Commun.*, in press.

(**85**) Doucet, J.P. and Weber, J., *Computer-Aided Molecular Design: Theory and Applications*, Academic Press, London, 1996, p. 127.

(**86**) Cerius^2, v 4.0, Molecular Simulations Inc.

(**87**) Comba, P. and Hambley, T.W., *Molecular Modeling of Inorganic Compounds*, VCH, Wienheim, 1995, pp. 80-89.

(**88**) Bode, M. L., Ph.D. Thesis, Rhodes University, 1994.

(**89**) George, R., M.Sc. Thesis, Rhodes University, 1994.

(**90**) Deane, P. O., M.Sc. Thesis, Rhodes University, 1995.

(**91**) Whittaker, R., M.Sc. Thesis, Rhodes University, 1995.

(92) Wilkinson, G., Gillard, R.D. and McCleverty, J.A., *Comprehensive Coordination Chemistry, Vol. 5*, Pergamon Press, Oxford, 1987, pp. 775-*ff*.

(**93**) Paquette, L. A., *Organic Reactions, Vol.*, New York, 1997, **51**, 205.

(**94**) Sabbagh, L.V., Ph.D. Thesis, Rhodes University, 2000.

(**95**) March, J., *Advanced Organic Synthesis: Reactions, Mechanisms and Structure*, 4th Ed., Wiley and Son, New York, 1992, pp. 217.

(**96**) Iveson, P. B., Drew, M. G. B., Hudson, M. J. and Madic, C., *J. Chem. Soc., Dalton Trans.*, 1999, 3605-3610.

(**97**) Hammet, L.P., *Physical Organic Chemistry*, McGraw-Hill, London, 1940, pp. 73.

(**98**) Isaacs, N.S., *Physical Organic Chemistry*, Longman Scientific and Technical, Harlow, 1987, pp. 355.

(**99**) Kabalka, G.W., Varma, M. and Varma, R.S., *J. Org. Chem.*, 1986, **51**, 2386-2388.

(**100**) Kofod, H., *Org. Syn., Coll. Vol.*, 1963, **4**, 491.

(**101**) Ramalingam, K., Raju, N., Nanjappan, P., Linder, K.E., Pirro, J., Zeng, W., Rumsey, W., Nowotnik, D.P. and Nunn, A.D., *J. Med. Chem.*, 1994, **37**(24), 4155-4163.

(**102**) Leach, C.A., Brown, T.H., Ife, R.J., Keeling, D.J., Laing, S.M., Parsons, M.E., Price C.A. and Wiggall, K.J., *J. Med. Chem.*, 1992, **35**(10), 1845-1852.

(**103**) Murphy, S.T., Ritchie, E. and Taylor, W.C., *Aust. J. Chem.*, 1974, **27**, 187-194.

(**104**) Yde, B., Yousif, N.M., Pedersen, U., Thomsen, I. and Lawesson, S.O. *Tetrahedron*, 1984, **40**(11), 2047-2052.

(**105**) Kingston, H.M. and Haswell, S.J., *Microwave-Enhanced Chemistry: Fundamentals, Sample Preparation, and Applications*, American Chemical Society, Washington, DC, 1997, pp. 1-*ff*.

(**106**) Goncalo, P., Roussel, C., Mélot, J.M. and Vébrel, J., *J. Chem. Soc., Perkin Trans. 2*, 1999, 2111-2115.

(**107**) PC Spartan Pro, v1.1, Wavefunction Inc.

(**108**) Wong, W.K, Chik, T.W., Hui, K.N., Williams, I., Feng, X., Mak, T.C.W. and Che, C.M., *Polyhedron*, 1996, **15**, 4447.

(**109**) Sweeney, D.M., Mizushima, S. and Quagliano, J.V., *J. Am. Chem. Soc*., 1955, **77**, 6521-6522.

(**110**) McAuliffe, C.A., Quagliano, J.V. and Vallarino, L.M, *Inorg. Chem.*, 1966, **11**, 1996-2003.

(**111**) Sole, K.C., Personal Communication.

(**112**) Sole, K.C. and Hiskey, B., *Hydrometallurgy*, 1992, **30**, 345-365.

(**113**) MINTEK, 200 Hans Strijdom Drive, Randburg, South Africa.

(**114**) Bode, M. L. and Kaye, P. T., *J. Chem. Soc., Perkin Trans, 1*., 1993, 1809-1813.

(115) *Beilstein's "Handbuch der Organischen Chemie"*; (a) H **2**, 629; (b) H **2**, 644; (c) EI **2**, 282 and (d) H **9**, 869.

(**116**) Cahiez, G. and Alami, M., *Tetrahedron*, 1989, **45**(13), 4163-4176.

(**117**) Wong, O. and McKeown, H.R, *J. Pharm. Sci*, 1988, **77**(11), 926-932.

(**118**) Weigand, S. and Brueckner, R., *Synthesis*, 1996, 475-482.

(**119**) Dhar, M.L., *J. Chem. Soc.*, 1964, 842-861.

(**120**) Wojcik and Adkins, *J. Am. Chem. Soc*., 1934, **56**, 2425.

(**121**) Rauscher, W.H. and Clark, W.H., *J. Am. Chem. Soc*., 1948, **70**, 438.

(122) Chemical Abtracts, CRN 98951-65-6.

(123) Chemical Abtracts, CRN 99850-07-4.

(124) Kazluskas, D. and Balsite, E., *Zh. Org. Khim.*, 1972, **8**(11), 2291-7 (Chemical Abstracts, 78:123969,).

(125) Nishino, H., Ishida, K., Hashimoto, H. and Kurosawa, K., *Synthesis*, 1996, 888-896.

5 Appendix

Crytallographic Data for *N,N´*-Bis(2-methoxyphenyl)malonamide 196

Table 46. Crystal data and structure refinement for **196**.

Identification code	**196**	
Empirical formula	C34 H36 N4 O8	
Formula weight	628.67	
Temperature	173(2) K	
Wavelength	0.71073 Å	
Crystal system	Monoclinic	
Space group	P 21/n	
Unit cell dimensions	a = 8.5670(1) Å	α= 90°.
	b = 15.3299(3) Å	β= 99.116(1)°.
	c = 23.516(1) Å	γ = 90°.
Volume	3049.4(2) $Å^3$	
Z	4	
Density (calculated)	1.369 Mg/m^3	
Absorption coefficient	0.099 mm^{-1}	
F(000)	1328	
Crystal size	0.27 x 0.25 x 0.25 mm^3	
Theta range for data collection	2.20 to 25.35°.	
Index ranges	-10<=h<=6, -18<=k<=18, -18<=l<=28	
Reflections collected	15787	
Independent reflections	5458 [R(int) = 0.0348]	
Completeness to theta = 25.35°	97.5 %	
Max. and min. transmission	0.9758 and 0.9739	
Refinement method	Full-matrix least-squares on F^2	
Data / restraints / parameters	5458 / 4 / 436	
Goodness-of-fit on F^2	1.056	
Final R indices [I>2sigma(I)]	R1 = 0.0424, wR2 = 0.0850	
R indices (all data)	R1 = 0.0808, wR2 = 0.0953	
Extinction coefficient	0.0018(4)	
Largest diff. peak and hole	0.216 and -0.214 $e.Å^{-3}$	

Table 47. Atomic coordinates (x 10^4) and equivalent isotropic displacement parameters ($Å^2$x 10^3) for **196**. U(eq) is defined as one third of the trace of the orthogonalized U^{ij} tensor.

	x	y	z	U(eq)
O(3)	9173(2)	2684(1)	101(1)	27(1)
O(3')	15094(2)	3547(1)	1212(1)	31(1)
O(1')	18874(2)	833(1)	2339(1)	34(1)
O(2)	9855(2)	2374(1)	1465(1)	36(1)
O(2')	14183(2)	1528(1)	1009(1)	33(1)
O(1)	15073(2)	2945(1)	2500(1)	37(1)
C(8')	15568(2)	1761(1)	1145(1)	23(1)
O(4')	19654(2)	4887(1)	734(1)	38(1)
N(1')	16516(2)	1486(1)	1628(1)	24(1)
N(2')	17069(2)	3886(1)	702(1)	25(1)
O(4)	13391(2)	1107(1)	-428(1)	38(1)
N(1)	12331(2)	2861(1)	1830(1)	26(1)
N(2)	11312(2)	1778(1)	168(1)	24(1)
C(11')	16903(2)	4809(1)	695(1)	24(1)
C(10')	16102(2)	3321(1)	924(1)	24(1)
C(10)	10521(2)	2471(1)	328(1)	22(1)
C(16)	9201(2)	895(1)	-390(1)	28(1)
C(12')	15442(2)	5212(1)	664(1)	28(1)
C(12)	11869(2)	803(1)	-579(1)	28(1)
C(14')	16643(3)	6616(1)	646(1)	35(1)
C(2)	13818(2)	2800(1)	2782(1)	27(1)
C(9)	11429(2)	2997(1)	812(1)	23(1)
C(9')	16338(2)	2374(1)	772(1)	25(1)
C(11)	10754(2)	1168(1)	-274(1)	23(1)
C(16')	18244(2)	5324(1)	702(1)	27(1)
C(3)	12343(2)	2742(1)	2427(1)	25(1)
C(4)	11004(3)	2605(1)	2674(1)	32(1)
C(6)	12572(3)	2586(1)	3616(1)	35(1)
C(13')	15310(3)	6111(1)	641(1)	33(1)
C(7')	16145(2)	872(1)	2036(1)	24(1)
C(8)	11122(2)	2698(1)	1398(1)	24(1)
C(6')	14626(3)	596(1)	2083(1)	35(1)
C(2')	17425(2)	517(1)	2411(1)	27(1)
C(13)	11405(3)	178(1)	-995(1)	34(1)
C(15)	8746(3)	267(1)	-811(1)	33(1)
C(14)	9843(3)	-87(1)	-1107(1)	35(1)
C(5')	14402(3)	-35(2)	2485(1)	45(1)

Table 47 (continued).

C(5)	11124(3)	2525(1)	3268(1)	36(1)
C(15')	18105(3)	6229(1)	675(1)	33(1)
C(3')	17184(3)	-106(1)	2815(1)	35(1)
C(7)	13922(3)	2727(1)	3376(1)	33(1)
C(1)	16619(3)	2896(2)	2826(1)	44(1)
C(4')	15665(3)	-380(2)	2846(1)	44(1)
C(17')	21067(3)	5403(2)	837(1)	57(1)
C(1')	20234(3)	441(2)	2670(1)	44(1)
C(17)	14585(3)	732(2)	-707(1)	56(1)

Table 48. Bond lengths [Å] and angles [°] for **196**.

O(3)-C(10)	1.237(2)
O(3')-C(10')	1.228(2)
O(1')-C(2')	1.368(2)
O(1')-C(1')	1.427(2)
O(2)-C(8)	1.227(2)
O(2')-C(8')	1.232(2)
O(1)-C(2)	1.367(3)
O(1)-C(1)	1.423(2)
C(8')-N(1')	1.355(2)
C(8')-C(9')	1.506(3)
O(4')-C(16')	1.372(2)
O(4')-C(17')	1.435(3)
N(1')-C(7')	1.415(2)
N(2')-C(10')	1.358(3)
N(2')-C(11')	1.423(3)
O(4)-C(12)	1.378(2)
O(4)-C(17)	1.421(3)
N(1)-C(8)	1.354(3)
N(1)-C(3)	1.413(3)
N(2)-C(10)	1.345(2)
N(2)-C(11)	1.422(2)
C(11')-C(12')	1.387(3)
C(11')-C(16')	1.392(3)
C(10')-C(9')	1.517(3)
C(10)-C(9)	1.507(3)
C(16)-C(11)	1.380(3)
C(16)-C(15)	1.393(3)
C(12')-C(13')	1.382(3)
C(12)-C(13)	1.383(3)
C(12)-C(11)	1.399(3)
C(14')-C(13')	1.379(3)
C(14')-C(15')	1.378(3)
C(2)-C(7)	1.390(3)
C(2)-C(3)	1.403(3)
C(9)-C(8)	1.515(3)
C(16')-C(15')	1.393(3)
C(3)-C(4)	1.381(3)
C(4)-C(5)	1.392(3)
C(6)-C(5)	1.376(3)
C(6)-C(7)	1.382(3)
C(7')-C(6')	1.389(3)
C(7')-C(2')	1.405(3)
C(6')-C(5')	1.385(3)

Table 48 (continued).

C(2')-C(3')	1.384(3)
C(13)-C(14)	1.383(3)
C(15)-C(14)	1.367(3)
C(5')-C(4')	1.372(3)
C(3')-C(4')	1.381(3)
C(2')-O(1')-C(1')	117.49(17)
C(2)-O(1)-C(1)	117.84(17)
O(2')-C(8')-N(1')	123.57(18)
O(2')-C(8')-C(9')	121.49(18)
N(1')-C(8')-C(9')	114.93(17)
C(16')-O(4')-C(17')	116.89(16)
C(8')-N(1')-C(7')	127.27(17)
C(10')-N(2')-C(11')	124.94(17)
C(12)-O(4)-C(17)	117.78(17)
C(8)-N(1)-C(3)	127.25(17)
C(10)-N(2)-C(11)	126.65(16)
C(12')-C(11')-C(16')	119.03(18)
C(12')-C(11')-N(2')	122.09(17)
C(16')-C(11')-N(2')	118.85(17)
O(3')-C(10')-N(2')	123.86(18)
O(3')-C(10')-C(9')	122.10(18)
N(2')-C(10')-C(9')	114.02(18)
O(3)-C(10)-N(2)	124.40(18)
O(3)-C(10)-C(9)	121.32(18)
N(2)-C(10)-C(9)	114.28(17)
C(11)-C(16)-C(15)	120.2(2)
C(13')-C(12')-C(11')	120.9(2)
O(4)-C(12)-C(13)	124.75(19)
O(4)-C(12)-C(11)	115.40(17)
C(13)-C(12)-C(11)	119.8(2)
C(13')-C(14')-C(15')	120.2(2)
O(1)-C(2)-C(7)	124.70(19)
O(1)-C(2)-C(3)	115.20(19)
C(7)-C(2)-C(3)	120.09(19)
C(10)-C(9)-C(8)	112.44(16)
C(8')-C(9')-C(10')	111.89(17)
C(16)-C(11)-C(12)	119.45(18)
C(16)-C(11)-N(2)	123.10(18)
C(12)-C(11)-N(2)	117.36(17)
O(4')-C(16')-C(15')	123.82(19)
O(4')-C(16')-C(11')	116.24(17)
C(15')-C(16')-C(11')	119.94(19)

Table 48 (continued).

C(4)-C(3)-C(2)	119.3(2)
C(4)-C(3)-N(1)	124.14(19)
C(2)-C(3)-N(1)	116.53(18)
C(3)-C(4)-C(5)	120.1(2)
C(5)-C(6)-C(7)	120.2(2)
C(14')-C(13')-C(12')	119.8(2)
C(6')-C(7')-C(2')	118.62(19)
C(6')-C(7')-N(1')	124.82(18)
C(2')-C(7')-N(1')	116.55(17)
O(2)-C(8)-N(1)	124.4(2)
O(2)-C(8)-C(9)	121.64(18)
N(1)-C(8)-C(9)	113.87(17)
C(5')-C(6')-C(7')	120.0(2)
O(1')-C(2')-C(3')	124.52(19)
O(1')-C(2')-C(7')	114.70(18)
C(3')-C(2')-C(7')	120.77(19)
C(12)-C(13)-C(14)	120.0(2)
C(14)-C(15)-C(16)	119.9(2)
C(15)-C(14)-C(13)	120.6(2)
C(4')-C(5')-C(6')	120.7(2)
C(6)-C(5)-C(4)	120.4(2)
C(14')-C(15')-C(16')	120.1(2)
C(2')-C(3')-C(4')	119.4(2)
C(6)-C(7)-C(2)	119.9(2)
C(5')-C(4')-C(3')	120.4(2)

Table 49. Anisotropic displacement parameters ($Å^2 x\ 10^3$) for **196**. The anisotropic displacement factor exponent takes the form: $-2p^2[\ h^2\ a^{*2}U^{11} + ...\ + 2\ h\ k\ a^*\ b^*\ U^{12}\ ]$

	U^{11}	U^{22}	U^{33}	U^{23}	U^{13}	U^{12}
O(3)	22(1)	32(1)	26(1)	-2(1)	2(1)	5(1)
O(3')	29(1)	30(1)	36(1)	-2(1)	14(1)	-3(1)
O(1')	24(1)	39(1)	37(1)	7(1)	-3(1)	2(1)
O(2)	28(1)	55(1)	26(1)	-3(1)	4(1)	-14(1)
O(2')	22(1)	33(1)	40(1)	6(1)	-3(1)	-3(1)
O(1)	22(1)	54(1)	33(1)	1(1)	2(1)	-3(1)
C(8')	21(1)	20(1)	27(1)	-4(1)	3(1)	1(1)
O(4')	24(1)	27(1)	66(1)	-2(1)	15(1)	-4(1)
N(1')	21(1)	25(1)	26(1)	3(1)	3(1)	0(1)
N(2')	23(1)	23(1)	31(1)	1(1)	8(1)	-1(1)
O(4)	28(1)	37(1)	52(1)	-11(1)	17(1)	2(1)
N(1)	23(1)	37(1)	20(1)	-2(1)	3(1)	-3(1)
N(2)	20(1)	26(1)	24(1)	-2(1)	2(1)	4(1)
C(11')	28(1)	24(1)	21(1)	-1(1)	7(1)	-1(1)
C(10')	18(1)	29(1)	23(1)	0(1)	-1(1)	-2(1)
C(10)	21(1)	25(1)	22(1)	4(1)	8(1)	0(1)
C(16)	28(1)	29(1)	26(1)	1(1)	5(1)	3(1)
C(12')	26(1)	32(1)	26(1)	1(1)	7(1)	-1(1)
C(12)	31(1)	23(1)	31(1)	1(1)	9(1)	0(1)
C(14')	45(1)	24(1)	35(1)	0(1)	11(1)	3(1)
C(2)	29(1)	24(1)	26(1)	0(1)	3(1)	-2(1)
C(9)	24(1)	23(1)	23(1)	0(1)	4(1)	0(1)
C(9')	23(1)	25(1)	26(1)	1(1)	1(1)	-1(1)
C(11)	26(1)	21(1)	23(1)	1(1)	3(1)	2(1)
C(16')	26(1)	29(1)	29(1)	0(1)	11(1)	2(1)
C(3)	29(1)	24(1)	21(1)	-3(1)	5(1)	-2(1)
C(4)	28(1)	40(1)	27(1)	-1(1)	4(1)	-4(1)
C(6)	50(2)	33(1)	21(1)	0(1)	5(1)	-6(1)
C(13')	35(1)	32(1)	31(1)	-1(1)	7(1)	9(1)
C(7')	30(1)	20(1)	24(1)	-1(1)	7(1)	2(1)
C(8)	24(1)	23(1)	25(1)	-5(1)	4(1)	0(1)
C(6')	30(1)	34(1)	42(2)	6(1)	10(1)	3(1)
C(2')	29(1)	28(1)	24(1)	-3(1)	4(1)	2(1)
C(13)	45(1)	28(1)	34(1)	-3(1)	17(1)	4(1)
C(15)	32(1)	31(1)	34(1)	0(1)	1(1)	-2(1)
C(14)	47(2)	28(1)	31(1)	-5(1)	5(1)	-4(1)
C(5')	37(1)	43(1)	58(2)	13(1)	20(1)	2(1)
C(5)	39(1)	40(1)	32(2)	-3(1)	10(1)	-8(1)
C(15')	36(1)	27(1)	38(1)	-2(1)	11(1)	-6(1)

Table 49 (continued).

C(3')	43(1)	33(1)	28(1)	5(1)	5(1)	6(1)
C(7)	34(1)	35(1)	29(1)	-1(1)	-4(1)	-2(1)
C(1)	24(1)	59(2)	47(2)	-4(1)	-5(1)	-3(1)
C(4')	50(2)	41(1)	43(2)	14(1)	16(1)	4(1)
C(17')	27(1)	36(1)	110(2)	-4(1)	18(1)	-7(1)
C(1')	32(1)	48(2)	47(2)	3(1)	-8(1)	8(1)
C(17)	35(2)	59(2)	80(2)	-20(2)	25(1)	4(1)

Table 50. Hydrogen coordinates (x 10^4) and isotropic displacement parameters ($Å^2$x 10^3)for **196**.

	x	y	z	U(eq)
H(16)	8440	1136	-182	33
H(12')	14520	4866	658	33
H(14')	16554	7233	630	41
H(9A)	11128	3619	759	28
H(9B)	12574	2949	796	28
H(9'A)	15887	2274	363	30
H(9'B)	17485	2246	820	30
H(4)	10000	2566	2437	38
H(6)	12643	2533	4021	42
H(13')	14303	6379	623	39
H(6')	13742	839	1840	42
H(13)	12159	-69	-1204	41
H(15)	7674	84	-893	40
H(14)	9530	-519	-1392	42
H(5')	13363	-230	2510	54
H(5)	10200	2427	3436	44
H(15')	19020	6580	676	39
H(3')	18056	-342	3068	42
H(7)	14920	2773	3616	40
H(1A)	16743	3350	3123	66
H(1C)	17404	2982	2570	66
H(1B)	16773	2321	3009	66
H(4')	15493	-812	3119	52
H(17'A)	21122	5777	502	85
H(17'B)	21991	5018	900	85
H(17'C)	21055	5767	1178	85
H(1'A)	20210	533	3080	66
H(1'C)	21192	706	2567	66
H(1'B)	20236	-186	2589	66
H(17B)	14643	103	-631	84
H(17A)	15606	1001	-560	84
H(17C)	14329	832	-1123	84
H(2)	12411(10)	1697(15)	379(8)	46(7)
H(1)	13367(13)	3028(14)	1717(10)	48(7)
H(1')	17658(8)	1653(15)	1681(10)	49(7)
H(2')	17900(20)	3629(14)	500(9)	53(7)

Table 51. Torsion angles [°] for **196**.

O(2')-C(8')-N(1')-C(7')	3.4(3)
C(9')-C(8')-N(1')-C(7')	-175.74(17)
C(10')-N(2')-C(11')-C(12')	-30.1(3)
C(10')-N(2')-C(11')-C(16')	151.78(19)
C(11')-N(2')-C(10')-O(3')	-10.0(3)
C(11')-N(2')-C(10')-C(9')	168.44(17)
C(11)-N(2)-C(10)-O(3)	-1.0(3)
C(11)-N(2)-C(10)-C(9)	180.00(17)
C(16')-C(11')-C(12')-C(13')	-0.1(3)
N(2')-C(11')-C(12')-C(13')	-178.24(19)
C(17)-O(4)-C(12)-C(13)	-2.2(3)
C(17)-O(4)-C(12)-C(11)	177.4(2)
C(1)-O(1)-C(2)-C(7)	9.3(3)
C(1)-O(1)-C(2)-C(3)	-171.88(18)
O(3)-C(10)-C(9)-C(8)	89.3(2)
N(2)-C(10)-C(9)-C(8)	-91.7(2)
O(2')-C(8')-C(9')-C(10')	88.9(2)
N(1')-C(8')-C(9')-C(10')	-91.9(2)
O(3')-C(10')-C(9')-C(8')	-16.4(3)
N(2')-C(10')-C(9')-C(8')	165.18(16)
C(15)-C(16)-C(11)-C(12)	-0.6(3)
C(15)-C(16)-C(11)-N(2)	-177.11(18)
O(4)-C(12)-C(11)-C(16)	-179.17(17)
C(13)-C(12)-C(11)-C(16)	0.4(3)
O(4)-C(12)-C(11)-N(2)	-2.4(3)
C(13)-C(12)-C(11)-N(2)	177.11(18)
C(10)-N(2)-C(11)-C(16)	-36.1(3)
C(10)-N(2)-C(11)-C(12)	147.3(2)
C(17')-O(4')-C(16')-C(15')	10.2(3)
C(17')-O(4')-C(16')-C(11')	-170.1(2)
C(12')-C(11')-C(16')-O(4')	179.86(18)
N(2')-C(11')-C(16')-O(4')	-1.9(3)
C(12')-C(11')-C(16')-C(15')	-0.4(3)
N(2')-C(11')-C(16')-C(15')	177.81(18)
O(1)-C(2)-C(3)-C(4)	-179.36(18)
C(7)-C(2)-C(3)-C(4)	-0.5(3)
O(1)-C(2)-C(3)-N(1)	-1.5(3)
C(7)-C(2)-C(3)-N(1)	177.36(18)
C(8)-N(1)-C(3)-C(4)	-13.9(3)
C(8)-N(1)-C(3)-C(2)	168.42(18)
C(2)-C(3)-C(4)-C(5)	-0.1(3)
N(1)-C(3)-C(4)-C(5)	-177.75(19)
C(15')-C(14')-C(13')-C(12')	-0.2(3)

Table 51 (continued).

C(11')-C(12')-C(13')-C(14')	0.4(3)
C(8')-N(1')-C(7')-C(6')	-15.9(3)
C(8')-N(1')-C(7')-C(2')	163.32(19)
C(3)-N(1)-C(8)-O(2)	-3.8(3)
C(3)-N(1)-C(8)-C(9)	173.07(17)
C(10)-C(9)-C(8)-O(2)	-30.0(3)
C(10)-C(9)-C(8)-N(1)	152.96(17)
C(2')-C(7')-C(6')-C(5')	-1.7(3)
N(1')-C(7')-C(6')-C(5')	177.6(2)
C(1')-O(1')-C(2')-C(3')	5.4(3)
C(1')-O(1')-C(2')-C(7')	-174.31(18)
C(6')-C(7')-C(2')-O(1')	-179.29(18)
N(1')-C(7')-C(2')-O(1')	1.4(3)
C(6')-C(7')-C(2')-C(3')	1.0(3)
N(1')-C(7')-C(2')-C(3')	-178.31(18)
O(4)-C(12)-C(13)-C(14)	179.25(19)
C(11)-C(12)-C(13)-C(14)	-0.2(3)
C(11)-C(16)-C(15)-C(14)	0.6(3)
C(16)-C(15)-C(14)-C(13)	-0.5(3)
C(12)-C(13)-C(14)-C(15)	0.3(3)
C(7')-C(6')-C(5')-C(4')	1.3(4)
C(7)-C(6)-C(5)-C(4)	-0.2(3)
C(3)-C(4)-C(5)-C(6)	0.4(3)
C(13')-C(14')-C(15')-C(16')	-0.3(3)
O(4')-C(16')-C(15')-C(14')	-179.7(2)
C(11')-C(16')-C(15')-C(14')	0.6(3)
O(1')-C(2')-C(3')-C(4')	-179.5(2)
C(7')-C(2')-C(3')-C(4')	0.1(3)
C(5)-C(6)-C(7)-C(2)	-0.4(3)
O(1)-C(2)-C(7)-C(6)	179.5(2)
C(3)-C(2)-C(7)-C(6)	0.7(3)
C(6')-C(5')-C(4')-C(3')	-0.1(4)
C(2')-C(3')-C(4')-C(5')	-0.6(4)

Table 52. Hydrogen bonds for **196** [Å and °].

D-H...A	d(D-H)	d(H...A)	d(D...A)	<(DHA)
N(2)--H(2)..O(2')	0.9997	1.9591	2.9247	161.1
N(1)--H(1)..O(1) [Intra]	0.9999	2.1677	2.6162	105.4
N(1)--H(1)..O(3')	0.9999	2.1877	3.1477	160.8'
				93.33' 359.3
N(2')--H(2')..O(3)	0.9999	2.1216	3.0752	158.81
N(1')--H(1')..O(2)	0.9997	2.3083	3.2444	155.48
N(1')--H(1')..O(1') [Intra]	0.9997	2.1311	2.6084	107.24'
				96.91' 359.63

Table 53. Hydrogen bonds for **196** [Å and °] involving H-atoms bonded to carbon

D-H...A	d(D-H)	d(H...A)	d(D...A)	<(DHA)
C(9)--H(9A)..O(4')	0.9900	2.3140	3.2634	160.36
C(4)--H(4B)..O(3')	0.9900	2.4063	3.2430	141.84
C(9) --H(9B)..O(2')	0.9900	2.5836	3.2407	123.81'
				79.96' 345.61
C(16) --H(16)..O(3)[Intra]	0.9500	2.5167	2.9777	109.93
C(4)--H(4)..O(2) [Intra]	0.9500	2.2878	2.8783	119.62
C(9')--H(9B')..O(3)	0.9900	2.4859	3.1371	123.01
C(9')--H(9A')..O(2)	0.9900	2.3444	3.1912	143.01'
				83.11' 349.13
C(14)--H(14)..O(4)	0.9500	2.5902	3.5278	169.18
C(12)--H(12)..O(3') [Intra]	0.9500	2.4134	2.8965	111.27
C(6')--H(6')..O(2') [Intra]	0.9500	2.3039	2.8751	118.01